Imperial College London

Investigating the role of extracellular ATP in Chronic Respiratory Diseases

Sabina Issop

2024

A thesis submitted for the Degree of Doctor of Philosophy

in the Faculty of Medicine, Imperial College London

Respiratory Pharmacology Group
National Heart and Lung Institute
Faculty of Medicine
Imperial College London
Sir Alexander Fleming Building
Exhibition Road
London
SW7 2AZ

Thesis Abstract

Chronic cough is a common symptom of respiratory diseases driven by activation of airway sensory nerves that express ion channels and receptors, including purinergic P2X3 channels, which are activated by ATP. A non-selective P2X3 receptor antagonist, Gefapixant, was one of the first drugs to show antitussive efficacy in clinical trials in treatment-refractory chronic cough patients. However, there are no data demonstrating levels of eATP in patients with refractory or unexplained chronic cough (RUCC) which is hypothesised to be increased in bronchoalveolar lavage fluid (BALF) and plasma samples.

Current methods used to measure eATP in biological samples are not always reliable or reproducible given that eATP rapidly degrades in the extracellular space. As such, a reliable and reproducible method for the collection and assessment of eATP in biological samples was developed.

In vitro and *ex vivo* experiments were used to show activation of vagal sensory nerves by the endogenous ATP ligand which could be blocked using P2X3 antagonists. However, in the clinic, P2X3 antagonists are commonly associated with taste disturbance side effects. Alternative strategies could include CD39, an ecto-nucleotidase enzyme that breaks down ATP and reduces activation of vagal sensory nerves by depleting levels of ATP. eATP levels were investigated in several airway disease models where decreases in eATP were measured in BALF samples. CD39 was also tested in an acute cigarette smoke model but had no impact on several key inflammatory markers, highlighting the need for alternative animal models with elevated eATP.

In patients with RUCC, the levels of eATP were reduced in BALF samples, but were increased in plasma samples. This increase supports the hypothesis that eATP is a driver in chronic cough and may have potential use as a clinical biomarker to select patient populations with elevated eATP who are more likely to respond to ATP-targeted therapies.

Acknowledgements

I would like to thank my supervisors Professor Maria Belvisi, Professor Terry Tetley and Dr Mark Birrell for giving me the opportunity to pursue my PhD within the Respiratory Pharmacology group and for their support and guidance throughout. I am grateful for the knowledge, opportunities and experiences I acquired at the National Heart and Lung Institute.

I would also like to thank members of the respiratory pharmacology team for their contributions and support, without which this work would not have been possible. A very special thank you to Dr Sara Bonvini, Dr Michael Wortley and Dr Eric Dubuis for your guidance, supervision and continuous support throughout this project. I would also like to thank Bilel Dekkak for always being of assistance in the lab and Dr Fisnik Shala for all his time carrying out single fibre experiments.

I am also grateful for the collaboration with Professor Jacky Smith and her team at Manchester University Hospital. Thank you to my PhD assessors Professor Omar Usmani and Professor Onn Min Kon for your suggestions and advice throughout the project.

I would also like to thank my friends at the NHLI, in particular Billy, Charlotte, Julia and Yasmine who have supported me over the years.

Finally, to my parents and the rest of my family and friends, thank you for your continuous support and encouragement to strive further.

This work was funded by the Wellcome Trust.

Statement of Originality

The work contained in this thesis is my own work, except where otherwise indicated and referenced appropriately.

In Chapter 3, mass spectrometry analysis of samples were performed by clinical collaborators in the Dynamic Omics team, AstraZeneca, Sweden.

In Chapter 4, vagus nerve experiments were performed by Dr Sara Bonvini, with my assistance and electrophysiological tracheal recordings were performed by Dr Eric Dubuis, with my assistance. Human vagal tissue dissection was performed by Dr Eric Dubuis.

In Chapter 5, single fibre experiments were performed by Dr Fisnik Shala.

In Chapter 6, the 2 months and 4 months chronic smoke exposure models were run by collaborators in the Bioscience In Vivo team, AstraZeneca, Sweden.

In Chapter 7, the collection of patient BALF and plasma samples and analysis using the SystemSure Plus ATP monitor were performed by clinical collaborators in Professor Jacky Smith's team at the University Hospital of South Manchester, UK.

Copyright Declaration

The copyright of this thesis rests with the author. Unless otherwise indicated, its contents are licensed under a Creative Commons Attribution-Non Commercial 4.0 International Licence (CC BY-NC). Under this licence, you may copy and redistribute the material in any medium or format. You may also create and distribute modified versions of the work. This is on the condition that: you credit the author and do not use it, or any derivative works, for a commercial purpose. When reusing or sharing this work, ensure you make the licence terms clear to others by naming the licence and linking to the licence text. Where a work has been adapted, you should indicate that the work has been changed and describe those changes. Please seek permission from the copyright holder for uses of this work that are not included in this licence or permitted under UK Copyright Law.

Table of Contents

Thesis Abstract 2

Acknowledgements 3

Statement of Originality 4

Copyright Declaration 5

List of Figures 11

List of Tables 13

List of Abbreviations 14

Chapter 1: Introduction 17

1.1 ATP 17

1.1.1 Introduction to ATP 17

1.1.2 Mechanisms of eATP release 19

1.1.3 Degradation of eATP 22

1.1.4 Measuring eATP 22

1.2 eATP in chronic respiratory diseases 24

1.2.1 eATP in asthma 26

1.2.2 eATP in COPD 27

1.2.3 eATP in IPF 30

1.2.4 eATP in chronic cough 31

1.3 Chronic cough 32

1.3.1 Prevalence of chronic cough 32

1.3.2 The cough reflex and airway sensory nerves 32

1.3.3 Activation of airway sensory nerves 34

1.3.4 Sensory nerve subtypes 35

1.3.5 Ion channels implicated in cough 37

1.3.6 Cough hypersensitivity 41

1.3.7 Assessment of the cough reflex 43

1.3.8 Cough therapies 46

1.4 Thesis plan 50

Chapter 2: General Methods 52

2.1 Animal samples 52

2.1.1 Animal husbandry 52

2.1.2 Animal sample collection and processing 52

2.2 Human samples 54

2.2.1 Human sample collection and processing 54

2.3 ATP measurements 55
2.3.1 ATPlite assay 55
2.3.2 ATP detection assay 56
2.3.3 Hygiena Ultrasnap Device 56
2.4 Electrophysiological recordings 58
2.4.1 *In vitro* isolated vagus nerve preparation 58
2.4.2 Isolated neuron recordings 60
Chapter 3: Developing Methods to Measure Extracellular ATP in Biological Samples 64
3.1 Rationale 64
3.1.1 Chapter hypothesis 65
3.1.2 Aims 65
3.2 Methods 65
3.2.1 ATPlite assay 66
3.2.2 ATP detection assay 66
3.2.3 Hygiena Device 66
3.2.4 Mass spectrometry Analysis 67
3.2.5 Data analysis 67
3.3 Results 68
3.3.1. Evaluating cross-talk of wells between different plate types using the ATPlite assay 68
3.3.2. Sensitivity of plate-based luminescent assays 69
3.3.3 Comparing the sensitivity of the ATP detection assay to the Hygiena Ultrasnap device 70
3.3.4 Effects of EDTA on BALF eATP measurements 71
3.3.5 Effects of different anticoagulants on plasma eATP measurements 73
3.3.6 Use of CD39 to confirm luminescent signals 74
3.3.7 Use of Mass spectrometry to measure ATP and metabolites 75
3.4 Discussion 77
Chapter 4: Investigating Extracellular ATP in Airway Sensory Nerves 81
4.1 Rationale 81
4.1.1 Chapter hypothesis 82
4.1.2 Aims 82
4.2 Methods 83
4.2.1 Calcium imaging of airway sensory nerves 83
4.2.2 *In vitro* isolated vagus nerve recordings 84
4.2.3 Electrophysiological tracheal recording of the Recurrent Laryngeal Nerve 85
4.3 Results 88

4.3.1. Effects of ATP on $[Ca^{2+}]_i$ in guinea pig jugular and nodose airway-specific ganglia neurons and single cell expression data 88
4.3.2. Effects of ATP concentration response on guinea pig vagus nerve 90
4.3.3 Effects of ATP on guinea pig recurrent laryngeal nerve 91
4.3.4 Effects of P2X3 antagonists on direct and indirect ATP-induced guinea pig vagus nerve depolarisation 93
4.3.5 Effects of P2X3 antagonists on direct and indirect ATP-induced firing of the recurrent laryngeal nerve 95
4.3.6 Effects of P2X3 antagonists on direct and indirect ATP-induced human vagus nerve depolarisation 97
4.4 Discussion 99
Chapter 5: Investigating the Effects of Ecto-nucleotidases on ATP-Induced Activation of Airway Sensory Nerves 103
5.1 Rationale 103
5.1.1 Chapter hypothesis 104
5.1.2 Aims 104
5.2 Methods 105
5.2.1 Cell Titer Glo assay 105
5.2.2 *In vitro* isolated vagus nerve recordings 105
5.2.3 *In vivo* single fibre recordings 106
5.2.4 Aerosol-induced conscious guinea pig cough model 107
5.3 Results 109
5.3.1. Concentration response of CD39 variants on 100µM ATP using a plate-based luminescent assay 109
5.3.2. Effects of CD39-His concentration response on ATP and GSK101 induced depolarisation of guinea pig vagus nerve 109
5.3.3. Effects of CD39-analogue concentration response on ATP and GSK101-induced depolarisation of guinea pig vagus nerve 110
5.3.4. Effects of CD39-analogue on single fibre firing in guinea pig Aδ- fibres 111
5.3.5. Effects of CD39-His on GSK101 induced cough in guinea pigs 112
5.3.6. Effects of CD39-His on BALF eATP levels in a conscious guinea pig cough model 113
5.3.7. Effects of CD39-His on plasma eATP levels in a conscious guinea pig cough model 114
5.4 Discussion 116
Chapter 6: Investigating Extracellular ATP in Animal Models of Respiratory Disease 118
6.1 Rationale 118
6.1.1 Chapter hypothesis 120
6.1.2 Aims 120
6.2 Methods 121

6.2.1 *In vivo* dose-ranging and timecourse experiments 121
6.2.2 Mouse cigarette smoke models 122
6.2.3 Acute Ozone exposure model 123
6.2.3 Poly I:C model 123
6.3 Results 125
6.3.1. Effects of intratracheal dose-response of CD39-His on BALF eATP levels in naïve mice 125
6.3.2. Effects of intratracheal dose-response of CD39-His on plasma eATP levels in naïve mice 126
6.3.3. Effects of intratracheal timecourse of CD39-His on BALF eATP levels in naïve mice 126
6.3.4. Effects of intranasal dose-response of CD39 on BALF eATP levels in naïve mice 127
6.3.5. Investigating effects of CD39-His in an acute 3-day cigarette smoke mouse model 128
6.3.6. eATP levels in acute and chronic mouse CS models 131
6.3.7. eATP levels in an acute ozone exposure model 132
6.3.8. eATP levels in a Poly I:C model 134
6.4 Discussion 136
Chapter 7: Measuring Extracellular ATP in Refractory and Unexplained Chronic Cough Patient Samples 142
7.1 Rationale 142
7.1.1 Chapter hypothesis 142
7.1.2 Aims 142
7.2 Methods 143
7.2.1 Cough Central clinical study 143
7.2.2 ANTHEM Clinical study 144
7.2.3 Human sample collection and processing 145
7.2.4 ATP measurements 146
7.3 Results 148
7.3.1 eATP measurements in Cough Central plasma samples 148
7.3.2 eATP measurements in male versus female Cough Central samples 149
7.3.3 Correlations between eATP measurements and cough counts in Cough Central 149
7.3.4 eATP measurements in ANTHEM BALF samples 150
7.3.5 eATP measurements in ANTHEM plasma samples 151
7.3.6 Comparing eATP measurements using the Cayman assay and Hygiena device 153
7.3.7 Correlations between eATP measurements and cough counts in the ANTHEM study 154
7.4 Discussion 155
Chapter 8: Summary and Future Studies 159
8.1 Summary of thesis 159

8.2 Limitations of this research and experimental challenges 166
8.3 Future work 167
8.3.1 Mass spectrometry analysis of eATP and metabolites in biological samples 167
8.3.2 Real-time imaging of ATP release *in vitro* 167
8.3.3 Real-time imaging of ATP release *in vivo* 167
8.3.4 Assessing ecto-nucleotidase activity in biological samples 168
8.3.5 Investigating levels of eATP in a systemic bleomycin model of IPF 171
8.3.6 BALF collection using bronchosorption 172
8.4 Concluding Remarks 173
Chapter 9: Bibliography 174
Appendix 194

List of Figures

Figure 1. 1 Schematic of purinergic signalling. 19
Figure 1. 2 Schematic of ATP release through vesicular exocytosis 20
Figure 1. 3 Basic structure of connexin and pannexin-based channels 21
Figure 1. 4 Purinergic signalling pathways involved in chronic respiratory diseases. 24
Figure 1. 5 P2X7 receptor mediated activation of the NLRP3 inflammasome. 25
Figure 1. 6 The cough reflex. 34

Figure 2. 1 Schematic of hygiena ultrasnap device eATP measurements. 57
Figure 2. 2 Schematic of isolated vagus nerve preparation 59
Figure 2. 3 DiI staining of airway specific nodose neurons. 61
Figure 2. 4 Brief summary of airway terminating-neuron isolation process and calcium imaging example trace. 63

Figure 3. 1 Evaluating the effects of different plate types on cross talk of luminescent signal between wells. 69
Figure 3. 2 ATP standard curve comparison between plate-based ATP luminescence assays. 70
Figure 3. 3 ATP standard curve comparison between the ATP detection assay and Hygiena device. . 71
Figure 3. 4 Comparing effects of spiked ATP concentration response (CR) in different BALF treatment groups using the ATP detection assay. 72
Figure 3. 5 Comparing effects of spiked ATP concentration response (CR) in different plasma treatment groups using the ATP detection assay. 74
Figure 3. 6 Comparing effects of CD39 on biological samples between different species. 75
Figure 3. 7 Mass spectrometry analysis of ATP and metabolites from Naïve rat samples. 76

Figure 4. 1 A schematic to demonstrate the set-up of the electrophysiological tracheal recording system as it records recurrent laryngeal nerve (RLN) activity. 86
Figure 4. 2 Effect of ATP and αβMe-ATP concentration response on intracellular calcium levels in guinea pig jugular and nodose airway neurons and purinergic receptor expression. 89
Figure 4. 3 Effect of ATP concentration response on guinea pig vagal nerve depolarisation. 90
Figure 4. 4 Effect of ATP, αβMe-ATP and GSK1016790A on guinea pig RLN activity. 92
Figure 4. 5 Effect of P2X3 antagonists on direct and indirect ATP-induced vagus nerve depolarisation in the guinea pig. 94
Figure 4. 6 Effect of P2X3 antagonist AF-353 against direct and indirect ATP-induced activation of the recurrent laryngeal nerve. 96
Figure 4. 7 Effect of P2X3 antagonists on- direct and indirect ATP-induced depolarisation of human vagus nerve. 97

Figure 5. 1 Schematic demonstrating ATP breakdown in the extracellular space by ecto-nucleotidase enzymes. CD39 metabolises ATP to AMP which is then further metabolised by CD73 to adenosine. 104
Figure 5. 2 Concentration response of CD39 enzymes on 100µM ATP. 109
Figure 5. 3 Concentration response of CD39-His on ATP and GSK101 induced depolarisation of guinea pig vagus nerve. 110
Figure 5. 4 Concentration response of CD39-analogue on ATP and GSK101 induced depolarisation of guinea pig vagus nerve. 111
Figure 5. 5 Effect of CD39 tools on TRPV4 induced Aδ-fibre firing in guinea pigs. 112

Figure 5. 6 Investigating the effect of CD39-His on GSK101 induced cough in guinea pigs. 113
Figure 5. 7 Investigating the effect of CD39-His on eATP in BALF from GSK101 induced cough in guinea pigs. 114
Figure 5. 8 Investigating the effect of CD39-His on eATP in plasma from GSK101 induced cough in guinea pigs. 115

Figure 6. 1 Effect of CD39-His dose-response on BALF eATP levels in naïve mice. 125
Figure 6. 2 Effect of CD39 dose-response on plasma eATP levels in naïve mice. 126
Figure 6. 3 Effect of CD39 timecourse on BALF eATP levels in naïve mice. 127
Figure 6. 4 Effect of CD39-His dosed intranasally and intratracheally on BALF eATP levels in naïve mice. 128
Figure 6. 5 Effect of CD39-His on BALF eATP levels and inflammatory markers in a 3-day CS model. 130
Figure 6. 6 eATP levels in an acute 3-day cigarette smoke model. 131
Figure 6. 7 eATP levels in chronic cigarette smoke models. 132
Figure 6. 8 eATP levels and inflammatory markers in an acute 3-hour ozone exposure model. 133
Figure 6. 9 eATP levels and inflammatory markers in a poly I:C exposure model. 135

Figure 7. 1 Cough Central plasma eATP measurements. 148
Figure 7. 2 Cough Central plasma eATP measurements in males versus females. 149
Figure 7. 3 Correlations between Cough Central plasma eATP measurements and 24 hour cough counts in chronic cough patient samples. 150
Figure 7. 4 ANTHEM BALF eATP measurements. 151
Figure 7. 5 ANTHEM plasma eATP measurements. 152
Figure 7. 6 Correlations between eATP measurements using the Cayman assay and Hygiena device. 153
Figure 7. 7 Correlations between ANTHEM eATP measurements and average daily cough counts in chronic cough patient samples. 154

Figure 8. 1 Schematic illustrating TRPV4 induced release of eATP activating P2X2/3 receptors. 162
Figure 8. 2 Assessing ATP breakdown over time using the Cayman ATP detection assay. 169
Figure 8. 3 Assessing ecto-nucleotidase activity in naïve mouse BALF. 170
Figure 8. 4 eATP levels in BALF from a systemic bleomycin model. 172

List of Tables

Table 1. 1 Drugs investigated for the treatment of chronic cough. 49

Table 2. 1 Imaging dyes maximum excitation and emission wavelengths. 61

Table 3. 1 Comparison of characteristics for the different luciferin/luciferase methods used to measure ATP. 78

Table 4. 1 Table of pIC50 of P2X3 antagonists on P2X3 and P2X2/3 receptors from the literature. ... 95

Table 7. 1 Recruitment criteria for Cough Central study. 144

Table 7. 2 Recruitment criteria for ANTHEM study. 145

List of Abbreviations

ACCP:	American College of Clinical Pharmacy
ADP:	Adenosine Diphosphate
AITC:	Allyl Isothiocynate
AM:	Acetoxymethyl
AMP:	Adenosine Monophosphate
ATP:	Adenosine Triphosphate
AUC:	Area Under the Curve
BALF:	Bronchoalveolar Lavage Fluid
cAMP:	Cyclic Adenosine Monophosphate
CC:	Chronic Cough
CD39:	Ectonucleotide triphosphate diphosphohydrolase 1
CD39-His:	Ectonucleotide triphosphate diphosphohydrolase 1 – Histidine tag
CD39L1:	Ectonucleoside triphosphate diphosphohydrolase 2
CD39L3:	Ectonucleoside triphosphate diphosphohydrolase 3
CD39-Mut:	Ectonucleotide triphosphate diphosphohydrolase 1 – Mutant
CD73:	Ecto-5’-nucleotidase
CNS:	Central Nervous System
COPD:	Chronic Obstructive Pulmonary Disease
CQLQ:	Cough Quality of Life Questionnaire
CR:	Concentration Response
CS:	Cigarette Smoke
CV:	Conduction Velocity
CVA:	Cough Variant Asthma
DAMP:	Danger Associated Molecular Pattern
DiI:	DiIC18 (3) (1,1’-dioctadecyl-3,3,3’,3’-tetramethyl-indocarbocyanine perchlorate
DMSO:	Dimethyl Sulfoxide
DNA:	Deoxyribose Nucleic Acid
eATP:	Extracellular Adenosine Triphosphate
ECS:	Extracellular Solution
EDTA:	Ethylenediamine Tetraacetic Acid
ED50:	Capsaicin concentration evoking at least half of the Emax
Emax:	Maximum number of coughs evoked by any capsaicin concentration
ENTPDase:	Ectonucleoside triphosphate diphosphohydrolase

ERS:	European Respiratory Society
eTRec:	Electrophysiological tracheal recording
EU:	European Union
FDA:	Food and Drug Administration
FEV_1:	Forced Expiry Volume in 1 second
fMRI:	Functional Magnetic Resonance Imaging
GPCR:	G Protein Coupled Receptor
GSK101:	GSK1016790a
HBSS:	Hanks Balanced Salt Solution
HV:	Healthy Volunteer
ICS:	Inhaled Corticosteroids
i.n:	Intranasal
i.p:	Intraperitoneal
i.t:	Intratracheal
IPF:	Idiopathic Pulmonary Fibrosis
IIAM:	International Institute for the Advancement of Medicine
IL:	Interleukin
ILD:	Interstitial Lung Disease
KH:	Krebs-Henseleit
LLOD:	Lower Limit of Detection
LPS:	Lipopolysaccharides
MEU:	Medicines Evaluation Unit
MFT:	Manchester University National Health Service Foundation Trust
MHRA:	Medicines and Healthcare products Regulatory Agency
MMP-9:	Metalloproteinase-9
NLRP3:	Nucleotide-Binding Domain, Leucine-Rich–Containing Family, Pyrin Domain–Containing-3
nTS:	Nucleus of the Solitary Tract
PAS:	Papain Activation Solution
PAMP:	Pathogen-Associated Molecular Mattern
PCR:	Polymerase Chain Reaction
PBS:	Phosphate Buffered Saline
Poly IC:	Polyinosinic:Polycytidylic Acid
RAR:	Rapidly Adapting Receptor

RCC:	Refractory Chronic Cough
RLN:	Recurrent Laryngeal Nerve
RLU:	Relative Light Unit
RNA:	Ribonucleic Acid
ROS:	Reactive Oxygen Species
RT:	Room Temperature
RTPCR:	Reverse Transcription Polymerase Chain Reaction
RUCC:	Refractory Unexplained Chronic Cough
Saline:	0.9% w/v sodium chloride
SAM:	Synthetic Absorptive Matrices
SAR:	Slowly Adapting Receptor
S.E.M:	Standard Error of the Mean
SNARE:	Soluble N-Ethylmaleimide-Sensitive-Factor Attachment Receptor
SLN:	Superior Laryngeal Nerve
TIMP-1:	Tissue Inhibitor of Matrix Metalloproteinase-1
TLR3:	Toll-like receptor 3
TRP:	Transient Receptor Potential
UCC:	Unexplained Chronic Cough
ULOD:	Upper Limit of Detection
VGSC:	Voltage Gated Sodium Channel
VNUT:	Vesicular Nucleotide Transporter
WT:	Wild Type
W/V:	Weight/Volume
αβ-MeATP:	αβ-MethyleneATP

Chapter 1: Introduction

1.1 ATP

1.1.1 Introduction to ATP

Adenosine 5'-triphosphate (ATP) is a molecule that can be found in all living cells and intracellular ATP plays a fundamental role in cellular metabolism and energetics (Nirody et al., 2020). Intracellular ATP can be found in the millimolar range and is often referred to as the "energy currency" of the cell whereby the breakdown of ATP provides readily releasable energy which is used for a broad range of cellular functions including cell growth and division, metabolism, and cell signalling (Nirody et al., 2020).

As well as providing energy for the cell, ATP can be released from cells into the extracellular space under both physiological and pathophysiological conditions. This extracellular ATP (eATP) is ubiquitously used for cell-to-cell communication where it functions as an autocrine and paracrine agent through activation of P2 purinergic cell-surface receptors. eATP is also part of the family of pathogen-associated molecular patterns (PAMPs) and damage-associated molecular patterns (DAMPs) which exerts effects on innate and adaptive immune responses by pro-actively modulating inflammatory processes (Newton and Dixit, 2012, Tang et al., 2012). For example, cell death can be associated with the release of large amounts of eATP as a 'danger' and 'find me' signal. There is a growing amount of research which implicates eATP in the pathophysiology of a range of chronic respiratory diseases and therefore the focus of this thesis will be on the role eATP in chronic respiratory diseases (Burnstock et al., 2012, Jacobson et al., 2023, Pelleg, 2021).

eATP exerts its effects through activation of P2 purinergic cell-surface receptors which contributes to the induction of immune responses in damaged tissues through recruitment and activation of a range of inflammatory immune cell types including eosinophils, mast cells, dendritic cells, alveolar macrophages and phagocytes resulting in a heightened inflammatory response (Idzko et al., 2007, Ferrari et al., 2020, Gao and Jacobson, 2017, Li et al., 2020, Iyer et al., 2009, Trautmann, 2009). Given the signalling effects of eATP, concentrations of eATP is tightly regulated in the extracellular space within the micromolar range through rapid degradation of eATP to adenosine 5'-diphosphate (ADP) and adenosine by ecto-enzymes, primarily ectonucleoside triphosphate diphosphorylase-1 (CD39) and ecto-5'-nucleotidase (CD73) (Zimmermann et al., 2012).

P2 purinergic cell-surface receptors can be divided into two families; metabotropic P2Y receptors which are seven trans-cell membrane domain G-protein coupled receptors (GPCRs) and ionotropic P2X receptors which are trans-cell membrane cationic channels (Burnstock et al., 2012). P2X receptors are ATP-gated ion channels permeable to calcium, sodium and potassium ions. There are eight P2Y receptors and seven homotrimeric P2X receptors (P2X1-7). Multiple heterotrimeric assemblies comprising of these P2X subunits have been described such as P2X2/P2X2/3 heterotrimers (Saul et al., 2013).

Given the role of eATP in respiratory diseases, bioinformatic studies on RNA expression have shown that P2X1, P2X4 and P2X7 are the mostly highly expressed P2X receptors in human lung and airway tissues. Protein expression data showing higher levels of P2X4 and P2X7 expression also supports this (Saul et al., 2013). The role of these receptors in respiratory disease is outlined in sections 1.2 and 1.3. The breakdown of eATP by ecto-enzymes into ADP and adenosine are also involved in purinergic signalling whereby ADP can activate metabotropic P2Y receptors and adenosine can activate P1 purinergic cell-surface receptors (Figure 1.1).

These receptors are expressed by a variety of cell types in the lungs, the activation of which can be associated with the development and pathology of a number of chronic respiratory diseases including asthma, chronic obstructive pulmonary disease (COPD) and idiopathic pulmonary fibrosis (IPF) (Burnstock, 2018). Purinergic signalling pathways specific to different chronic respiratory diseases are outlined in section 1.2. These diseases represent a significant global healthcare burden, where new safe and effective therapies are required. The focus of this thesis will be on eATP and its role in chronic respiratory diseases, particularly chronic cough which is a common symptom across respiratory diseases.

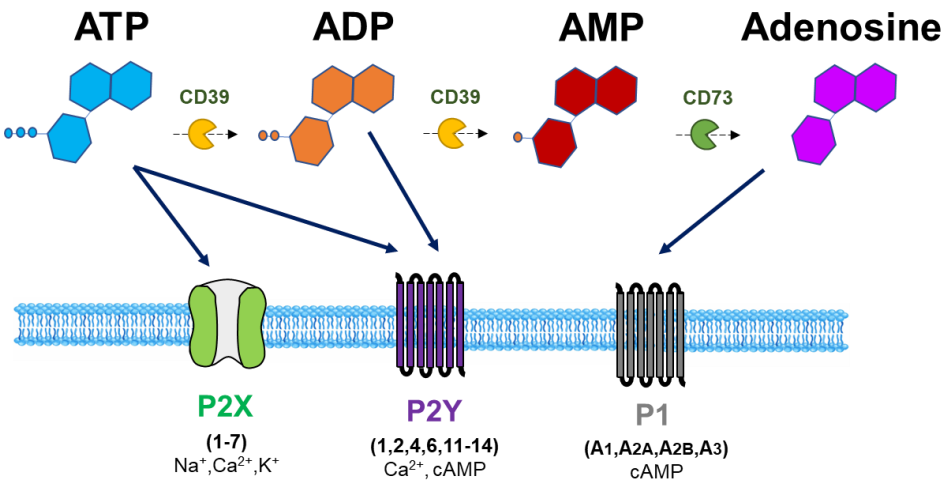


Figure 1. 1 Schematic of purinergic signalling.

eATP can activate P2X and P2Y receptors causing changes in intracellular ion concentrations and/or levels of cyclic adenosine monophosphate (cAMP). ATP can by metabolised by the ecto-nucleotidases CD39 and CD73 into ADP, AMP and adenosine. ADP can activate P2Y receptors whilst adenosine activates P1 receptors to alter intracellular cAMP levels. Figure adapted from (Thompson et al., 2021).

1.1.2 Mechanisms of eATP release

ATP is released from various cell types under physiological and pathophysiological conditions in response to different stimuli or micro-environmental conditions. For example, increased eATP has been found in inflammatory conditions such as in the lungs of COPD patients and in mouse models of smoke-induced acute lung inflammation and emphysema (Baxter et al., 2014, Lázár et al., 2008, Mortaz et al., 2009, Cicko et al., 2010, Jacobson et al., 2023). A variety of different cell types in the lungs have been linked to increased ATP release in different chronic respiratory diseases (Ryan et al., 2016, Bonvini et al., 2020, Rahman et al., 2018, Baxter et al., 2014) leading to the activation of various purinergic receptors involved in inflammatory and neuronal responses. Cell death can lead to non-specific release of eATP. However, it can also be released into the extracellular space in a controlled manner via exocytosis, large membrane pores and specific trans-cell membrane ion channels (Taruno, 2018, Vultaggio-Poma et al., 2020).

Controlled release mechanisms include vesicular exocytosis and channel-mediated release of ATP via connexin or pannexin hemichannels (Dosch et al., 2018). In inflammatory conditions, the release of ATP allows activation of inflammatory immune cells such as macrophages, neutrophils and endothelial cells to tightly regulate autocrine and paracrine responses (Kim et al., 2018, Shishikura et al., 2016, Wang et al., 2014).

The biochemical properties of eATP make it an efficient damage signalling molecule as it is rapidly released via vesicular exocytosis or cellular pores upon cell activation. ATP is also water-soluble and can freely diffuse in the extracellular environment as it contains negatively charged phosphate residues (Di Virgilio and Vuerich, 2015). Additionally, there is a high concentration gradient between eATP in the micromolar range and intracellular ATP in the millimolar range. This creates a strong signal to noise ratio with very low background noise making the extracellular environment hypersensitive to even the smallest changes in eATP (Di Virgilio and Vuerich, 2015).

1.1.2.1 Active ATP release via vesicular exocytosis

Specialised cytosolic vesicles within cells can store ATP that is rapidly released through fusion of the vesicle with the plasma membrane (Martens and McMahon, 2008, Moriyama et al., 2017). ATP storage within these vesicles are dependent on vesicular nucleotide transporters (VNUT) which are secondary active transporters ensuring the accumulation of cytosolic ATP into the vesicles in a chloride-dependent manner. This is driven by an electrochemical proton gradient where vesicles are positively charged (Sawada et al., 2008, Miyaji et al., 2011). The mechanisms of vesicular exocytosis have been shown to be dependent on intracellular calcium levels and the SNARE (soluble N-ethylmaleimide-sensitive-factor attachment receptor) family of proteins which mediates membrane fusion as seen in macrophages (Imura et al., 2013, Südhof and Rothman, 2009). The stages of ATP release through vesicular exocytosis are illustrated in figure 1.2.

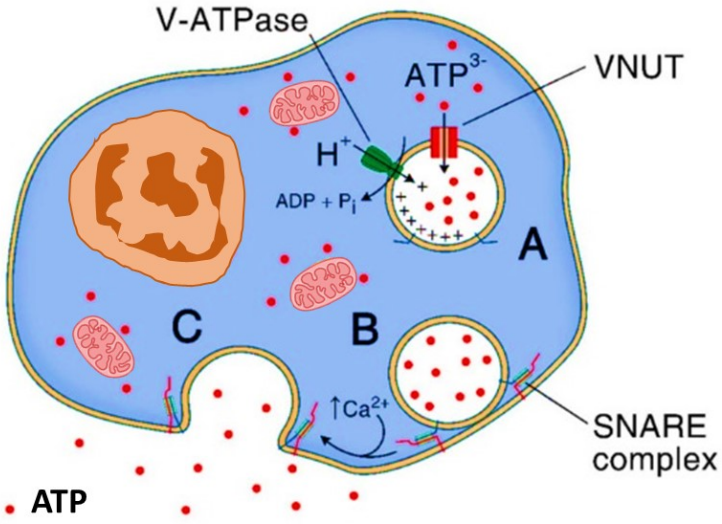


Figure 1. 2 Schematic of ATP release through vesicular exocytosis

(A) V-ATPase generates a proton gradient as a driving force to active transport ATP inside vesicles through the vesicular nucleotide transport (VNUT). (B) SNARE zippering occurs spontaneously. (C) Increased intracellular calcium concentrations causes fusion of the two membranes mediated by

SNARE proteins leading to the release of ATP into the extracellular space. Figure adapted from (Dosch et al., 2018).

1.1.2.2 Active ATP release via pore-forming channels

In addition to vesicular exocytosis, inflammatory cells release ATP into the extracellular space via connexin hemichannels or pannexin channels, primarily connexin-43 and pannexin-1 (Junger, 2011). Connexin proteins can form both gap junctions and hemichannels, whereas pannexin proteins can only form hemichannels (Sosinsky et al., 2011). Both channels mediate the release of small molecules in the extracellular space, including ATP, glutamate, prostaglandins and other molecules including the influx of ions such as sodium and calcium as illustrated in figure 1.3 (Penuela et al., 2013, Baroja-Mazo et al., 2013). Gating of both these channels are regulated by changes in transmembrane voltage, intracellular and extracellular calcium concentrations, mechanical strain and post-translational modifications (Retamal et al., 2007, Lopez et al., 2016, Wang et al., 2013).

Pannexin-1 channels are widely expressed in the airways and lungs and has been shown to play a role in ATP release (Penuela et al., 2013). For example, in cough, the activation of airway sensory nerves following stimulation of TRPV4 receptors has been shown to cause ATP release via pannexin-1 channels, outlined in section 1.3.5.2 (Bonvini et al., 2016).

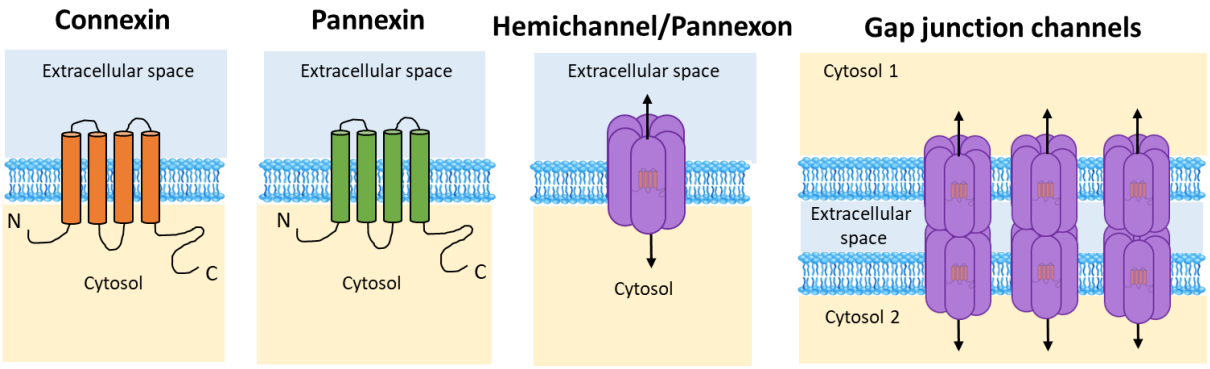


Figure 1. 3 Basic structure of connexin and pannexin-based channels

Both connexins and pannexins have four transmembrane domains. Hemichannels are formed of six connexin subunits around a central pore whereas pannexons are composed of six pannexin subunits. Hemichannels can also dock each other to form functional cell-cell channels called gap junction channels. Under resting conditions, hemichannels and pannexons remain preferentially closed, but they may be activated by diverse physiological and pathological conditions. Figure adapted from (Abudara et al., 2018).

1.1.3 Degradation of eATP

Extracellular signalling molecules such as eATP and other extracellular nucleotides and nucleosides are controlled by a network of cell surface receptors known as ecto-nucleotidases. These tightly regulate local concentrations of these molecules by ectonucleoside triphosphate diphosphohydrolases (ENTPDases). mRNA expression of several ENTPDases have been reported in human lungs and bronchial epithelial cells including ENTPDase-1 (CD39), ENTPDase-2 (CD39L1) and ENTPDase-3 (CD39L3) (Chadwick and Frischauf, 1998, Burch and Picher, 2006). Studies have shown that mRNA expression of CD39 and CD39L3 increases along the human airway towards the alveoli, though expression levels of CD39 are much higher compared to CD39L3 (Burch and Picher, 2006).

eATP is normally highly regulated in the extracellular environment on the cell surface by CD39 and CD73, which rapidly metabolises ATP to AMP and AMP to adenosine respectively (Zimmermann et al., 2012). However, for patients with chronic lung diseases including asthma, COPD and IPF, eATP is elevated in their lungs suggesting an increased production or breakdown dysregulation of eATP (Idzko et al., 2007, Hlapčić et al., 2019, Riteau et al., 2010). This is supported by a study that showed an attenuation of CD39 expression in the lung tissue of patients with COPD, which could be responsible for pulmonary ATP accumulation (Aliagas et al., 2018).

1.1.4 Measuring eATP

The most common method for measuring ATP is based on the biochemical luciferase-luciferin reaction whereby luciferase catalyses the oxidation of luciferin to oxyluciferin in the presence of ATP and oxygen. This was discovered in 1947 whereby luciferin and luciferase were isolated from firefly tails and were shown to be responsible for the production of light (McElroy, 1947).

For decades, luminescence-based assays have been the commonly used method to measure bulk ATP concentrations in extracellular solutions (Schwiebert and Zsembery, 2003). The oxyluciferin produced by this reaction is a highly unstable compound that emits light in the form of luminescence. The experimental premise is that levels of eATP in the sample are proportional to the amount of luminescence measured. The reaction occurs as follows:

$$\textbf{ATP + D-Luciferin + } O_2 \xrightarrow[Mg^{2+}]{\text{Luciferase}} \textbf{Oxyluciferin + AMP + } CO_2 \textbf{ + Pyrophosphate + Light}$$

Commercially available assays utilising this reaction have been used to measure eATP in biological samples as described in section 1.2, the most common used in the literature being the ATPlite kit assay by PerkinElmer. Using this assay, increased eATP has been reported in the lungs of asthma, COPD and

IPF patients (Idzko et al., 2007, Lommatzsch et al., 2010, Riteau et al., 2010). However, across the literature, levels of eATP measured are variable and range from picomolar to micromolar concentrations. Furthermore, different techniques, methods and chelating agents are used for the retrieval and assessment of eATP in these biological samples which differ in sensitivity and reliability as they are not always reproducible. Accurately measuring eATP is also challenging as it is highly regulated in the extracellular environment by ecto-nucleotidases (see section 1.1.3).

Modification of these assays have also been used to visualise ATP release from individual cells in real-time using microscopy (Takahara et al., 2014, Takahashi et al., 2017). However, these methods are not standardised and are not easily reproducible as the formulation of luciferase-luciferin mixtures used are not known. Nonetheless this may be a promising approach to identifying ATP release from cells in sensory nerves and the airways.

1.2 eATP in chronic respiratory diseases

Increased eATP in the lungs of patients with chronic respiratory diseases leads to the activation of purinergic receptors widely expressed by different cell types in the lungs (Pelleg et al., 2016). Activation of these purinergic receptors play a mechanistic role in the pathophysiology of a number of pulmonary disorders as illustrated in figure 1.4.

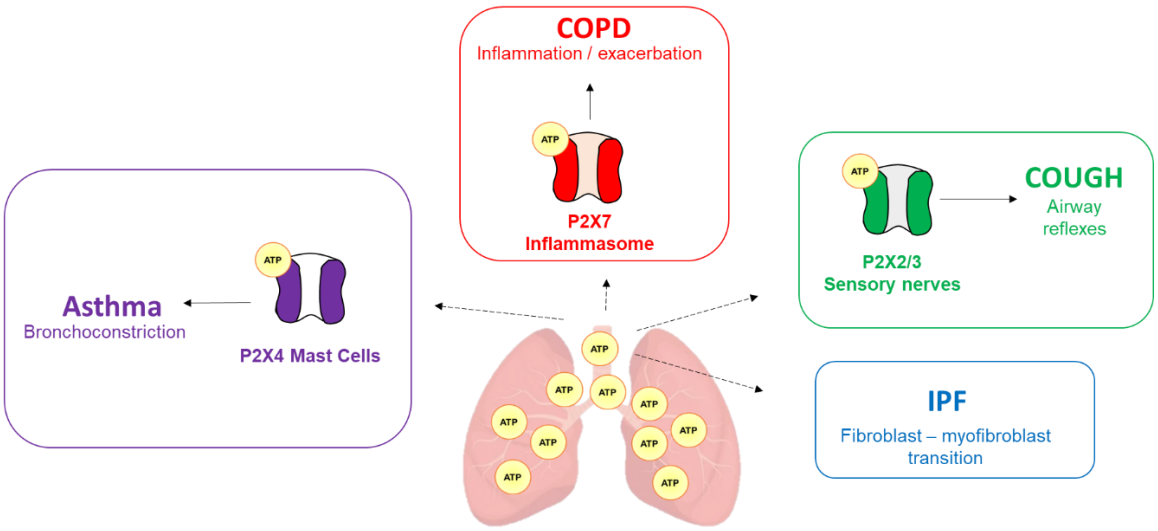


Figure 1. 4 Purinergic signalling pathways involved in chronic respiratory diseases.

eATP can stimulate different purinergic receptors involved in the pathogenesis of chronic respiratory diseases such as P2X4 receptors involved in asthma and bronchoconstriction, P2X7 involved in inflammation and exacerbations observed in COPD, P2X2/3 receptors involved in cough and airway reflexes and the transition of fibroblasts to myofibroblasts in IPF (Bonvini et al., 2016, Baxter et al., 2014, Bonvini et al., 2020, Rahman et al., 2018).

This section will focus on eATP in asthma, COPD and IPF which are all characterised by pulmonary inflammation. There is an unmet clinical need for the development of novel effective therapies for these chronic respiratory diseases. The involvement of eATP and its purinergic signalling pathways involved in the pathogenesis of these conditions could be targeted for the development of novel effective therapies. Chronic cough is a common symptom of these diseases and the role of eATP in chronic cough will also be highlighted in section 1.2.4 and in section 1.3.

There is growing amounts of research to suggest that the multimeric protein complex referred to as the nucleotide-binding domain, leucine-rich–containing family, pyrin domain–containing-3 (NLRP3) inflammasome plays a key role in pulmonary inflammation observed in these chronic respiratory

diseases (Leszczyńska et al., 2022). Importantly, eATP is a key damage-associated molecular pattern (DAMP) that has been shown to induce formation of the NLRP3 inflammasome by signalling through the purinergic P2X7 cell surface receptor (Idzko et al., 2014, Di Virgilio et al., 2017, Ferrari et al., 2006). Stimulation of the NLRP3 inflammasome leads to the cleavage of pro-caspase 1 into its active form (Martinon et al., 2002). Caspase-1 is an enzyme that cleaves the pro-forms of two potent pro-inflammatory cytokines interleukin-1β (IL-1β) and interleukin-18 (IL-18) as illustrated in Figure 1.5. These cytokines are then released from cells and play a key role in modulating immune responses and are involved in signalling pathways that promote infiltration of inflammatory cells into the lungs (Birrell and Eltom, 2011). Further details highlighting the role of eATP, the NLRP3 inflammasome and other purinergic signalling pathways involved in the pathogenesis of asthma, COPD and IPF can be found in the subsequent sections.

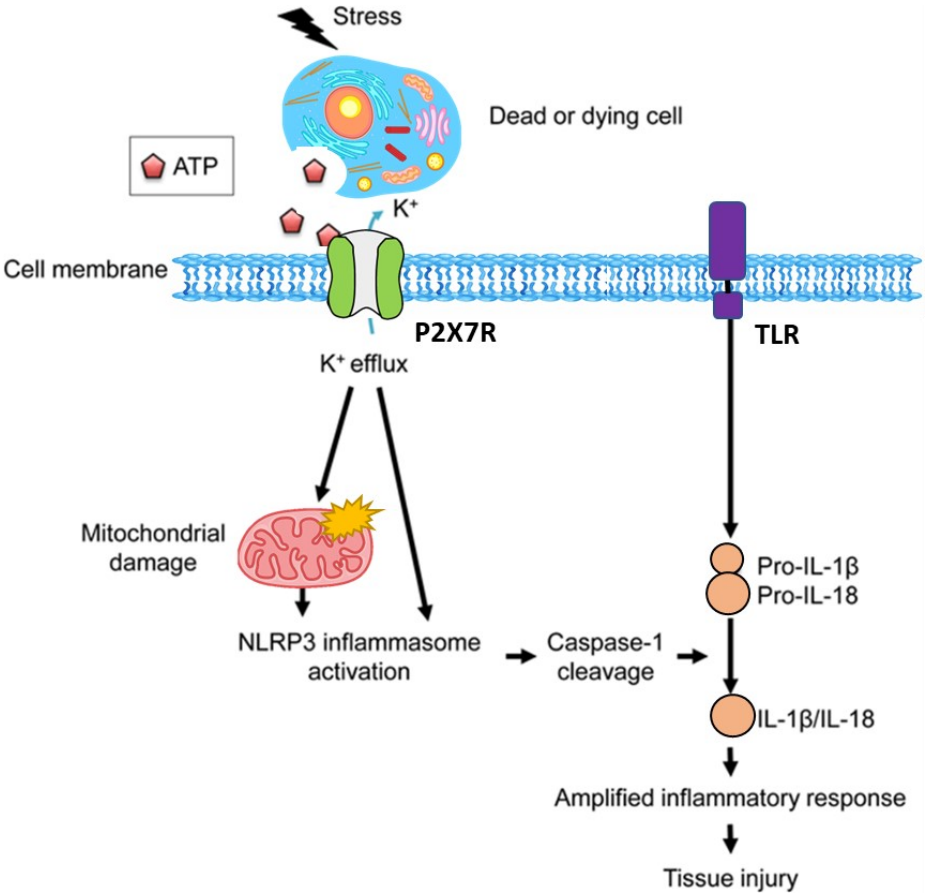


Figure 1. 5 P2X7 receptor mediated activation of the NLRP3 inflammasome.

An overview of the signalling cascade associated with P2X7 induced activation of the NLRP inflammasome in macrophages. High concentrations of eATP in the extracellular space can potently stimulate P2X7 receptors on macrophages triggering potassium efflux from the cytosol to the

extracellular space. This can activate the NLRP3 inflammasome directly or indirectly by inducing reactive oxygen species (ROS) produced from the mitochondria. Once the inflammasome is activated it leads to the maturation and release of the pro-inflammatory cytokines IL-1β and IL-18 which further amplifies the inflammatory response. Figure adapted from (Wang et al., 2021).

1.2.1 eATP in asthma

Asthma is a chronic inflammatory disease of the airways which is characterised by airflow obstruction and symptoms such as cough, shortness of breath, wheezing and tightness of the chest (Lemanske and Busse, 2003, Bateman et al., 2008). Asthma is a global health problem that affects over 300 million people worldwide carrying a significant morbidity and mortality burden to society (Wong et al., 2023, Stern et al., 2020). Although inhaled corticosteroids (ICS) are the gold standard therapy used to control asthma, a subset of patients have persistent symptoms despite high doses of ICS (Samitas et al., 2017). This highlights the need for the development of novel treatments, particularly for patients who are steroid insensitive.

Studies have shown that eATP and the product of its enzymatic breakdown, adenosine, plays a role in the pathophysiology of asthma through its effects on various cell types in the lungs (Adriaensen and Timmermans, 2004). Increased levels of eATP were found in the bronchoalveolar lavage fluid (BALF) of patients with asthma and in mouse models of allergic asthma following allergen challenge (Idzko et al., 2007).

In these asthmatic mouse models, disease features such as Th2 and Th17 cytokine production and bronchospasm were reduced in mice treated with the ATP-hydrolysing enzyme apyrase or purinergic P2 receptor antagonists (Idzko et al., 2007). Additionally, application of exogenous ATP was shown to enhance Th2-type sensitisation to inhaled antigens in mice highlighting the role of ATP in the recruitment of Th2-inducing lung myeloid dendritic cells to mediastinal lymph nodes (Idzko et al., 2007).

Allergic asthma has also been associated with activation of the NLRP3 inflammasome which can be triggered by eATP and leads to the subsequent release of cytokines such as IL-1β. Studies using NLRP3 gene-deficient (*Nlrp3-/-*) mice in mouse models of allergic asthma were shown to have reduced infiltration of inflammatory immune cells and levels of IL-1β measured in the BALF compared with wildtype (WT) mouse models of allergic asthma (Besnard et al., 2011). Furthermore, the levels of inflammatory interleukins dependent on the NLRP3 inflammasome (IL-1β and IL-18) were found to be

lower in the BALF of asthma models treated with the steroid Dexamethasone, one of the main ICS used for the treatment of asthma, compared to non-treated models (Guan et al., 2020). Both ATP and adenosine have also been shown to have pro-asthmatic roles within airway epithelia through stimulation of mucin production (Kim et al., 2018, McNamara et al., 2004). Adenosine has also been shown to upregulate fibronectin expression and may therefore play a role in airway remodelling (Roman et al., 2006). Increased levels of eATP were also found in BALF samples from a mouse model of neutrophilic asthma following allergen challenge which correlated with neutrophil counts and the production of the cytokine interleukin-17 (Zhang et al., 2017).

Eosinophils also play a role in regulating local immune and inflammatory responses in asthma (Fulkerson and Rothenberg, 2013). ATP through activation of P2Y2 receptors was shown to increase intracellular calcium levels in human eosinophils (Mohanty et al., 2001). This is associated with the chemotactic action of platelet-derived ATP on eosinophils (Burgers et al., 1993).

Mast cells are also key players in the inflammatory response and can be activated by ATP and adenosine to release a wide variety of inflammatory mediators such as histamine (Gao and Jacobson, 2017). In non-allergic asthma, studies have shown that activation of TRPV4 on human airway smooth muscle leads to the release of ATP which activates P2X4 on human lung mast cells. This induces the release of cysteinyl leukotrienes, a family of inflammatory lipid mediators involved in bronchoconstriction (Bonvini et al., 2020). Clinical studies have also shown that asthmatic patients are hypersensitive to aerosolised ATP which increases breathing difficulty in people with asthma compared to healthy non-smokers and has potent effects on bronchoconstriction (Basoglu et al., 2005). Taken together, these data demonstrate a role for ATP in the pathophysiology of asthma which may be an alternative target in the development of novel therapies.

1.2.2 eATP in COPD

COPD affects approximately 300 million people worldwide and is the third leading cause of death globally (Ruvuna and Sood, 2020, Barnes et al., 2015). COPD encompasses several heterogenous lung conditions associated with chronic inflammation affecting the lung parenchyma and peripheral airways resulting in persistent and progressive airflow limitations. Features of COPD include emphysema, characterised by enlargement of the alveoli and destruction of alveolar walls (Barnes, 2014). Patients diagnosed with COPD typically present with cough, shortness of breath, mucus production and exacerbations of these symptoms (Barnes et al., 2015). Cigarette smoking is the most common causative risk factor for the development of COPD as it results in chronic inflammation of the

peripheral airways (Barnes, 2014). This is characterised by an increase in inflammatory immune cells in the lungs such as neutrophils, macrophages and lymphocytes which increase with disease progression (Hogg, 2004).

Many patients with COPD have poorly controlled symptoms and are at risk of exacerbations and death (Abbafati et al., 2020). Bronchodilators such as anticholinergics which block muscarinic M3 receptors and long acting β2-adrenergic receptor agonists are commonly used to treat some of the symptoms of COPD (Barnes et al., 2015). However, these only reduce exacerbations in COPD patients by approximately 20% (Barnes, 2013). To date there are currently no therapies which affect the underlying inflammation, disease progression or improve mortality in patients with COPD highlighting the need for novel effective therapies.

Cigarette smoke exposure is the most common underlying mechanism for the development of COPD, with the majority of COPD patients current or former smokers (Hlapčić et al., 2019). Cigarette smoke exposure is commonly used in the development of COPD animal models as it is shown to induce features of COPD including lung inflammation marked by increases in inflammatory immune cells and pro-inflammatory cytokines into the lungs, increased protease activity, apoptosis, oxidative stress and emphysema (Wright et al., 2008, Jones et al., 2017, Vlahos and Bozinovski, 2014).

Importantly, increased levels of eATP have been found in BALF of COPD patients and animal models of COPD (Mortaz et al., 2009, Cicko et al., 2010, Baxter et al., 2014, Lommatzsch et al., 2010, Eltom et al., 2014). Elevated eATP has also been measured in the blood of COPD patients which positively correlates with disease severity (Hlapčić et al., 2019). Studies have also shown that gene expression of ATP-degrading enzymes such as CD39 are downregulated in the lung tissue of COPD patients which may contribute to increased eATP in diseased lungs (Aliagas et al., 2018, Careta et al., 2019). Clinical studies have also shown that COPD patients have a hypersensitive response to aerosolised ATP which induces acute bronchoconstriction (Basoglu et al., 2005). A more recent study comparing patients with COPD, smokers and healthy non-smokers found that aerosolised ATP provoked a more pronounced cough, reduced forced expiry volume in 1 second (FEV_1) by ≥20% and difficulty breathing in people with COPD and smokers compared to healthy volunteers (Basoglu et al., 2015). In this study 90% of all participants coughed in response to aerosolised ATP, with 81% reporting of throat irritation and 29% sputum production (Basoglu et al., 2015).

Pre-clinical studies found that BALF from mouse models of smoke-induced lung inflammation had increased eATP (Mortaz et al., 2009, Cicko et al., 2010). Cigarette smoke exposure in human bronchial epithelial cells was also shown to induce ATP release, which was blocked using a TRPV4, TRPV1 and pannexin-1 blocker (Baxter et al., 2014). eATP-induced activation of P2Y2 receptors is also important in mediating the recruitment of macrophages and neutrophils to the site of inflammation where damaged cells are being phagocytosed (Idzko et al., 2014). Studies have shown an upregulation in P2Y receptor subtypes in neutrophils, macrophages, and lung tissues from animal models with cigarette-smoke induced lung inflammation (Cicko et al., 2010, Mortaz et al., 2010).

Ozone is another major pollutant which is associated with airway inflammation and is used to develop COPD models (Sokolowska et al., 2019). Studies have shown that human lung epithelial cells release eATP during ozone exposure (Kong et al., 2021). *In vivo* studies have also shown that ozone exposure in mice induces airway hyperreactivity and neutrophilic inflammation in the lungs where increased eATP levels have been reported (Kong et al., 2021).

Respiratory viruses are also a major cause of COPD development and exacerbations. Polyinosinic:polycytidylic acid (Poly I:C) is a synthetic analogue of dsRNA and a toll-like receptor 3 (TLR3) agonist commonly used to mimic viral infection. TLR3 is a member of the toll-like receptor family of pattern recognition receptors involved in activating the innate immune system. Pre-clinical *in vitro* studies have shown that Poly I:C causes increased eATP release and mucus release from human bronchial epithelial cells (Shishikura et al., 2016). *In vivo* studies have also shown that Poly I:C exacerbates airway inflammation and remodelling in cigarette smoke exposed mice (Mei et al., 2022).

eATP is known to trigger the NLRP3 inflammasome through activation of P2X7 which is associated with inflammation observed in COPD. P2X7 receptor expression was found to be upregulated in BALF macrophages and blood neutrophils from patients with COPD (Lommatzsch et al., 2010). Gene expression analysis of patients with COPD also reported an upregulation of genes related to an inflammatory profile, particularly IL-1β which was upregulated in small airway epithelial cells and positively correlated with disease severity (Yi et al., 2018). Several studies have also shown that levels of IL-1β and IL-18 in the BALF and serum of COPD patients and COPD animal models were significantly elevated compared to healthy controls (Wang et al., 2018, Churg et al., 2009, Baxter et al., 2014, Petersen et al., 2007, Lucey et al., 2002). *In vitro* models of COPD also suggest that the NLRP3 inflammasome is involved in the development of COPD as a pulmonary adenocarcinoma derived cell

line treated with cigarette-smoke extract showed increasing levels of the NLRP3 protein and IL-1β production in a dose-dependent manner (Nachmias et al., 2019).

Taken together, these data suggest a role for eATP and purinergic signalling in the development of COPD. Therapies aimed at modulating eATP and its signalling pathways may therefore be an alternative target for the development of novel effective therapies that address the underlying mechanisms driving chronic inflammation in the pathophysiology of COPD.

1.2.3 eATP in IPF

IPF is one of the most common Interstitial Lung Diseases (ILD) which accounts for 17 to 37% of ILD diagnoses (Ley and Collard, 2013). IPF is characterised by progressive scarring of the lungs and symptoms include a dry, non-productive cough, dyspnoea on exertion and inspiratory crackles on lung examination (Munchel and Shea, 2021). Mechanisms underlying the pathogenesis of IPF is thought to be driven by abnormal healing responses following damage to epithelial cells. This damage can be caused by endogenous insults or by external sources such as exposure to asbestos, cigarette smoke or viruses (Daccord and Maher, 2016, Kropski et al., 2013). This results in an overgrowth of fibroblasts that migrate to areas of injury and transition to myofibroblasts. These myofibroblasts secrete excessive amounts of extracellular matrix proteins which results in a loss of lung architecture, fibrosis, progressive scarring of the lungs and subsequent respiratory dysfunction (Daccord and Maher, 2016). Pirfenidone and Nintedanib are current therapies used to slow down disease progression in IPF (Raghu et al., 2022). However, there is an unmet clinical need for the development of therapies which can halt or reverse the pathophysiological mechanisms driving IPF.

A number of studies have shown that ATP and P2X7 mediate lung inflammation and fibrosis. Increased eATP was found in BALF of IPF patients and similar increases were found in a murine bleomycin model of lung injury where increased BALF neutrophils and markers of fibrosis were observed (Riteau et al., 2010). The role of P2X7 in the pathogenesis of fibrosis in this model was highlighted in studies using P2X7 receptor knock-out mice. In these mice, there was a significant reduction in BALF neutrophils and markers of tissue fibrosis such as lung collagen content, matrix-remodelling proteins metalloproteinase-9 (MMP-9), and tissue inhibitors of matrix metalloproteinase-1 (TIMP-1) (Riteau et al., 2010). The NLRP3 inflammasome which can be activated by ATP stimulation of P2X7 receptors were also shown to be involved in the pathogenesis of IPF. BALF samples from IPF patients were shown to have elevated levels of IL-1β and IL-18 compared to healthy controls as well as increased caspase-1 activity (Jäger et al., 2021). Furthermore, in patients with acute exacerbations of IPF, IL-1β levels

were massively elevated (Jäger et al., 2021). These data suggest a role for ATP-induced P2X7 activation in the pathophysiology of IPF which may be an alternative target in the development of novel therapies.

1.2.4 eATP in chronic cough

Chronic cough is a common symptom across several respiratory diseases such as asthma, COPD and IPF and can also be idiopathic in nature. Cough is driven by activation of airway sensory nerves, which express a variety of ion channels and receptors, including transient receptor potential (TRP) channels and purinoreceptor (P2X/P2Y) channels, which are activated by ATP. Early studies have implicated a role for eATP in cough as it has been shown to reduce the threshold for cough induction in *in vivo* guinea pig cough models (Kamei et al., 2005, Kamei and Takahashi, 2006). Pre-clinical studies have also shown that the tussigenic action of ATP is mediated by P2X3 receptors (Pelleg et al., 2019, Bonvini et al., 2016). Throughout this thesis the term P2X3 antagonist will be used to describe both P2X3 homotrimers and P2X2/3 heterotrimers unless specified as selective for P2X3 or non-selective referring to P2X2/3.

Importantly, a non-selective P2X2/3 receptor antagonist, Gefapixant, was one of the first drugs to show antitussive efficacy in clinical trials in treatment-refractory chronic cough patients. These antagonists are currently the most promising antitussives in development with recent approval of the P2X2/3 antagonist Gefapixant in Japan, Switzerland, and Europe (McGarvey et al., 2022, Drake et al., 2023). Furthermore, recent studies have shown increased airway epithelial sensory nerve density in chronic cough patients (Shapiro et al., 2021). Taken together, these data suggest a role for eATP in chronic cough. Further details including the prevalence of chronic cough and the mechanisms involved in the cough reflex, activation of airway sensory nerves and ion channels implicated in cough is outlined in section 1.3.

1.3 Chronic cough

Under normal physiological circumstances, cough is a protective reflex which prevents the inhalation of irritants into the airways and can be triggered to clear the airways of unwanted secretions. However, when cough persists and becomes excessive or inappropriately activated for more than 8 weeks it is termed chronic cough. Chronic cough can be idiopathic in nature, known as unexplained chronic cough (UCC), but can also be a common feature in a range of chronic respiratory diseases which can have detrimental impacts on quality of life (Chamberlain et al., 2015). This includes conditions such as asthma, COPD and IPF. Chronic cough that persists despite treatments that target those underlying respiratory conditions is described as refractory chronic cough (RCC).

1.3.1 Prevalence of chronic cough

Cough is one of the most common symptoms presented in primary care clinics globally (Finley et al., 2018). Chronic cough has a worldwide prevalence of 4% to 5% and is associated with additional symptoms including pain, dizziness, urinary incontinence and in some cases loss of consciousness (Everett et al., 2007, Çolak et al., 2017, Meltzer et al., 2021). As a result, chronic cough can have a significant negative impact on quality of life and can impair daily activities and work productivity (Meltzer et al., 2021, Kuzniar et al., 2007). Approximately 5% of adults in the UK suffer from chronic cough which is estimated to have an economic burden of approximately £128 million (Mcgarvey et al., 2019, Irwin et al., 2014).

To date, there are no licensed therapies in the UK for the treatment of chronic cough (Smith and Badri, 2019). This highlights the importance of understanding the pathophysiological mechanisms that drive chronic cough to help inform the development of safe and effective antitussive therapies.

1.3.2 The cough reflex and airway sensory nerves

The cough reflex is a forced event that clears the larynx, trachea and large bronchi of foreign materials and airway secretions (Chung and Pavord, 2008). Cough can be described in three physiological phases beginning with a deep rapid inspiration, followed by a compressive phase involving the build-up of intrathoracic pressure following closure of the glottis, and finally an expiratory phase where there is a rapid expulsion of air to clear the lungs and airways (Bianco et al., 1988). This release of air makes a characteristic cough sound that can occur singly, or in bouts referred to as cough trains where repetitive coughs occur in succession (Smith, 2010, Nasra and Belvisi, 2009).

The cough reflex is initiated through activation of airway sensory nerves housed within the vagus nerve (Bonvini et al., 2015). Pre-clinical studies have shown that cough is predominantly driven by activation of two types of vagal sensory afferent fibres; C-fibres and Aδ-fibres whose cell bodies are housed within the jugular and nodose ganglia of the vagus nerve (Mazzone and Undem, 2016). The embryological origins of these ganglia differ causing them to house different nerve fibre populations as the jugular is neural crest derived whereas the nodose is epibranchial placode derived (Nasra and Belvisi, 2009). The cell bodies of the vagus nerve then branch into the superior laryngeal nerves (SLN) and recurrent laryngeal nerves (RLN) which carry airway fibres to the trachea and bronchi (Canning et al., 2004, Belvisi, 2003).

These airway sensory nerves detect changes in the physical and chemical environment and there are several endogenous and exogenous stimuli capable of activating these nerves. These nerve fibres express a variety of ion channels present on nerve terminals found within and under the airway epithelium, some of which have been implicated in the pathways controlling cough, including purinoreceptor (P2X/P2Y) channels and cationic selective transient receptor potential (TRP) channels (Belvisi et al., 2016). Of these, TRPV1 and TRPA1 receptors have been extensively researched and their activation has been shown to elicit cough in human challenge studies (Lalloo et al., 1995, Carr et al., 2003, Trevisani et al., 2004, Birrell et al., 2009, Grace et al., 2012, Andre et al., 2009). However, there are limited studies investigating antagonists of these receptors in clinical trials (Khalid et al., 2014, Smith and Badri, 2019, Belvisi et al., 2017).

Activation of these airway sensory nerves relay pulmonary sensory information to the central nervous system (CNS), more specifically to the paratrigeminal nucleus (Pa5) and the nucleus of the solitary tract (nTS) in the brainstem (Polverino et al., 2012). Cough centres are then involved in triggering efferent nerves in the vagus, phrenic and spinal motor nerves to coordinate activation of the diaphragm and muscles involved in cough (Polverino et al., 2012). Activation of these airway sensory nerves lead to the cough reflex as illustrated in figure 1.6 (Belvisi et al., 2016, Brouns et al., 2012, Bonvini et al., 2015).

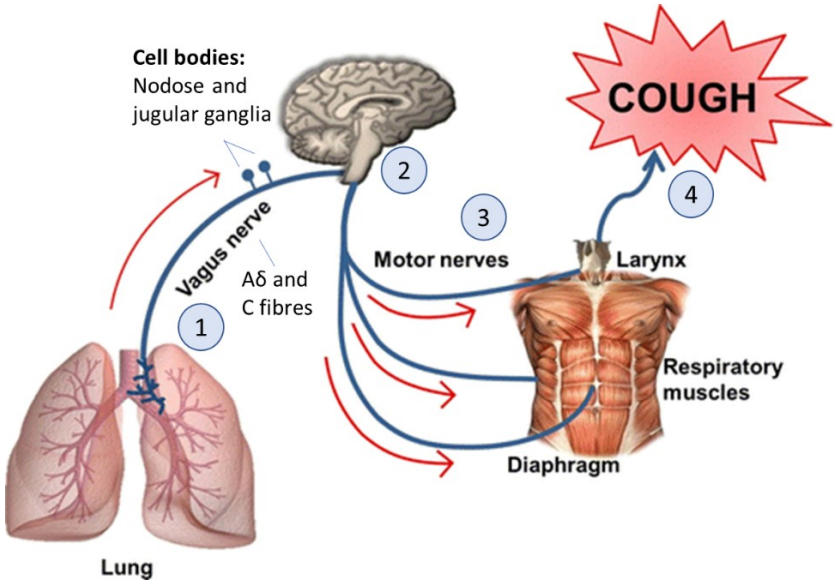


Figure 1. 6 The cough reflex.

Cough is initiated when endogenous or exogenous irritants activate receptors/ions channels present on sensory afferent nerves in the airways. If activation reaches a certain threshold, an action potential travels through the vagus nerve which synapses in the brainstem. Signals are then sent to effector muscles via motor neurons resulting in cough. Figure adapted from (Bonvini et al., 2015).

1.3.3 Activation of airway sensory nerves

A range of different stimuli can activate airway sensory nerves including mechanical irritation, inflammatory mediators and environmental stimuli as well as changes in pH, temperature and osmolarity (Belvisi et al., 2011, Canning, 2006, Grace et al., 2012, Koskela et al., 2005, Morice et al., 1987, Maher et al., 2009, McGarvey et al., 1998, Undem et al., 2004, Wong et al., 1999, Bonvini et al., 2016). Activation of sensory receptors causes an inward flow of current that depolarises the membrane and if this is sufficient in magnitude and reaches the threshold potential, it can trigger an action potential (Brouns et al., 2012). When this occurs at a specific location along the neuronal axon, adjacent locations along the axon also depolarise which causes nerve impulses to propagate along the length of the axon (Brouns et al., 2012).

Voltage gated sodium channels (VGSCs) are embedded in the plasma membrane of neurons and are required for action potentials to occur (Barnett and Larkman, 2007). The resting potential of a neuronal cell membrane is around -70mV but if an influx of sodium ions from a generator potential reaches the threshold potential, typically between -50mV and -55mV, VGSCs rapidly open causing an influx of positively charged sodium ions into the cell. This causes the membrane potential to increase

up to +30mV which further triggers neighbouring VGSCs to open causing propagation of a nerve impulse along the axon to the neuronal terminal in the CNS (Barnett and Larkman, 2007).

Following the opening of VGSCs, potassium channels open to allow potassium ions to leave the cell. Once the peak of the action potential is reached, VGSCs close whilst potassium channels remain open. This efflux of potassium causes a decrease in membrane potential allowing for repolarisation of the membrane. Although the size and magnitude of action potentials remain the same as they propagate along the neuron, the firing rate of these action potentials can vary. A sustained high frequency of action potentials is required to activate the afferent pathways of the cough reflex resulting in an urge-to-cough preceding the cough reflex (Canning and Mori, 2011).

The processing of the cough reflex in the human brain has been studied using functional brain imaging where regional brain responses can be monitored during exposure to airway irritants and coughing. These studies have shown that cough neural pathways form a widely distributed complex network within the brain in brain regions including the thalamus, insula, primary somatosensory and motor cortices, posterior parietal cortex, orbitofrontal cortex and the cerebellum (Ando et al., 2016). This is further complicated by different types of cough events as they can be voluntary or involuntarily executed and can also be supressed when there is an urge-to-cough (Ando et al., 2016). Neuroimaging studies show that the involuntary cough reflex only requires brainstem circuitry whereas neural processing of the urge-to-cough, voluntary coughing or inhibition of cough requires higher order neural networks within the cerebral cortex (Mazzone et al., 2011, Pacheco, 2014).

1.3.4 Sensory nerve subtypes

There is a wide range of stimuli that can activate airway sensory nerves which can broadly be categorised into mechanosensitive fibres which respond to mechanical forces in the lungs such as inflation and deflation during respiration, and chemosensitive fibres which respond to exogenous irritants such as cigarette smoke or inflammatory mediators such as bradykinin (Poliacek, 2020, Brouns et al., 2012).

The vagal sensory afferent nerves innervating the airways can be subdivided into four types according to characteristics including conduction velocity, diameter, adaptation index, physiochemical sensitivity, myelination and embryological origin (Canning, 2006). These 4 subtypes are Aα, Aβ, Aδ and C-fibres. Single fibre recording studies have described three classes of afferent fibre endings: slowly

adapting stretch receptors (Aδ-SARs), rapidly adapting stretch receptors (Aδ-RARs) and C-fibre endings (Belvisi, 2003).

1.3.4.1 Rapidly Adapting Receptors (Aδ-RARs)

These are fast conducting, myelinated Aδ-fibres that rapidly cease firing following maintained mechanical stimuli (Sant'Ambrogio and Widdicombe, 2001). These fibres have a conduction velocity of over 3 milliseconds and are also known as classical RARs, irritant receptors or just Aδ-fibres (Adcock et al., 2014, Adcock et al., 2003). These fibres can be found throughout the respiratory tract, but the majority are found in the larger airways (Sant'Ambrogio and Widdicombe, 2001, Canning, 2006). The cell bodies of RARs are thought to be mostly housed in the nodose ganglia (Ricco et al., 1996, Canning, 2006). These fibre types are not thought to be directly activated by chemical stimuli although these can be indirectly activated following mucus production and bronchoconstriction (Widdicombe, 2003). Nonetheless, some experiments suggest a subset of RAR fibres respond to capsaicin regardless of conduction velocity (Adcock et al., 2014). RARs are thought to provide defensive cough reflexes as they are able to cause a cough response even under anaesthesia (Nasra and Belvisi, 2009, Dicpinigaitis et al., 2014).

1.3.4.2 Slowly Adapting Receptors (Aδ-SARs)

SARs are nodose derived myelinated Aδ-fibres which adapt more slowly to a maintained stimulus and are less sensitive than RARs to sustained lung inflation (Schelegle and Green, 2001). SARs have a conduction velocity of approximately 18 milliseconds and are not thought to be involved in cough (Canning, 2006). Instead they are thought to play a role with autonomic functions such as tidal breathing and the Hering-Breur reflex, a stretch reflex that causes the cessation of inspiration and the start of expiration (Schelegle, 2003). The nerve termini of SARs can be found within the smooth muscle of the airways (Schelegle and Green, 2001, Bartlett et al., 1976).

1.3.4.3 C-fibres

C-fibres are slower conducting, unmyelinated fibres that make up the majority of afferent nerves that innervate the airways (Coleridge and Coleridge, 1984, Lee and Pisarri, 2001). These fibres can originate from both the nodose and jugular ganglia and innervate the epithelium and other structures within the intrapulmonary and extrapulmonary airway walls. These fibre types are thought to be responsible for the conscious perception of airway irritation and their activation is blocked by anaesthesia (Mazzone, 2004).

A range of chemical stimuli are capable of activating C-fibres which express members of the transient receptor potential (TRP) family of ion channels. For instance, bronchopulmonary C-fibres express TRPV1 and TRPA1 which can be activated by environmental tussive agents or endogenous inflammatory mediators to cause cough (Adcock et al., 2014, Birrell et al., 2009, Canning et al., 2004, Coleridge and Coleridge, 1984, Dicpinigaitis et al., 2014, Grace et al., 2012, Lalloo et al., 1995).

C-fibres are also able to release neuropeptides such as substance P from peripheral nerves lining the lungs via an axon reflex (Mazzone et al., 2003). Animal studies suggest these neuropeptides trigger local reflex responses such as mucus secretion and bronchoconstriction and may also have a sensitising role in cough (Kohrogi et al., 1988, Moreaux et al., 2000). Interestingly, increased levels of substance P have been found in BALF samples from patients with IPF and in the plasma and sputum of chronic cough patients which could suggest there is sustained activation of C-fibres in these patients (Takeyama et al., 1996, Otsuka et al., 2011). Substance P has also been shown to elicit cough in IPF patients but not in healthy volunteers (Hope-Gill et al., 2003).

There are two distinct populations of C-fibres; bronchial and pulmonary C-fibres which differ in their site of termination. Bronchial C-fibres innervate the extrapulmonary airways, are primarily derived from jugular ganglia and are stimulated by chemicals in the bronchial and systemic circulation (Coleridge and Coleridge, 1984). These fibres express neuropeptides such as substance P and are thought to be responsible for mediating the cough response based on their positioning within the airways (Undem and Kollarik, 2002). On the other hand, pulmonary C-fibres are thought to innervate the lower airways, do not express neuropeptides and have been shown to inhibit cough in animal models (Coleridge and Coleridge, 1984, Undem et al., 2003, Undem et al., 2004, Tatar et al., 1994, Widdicombe and Undem, 2002, Chou et al., 2008). This is thought to be through inhibition of the cough centres within the CNS rather than a direct inhibition of the cough reflex (Karlsson and Fuller, 1999).

1.3.5 Ion channels implicated in cough

1.3.5.1 P2X3 receptors

P2X3 receptors are purinergic receptors that are activated by ATP. Several studies have shown that receptors containing P2X3 subunits play a crucial role in activation of airway sensory nerves (Bodin and Burnstock, 2001, Jarvis, 2003, Bonvini et al., 2016). Airway expression of P2X3 is predominantly found on small to medium diameter C-fibres and Aδ-fibres originating from the jugular and nodose ganglia (Kwong et al., 2008, Undem and Nassenstein, 2009). P2X3 receptors form homotrimeric P2X3

receptors consisting of 3 P2X3 subunits, or heterotrimeric P2X2/3 receptors consisting of two P2X3 subunits and one P2X2 subunit (Ford, 2012). P2X3 receptors are predominantly activated by ATP and the ATP analogue αβ-Methylene ATP (αβ-MeATP) which is a more stable ligand selective for P2X1 and P2X3 subunit containing receptors. Activation of P2X receptors requires three molecules of ATP to bind to the extracellular portion of the open P2X channel (Jiang et al., 2003). Studies have shown that P2X3 receptors are rapidly desensitised. Following activation, P2X3 receptors open for milliseconds and then rapidly deactivate within tens of milliseconds (North and Jarvis, 2013).

Pre-clinical studies have shown that ATP-induced activation of airway sensory nerves could be blocked by the P2X3 antagonist AF-353 (Bonvini et al., 2016). ATP-induced activation of sensory fibres from nodose and jugular ganglia was also shown to be blocked by the selective P2X3 antagonist A-317492 (Kwong et al., 2008). Application of a P2X1/P2X3 inhibitor TNP-ATP was also able to block ATP enhanced coughs to citric acid (Kamei et al., 2005).

Antagonists of the P2X3 receptor which are activated by ATP are currently the most promising antitussive therapies in development which further implicates ATP and P2X3 in the pathophysiology of chronic cough, (see section 1.3.7) (Drake et al., 2023).

1.3.5.2 Transient Receptor Potential Ion channels

Transient receptor potential (TRP) channels are a family of non-selective cationic channels that show a preference for calcium. These channels are widely expressed throughout the body and respiratory system including immune, neuronal and structural cells in the lung. A number of TRP channels have been implicated in the mechanisms driving chronic cough (Grace et al., 2013). This section will briefly highlight the role of TRPV4 in cough given its association with the release of eATP (Bonvini et al., 2015, Bonvini et al., 2016) as well as the roles of TRPA1 and TRPV1.

TRPV4

The TRPV4 ion channel is expressed in a variety of cell types in the lungs including airway smooth muscle cells, fibroblasts, epithelial cells and inflammatory cells such as macrophages and neutrophils (Nilius and Szallasi, 2014, Jia et al., 2004, Rayees et al., 2019, Weber et al., 2020). TRPV4 expression has been found on dorsal root ganglion neurons. However, single cell PCR data suggests that there is no expression on neurons from pulmonary sensory ganglia which suggests TRPV4 exerts its effects through indirect mechanisms (Grant et al., 2007, Bonvini et al., 2016).

TRPV4 can be activated by endogenous ligands such as phorbol ester 4αPDD and synthetic activators such as GSK1016790a (GSK101), both of which are commonly used pre-clinically (Watanabe et al., 2002, Thorneloe et al., 2008). TRPV4 is also activated by hypo-osmolarity (Strotmann et al., 2000, Suzuki et al., 2003, Liedtke et al., 2000). Importantly, the activation of TRPV4 is linked to the release of ATP via pannexin-1 channels from a number of different cell types in the lungs (Ryan et al., 2016, Bonvini et al., 2020, Rahman et al., 2018, Baxter et al., 2014) leading to the activation of various purinergic receptors involved in inflammatory and neuronal responses.

TRPV4 has been shown to induce increases in intracellular calcium levels in cells from the nodose ganglia and causes depolarisation of guinea pig and human vagal nerves (Bonvini et al., 2016). Additionally, TRPV4 activation was shown to cause firing of Aδ-fibres (but not C-fibres) and induced cough in the conscious guinea pig (Bonvini et al., 2016). However, little to no expression of TRPV4 was found on neurons from pulmonary sensory ganglia and its effects were attributed to the release of ATP from satellite cells surrounding airway sensory nerves, and activation of P2X3 receptors on airway sensory nerve terminals (Bonvini et al., 2016). This is supported by experiments which showed that TRPV4 induced activation of airway sensory nerves could be blocked using a TRPV4 antagonist GSK2193874, as well as a P2X3 antagonist AF-353 (Bonvini et al., 2016). This TRPV4-ATP-P2X3 axis is thought to play a key role in the mechanisms that drive chronic cough which is supported by the investigation of P2X3 antagonists as potential antitussive therapies in people with refractory chronic cough, as described in section 1.3.8 (Dicpinigaitis et al., 2020).

In addition, hypo-osmolar solutions which are known to activate TRPV4 channels were shown to induce cough and bronchospasm in human subjects and is commonly used as a tussive agent in the clinic, the effects of which can be inhibited by the P2X3 antagonist Gefapixant (Schoeffel et al., 1981, Fuller and Collier, 1984, Naumov et al., 2016, Morice et al., 2007a, Morice et al., 2019). The antitussive efficacy of an oral TRPV4 antagonist GSK2798745 was investigated in a phase 2 clinical trial in 17 patients with chronic cough, however this trial was terminated early due to a lack of efficacy with 24-hour objective cough counts being the primary endpoint (Ludbrook et al., 2021). However, this compound was recently found to be rapidly metabolised to a less potent compound in human pharmacokinetic studies which may explain the lack of antitussive efficacy with this TRPV4 antagonist (Pero et al., 2021).

TRPA1

TRPA1 is a voltage dependent cation channel that is the only ankyrin member of the TRP channels (Story et al., 2003). It was initially found in human cultured fibroblasts and is expressed on a range of airway relevant cells including fibroblasts, epithelial cells, airway smooth muscle cells and inflammatory cells as well as vagal sensory neurons originating from the nodose and jugular ganglia (Jaquemar et al., 1999, Nassini et al., 2012, Nassenstein et al., 2008, Wortley et al., 2016, Story et al., 2003). TRPA1 channels are primarily activated by electrophilic compounds such as allyl isothiocynate (AITC) found in mustard oil and cannabinol found in cannabis as well as environmental irritants such as acrolein found in cigarette smoke and diesel particles (Jordt et al., 2004, Andrè et al., 2008, Bautista et al., 2006, Robinson et al., 2018).

TRPA1 activation has been shown to cause cough in humans and animal models (Birrell et al., 2009). Interestingly, TRPA1 only seems to activate C-fibres and not Aδ-fibres (Grace and Belvisi, 2011). Agonists of TRPA1 including acrolein and AITC have been shown to cause depolarisation of guinea pig and human vagal nerve tissues and can cause cough in conscious naïve guinea pigs (Raemdonck et al., 2012, Birrell et al., 2009, Caceres et al., 2009, Andre et al., 2009, Brozmanova et al., 2011). Antagonist studies found that the TRPA1 antagonist GDC-0334 was able to cause a dose-dependent reduction of citric acid induced cough in guinea pigs (Balestrini et al., 2021). Diesel particles have also been shown to activate airway sensory nerves through TRPA1 and interestingly, controlled human exposure studies found increased objective cough counts over 24 hours following exposure to diesel particles. A positive association between increased genetic risk scores of cough associated genes including TRPA1 was also identified (Robinson et al., 2018, Taylor-Clark and Undem, 2011).

Clinical studies investigating TRPA1 antagonists are limited due to a lack of potent small molecule inhibitors which demonstrate good oral bioavailability and as such it remains inconclusive whether TRPA1 antagonists may be useful in inhibiting chronic cough (Koivisto et al., 2022).

TRPV1

TRPV1 is well-studied in the scientific literature and is known to mediate hot sensations from the chilli pepper extract capsaicin and is commonly referred to as the ‘capsaicin receptor’ (Caterina et al., 1997). TRPV1 can be activated by capsaicin as well as other stimuli such as noxious heat (>42°C) and inflammatory molecules such as bradykinin. Interestingly, the 2021 Nobel Prize in Physiology or Medicine jointly awarded to David Julius and Ardem Patapoutian was for their discoveries of receptors

for temperature and touch which included the discovery of TRPV1 as a sensor of noxious heat and thermosensation (Latorre and Díaz-Franulic, 2022).

TRPV1 is highly expressed in airway innervating nerve fibres (Wortley et al., 2016, Sato et al., 2014, Atsumi et al., 2020). A range of TRPV1 agonists have been shown to evoke sensory nerve activation and/or cough in guinea pigs and humans (Grace et al., 2012, Kollarik and Undem, 2004, Fox et al., 1995, Choudry et al., 1989, Costello et al., 1985, Hewitt et al., 2016, Yılmaz, 2019). In fact, the use of capsaicin to provoke cough is widely accepted as a measure of cough reflex sensitivity (Chung, 2011, Millqvist, 2011).

Pre-clinical studies have shown that TRPV1 expression in airway sensory neurons can be increased and/or expressed in additional neurons in disease models of IPF, asthma and COPD (Belvisi et al., 2016, Lieu et al., 2012, Hu et al., 2014, Lv et al., 2016, Guan et al., 2021). TRPV1 expression has also been shown to be increased in patients with airway diseases such as asthma (McGarvey et al., 2014, Gao et al., 2022). However, clinical studies using TRPV1 antagonists suggest it does not reduce objective cough counts in patient with refractory chronic cough (Khalid et al., 2014, Belvisi et al., 2017). To date there are currently no clinical trials in progress with a TRPV1 antagonist for respiratory conditions.

1.3.5.3 Nicotinic receptor channels

Preclinical studies have found that central administration of nicotine inhibits cough in cats, and more recently the α7 nicotinic-receptor agonist ATA-101 was found to dose-dependently inhibit cough in guinea pigs (Poliacek et al., 2015, Canning et al., 2022). Although TRP channels and nicotinic-receptor agonists have been shown to play a mechanistic role in cough, they have not been shown to significantly reduce chronic cough in clinical trials (Belvisi et al., 2017, Khalid et al., 2014, Ludbrook et al., 2021, Smith et al., 2017, Kanemitsu et al., 2020).

These findings suggest that targeting single peripheral receptors or channels may not be sufficient to reduce chronic cough as there are more complex processes underlying the pathophysiology. Species-specific differences in cough triggers may also impact the translation of preclinical research into chronic cough therapies for humans (Drake et al., 2023).

1.3.6 Cough hypersensitivity

Excessive coughing has been attributed to increased activation and hypersensitivity in the neuronal pathways responsible for the cough reflex (Young and Smith, 2011). This may be due to changes in the excitability of the neuronal pathways involved in the cough reflex and/or increased exposure of sensory nerve terminals to chemical irritants such as ATP (Smith and Badri, 2019).The exact

mechanisms driving the development of cough hypersensitivity have not been fully elucidated. However, sensitisation of these neural pathways is believed to contribute to excessive cough and cough hypersensitivity.

Most patients with chronic cough have cough hypersensitivity. This is characterised by increased neural responsivity to a range on stimuli that affect the airways and lungs. Patients with cough hypersensitivity typically present with persistent urges to cough with frequent bouts of coughing usually triggered by innocuous stimuli (Chung et al., 2022). Although cough is a common feature of many chronic respiratory conditions, many present with unexplained chronic cough as they have no identifiable cause despite thorough investigation. These observations suggest that chronic cough may be a distinct clinical condition which results in sensitisation of the neural pathways that evoke cough (Chung et al., 2013, Morice, 2010, Morice et al., 2014b, Niimi and Chung, 2015). The development of sensitive tests or biomarkers for diagnosing cough hypersensitivity remains an unmet clinical need.

Clinical inhalation studies support the concept of cough hypersensitivity as patients with chronic cough exhibit heightened responses to a wide range of tussive stimuli including capsaicin, citric acid and hypertonic saline (Choudry and Fuller, 1992, Nurmi et al., 2019, Koskela et al., 2008). Studies have also found sex-related differences in cough hypersensitivity. Women with and without chronic cough were found to have heightened cough sensitivity to tussive stimuli compared to men which is likely due to enhanced central responses in the somatosensory cortex (Varechova et al., 2008, Morice et al., 2014a). This is likely to explain the overrepresentation of women in cough clinics and observational studies showing a higher prevalence of chronic cough in women relative to men (Meltzer et al., 2021, Morice et al., 2014a). For example, A survey of 10032 adults found that two thirds of patients with chronic cough were female (Morice et al., 2014a).

Clinical studies have also shown that chronic cough patients have increased airway epithelial sensory nerve density in the lower airways relative to healthy volunteers which suggests that sensory neuroplasticity is a contributing factor to cough hypersensitivity (Shapiro et al., 2021). The location of these nerve fibres and morphology suggest that they are most likely to be ATP-sensitive vagal C-fibres (Smith and West, 2021).

1.3.6.1 eATP in cough hypersensitivity

eATP is suggested to play an important role in cough hypersensitivity observed in most chronic cough cases. eATP is released during cellular injury and inflammation to alert neighbouring cells to damage. Excess eATP release may contribute to sensitisation of peripheral afferent neurons and subsequent

increased neural activation and coughing (Ford and Undem, 2013). It has been suggested that ATP is an important 'priming autocoid' in the airways by priming sensory neurons to reduce its activation to stimuli that drive afferent excitatory signals, and therefore contributing to sensitisation (Ford and Undem, 2013). eATP activates several ionotropic P2X and metabotropic P2Y purinoceptor subtypes. This includes homomeric P2X3 and heteromeric P2X2/3 receptors which are expressed by airway sensory neurons that mediate cough (Mazzone and Undem, 2016).

Early studies have shown that administering ATP significantly enhances the number of citric acid-induced coughs in a conscious guinea pig cough model. eATP enhanced cough in a concentration-dependent manner highlighting its role in enhancing cough reflex sensitivity (Kamei et al., 2005, Kamei and Takahashi, 2006). This data was to be expected given that eATP has been shown to stimulate both vagal C and Aδ-fibres in the lungs, both of which are important in the cough reflex (Widdicombe, 2002). Pre-clinical studies have also shown that the tussive effects of ATP are mediated by the P2X3 receptor. A selective P2X3 receptor antagonist, DT-0111 delivered to guinea pigs as an aerosol was able to effectively suppress aerosolised ATP-induced cough in free moving guinea pigs (Pelleg et al., 2019).

Clinical inhalation studies have also shown that patients with COPD and asthma have more pronounced coughs in response to aerosolised ATP compared to healthy volunteers (Basoglu et al., 2005, Basoglu et al., 2015). A cohort of people with idiopathic chronic cough also had significantly increased cough sensitivity to inhaled ATP relative to healthy volunteers (Fowles et al., 2017). These findings support that in chronic respiratory diseases, ATP has a mechanistic role in cough hypersensitivity.

1.3.7 Assessment of the cough reflex

1.3.7.1 Pre-clinical models of cough

Guinea pigs are the most relevant model species to investigate the cough reflex as they have very similar airway anatomy and physiology to man and demonstrate similar sensitivities to tussive stimuli such as capsaicin and citric acid (Belvisi and Hele, 2003, Canning et al., 2006, Karlsson and Fuller, 1999). The guinea pig can be used in a number of *in vitro* and *in vivo* model systems to pre-clinically investigate the cough reflex. Those used in this thesis are summarised below, and further details can be found in chapter 2.

Calcium imaging of airway ganglia

Jugular and nodose ganglionic neurons from guinea pigs can be harvested and investigated. 12-14 days prior to analysis a retrograde tracer dye DiIC18(3),1,1'-dioctadecyl-3,3,3',3'-tetramethylindocarbocyanine perchlorate (DiI) is administered to the airways which enables identification of airway specific neurons (Undem et al., 2003, Kwong et al., 2008, Lieu et al., 2012). These neurons can be loaded with a calcium specific dye and intracellular calcium levels investigated in the presence of agonists and antagonists (Dubuis et al., 2013, Grace et al., 2012). These cells can also be used for electrophysiological assessments such as patch clamp and for assessing gene expression (Dubuis et al., 2013, Nassenstein et al., 2008).

Isolated vagus nerve experiments

The vagus nerve trunk can be isolated from guinea pigs and placed in a grease gap recording chamber. This enables compounds to be applied to one end of the nerve trunk and membrane depolarisation to be measured at the other end of the nerve trunk as a measure of nerve activation (Birrell et al., 2009, Grace and Belvisi, 2011, Bonvini et al., 2016). Several compounds which induce vagus nerve depolarisation in this preparation have also been shown to induce cough *in vivo* (Patel et al., 2003, Maher et al., 2009, Belvisi and Smith, 2017, Bonvini et al., 2016). A major advantage of this preparation is that it can also be used with donor human vagal tissues which provides key translational data.

Electrophysiological tracheal recordings

Electrophysiological tracheal recording (eTRec) is an *ex vivo* technique this is used to measure action potentials firing from airway sensory nerve endings within the recurrent laryngeal nerve (RLN). The protocol used is similar to a technique previously described (Riccio et al., 1996). Briefly, the trachea is dissected out whilst the nerves innervating the trachea are left intact. The trachea is then placed in an organ bath and independently perfused with a buffered solution to which different compounds can be added and their effects on action potential firing of the RLN can be assessed. This technique enables the measurement of nerve activity following activation of receptors on the nerve termini.

In vivo single fibre recordings

In vivo electrophysiological recordings can be used to investigate tussive or antitussive compounds on action potential firing of airway specific afferent fibres (Adcock et al., 2003, Canning et al., 2004). Specific criteria are used to identify individual fibre types such as patterns of spontaneous activity, responses to hyperinflation and deflation, responses to capsaicin and citric acid and conduction

velocity. The effects of compounds can then be investigated on the nerve termini in a whole animal which is a more physiologically relevant technique.

Conscious guinea pig cough model

Cough responses can be investigated in conscious guinea pigs by placing them in individual perspex chambers and monitoring the effects of aerosolised compounds on cough counts. Studies have shown that guinea pig cough responses are similar to those seen in man (Birrell et al., 2009, Belvisi and Smith, 2017).

1.3.7.2 Clinical assessment of cough

Clinical assessment of cough can be broadly categorised into subjective or objective measures of cough. Subjective measurements are in the form of questionnaires which assess the impact of cough on quality of life. One example is the 'cough quality of life questionnaire' which contains 28 questions about the physical, psychosocial, functional and emotional effects of cough (Lechtzin et al., 2013). Another example is the 'Leicester cough questionnaire' which contains 19 items divided into three domains to assess the social, psychological and physical impacts of cough (Birring et al., 2003).

Objective measures of cough include ambulatory cough counts which enables cough counts to be counted in a patient's natural environment (Smith, 2010). Patients wear a cough monitor which is a discrete recording device equipped with a microphone to detect cough over a defined period of time for up to 24 hours (Smith, 2010, Smith and Woodcock, 2008, Kelsall et al., 2011). Objective cough frequency has become the gold standard primary endpoint for assessing the efficacy of novel antitussive agents (Hall et al., 2020, Turner and Birring, 2023). A variety of different cough monitors have been trialled with the Leicester Cough Monitor (LCM) and the VitaloJAK device being the main monitors widely used in cough research (Smith and Woodcock, 2008).

The LCM contains a portable digital recording device and a lapel microphone whereby audio data is analysed using an automated algorithm that selectively detects cough sounds and their timings (Birring et al., 2008). The LCM has proven useful in providing cough counts in clinical trials of potential antitussive therapies and non-pharmacological interventions (Ryan et al., 2012, Vertigan et al., 2016, Birring et al., 2017, Chamberlain Mitchell et al., 2017).

The vitaloJAK monitoring system differs from the LCM as it uses a digital recorder to record sounds through a chest wall contact microphone in addition to one attached to the lapel (Smith et al., 2021b).

Cough recordings are not automated but compressed and shortened to remove silences and most non-cough sounds. This is then processed by human cough counters aided by software providing visual representation of the audio file (Smith et al., 2021b). The VitaloJAK monitoring system has been used for a range of antitussive clinical trials including those for novel P2X3 receptor antagonists and this is the only monitor that currently has Food and Drug Administration (FDA) approval (McGarvey et al., 2022, Smith et al., 2020a).

Another objective measure of cough includes cough challenge studies which assesses cough reflex sensitivity in individuals. Similar to pre-clinical cough models, subjects inhale a nebulised tussive agent, most commonly capsaicin which induces cough in a reproducible and dose-dependent manner and is safe to use (Dicpinigaitis and Alva, 2005). This is a standardised method published by the European Respiratory Society (ERS) to enable universal interpretation and comparison between different cough clinics (Morice et al., 2007a). A key advantage of this technique is that it allows clinicians to identify differences in cough sensitivity across different airway diseases such as asthma, COPD and chronic cough. The sensitivity of the cough reflex is commonly measured as the concentration of the tussive agent that produces 2 coughs (C2) and 5 coughs (C5) (Morice et al., 2007b, Dicpinigaitis, 2006). However, the disadvantage of using the C2 and C5 parameters is that it weakly correlates to ambulatory cough counts (Birring et al., 2006, Decalmer et al., 2007, Hilton et al., 2013). Alternative parameters such as the maximum number of coughs evoked by any capsaicin concentration (Emax) and the capsaicin concentration evoking at least half of the Emax (ED50), instead of C2 and C5, could enable better correlation with objective cough counts and distinguishing different disease types from healthy controls (Hilton et al., 2013). This type of analysis has also been used in animal cough studies (Smith et al., 2012).

1.3.8 Cough therapies

For patients with RCC or UCC, clinicians commonly recommend therapies that globally supress cough, the most common of which are opioid receptor agonists (Morice et al., 2007b). Although these opioid based therapies can provide relief of cough in some situations, they have potential for dependency and can be associated with side effects including drowsiness and constipation. Furthermore, these drugs may cause unwanted suppression of protective cough reflexes (Morice et al., 2007b, Fuller et al., 1988).

Drugs that impact the central nervous system including gabapentin and pregabalin were shown to have some antitussive efficacy in a small number of randomised clinical trials. However, side effects

of these neuromodulators include respiratory depression, sedation, and drowsiness which limits their use for treating chronic cough (Ryan et al., 2012, Vertigan et al., 2016, Morice et al., 2007b). These drugs are thought to target central sensitisation by blocking central voltage-gated calcium channels that may be involved in driving cough (Morice et al., 2020, Mazzone and McGarvey, 2021). Although neuromodulators have occasionally shown antitussive potential, they infrequently improve objective cough frequency which suggests their efficacy is not driven by direct antitussive activity (Smith and Badri, 2019).

Studies exploring more targeted therapies have shown more potential in addressing peripheral mechanisms underlying chronic cough which may reduce cough hypersensitivity rather than broadly supressing all cough including protective cough. These drugs are summarised in table 1.1. Antagonists of P2X3 receptors supported by the role of ATP in airway inflammation and cough hypersensitivity have shown promising results (Smith and Badri, 2019).

Most cough therapies in development are targeted towards ion channels and receptors involved in peripheral activation of cough such as TRP channels and P2X3 receptors. Antagonists of the P2X3 receptor which are activated by ATP are currently the most promising antitussive therapies in development and several compounds have been tested in clinical trials. This includes drugs such as gefapixant, camlipixant, sivopixant, eliapixant and filapixant as summarised in Table 1.1 (Drake et al., 2023). Gefapixant is a non-selective P2X3 receptor antagonist and the most clinically advanced with data from two large, phase 3, randomised trials. Data from the phase 3b randomised trial demonstrated significant improvement in objective cough frequency and quality of life in patients with RCC or UCC (McGarvey et al., 2022, McGarvey et al., 2023a). Gefapixant is currently approved for RCC and UCC in Japan, Switzerland and the European Union (EU) with approval being sought in the United Kingdom and United States (Markham, 2022). However, in a recent FDA advisory committee meeting, the panel voted against Gefapixant for chronic cough due to concerns over the small reduction in cough frequency between Gefapixant and placebo (Hornick, 2023). A lack of efficacy observed over placebo may be due to trial design and patient selection as both UCC and RCC patients were selected for the study. Furthermore, there may have been a lack in diagnosing patients with underlying conditions and there were no controls for the background medications patients were already on. Additionally, there was no long run-in period to complete all 3 phases of clinical trials which is typically a lot longer for asthma trials.

Initial trials in RCC and UCC patients found camlipixant did not meet its primary endpoint in a phase 2a study which was terminated early due to the COVID-19 pandemic (Smith et al., 2021a). A subsequent study enrolling an enriched patient population based on baseline cough frequency found that camlipixant met its primary endpoint of significant reductions in 24 hour cough frequency and is currently in phase 3 clinicals with anticipated regulatory approval and launch in 2026 (Smith et al., 2022). Sivopixant was another P2X3 antagonist being trialled, however it did not show significant reduction in 24-hour cough frequency in a phase 2b study (McGarvey et al., 2023b). Eliapixant and filapixant were also under clinical development, however their programs have been discontinued despite showing efficacy in clinical trials (Friedrich et al., 2023, Morice et al., 2021, Drake et al., 2023).

Although P2X2/3 and P2X3 antagonists are generally safe, taste-related adverse events particularly with P2X2/3 antagonists such as Gefapixant are observed and is likely due to the presence of P2X receptors expressed on the gustatory nerves innervating the taste buds (Smith et al., 2020b, Morice et al., 2021). Although more selective P2X3 antagonists generally exhibited lower incidences of taste-related adverse events, recent trials of eliapixant and filapixant suggest selectivity of P2X3 homotrimeric receptors over other P2X2/3 heterotrimeric receptors may not completely be attributed to taste-related side effects and other factors such as pharmacokinetic properties and allosteric binding sites may contribute to these adverse events (Friedrich et al., 2023, High et al., 2023).

Many studies investigating P2X3 antagonists have consistently observed a large placebo effect, though reasons for these observations are not well understood (McGarvey et al., 2022, Smith et al., 2020b). Differences in the clinical efficacy between P2X3 antagonists are also unclear but could potentially be due to placebo effects, individual factors such as selection for baseline cough frequency and/or the pharmacokinetic properties of individual drug compounds such as their receptor selectivity and bindings sites. Additional data from phase 3 studies are required to better compare the efficacy and safety profiles of these P2X3 antagonists.

Support for the role of ATP in chronic cough is that Merck, Bayer, Shinogi and Bellus all had P2X2/3 or P2X3 compounds that demonstrated efficacy through improved objective cough frequency and/or subjective patient experiences related to their cough. In addition to this the phase 2 data with Gefapixant showed a significant reduction in cough over placebo in chronic cough patients, although this efficacy was reduced in phase 3 studies where the patient population was broadened (Drake et al., 2023).

Drug (manufacturer)	Mechanism of action	Development phase
Gefapixant (Merck)	P2X3 receptor antagonist	Phase 3 and 3b completed, Approved in Japan, Switzerland and the EU
Eliapixant (Bayer)	P2X3 receptor antagonist	Phase 2 completed, Development discontinued
Filapixant (Bayer)	P2X3 receptor antagonist	Phase 2 completed, Development discontinued
Camlipixant (Bellus)	P2X3 receptor antagonist	Phase 2 completed, Phase 3 in progress
Sivopixant (Shionogi)	P2x3 receptor antagonist	Phase 2 completed

Table 1. 1 Drugs investigated for the treatment of chronic cough.

Table Adapted from (Drake et al., 2023).

1.4 Thesis plan

Hypothesis: eATP is a key driver of chronic respiratory diseases including chronic cough through the activation of airway sensory nerves. Increasing the breakdown of eATP using the ecto-nucleotidase enzyme CD39 may reduce activation of airway sensory nerves and lung levels of eATP which may be a therapeutic option for treating patients with chronic cough and other ATP-driven chronic respiratory diseases.

In order to address this hypothesis, the aims of this thesis are:

- Optimise the methodology for the retrieval and assessment of eATP in biological samples using luminescent-based assays (**Chapter 3**).
- Investigate whether ATP can activate airway sensory nerves in guinea pig and human tissues and investigate its pharmacology using P2X3 antagonists (**Chapter 4**).
- Determine whether ATP-induced activation of sensory nerves can be reduced by increasing its breakdown using the ecto-nucleotidase enzyme CD39 (**Chapter 5**).
- Investigate the role of eATP in animal models of airway inflammation such as COPD and determine whether eATP is increased in these disease models. These can then be used to test whether increases in eATP and other airway disease markers can be inhibited by CD39 ligands once the pharmacodynamic and pharmacokinetic properties of CD39 have been characterised *in vivo*. A reduction in airway disease markers would suggest CD39 has therapeutic potential (**Chapter 6**).
- Investigate whether eATP is elevated in refractory and unexplained chronic cough patient samples (**Chapter 7**).

These aims will be achieved using the following techniques:

- Comparison of different luminescent-based assays for the detection of eATP in biological samples.
- Using *in vitro* and *ex vivo* pre-clinical nerve recording systems to investigate the pharmacology of ATP on airway sensory nerves.
- Using *in vitro* and *in vivo* pre-clinical nerve recording systems to investigate the pharmacology of CD39 on airway sensory nerves.
- Using naïve guinea pigs in an ATP-induced cough model to investigate the anti-tussive capabilities of CD39.

- Using naïve mice to investigate the dose response, duration of action and best route of administration of CD39 *in vivo*.
- Using cigarette smoke-, ozone- and Poly IC- exposed animal models of COPD and airway inflammation to investigate levels of eATP.
- Using an acute cigarette smoke-exposed mouse model to investigate the *in vivo* impact of CD39 on eATP levels and other ATP-driven disease markers.
- Using luminescent-based assays to measure eATP in refractory and unexplained chronic cough patient samples.

Chapter 2: General Methods

This chapter outlines the general methodology used throughout this thesis. Specific protocols with further details including statistical analysis can be found within each results chapter.

2.1 Animal samples

All animal work was performed in accordance with the UK Home Office guidelines for animal welfare based on the Animals (Scientific Procedures) Act of 1986 and the ARRIVE guidelines, under project licence number PP5469104.

2.1.1 Animal husbandry

Male Dunkin Hartley guinea pigs (250-400g) were purchased from Marshall, UK, male Brown Norway rats (225-250g) were purchased from Charles River Laboratories, UK, and male and female C57/BL6J mice (20-25g) were purchased from Envigo, UK. Animals were housed in groups within temperature controlled (21°C) individually ventilated cages with access to food and water. All animals were acclimatised to their environment for at least one week prior to experimentation.

2.1.2 Animal sample collection and processing

To evaluate levels of extracellular ATP (eATP) and measure other endpoints specified in the relevant results chapters, plasma, bronchoalveolar lavage fluid (BALF) and lung samples were collected from animals.

Animals were euthanised with an intraperitoneal overdose of sodium pentobarbitone (200mg/kg, 1ml/kg) which was administered by a trained individual. This was done at specified timepoints detailed in the relevant result chapters. Animals were exsanguinated via cardiac puncture and their tracheas were cannulated to enable collection of plasma and BALF, respectively followed by collection of lung samples.

BALF and plasma samples were taken with specified concentrations of ethylenediamine tetraacetic acid (EDTA) solution, to ensure all samples contained approximately 6mM EDTA. This is the concentration of EDTA found to prevent blood coagulation and allows reproducible detection of ATP levels in biological fluids by preventing rapid breakdown of ATP as described in chapter 3 of this thesis (see section 3.3.4 and 3.3.5).

2.1.2.1 Animal Plasma

Blood was collected via cardiac puncture using syringes pre-filled with EDTA and immediately placed on ice. For mice, blood was collected into 1ml syringes containing 10µl of 0.12M EDTA using a 23g

needle. For guinea pigs and rats, blood was collected into 5ml syringes containing 60µl of 0.5M EDTA using a 21g needle. All blood samples were centrifuged (1200g, 10min, 4°C) to separate cells from the plasma supernatant. The plasma was aliquoted and stored at -80°C until further analysis.

2.1.2.2 Animal Bronchoalveolar lavage fluid (BALF)

BALF was collected by injecting 0.9% w/v sodium chloride (saline) into the lungs of animals through a tracheal cannula. For mice 0.3ml saline was injected and left to equilibrate in the lungs for 30 seconds before being aspirated. This was repeated twice and the BALF was combined into a single tube containing 8µl of 0.5M EDTA. For guinea pigs and rats, 3ml saline was injected and left to equilibrate in the lungs for 30 seconds before being aspirated. This was repeated once and the BALF was combined into a single tube containing 60 µl of 0.5M EDTA. All BALF samples were centrifuged (800g, 10min, 4°C) to separate cells from the supernatant. The supernatant BALF was aliquoted and stored at -80°C until further analysis.

2.1.2.3 Mouse Lungs

Lung samples were taken from mouse models of airway disease to investigate changes in gene expression of specific ecto-nucleotidases following acute exposure to cigarette smoke, PolyI:C and ozone in C57/BL6J mice. Lung lobes were dissected, cut into smaller pieces, placed into cryovial tubes, and then flash frozen in liquid nitrogen. Frozen samples were then stored at -80°C for future assessment of gene expression.

2.2 Human samples

Donor human tissue that was not suitable for transplantation was obtained from the International Institute for the Advancement of Medicine (IIAM, New Jersey, USA). Ethical approval for the use of human tissue was obtained from the Royal Brompton and Harefield Trust.

Levels of eATP in human plasma and BALF samples from chronic cough patients and healthy volunteers were also investigated. This data was collected alongside data from animal models of respiratory disease to give insight into the translatability of measuring endpoints such as eATP.

Human plasma and BALF samples were obtained from our clinical collaborators, professor Jacky Smith and her team at the University Hospital of South Manchester, UK. This study was approved by the London-Dulwich Research Ethics Committee (REC reference: 21/PR/1233).

2.2.1 Human sample collection and processing

Having shown that adding EDTA to the collection protocol of biological fluids allows reproducible detection of ATP levels (see chapter 3, section 3.3.4 and 3.3.5), this methodology was fed back to our clinical collaborators. They were able to use this information to inform clinical sample collection allowing us to investigate levels of eATP in chronic cough patients and determine susceptible patient groups who may respond to ATP-targeted treatments. BALF and plasma samples were taken with specified concentrations of EDTA solution, to ensure all samples contained approximately 6mM EDTA.

2.2.1.1 Human Plasma

Plasma samples were drawn from the median cubital or cephalic vein in the arms of subjects and collected into K2E K2EDTA blood collection tubes (Avantor, USA) and immediately placed on ice. Blood samples were then centrifuged (1200g, 10min, 4°C) to separate cells from the plasma supernatant and the plasma was aliquoted and stored at -80°C until further analysis.

2.2.1.2 Human Bronchoalveolar lavage fluid (BALF)

Fibreoptic bronchoscopy was performed under conscious sedation and BALF was collected according to the ATS guidelines (Meyer et al., 2012) at a specialist cough clinic at the University Hospital of South Manchester, UK as previously described (West et al., 2012). BALF was combined into K2E K2EDTA blood collection tubes (Avantor, USA). All BALF samples were centrifuged (800g, 10min, 4°C) to separate cells from the supernatant. The supernatant BALF was aliquoted and stored at -80°C until further analysis.

2.3 ATP measurements

There is a growing body of research which suggests that increased levels of extracellular adenosine triphosphate (eATP) in the lungs contributes to the pathogenesis and symptoms of chronic lung diseases. However, measuring eATP is challenging as it is rapidly broken down by enzymes in the extracellular space. Although several publications have measured eATP in biological samples (Idzko et al., 2007, Riteau et al., 2010, Hlapčić et al., 2019), different methods and protocols are used highlighting the need to develop a more standardised technique for the retrieval and accurate assessment of eATP in biological samples which is both reliable and reproducible.

To determine the most accurate method to use for assessing levels of eATP in biological samples, several methods including plate-based assays and a handheld device was tested. These methods utilise luciferase which catalyses the reaction of luciferin in the presence of ATP to produce oxyluciferin and light in the form of luminescence, where the amount of light emitted is proportional to the amount of ATP present in the sample. The reaction occurs as follows:

$$\textbf{ATP + D-Luciferin + } O_2 \xrightarrow[Mg^{2+}]{\text{Luciferase}} \textbf{Oxyluciferin + AMP + } CO_2 \textbf{ + Pyrophosphate + Light}$$

For the plate-based assays, plates were read using the SpectraMax iD5 multi-mode microplate reader. Plate settings were customised using the SoftMax Pro software package (Molecular Devices, USA) to include the exact dimensions of the 96-well black ½ area optiplates which minimised cross-talk between wells. Luminescence was read with a 1 second per well integration time at room temperature.

2.3.1 ATPlite assay

The ATPlite Luminescence ATP Detection Assay System (PerkinElmer, USA) was used to measure levels of eATP in samples to compare the sensitivity of this kit to the ATP detection assay. This kit was based on the same luciferase-luciferin reaction. The assay was performed according to the manufacturer's protocol with the following modifications:

- The accompanying mammalian cell lysis solution was not used as eATP was measured in supernatant samples not containing cells (saline was used to collect BALF samples)
- ATP standards were prepared in nuclease-free water (Promega, USA)
- The assay was performed using 96-well black ½ area optiplates (PerkinElmer, USA)
- Plates were put to shake for 5 minutes in an orbital shaker at 700 rpm in the dark at room temperature and dark adapted for a further 5 minutes in the plate reader

2.3.2 ATP detection assay

The ATP Detection Assay kit- Luminescence assay (Cayman chemical, USA) was also used to measure levels of eATP in BALF and plasma samples. The assay was performed as per the manufacturer's protocol, with the following modifications:

- The accompanying ATP detection sample buffer was not used as eATP was measured in supernatant not containing cells (saline was used to collect BALF samples)
- ATP standards were prepared in nuclease-free water (Promega, US)
- The assay was performed in 96-well black ½ area optiplates (PerkinElmer, USA)
- Plates were put to shake for 5 minutes in an orbital shaker at 700 rpm in the dark at room temperature and dark adapted for a further 15 minutes in the plate reader

2.3.3 Hygiena Ultrasnap Device

ATP measurements taken using the plate-based assay were also compared to those taken using a Hygiena ensure touch luminometer (Hygiena, USA) which is a handheld device originally intended for food-safety monitoring. This device has the advantage of immediate sample measurements which may be useful in the clinic to get immediate read-out of eATP levels present in biological samples. By contrast, plate-based assays require the purchase of and training to use plate readers, and time to dark adapt and read plates. For plate-based assays samples are best stored and then measured on the same plate; whilst this confers greater accuracy (reduced variability when comparing between samples) it requires sample storage at ultra-cold temperatures compared to the immediate results obtained with a handheld device.

Measurements were taken by using the hygiena Ultrasnap swab where the swab was removed from its casing and the cotton bud tip was placed in 25µl of sample within a 2ml Eppendorf tube. The swab was rotated round 5 times and then placed back into its casing. The top of the swab was then snapped where the liquid reagent is located. The top of the swab was then squeezed so all the reagents fell to the bottom of the swab towards the cotton bud tip. The casing containing the swab was then shaken for a few seconds to ensure the liquid cotton bud tip was submerged in solution and this was placed in the luminometer which provides relative light unit measurements from the samples within 10 seconds. An ATP standard curve (100pM – 100µM) was performed prior to sample measurements and ATP concentrations of samples were then interpolated from the standard curve linearly by plotting ATP concentration against relative light units (RLU).



Figure 2. 1 Schematic of hygiena ultrasnap device eATP measurements.

2.4 Electrophysiological recordings

To investigate whether eATP and its upstream mediators activates airway sensory nerves in naïve guinea pigs, three complementary electrophysiological techniques were used. The methodology for electrophysiological tracheal recordings of the recurrent laryngeal nerve is outlined in chapter 4 (see section 4.2.3). The methodology for in vivo single fibre recordings is outlined in chapter 5 (see section 5.2.3).

2.4.1 *In vitro* isolated vagus nerve preparation

This system allows relatively high throughput pharmacological investigation into a range of stimuli that causes depolarisation of the vagus nerve which houses the sensory nerves that innervate the airways. This preparation has the advantage of providing translational data as both animal and human vagus can be investigated. Furthermore, this *in vitro* model enables the study of drugs irrespective of *in vivo* pharmacokinetic interference or influences from bronchoconstriction, mucus secretion or airway inflammation. However, the depolarisation measured is a summation of changes in membrane potential in all nerve axons within the vagus nerve trunk, not just airway sensory nerves. Additionally, receptor expression and behaviour on the vagal nerve trunk may differ to that on peripheral airway sensory nerve termini *in vivo*.

2.4.1.1 Tissue Dissection: Animals

Male Dunkin Hartley guinea pigs were euthanised as described in section 2.1.2. An incision was made from the abdomen towards the neck, and skin, muscle, connective tissue and the ribcage was carefully removed to expose the trachea and vagal nerves. The vagal nerve trunks were dissected out caudal to the nodose ganglia and placed into modified Krebs-Henseleit (KH) solution containing (in mM: NaCl 118; KCl 5.9; $MgSO_4$ 1.2; $CaCl_2$ 2.5; NaH_2PO_4 1.2; $NaHCO_3$ 25.5 and glucose 5.6; pH 7.4) and bubbled with 95% O_2 / 5% CO_2. The nerve was cleared of any connective tissue, de-sheathed and cut into 10-15mm segments prior to experimentation. Care was taken to avoid stretching or damaging the nerve and they remained in oxygenated modified KH solution throughout the experiment.

2.4.1.2 Tissue Dissection: Human

Human tissue that was not suitable for transplant was purchased from IIAM. En bloc lungs, trachea and vagus nerves attached were harvested from a deceased 65-year old female donor, who was diagnosed with COPD. Tissues were received on ice within 36 hours of aortic cross clamping and immediately placed within bubbled KH solution as described previously. A dissecting microscope was used to free the nerve from surrounding connective tissue as the perineural and epineural sheath is much harder to remove in human tissue. As with guinea pig tissue, the vagus nerves were cut into 10-15mm segments and remained in oxygenated modified KH solution throughout the experiment.

2.4.1.3 Apparatus set-up

The dissected nerve segments were placed in a grease-gap recording chamber consisting of a custom-made perspex block as described in (Birrell et al., 2002) and shown in Figure 2.2. Briefly, individual nerve segments were threaded through a longitudinal channel within the perspex block, and the ends of the nerves were electrically and chemically isolated by injecting petroleum jelly in the middle of the channel. One side of the nerve was in contact with a recording electrode and was constantly perfused with 37°C oxygenated KH solution at a rate of 2ml/min. The other end of the nerve was in contact with a reference electrode and remained in 37°C oxygenated KH solution throughout the experiment. The electrodes used were Ag/AgCl pellet half-cell electrodes (ESP-F20N, Warner Instruments, USA) and a glass capillary tube was placed into the electrode. The glass tube was carefully filled with KH solution to avoid air bubbles and rested on each end of the nerve. The electrodes were connected to a DAM50 differential amplifier unit (WPI, UK) which amplified the direct current signal (x10 gain, low pass filter 0.1Hz, high pass filter 3kHz). This signal way relayed onto a computer using the Lab-Trax 4/16 data acquisition system (WPI, UK) at a sampling rate of 10KhZ and recorded and analysed using LabScribe 4 software (iWorx Systems, USA).

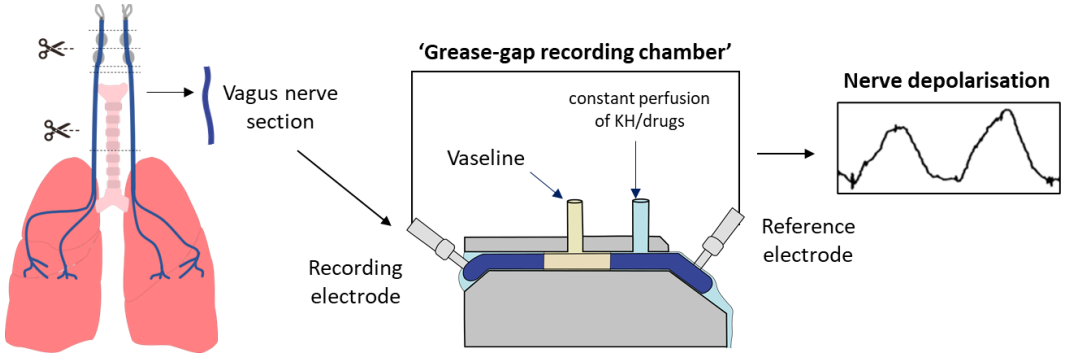


Figure 2. 2 Schematic of isolated vagus nerve preparation

2.4.1.4 Antagonist experiments

The inhibition of agonist responses by antagonists were investigated. The concentration of agonist used was based on the submaximal concentration responses which were previously determined. In each experiment, the agonist was perfused onto the nerve for 2 minutes followed by a washout period. This was repeated 2-3 times to achieve 2 reproducible responses. Once this was obtained, an antagonist was perfused onto the tissue for 10 minutes, immediately followed by a combination of agonist and antagonist for 2 minutes. Any responses were then washed to baseline by KH alone, and then a final stimulation with agonist was performed to test the viability of the nerve and reversibility of the antagonist. Specific protocols and concentrations of drugs used for antagonist experiments can be found in the relevant results chapters (See section 4.2.2).

2.4.2 Isolated neuron recordings

Isolated neuron recordings have the advantage of measuring responses from airway specific neurons whereas *in vitro* isolated vagus nerve recordings are not airway specific as the vagus nerve also contains axons that innervate visceral organs such as the heart. Isolated neuron recordings enable functional investigation into the effects of compounds on the cell bodies of airway terminating neurons by measuring changes in intracellular free calcium ($[Ca^{2+}]_i$). Calcium signals were measured in airway neurons dissociated from the nodose ganglia and jugular ganglia, which house the cell bodies of nerve fibres of the vagus nerve. Increases in intracellular calcium levels are indicative of neuronal activation which enables investigation of potential antitussive compounds against tussive stimuli. The methodology used in this section is as described in an established protocol (Dubuis et al., 2013).

2.4.2.1 Labelling of airway-terminating nodose ganglia and jugular ganglia

To ensure neurons experimented on were innervating the airways, male Dunkin Hartley guinea pigs were dosed with a retrograde tracer dye, 1,1'-dioctadecyl-3,3,3',3'-tetramethyl-indocarbocyanine perchlorate (DiI). The dye is a lipophilic fluorophore which infiltrates the membranes of sensory nerve endings and is moved towards the cell body via retrograde transport (Hofmann and Bleckmann, 1999). On the day of use, the DiI which is previously dissolved in 100% ethanol is diluted in 0.9% saline to give a final concentration of 2.2% V/V. Animals were dosed intranasally (i.n.) whilst remaining conscious and received 1ml/kg of 0.25mg/ml DiI, 12-14 days prior to experimentation. This ensured enough time was given for the dye to migrate from sensory nerve endings within the airways, along sensory nerve axons to the cell body in the vagal ganglia.

2.4.2.2 Ganglia dissection and dissociation

Male Dunkin Hartley guinea pigs were euthanised as described in section 2.1.2. The skin, connective tissues and muscles from the animal's head were removed to expose the skull. The top of the skull and brain were removed. The ear bone was then cut out to reveal the nodose and jugular ganglia found against the occipital bone. Both ganglia were carefully extracted from surrounding connective tissue and placed in ice cold sterile Hanks Balanced Salt Solution (HBSS: containing 5.33M KCl, 0.441mM KH_2PO_4, 138mM NaCl, 0.3mM Na_2HPO_4, 5.6mM glucose, 5mM HEPEs at pH 7.4). The ganglia were further cleared of connective tissues under the microscope and were enzymatically digested in a 2-step process as described previously (Grace et al., 2012, Dubuis et al., 2013). Briefly, the ganglia were incubated with activated papain (20units/ml, Sigma UK) in Papain Activation Solution (PAS: HBSS supplemented with 400mg/L L-Cysteine, 1ml/L EDTA 0.5M stock solution and 1.5ml/L $CaCl_2$ 1M stock solution). The ganglia were then incubated in HBSS solution containing Type IV collagenase (Worthington, USA, 2mg/ml) and Dispase II (Roche, UK, 2.4mg/ml), at 37°C for 40 minutes. Following

enzymatic digestion, the ganglia were washed, centrifuged and the supernatant removed. Cells were resuspended in sterile HBSS and dissociated by trituration with a heat-smoothed glass pasteur pipette coated with F12 media. To separate the large neuronal cells bodies and eliminate unwanted debris, the cell suspension was centrifuged through L15 medium containing 20% percoll v/v. The supernatant was then removed, and the remaining cell pellet was resuspended in L15 medium. The cells were centrifuged again and resuspended in complete F12 medium (containing 1% FBS, 1% penicillin and 100,000u/ml streptomycin). The dissociated cells were then plated onto Poly-D-Lysine (100µg/ml) and laminin (75µg/ml) coated fluorodishes (0.17 mm thick optical quality glass bottom) and left to adhere for 2 hours, after which plates were flooded with 2ml of complete F12 medium and incubated at 37°C (5% CO_2 / 95% O_2) for ~16 hours prior to experimentation.

2.4.2.3 Fluorescence imaging dyes

Fura2 (Invitrogen) is a Ca^{2+}-binding dye used to measure changes in $[Ca^{2+}]_i$ within the vagal ganglia following drug treatments. The esterified form of Fura2, Fura2-AM was used as it contains an acetoxymethyl ester (AM) group which is hydrophobic, enabling the dye to permeate through cell membranes. This dye was selected as it does not overlap with the excitation and emission wavelengths of the DiI dye used to identify airway-specific neurons (section 2.4.2.1) Figure 2.3.

Dye	Localisation	Peak excitation λ	Peak emission λ
DiI	Cell membrane	550nm	570nm
Fura-2 Ca^{2+} free	Cytoplasm	380nm	512nm
Fura-2 Ca^{2+} bound	Cytoplasm	340nm	510nm

Table 2. 1 Imaging dyes maximum excitation and emission wavelengths.

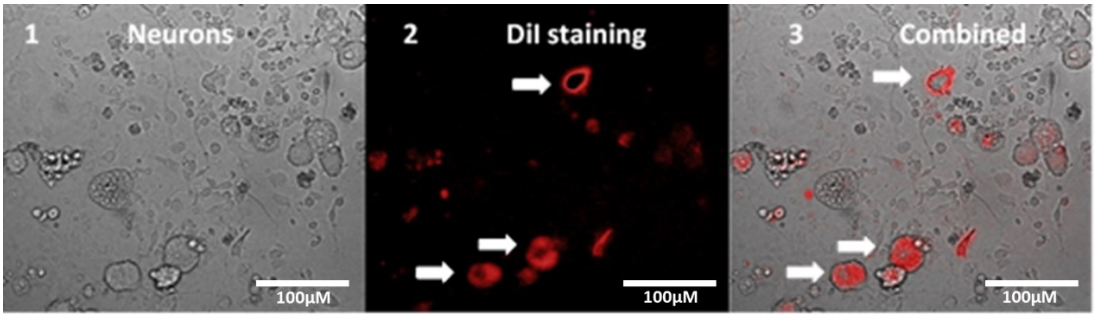


Figure 2. 3 DiI staining of airway specific nodose neurons.

(1) Image of nodose neurons recorded using bright-field microscopy. (2) DiI fluorescence with the light intensity expressed by a black (no light) to red (highest light) colour code. Airway specific neurons are indicated by DiI staining (white arrowheads). (3) Combined image of bright-field and fluorescence images.

Fura2-AM was dissolved in DMSO and combined with an equal volume of PowerLoad (Thermo Fisher Scientific, UK) which helps the dye permeate into cells. This mixture was diluted in Extracellular Solution (ECS containing in mM: KCl, 5.4; NaCl, 136; $MgCl_2$, 1; $CaCl_2$, 1.8; NaH_2PO_4, 0.33; glucose, 10; HEPES 10 at pH 7.4) to give a final concentration of 12µM Fura2-AM in the loading solution.

Initially, cells were washed three times with ECS to remove any traces of complete F12 media. Cells were then loaded with Fura2-AM/PowerLoad/ECS solution for 40 minutes in the dark at room temperature. This solution was then aspirated, and cells were washed twice with ECS and left in the dark for a further 30 minutes. This de-esterification step was necessary to allow intracellular esterases in the cytosol to cleave the AM group from the Fura2 molecule, trapping the dye within the cell membrane and allowing for full Ca^{2+} sensitive fluorescence responses (Takahashi et al., 1999).

2.4.2.4 Calcium imaging

An inverted epifluorescence microscope (Zeiss) was used to image the cells. The microscope contained a mercury arc lamp with a 500nm beam splitter, a set of excitation filters at 335/7nm (near UV) and 387/11nm (deep blue), and an emission filter at 529/24nm (green). Fluorodishes were mounted on the microscope stage within a 37°C heated chamber in a solution-changing perfusion system. Perfusion tubes were placed either end of the fluorodish to allow for the addition and removal of solutions to the cells. For all recordings, neurons were initially exposed to a hyper-potassium solution referred to as K_{50} (containing 50mM KCl, 91.4mM NaCl, 1mM $MgCl_2$, 2.5mM $CaCl_2$, 0.3M NaH_2PO_4, 10mM glucose 1mM HEPES at pH 7.4). K_{50} triggers a rapid increase of calcium into neurons through voltage gated calcium channels opened by cell depolarisation. After 15 seconds of exposure, the K_{50} was washed off with ECS until the calcium signal returned to baseline. K_{50} responses were used to normalise responses of neurons from different dishes and K_{50} was applied at the beginning and end of the recording to ensure cell viability. An example trace is shown in figure 2.4.

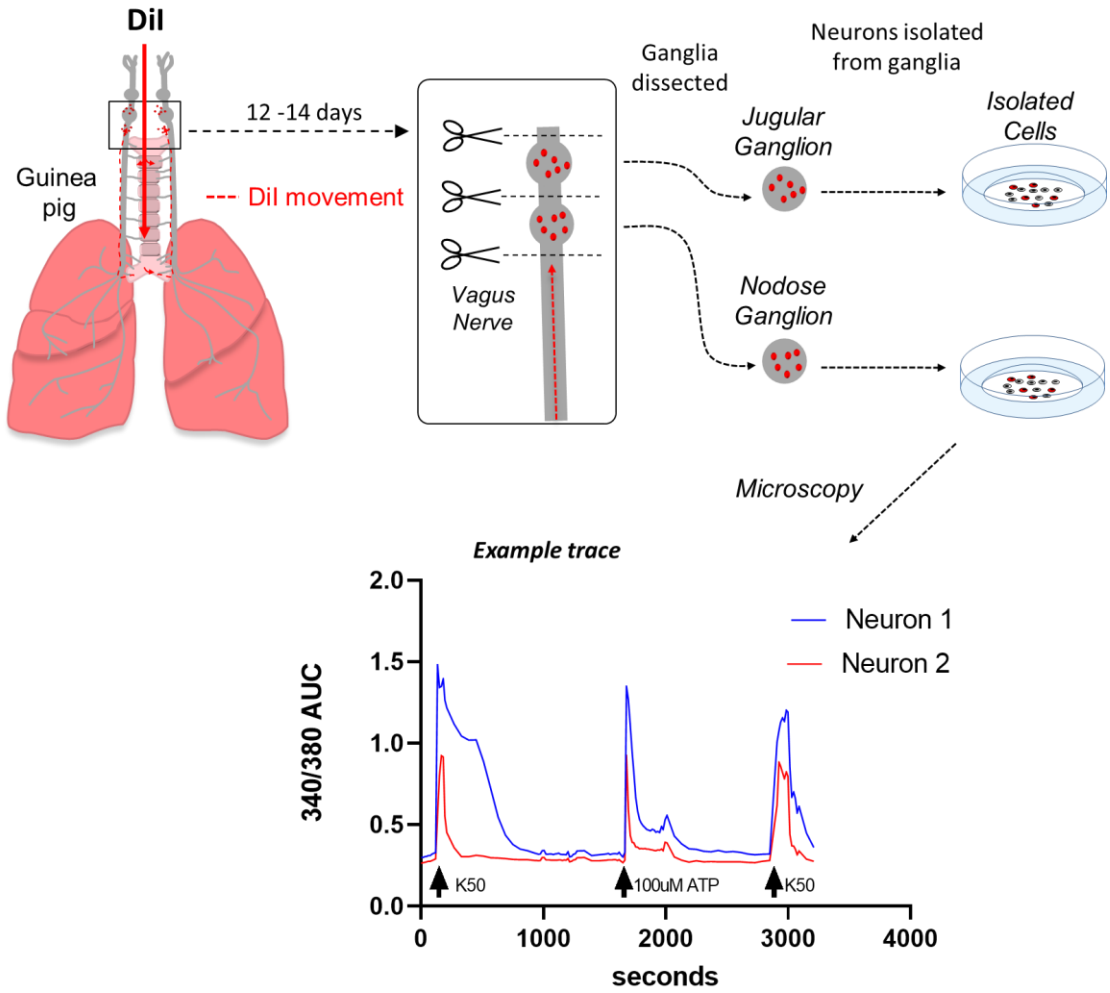


Figure 2. 4 Brief summary of airway terminating-neuron isolation process and calcium imaging example trace.

2.4.2.5 Data analysis

Cells were individually analysed using Fiji analysis software (version 1.53t). Regions of interest were drawn around each cell and the ratio of fluorescence (F340/F380) was calculated over time. Responses were calculated as total Area Under the Curve (A.U.C) which reflects changes in $[Ca^{2+}]_i$ from baseline over time. This was normalised to a percentage of the calcium response (A.U.C) induced by K_{50}.

Chapter 3: Developing Methods to Measure Extracellular ATP in Biological Samples

3.1 Rationale

There is a growing amount of research which suggests that increased levels of extracellular adenosine triphosphate (eATP) in the airways contributes to the pathogenesis and symptoms of chronic lung diseases. For instance, pre-clinical studies have shown that several cell types in the lungs release ATP into the extracellular space (Bonvini et al., 2020, Rahman et al., 2018, Baxter et al., 2014) leading to the activation of purinergic receptors which can subsequently cause activation of inflammatory and neuronal responses involved in chronic lung diseases (Burnstock, 2018).

Clinical data have also highlighted the role of ATP in driving chronic cough as antagonists of purinergic P2X3 receptors present on sensory afferent nerves have shown antitussive efficacy in refractory chronic cough patients in clinical trials (Abdulqawi et al., 2015, McGarvey et al., 2022, Bonvini et al., 2016). However, it remains unclear whether eATP is elevated in the airways of this patient group as this has not yet been measured.

Although increased eATP has been reported in the lungs of asthma (Idzko et al., 2007), Chronic Obstructive Pulmonary Disease (COPD) (Lommatzsch et al., 2010) and Idiopathic Pulmonary Fibrosis (IPF) (Riteau et al., 2010) patients, levels of eATP measured are variable and range from picomolar to micromolar concentrations. These measurements are based on enzymatic luciferin/luciferase assays that give an indirect read out of ATP levels. Across the literature, different techniques, methods and chelating agents are used for the retrieval and assessment of eATP in biological samples which differ in sensitivity and reliability as they are not always reproducible. Accurately measuring eATP is also challenging as it is highly regulated in the extracellular environment by numerous ATPase enzymes, including the CD39 family of ecto-nucleotidases. These enzymes rapidly break down ATP to adenosine diphosphate (ADP) and other breakdown products including adenosine monophosphate (AMP) and adenosine. This often means levels of eATP measured in biological samples such as plasma and bronchoalveolar lavage fluid (BALF) are below the limit of detection and/or not reflective of localised release of eATP levels. Mass spectrometry is an alternative method that could be investigated for the measurement of eATP as well as breakdown products in biological samples.

Given the suggested importance of ATP as a driver of chronic respiratory diseases, accurately measuring eATP in the airways is key to understanding its role in driving the pathophysiology of these conditions. Therefore, the aim of this chapter is to develop a more standardised technique for the

retrieval and accurate assessment of eATP in biological samples which is both reliable and reproducible. The use of the chelating agent ethylenediaminetetraacetic acid (EDTA) which binds to metal ions will be added to biological samples to determine whether EDTA reduces the enzymatic activity of ATPases and thereby reducing eATP breakdown. This is necessary to evaluate whether eATP is elevated in refractory chronic cough patients and in pre-clinical models of airway disease. This could contribute to the use of eATP to determine target engagement of compounds which impact eATP. These eATP measurements could also be used in the clinic as clinical biomarkers to help identify patients with elevated levels of eATP enabling a precision medicine approach to be taken for ATP-targeted treatments.

3.1.1 Chapter hypothesis

Luminescent-based assays can be optimised to measure eATP in mouse, rat and guinea pig plasma and BALF samples with the addition of ethylenediaminetetraacetic acid (EDTA) preventing rapid breakdown of eATP.

3.1.2 Aims

- Determine the sensitivity of commercially available ATP detection assays.
- Determine whether chelating agents can stabilise rapid breakdown of ATP.
- Show that eATP can be reliably measured in the mouse, rat, and guinea pig.
- Confirm luminescence detected is due to eATP using the ecto-nucleotidase enzyme CD39.

3.2 Methods

BALF and plasma samples were taken from male Brown Norway rats, male Dunkin Hartley guinea pigs and male C57/BL6J mice and processed as previously described in section 2.1.2. Samples were taken from these species and strains as they are commonly used in *in vivo* models of airway disease.

The ATP assays described below all utilise the biochemical reaction where luciferase catalyses the reaction of luciferin in the presence of ATP to produce oxyluciferin and light in the form of luminescence. The reaction occurs as follows:

$$\textbf{ATP + D-Luciferin + } O_2 \xrightarrow[Mg^{2+}]{\text{Luciferase}} \textbf{Oxyluciferin + AMP + } CO_2 \textbf{ + Pyrophosphate + Light}$$

The amount of light emitted is directly proportional to the amount of ATP present in the sample.

For all the assays described below, an ATP standard curve consisting of 100pM, 10nM, 100nM, 1µM, 10µM and 100µM of ATP was prepared in sterile water and used to compare the sensitivity of the assays.

3.2.1 ATPlite assay

The ATPlite Luminescence ATP Detection Assay System (PerkinElmer, USA) referred to as the ATPlite kit was performed as per the manufacturer's protocol with modifications detailed in section 2.2.1.

Briefly, bronchoalveolar lavage fluid and plasma samples were thawed on ice. The ATP standard was then prepared by serially diluting the ATP standard stock in sterile water ranging between 100pM – 100µM. 10µl of standard was added to the relevant wells of a black ½ area 96-well optiplate and 10µl of sterile water was added to remaining wells. This was followed by 100µl of media (saline with EDTA) to the standard wells and 100µl of sample to sample wells. Finally, to initiate the reaction, 50µl of the kit's substrate solution was added to all the wells. The plate was then dark adapted for 10 minutes at room temperature prior to being read in the SpectraMax iD5 multi-mode microplate reader.

3.2.2 ATP detection assay

The ATP Detection Assay kit- Luminescence assay (Cayman chemical, USA) referred to as the ATP detection assay was performed as per the manufacturer's protocol with modifications detailed in section 2.3.2.

Briefly, bronchoalveolar lavage fluid and plasma samples were thawed on ice. Next, ATP standard solutions were prepared by serially diluting the ATP standard stock in sterile water ranging between 100pM – 100µM. 10µl of standard was added to the relevant wells of a black ½ area 96-well optiplate and 10µl of sterile water was added to remaining wells. This was followed by 10µl of media (saline with EDTA) to the standard wells and 10µl of sample-to-sample wells. Finally, the reaction mix was prepared using the reagents provided in the kit and 100µl of reaction mix was added to all wells. The plate was then dark adapted for 20 minutes at room temperature prior to being read in the SpectraMax iD5 multi-mode microplate reader.

3.2.3 Hygiena Device

The Hygiena ensure touch luminometer (Hygiena, USA) referred to as the Hygiena device was used as described in section 2.3.3.

Briefly, 25µl of sample was placed in a 2ml Eppendorf tube and measurements were taken by using the Hygiena Ultrasnap swab. The swab was placed into the sample and rotated round 5 times and then placed back into its casing. The top of the swab was then snapped to release the liquid reagent to the bottom of the swab. The casing was then shaken for a few seconds before being placed into the luminometer which provided relative light unit (RLU) measurements from the samples.

3.2.4 Mass spectrometry Analysis

Biological samples collected were sent to collaborators in the Dynamic Omics team at AstraZeneca for mass spectrometry analysis. This was a novel Microfluidic Capillary Electrophoresis–Mass Spectrometry method used which allows measurements of ATP together with its metabolites, ADP, AMP and adenosine. Samples were assessed using a bare-glass ZipChip on a 908-device coupled to a Thermo Scientific ID-X as described in (Di Poto et al., 2024).

3.2.5 Data analysis

The ATP concentrations were interpolated from the ATP standard curve (100pM – 100µM) which was run in duplicate by linearly plotting log (concentration) in the x axis and average RLU in the y axis. All data are presented as mean ± S.E.M.

3.3 Results

3.3.1. Evaluating cross-talk of wells between different plate types using the ATPlite assay

The ATPlite assay is commonly used to measure levels of ATP in samples. However, during testing, well-to-well cross-talk of the luminescent signal was identified as an issue. Therefore, the first step was to examine a range of plate formats to determine which had the least amount of cross-talk between wells (Figure 3.1). Black and white plate types with varying well sizes were tested by measuring levels of luminescence in the wells containing the maximum ATP standard, 100µM ATP (max), wells directly adjacent to the max (next to max) and empty wells (blank).

When comparing RLU values in the blank wells, black plates had the lowest RLU compared to white plates which had an elevated baseline. The RLU values for the wells containing the 100µM ATP maximal response (max) was highest in the black and white isoplates. However, the important variable here was assessing the impact of different plate types on the RLU values in the wells directly adjacent to the maximal response (next to max). The ½ area black optiplates offered the least well-to-well cross-talk, with minimal signal in empty wells adjacent to the maximum ATP concentration (100µM ATP). These plates were therefore selected for future experiments.

A

Black optiplates	Black and white isoplates	½ area black optiplates	½ area white optiplates	White optiplates
				

B

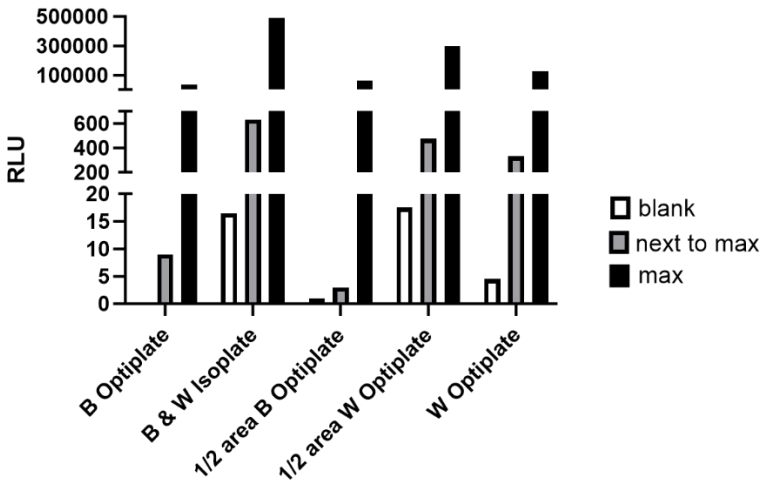


Figure 3. 1 Evaluating the effects of different plate types on cross talk of luminescent signal between wells.

(A) Images of different black [B] and white [W] plate types with standard or ½ area well sizes. (B) Different plate types were tested using an ATP standard curve. The 'blank value' represents the average signal from the blank addition to the standard curve containing no ATP. The 'max' value represents the average signal from the 100µM ATP sample and the 'next to max' value represents the average signal from the empty wells directly adjacent to the 100µM ATP sample well.

3.3.2. Sensitivity of plate-based luminescent assays

To determine which plate-based luminescence assay was more sensitive in measuring levels of ATP, comparisons were made by evaluating an ATP concentration response curve (100pM-100µM) using the ATP detection and ATPlite assay. The effect of time following addition of the reaction mix was also assessed to determine the impact of time on relative light unit (RLU) readings.

In both assays a concentration-dependent increase in luminescence was observed, however the ATP detection assay was more sensitive, with a lower limit of detection (LLOD) of 0.1nM ATP compared to 10nM for the ATPlite assay (Figure 3.2A). The luminescent signal in both assays appeared relatively stable for 20 minutes (Figure 3.2B) which meant that slight variations in read times between plates

did not affect comparability of the data. Given the increased sensitivity of the ATP detection assay, this plate-based assay was used for future experiments.

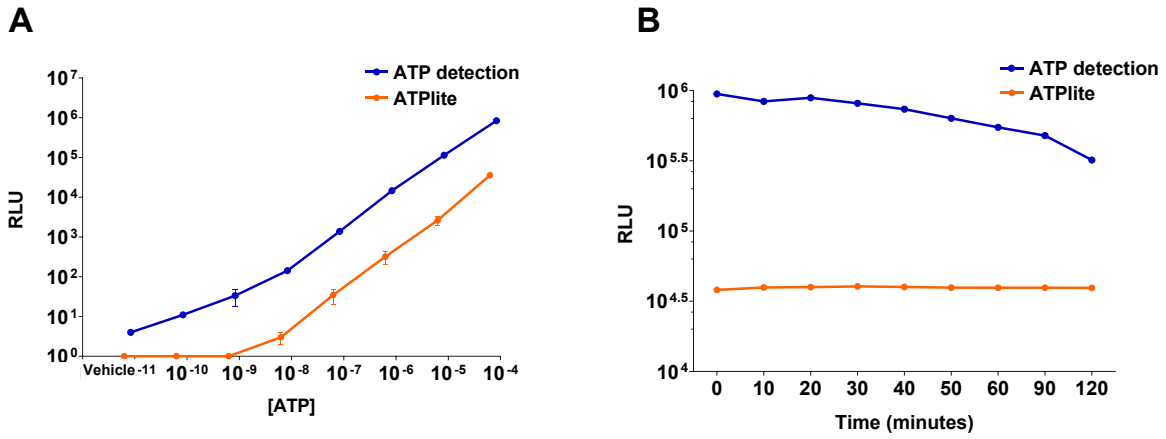


Figure 3. 2 ATP standard curve comparison between plate-based ATP luminescence assays.

(A) Comparisons of ATP concentration response (100pM-100µM) between the ATP detection and ATPlite assay. (B) The effect of time on the luminescent signal from the highest ATP value on the standard curve (100µM ATP). Data presented as Relative Light Units (RLU) N=3.

3.3.3 Comparing the sensitivity of the ATP detection assay to the Hygiena Ultrasnap device

The handheld Hygiena ensure touch luminometer (Hygiena device) is an alternative device also used to measure ATP which is more amenable to measurements in the clinic as it does not require the use of laboratory equipment. The sensitivity of this device was also investigated given its potential use as a point-of-care device for fast measurements of eATP.

The ATP standard curve produced with this device was compared to the ATP detection assay standard curve. The LLOD for the Hygiena device was 10nM, 100-fold less sensitive than the ATP detection assay. Additionally, luminescence values with the Hygiena device reached maximum values after 1µM ATP, indicating a much-reduced range of ATP concentrations compared to the ATP detection assay (Figure 3.3). Although the Hygiena device was not as sensitive as the ATP detection assay, further investigation and comparisons using clinical samples are required to determine whether the Hygiena device can be useful with regards to point-of-care use in the clinic.

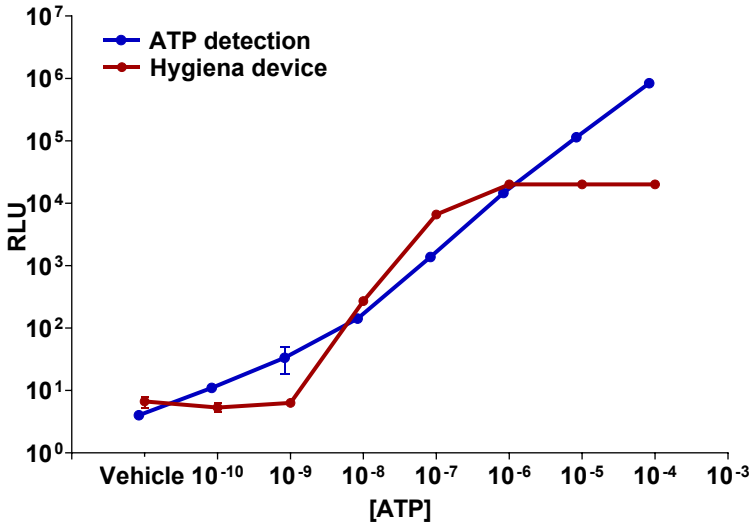


Figure 3. 3 ATP standard curve comparison between the ATP detection assay and Hygiena device.

Comparisons of ATP concentration response (100pM-100µM) between the ATP detection assay and the Hygiena device. Data presented as Relative Light Units (RLU) N=3.

3.3.4 Effects of EDTA on BALF eATP measurements

The next aim was to investigate whether EDTA can prevent rapid breakdown of eATP in biological samples using the ATP detection assay as eATP is rapidly broken down in the extracellular environment by ATPases (Zimmermann et al., 2012). EDTA is a chelating agent which binds metal ions such as calcium which is required for the activity of various enzymes including ATPases. Therefore, the addition of EDTA could potentially reduce the enzymatic activity of ATPases and reduce eATP breakdown. 6mM EDTA was tested as this is the concentration commonly used as an anticoagulant in human blood collection (Banfi et al., 2007).

Initial experiments examined the effects of freeze-thawing on ATP levels as biological samples are frozen soon after collection and stored at -80°C or transported on dry ice until they are thawed for analysis. These samples often go through various freeze/thaw cycles, particularly when experiments are repeated, or different analytes are being assessed. The effect of freeze-thawing on ATP levels was investigated by producing a spiked ATP concentration response curve (100pM-100µM) in saline or saline + 6mM EDTA. Solutions of saline and saline + 6mM EDTA were spiked with ATP at least 24 hours prior to running the assay and then stored at -80°C for at least 24 hours. A fresh ATP concentration response (CR) was prepared just prior to performing the assay. Using the ATP detection assay, lower luminescence was detected in frozen saline, which suggests some ATP degradation does occur once samples are freeze-thawed and this is not completely prevented by 6mM EDTA (Figure 3.4A).

BALF was collected from naïve brown Norway rats using different lavage solutions in the presence or absence of 6mM EDTA. Initially animals were lavaged with saline alone or saline containing 6mM of EDTA. As it is not safe to collect human BALF samples with saline containing EDTA, another group of animals was lavaged with saline alone and then immediately after collection BALF, samples were spiked with 6mM EDTA. This group was included as this is a potential way clinical BALF samples may be collected. BALF samples were then split to prepare a series which were spiked with various ATP concentrations (0.1nM-100µM) before freezing for 24 hours prior to assessment of ATP.

BALF treatment groups consisted of saline-only lavage, saline containing EDTA lavage, and a saline lavage followed by a 6mM EDTA spike once collected. As can be seen in Figure 3.4B, a baseline level of luminescence was recorded, equivalent to approximately 100nM of basal ATP. The ATP detection assay showed that BALF samples containing EDTA had higher levels of luminescence for samples with ATP concentrations below 1µM, suggesting reduced levels of ATP breakdown compared to the saline only lavage group. Including EDTA in the lavage solution did not appear to reduce the level of ATP recorded in BALF samples, compared to the addition of EDTA to lavaged saline solution. Based on this data, future BALF samples were immediately spiked with EDTA post-lavage to give a final concentration of 6mM EDTA.

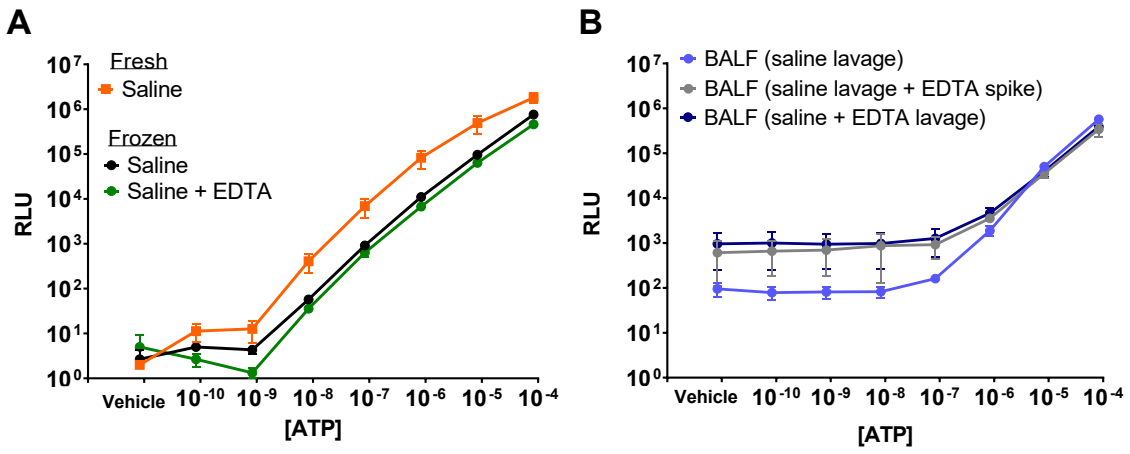


Figure 3. 4 Comparing effects of spiked ATP concentration response (CR) in different BALF treatment groups using the ATP detection assay.

(A) Comparisons between a spiked ATP concentration response (100pM-100µM) prepared 24 hours before the assay (frozen) in saline and saline + EDTA or freshly prepared in saline on the day of the experiment (fresh) N=3. (B) Comparisons between a spiked ATP concentration response (100pM-

100µM) prepared in BALF collected from naïve Brown Norway rats N=3 using saline-only lavage, a saline lavage followed by a EDTA spike once collected or saline containing EDTA lavage, N=3.

3.3.5 Effects of different anticoagulants on plasma eATP measurements

Compared to collection of BALF, blood collection is more routine and less invasive for patients, and plasma can be prepared for relatively easy clinical assessment of various biomarkers in disease. It is unknown whether eATP measurements in the plasma correlate with those in BAL, or whether a systemic measure would correlate with chronic cough or other respiratory disease. However, given the relative ease of access to/availability of samples it was important to establish the best collection method to assess eATP in plasma.

During blood collection anticoagulants are required to prevent blood clotting and ensures that concentrations of substances to be measured is changed as little as possible prior to analysis (Guder et al., 2002). EDTA and heparin are commonly used anticoagulants in blood collection, and final concentrations of 6mM (EDTA) and 50IU/ml (heparin) are sufficient to prevent coagulation (Nigam, 2016). By contrast to EDTA which chelates calcium required for coagulation enzymes, heparin activates antithrombin III, which then inactivates thrombin, factor Xa and other coagulating enzymes (Gray et al., 2012). The effects of heparin were therefore compared to that of EDTA.

A spiked ATP concentration response was prepared in saline containing a final concentration of 6mM EDTA and saline containing a final concentration of 50IU/ml heparin. These were prepared at least 24 hours prior to running the assay and then stored at -80°C. A fresh ATP concentration response (CR) was prepared just prior to performing the assay. Blood samples were collected from naïve Brown Norway rats into either EDTA (6mM final) or heparin (50IU/ml final) coated syringes and then centrifuged to obtain plasma. Plasma samples were then split to prepare a series which were spiked with various ATP concentrations (100pM-100µM) before freezing for 24 hours prior to assessment of ATP.

Using the ATP detection assay, a generally lower luminescent signal was detected in frozen saline + EDTA samples which suggests ATP degradation does occur once samples are freeze-thawed and this is not prevented by EDTA. However, heparin in the absence of ATP appeared to cause a high basal level of luminescence which suggests any signal below approximately 10^2 RLU is caused by heparin as opposed to eATP (Figure 3.5A).

In plasma samples collected in EDTA compared to heparin, a higher baseline level of luminescence was recorded, equivalent to approximately 1µM of ATP, suggesting there is reduced eATP breakdown in the presence of EDTA (Figure 3.5B). Based on this data 6mM EDTA was used going forward for the collection of plasma samples.

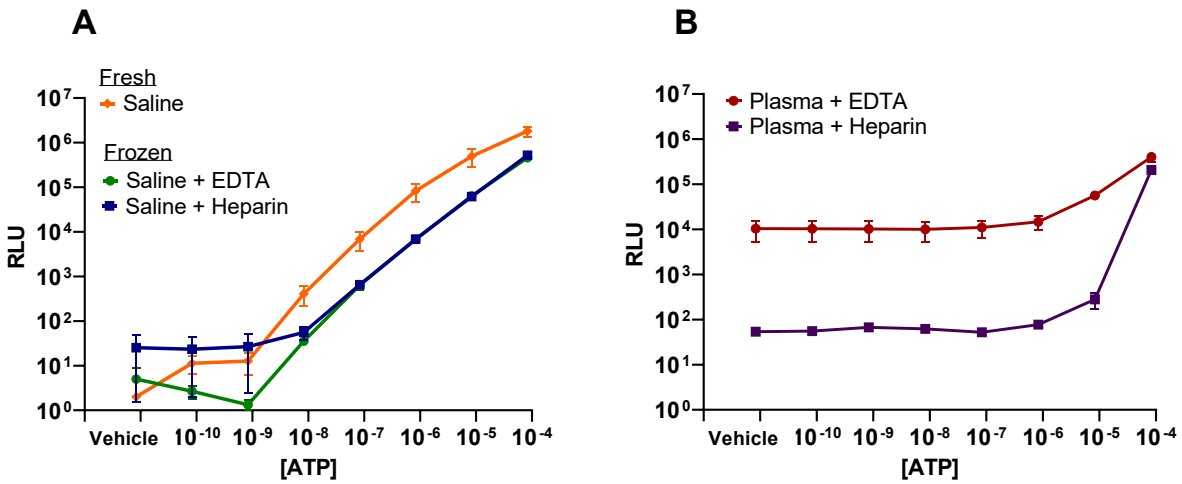


Figure 3. 5 Comparing the effects of spiked ATP concentration response (CR) in different plasma treatment groups using the ATP detection assay.

(A) Comparisons between a spiked ATP concentration response (100pM-100µM) prepared 24 hours before the assay (frozen) in saline + EDTA or saline + heparin, compared to freshly prepared in saline on the day of the experiment (fresh) N=3. (B) Comparisons between a spiked ATP concentration response (100pM-100µM) prepared in plasma collected from naïve Brown Norway rats using EDTA or heparin as the anticoagulant, N=3.

3.3.6 Use of CD39 to confirm luminescent signals

To confirm the luminescence signal observed with the ATP detection assay was reflective of eATP levels, an ecto-nucleotidase enzyme (CD39-His) was added to samples containing either endogenous eATP or a known amount of exogenously spiked ATP. This was tested across BALF and plasma samples from naïve rats, guinea pigs and mice as all three species are commonly used for models of airway disease. Across all species the enzyme was able to breakdown ATP and reduce its detection. The mutant version of the enzyme (CD39-Mut) had no effect (Figure 3.6). This confirms that the luminescent signal observed in biological samples is a measure of eATP levels found in the samples.

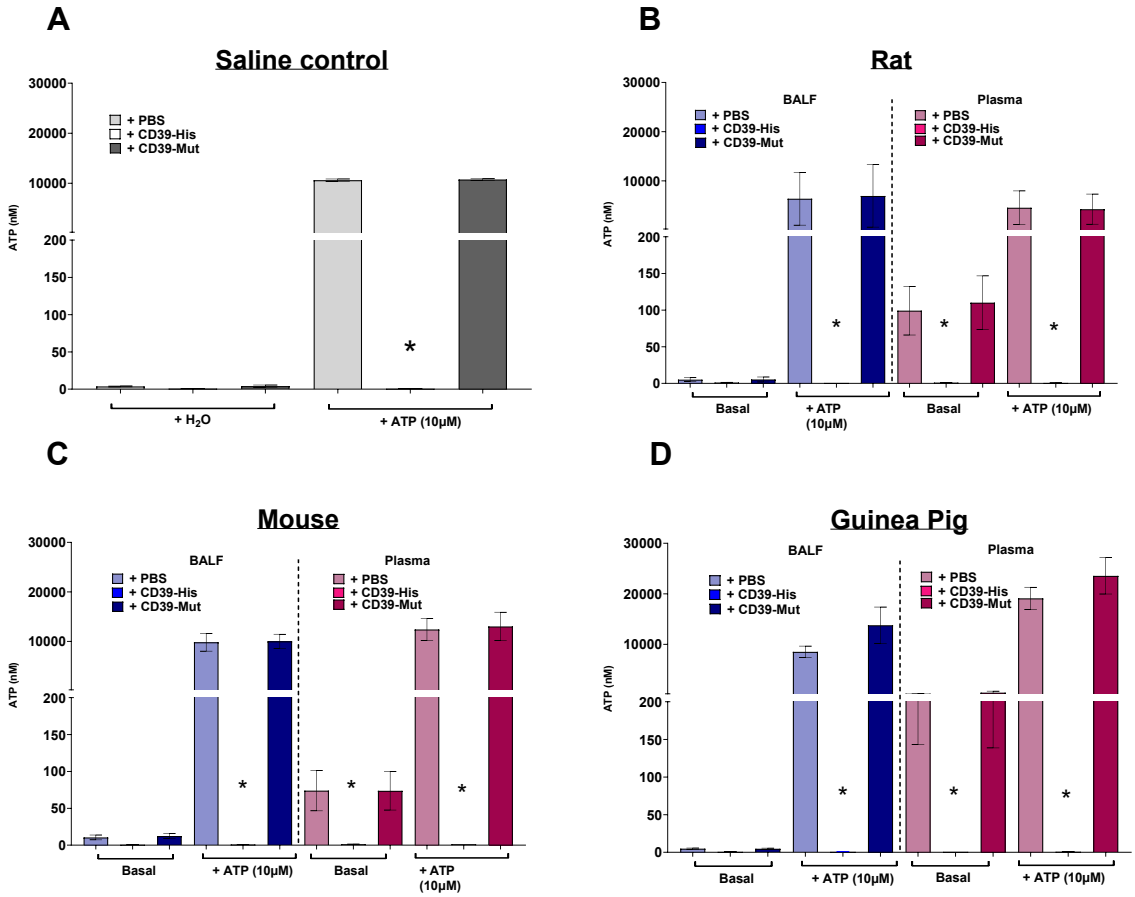


Figure 3. 6 Comparing effects of CD39 on biological samples between different species.

*Saline was used as a control (A) and BALF and plasma samples were taken from naïve rats (B), mice (C) and guinea pigs (D). Samples were spiked with either water or 10µM ATP and incubated with vehicle (PBS), CD39-His (300nM) or the mutant version of CD39 (CD39-Mut) (300nM). Data was collected using the ATP detection assay (N=3 per species). Data shown as mean ± SEM. * indicates significance at p<0.05, one way ANOVA comparing treatment groups within basal and ATP-spiked samples.*

3.3.7 Use of Mass spectrometry to measure ATP and metabolites

Previous data obtained were based on enzymatic luciferase-luciferin reactions where luminescence was used as in indirect read out of ATP levels. However, mass spectrometry has the advantage of direct ATP measurements as well as ATP metabolites such as ADP, AMP and adenosine. Samples were also sent for mass spectrometry analysis as the measurement of ATP and its metabolites is a novel technique being tested by AstraZeneca collaborators in the Dynamic Omics team. This team specialises in proteomics and metabolomics, using state-of-the-art mass spectrometry to identify and quantify proteins, metabolites and lipids in biological samples in order to identify changes that occur during disease or after treatment.

Preliminary data from BALF and plasma samples collected with EDTA showed that adenosine, AMP and ADP could all be detected. This confirms the potential use of mass spectrometry for measuring ATP metabolites in biological fluids collected with EDTA (Figure 3.7). Further investigation using mass spectrometry is required to determine whether it can be used to measure ATP and metabolites in clinical samples.

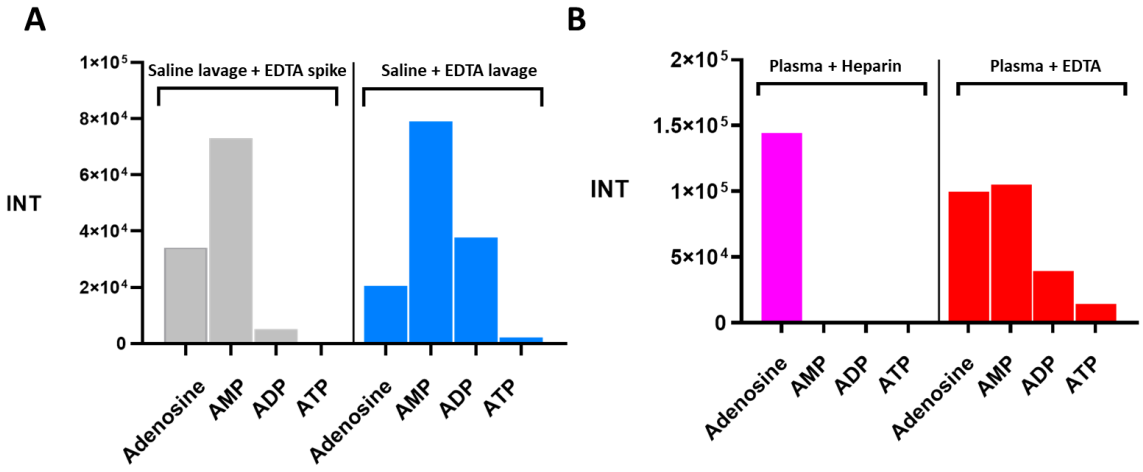


Figure 3. 7 Mass spectrometry analysis of ATP and metabolites from Naïve rat samples.

(A) ATP and metabolites analysis of BALF collected from naïve rat samples using saline lavage followed by an EDTA spike or saline with EDTA lavage. (B) ATP and metabolites analysis of plasma samples collected with heparin or EDTA anticoagulant. N=1, data presented as raw intensity values (INT).

3.4 Discussion

ATP is known to be a key driver of chronic cough as antagonists of the purinergic P2X3 receptors present on afferent sensory nerves have shown unprecedented efficacy in this patient group (Bonvini et al., 2016, McGarvey et al., 2022). However, it is yet to be demonstrated whether these patients show increased levels of ATP in the airways, and therefore, measuring extracellular levels of ATP surrounding the cells within the airways and lungs is key to understanding its role in driving the pathophysiology of these chronic lung diseases.

The aim of this chapter was to develop accurate methods for the recovery and reliable measurement of eATP in biological samples, with the ultimate future aim of demonstrating increased eATP levels in patient samples. Although there are a range of commercially available kits which can measure ATP, they differ in sensitivity and reliability, highlighting the need for a more standardised technique for eATP measurements.

In order to measure eATP levels in the airways and lungs, bronchoalveolar lavage fluid (BALF) samples were chosen. BALF samples are collected by introducing saline through the trachea into the airways and lungs to lavage the lining fluid from the airway lumen. The fluid recovered contains a range of airway lumen constituents, including eATP, at the apical surface of the cells which come into contact with the lavage solution. These samples are then spun down to remove any cells present and the supernatant is used to assess levels of eATP. The key advantage of using BALF is that it can be taken from animal models and from patients in the clinic to allow comparisons between species. Another option might have been to take ATP measurements from lung biopsies. However, these were not performed as these measurements would also include intracellular levels of ATP from lysed cells, whereas a measure of eATP was required to address the hypothesis that it is eATP driving the pathways involved in chronic lung diseases. As ATP is the energy currency of the cell which drives a range of metabolic processes, intracellular ATP levels are relatively high and in the millimolar range (Trautmann, 2009). In comparison, levels of eATP are much lower in the nanomolar range, and this is highly regulated in the extracellular environment by ATPases which rapidly breakdown ATP (Zimmermann et al., 2012). Alongside measuring levels of eATP in the lungs, eATP measurements were performed in plasma samples, as this is a useful indication of systemic levels of eATP circulating around the body to determine whether this is also elevated in lung disease. Again, this had the advantage of translatability between animal and clinical samples.

The first aim of this chapter was to determine the optimal assay, plate type, timing, and anticoagulant to use for sample collection to minimise ATP degradation. It was first important to determine which plate type was suitable to use with the plate-based assays, as cross-talk between wells was observed,

which would lead to inaccurate measures of eATP levels in samples adjacent to wells containing higher levels of eATP. Black ½ area plates had the least amount of cross-talk which meant that an entire 96-well plate could be used to measure samples without the need to leave empty wells to prevent bleed-over of the luminescent signal (Figure 3.1B).

The sensitivities of the assays were also investigated by determining the lower limit of detection (LLOD) and upper limit of detection (ULOD) of ATP. This was important as the levels of eATP found in BALF samples were likely to be low and in the nanomolar range. The commercially available plate-based assay method of ATP detection using the ATP detection assay was more sensitive with a LLOD of 0.1nM compared to the comparator kit, ATPlite assay which had a LLOD of 10nM (Figure 3.2A). The ATP detection assay also had the advantage of requiring only 10µl of sample compared to the ATPlite assay which required 100µl of sample. This is useful as the volume of biological samples recovered from animal models, particularly mouse models are relatively low.

The sensitivity of the hand-held Hygiena device was also investigated. Although this device has the advantage of immediate sample measurements, which could be key in the clinic, it had a LLOD of 10nM, 100-fold less sensitive than the ATP detection assay and reached maximum luminescent values (ULOD) after 1µM ATP, indicating a much-reduced detection range of ATP concentrations (Figure 3.3).

The different characteristics of each method are summarised in table 3.1. With regards to ease-of-use, the plate-based assays also require a trained individual to perform the assay as solutions have to be prepared and the use of laboratory equipment such as pipettes and a plate reader are required. In comparison, the Hygiena device is relatively easy to use as it does not require the use of laboratory equipment, solutions used to perform the assay are already provided within the ultrasnap swab and fast RLU read outs are obtained from placing the swab into the luminometer device. Although the Hygiena device is not as sensitive as the ATP detection assay, it does not require the use of laboratory equipment, and therefore further investigation and comparisons using clinical samples are required to determine whether the Hygiena device can be useful with regards to point-of-care use in the clinic.

Method	Format	LLOD	ULOD	Ease of use	Standardised
ATP detection assay	plate-based	0.1nM	100µM	No	Yes
Hygiena device	Hand-held device	10nM	1µM	Yes	No
ATPlite assay	Plate-based	10nM	100µM	No	Yes

Table 3. 1 Comparison of characteristics for the different luciferin/luciferase methods used to measure ATP.

Another major challenge with measuring eATP in biological samples is how rapidly it is broken down by extracellular ATPases and ADPases (Kaczmarek et al., 1996, Picher et al., 2003). The effects of EDTA, which is a well-known anticoagulant that has been in use since the early 1950's was investigated. EDTA works as a chelating agent that binds metal ions such as calcium which is necessary for a wide range of enzymatic reactions, such as those in the blood coagulation cascade (Banfi et al., 2007). It was found that 6mM EDTA which is the concentration used to prevent blood coagulation and ATP breakdown in human blood samples (Wood et al., 2009) could reduce rapid breakdown of eATP in both BALF and plasma samples. This is presumably by preventing enzymatic reactions that cause rapid breakdown of eATP.

Based on these findings BALF and plasma samples were taken using 6mM EDTA from naïve rats, guinea pigs and mice as all three species are commonly used for models of airway disease. CD39-His, an ecto-nucleotidase enzyme able to breakdown ATP was added to samples containing either endogenous eATP or a known amount of exogenously spiked ATP in order to confirm that the luminescence signal observed with the ATP detection assay was reflective of eATP levels. Across all species the enzyme was able to breakdown ATP and reduce its detection confirming that the luminescent signal observed correlates with eATP levels found in the samples (Figure 3.6).

Given that luciferase-luciferin assays can only be used to indirectly measure levels of ATP, the use of mass spectrometry to measure ATP and its metabolites in biological samples was investigated in collaboration with the Dynamic Omics team at AstraZeneca. Preliminary data found that ATP metabolites could be detected in naïve rat BALF and plasma samples collected with EDTA (Figure 3.7). However, very little ATP was detected which suggests that the majority of ATP may have been broken down prior to assessment. Therefore, this technique may only be useful to assess levels of ATP metabolites in pre-clinical disease models and clinical samples.

Overall, the data suggests that recovering BALF and blood in EDTA aids the recovery of eATP in biological samples. Furthermore, the ATP detection assay allows reproducible detection of eATP levels in the nanomolar range. Therefore, the hypothesis that luminescent-based assays can be optimised to measure eATP in biological samples with the addition of EDTA preventing rapid breakdown of eATP can be accepted.

This technique will be used to evaluate eATP release in pre-clinical disease models which could provide additional evidence for eATP associated mechanisms driving chronic lung diseases. Clinically, this could allow for investigation into levels of eATP in patients with chronic respiratory diseases. These patient sample measurements could be used to identify patients with high levels of eATP and could therefore allow a precision medicine approach to be taken. This could be utilised in patients with

chronic cough, where patient populations thought to be more likely to respond to P2X3 antagonists and other ATP-targeted therapies can be identified.

In addition to assessing levels of eATP in driving chronic lung diseases such as chronic cough, the next chapter aims to provide complimentary evidence for the role of endogenous ATP in activating airway sensory nerves that lead to the cough reflex. Pharmacological intervention studies will also be used to investigate the role of endogenous ATP and the efficacy of clinically relevant compounds in a number of model systems.

Chapter 4: Investigating Extracellular ATP in Airway Sensory Nerves

4.1 Rationale

ATP is known to be a key driver of chronic cough which is defined as excessive and/or inappropriately activated cough occurring for more than 8 weeks. Chronic cough can occur as a symptom of respiratory disease or can have undetermined aetiology referred to as unexplained chronic cough (UCC). Cough that persists despite treatments targeting those with underlying respiratory disease is described as refractory chronic cough (RCC).The role of ATP in UCC and RCC is supported by the antitussive effects of drugs that block purinergic P2X3 receptors which are activated by ATP. For example, Gefapixant, a non-selective P2X2/3 antagonist, has shown some efficacy in large scale clinical trials and is currently under evaluation for FDA and Medicines and Healthcare products Regulatory Agency (MHRA) approval (Smith et al., 2020b, McGarvey et al., 2022). A more selective P2X3 antagonist, BLU-5937 (Bellus Health) has also shown antitussive efficacy in RCC patients (Birring et al., 2022). These clinical data suggest ATP plays a key role in activation of purinergic receptors and subsequent neuronal responses such as the cough reflex.

Cough is driven by the activation of P2X3 purinergic receptors present on airway-innervating sensory nerves, which are housed within the vagus nerve (Brouns et al., 2012). The cell bodies of these nerves can be found in the jugular and nodose ganglia of the vagus nerve (Mazzone and Undem, 2016). Pre-clinical studies have demonstrated that airway afferent nerves can be activated by indirect release of ATP through activation of the TRPV4 receptor using the TRPV4 agonist GSK1016790A (GSK101), and directly through the metabolically stable analogue of ATP, αβMe-ATP (Bonvini et al., 2016).

Given that the clinical data suggests endogenous ATP is driving cough, more research is needed to demonstrate the ability of ATP (rather than analogues) to activate airway sensory nerves. The aim of this chapter is to investigate whether ATP can elicit effects in airway sensory nerves, similar to its more stable analogue αβMe-ATP. If so, then the pharmacology of ATP and the mechanisms driving airway sensory nerve activation will be further investigated.

In order to test this, the clinical P2X2/3 antagonist Gefapixant, as well as the pre-clinical tool AF-353 (an analogue of Gefapixant) will be investigated to determine their effect on ATP-induced activation of airway sensory nerves. These results could allow a better understanding of the pharmacological effects of endogenous ATP and its role in the activation of airway sensory nerves.

4.1.1 Chapter hypothesis

Airway sensory nerves from guinea pig and human tissue are activated by the endogenous ligand ATP, and this activation can be blocked using P2X3 receptor antagonists.

4.1.2 Aims

- Determine whether the endogenous ligand ATP is able to elicit an effect on guinea pig and human airway sensory nerves.
- Investigate the pharmacology of ATP on guinea pig and human airway sensory nerves using P2X3 antagonists in *in vitro* and *ex vivo* pre-clinical nerve recording models.

4.2 Methods

4.2.1 Calcium imaging of airway sensory nerves

Male Dunkin Hartley guinea pigs were dosed with 1 ml/kg of 0.25 mg/ml of the retrograde tracer dye DiI 14 days prior to experimentation to ensure staining of airway specific neurons by retrograde transport (Dubuis et al., 2013). The nodose and jugular ganglia were then dissected out and enzymatically digested as previously described in section 2.4.2. Neurons were placed into poly-D-lysine (100µg/ml) and laminin (75µg/ml) coated fluorodishes (0.17 mm thick optical quality glass bottom) and left to adhere for at least 12 hours in an incubator (37°C, 5% CO_2/95% O_2) in complete F12 medium.

Prior to experimentation, cells were loaded with a calcium dye (Fura2-AM) for 40 minutes at room temperature in the dark. This was followed by a de-esterification step for 30 minutes at room temperature in the dark. After several washes with Extracellular solution (ECS), the fluorodishes were mounted onto a widefield inverted microscope and neurons were excited sequentially with 340nm and 380nm light wavelengths and the emission signals recorded at 520nm as described in section 2.4.2.4. Changes in intracellular Ca^{2+} ($[Ca^{2+}]_i$) responses were investigated as previously described (Dubuis et al., 2013, Grace et al., 2012).

4.2.1.1 Agonist Concentration Response Curves

To investigate the effects of ATP on changes in $[Ca^{2+}]_i$ signal in the nodose and jugular ganglia, the following experimental protocol was followed. For all recordings, neurons were initially exposed to a hyper-potassium solution (50mM potassium chloride; K_{50}) for 30 seconds to trigger an increase in intracellular calcium levels which was used as a control response to assess neuron viability and against which all other responses were normalised. Once intracellular calcium levels had returned to baseline, drugs were perfused through a solution-changing perfusion system and changes in $[Ca^{2+}]_i$ were recorded. Cells were washed a minimum of 6 times following addition of each drug until baseline was reached. K_{50} was also applied at the end of the recording to ensure cell viability. Initially a concentration response to ATP was performed by addition of either vehicle (dH_2O), 0.1µM, 1µM, 10µM, 100µM or 1000µM ATP for 3 minutes. Only one ATP concentration was tested per dish as repeated exposures would increase the risk of photobleaching whereby increased light exposure could cause fading of the fluorescent signal.

4.2.1.2 Data Analysis

Cells with a diameter of over 20µM were used for analysis as these were more likely to be sensory neurons (Hunter et al., 2000). Changes in $[Ca^{2+}]_i$ induced by the agonists were calculated as the total

area under the curve, (A.U.C) of the fluorescence ratio over time from resting level. Responses were then normalised as a percentage of the initial K_{50} response and expressed as mean ± SEM, with statistical significance set at $P < 0.05$.

4.2.2 *In vitro* isolated vagus nerve recordings

Guinea pig vagal nerve trunks were dissected free from surrounding tissue, de-sheathed and maintained in modified Krebs-Henseleit (KH) buffer and bubbled with 95% O2 / 5% CO2. The isolated vagus nerve trunk was placed into a grease gap recording chamber, and depolarisation was recorded as previously described in section 2.4.1. Sub-maximal concentrations of agonists were previously determined from agonist concentration response curves previously carried out in this system (Bonvini et al., 2016). Key experiments were also repeated using human vagus nerve derived from a deceased 65-year-old female donor, who was diagnosed with COPD.

4.2.2.1 Agonist concentration response curves

To determine if ATP caused vagus nerve depolarisation, non-cumulative concentrations of either vehicle (dH_2O), 10µM, 30µM, 100µM, 300µM or 1000µM ATP were applied to the vagus nerve. A sub-maximal ATP concentration was used for antagonist studies.

4.3.2.2 Antagonist concentration response curves

A concentration response (0.01µM - 10µM) of non-selective P2X3 (clinically relevant Gefapixant and preclinical tool AF-353) or vehicle (0.1% DMSO) were measured against the sub-maximal concentrations of ATP (100µM) or the TRPV4 agonist, GSK1016790A (GSK101, 300nM) induced depolarisation. These concentrations were based on previous experiments performed in this system and by other groups (Bonvini et al., 2016, Garceau and Chauret, 2019).

Briefly, two reproducible agonist responses were established, followed by incubation with a single concentration of antagonist for 10 minutes and then re-stimulation of the nerve with agonist in the presence of antagonist to determine inhibition of the response. Nerves were then washed with Krebs until baseline was reached, followed by a final agonist response to ensure the nerve was still viable.

4.3.2.3 Data Analysis

Nerve depolarisation was assessed by measuring the peak amplitude of the response in millivolts (mV). The approximate IC_{50} and PIC_{50} values were calculated for each antagonist. All data are presented as mean ± S.E.M, with statistical significance set at $P < 0.05$.

4.2.3 Electrophysiological tracheal recording of the Recurrent Laryngeal Nerve

In addition to measuring nerve activity of receptors expressed along the vagus axon, electrophysiological tracheal recording (eTRec) is an *ex vivo* technique that can be used to measure nerve activity evoked from peripheral airway sensory nerve terminals. This is a more physiologically relevant setting as the trachea is constantly perfused with KH solution, to which drugs can be added to act on peripheral nerve terminals *in situ* within the tracheal lumen. Compound action potentials are then measured within the recurrent laryngeal nerve (RLN) which is a branch of the vagus nerve that innervates the upper airways (Figure 4.1).

4.2.3.1 Electrophysiological tracheal recording of the RLN set-up

Male Dunkin-Hartley guinea pigs (350 – 400g) were euthanised as described in section 2.1.2. The larynx, trachea, oesophagus, heart, lungs and innervating nerves from the vagal ganglia down to the superior mediastinum were dissected out *en bloc*. Care was taken to ensure all the nerve connections remained intact whilst any remaining connective tissue was removed. Heart, oesophagus, lung lobes, arteries and veins were carefully removed while preserving the innervation. All nerves connected to these organs were cut. The recurrent laryngeal nerve was exposed where it branches to the vagus nerve and the nerve bundles were carefully separated and held in place with micro-pins on a silicone block. A similar technique was used as previously described (Ricco et al., 1996). The trachea, primary bronchi and vagus nerves were part of the preparation. The left superior laryngeal nerve (SLN) and inferior branches of the laryngeal nerve and the left and right recurrent laryngeal nerve were also left intact. These tissues were placed inside a custom-made perspex bath and immersed in oxygenated KH solution at a pH of 7.4.

The airways were perfused with KH solution or drugs via cannulation of the larynx and bronchi at a rate of 2ml per minute and collected in a waste trap. Drugs were prepared in 37°C Krebs-Henseleit (KH) solution (containing, in mM: NaCl 118; KCl 5.9; $MgSO_4$ 1.2; $CaCl_2$ 2.5; NaH_2PO_4 1.2; $NaHCO_3$ 25.5 and glucose 5.6; pH 7.4) and bubbled with 95% O_2 / 5% CO_2.The tissues within the bath were separately perfused with KH solution at a rate of 10ml per minute. All solutions used were maintained at 37°C using an automated heating controller (TC-344C Warner Instruments, UK).

The left RLN was cut close to where it branches from the vagus nerve and the nerve bundles were carefully separated and held in place with micro-pins on a silicone block. A recording suction electrode made from a heat-pulled (narishige PC-10 puller) and fire polished (Narishige MF-900 Microforge) (tip 200-300 µm Int. Ø) borosilicate glass capillary (1.5 mm Ext. Ø, 1.17 mm Int. Ø; no inner filament; Clark glass capillary, Warner Instruments) that was pre-filled with KH solution was applied to each bundle sequentially until identification of the tracheal sensory bundle (increased firing in response to K_{50}

perfused in the tracheal lumen). The lumen was washed off with KH until its firing returned to normal after each application. Once the recording electrode was connected to the sensory bundle, the preparation was left to rest for 20 minutes. The reference electrode was placed in a side chamber filled with KH and connected to the bath by an agar bridge. Recording electrodes had a silver/silver-chloride filament and was inserted in a precision-made holder (QSW-M20P, Warner Instruments) connected to a recording headstage (NL100AK Neurolog headstage, Digitimer; FL, USA) and a neurology extracellular action potential recording system. The electrode was positioned using a thin three-Axis Coarse/Fine Micromanipulator (Narishige M-3333, Japan). The reference electrode was a silver/silver-chloride pellet electrode (WPI) connected to the recording headstage.

The difference in potential (µV) between the electrodes was recorded by connecting them to a pre-amplified headstage (NL104A – AC Preamplifier, Digitimer; FL, USA). Signals received were amplified (x10,000; NL106 – AC/DC Amplifier, Digitimer) and filtered (NL125 – Band-Pass Filter, Digitimer set to 500Hz High Pass and 2000Hz low pass). Any mains electrical 50 Hz interference was removed using a noise eliminator (Humbug, Digitimer; FL, USA). The output was converted to a digital signal at 50kHz and analysed with Spike 2 software (Cambridge Electronic Design Limited; Cambridge, England).

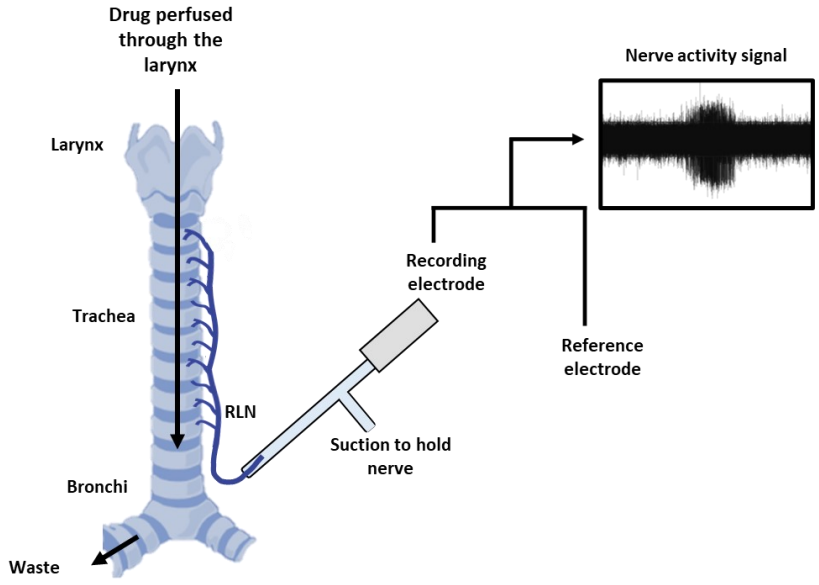


Figure 4. 1 A schematic to demonstrate the set-up of the electrophysiological tracheal recording system as it records recurrent laryngeal nerve (RLN) activity.

4.2.3.2 Interpretation of RLN recordings

Key differences between the isolated vagus nerve system and eTRec recordings of RLN (a distal branch of the vagus nerve in the upper airways) are that drugs used to activate the RLN are perfused through the trachea where they act on peripheral airway sensory nerve terminals within the trachea.

Additionally, in the isolated vagus nerve system, a localised depolarisation is measured (which may or may not represent action potential firing), whereas in eTrec the suction electrode records action potentials which have propagated along the nerve from the peripheral terminals in the trachea. The eTrec recorded signal therefore represents compound action potential firing initiated from the peripheral terminals of tracheal afferents.

4.2.3.3 Concentration response protocol

Initially to generate a positive control response, capsaicin (0.3µM) was perfused through the trachea for 2 minutes to confirm viability of the nerve. Following a wash-off period and once nerve firing had reached background activity, vehicle (0.1% dH_2O) and various concentrations of ATP (1µM-1mM), or vehicle (0.1% DMSO) and various concentrations of GSK101 (0.1-100nM) were applied in sequence, each for 10 min followed by a wash to baseline in order to determine their effect on nerve activity. A final application of capsaicin (0.3µM) was performed to confirm nerve viability.

4.2.3.4 Antagonist response protocol

A positive control response to capsaicin (0.3µM) was determined by perfusing capsaicin through the trachea for 2 minutes to confirm viability of the nerve. Following a wash-off period and once nerve firing had reached background activity, ATP (100µM) or GSK101 (300nM) was perfused through the trachea for 10 minutes followed by a wash-off period. This response was repeated and following wash off the trachea was perfused with the antagonist AF-353 for 10 minutes. ATP or GSK101 with AF-353 was then perfused through the trachea to assess inhibition of the antagonist and following 30 minutes of wash-off of all compounds, a final stimulation with ATP or GSK101 was applied to confirm nerve viability.

4.2.3.5 Data analysis

The effect of drugs were determined by subtracting the nerve mass activity of the RLN recorded prior to the addition of drugs from the nerve mass activity of the RLN whilst the trachea was perfused with a drug for the same amount of time (i.e. Δ NMA =.$\int^{test}$(Abs(µV)).sec.- $\int^{control}$(Abs(µV)).sec.). All data are presented as mean ± S.E.M, with statistical significance set at $P < 0.05$.

4.3 Results

4.3.1. Effects of ATP on $[Ca^{2+}]_i$ in guinea pig jugular and nodose airway-specific ganglia neurons and single cell expression data

The functional effects of ATP were investigated by measuring changes in $[Ca^{2+}]_i$ in jugular and nodose airway-specific ganglia neurons. These tissues were used as they contain the cell bodies of airway terminating vagal fibres which may mediate the cough reflex. A vehicle response (0.1% dH_2O) and a concentration range of ATP (0.1 - 1000µM) were tested in dishes containing jugular or nodose ganglia airway-specific neurons. ATP-induced a concentration-dependent increase in $[Ca^{2+}]_i$ which is indicative of activation of the neurons in both airway specific jugular and nodose ganglia neurons (Figure 4.2). However, αβMe-ATP-induced a concentration-dependent increase in $[Ca^{2+}]_i$ in airway specific nodose neurons but not in jugular neurons which is similar to the responses shown with the TRPV4 agonist, GSK101 (Bonvini et al., 2016).

Nodose and jugular neurons from a single naïve guinea pig were also sent for next generational RNA sequencing which showed that 2/11 and 4/11 jugular neurons expressed P2X2 and P2X3 respectively. All 10 nodose neurons sequenced expressed P2X2 and P2X3 (Figure 4.2D). Despite differences in receptor expression, both airway specific jugular and nodose ganglia neurons responded similarly to ATP in a concentration-dependent manner.

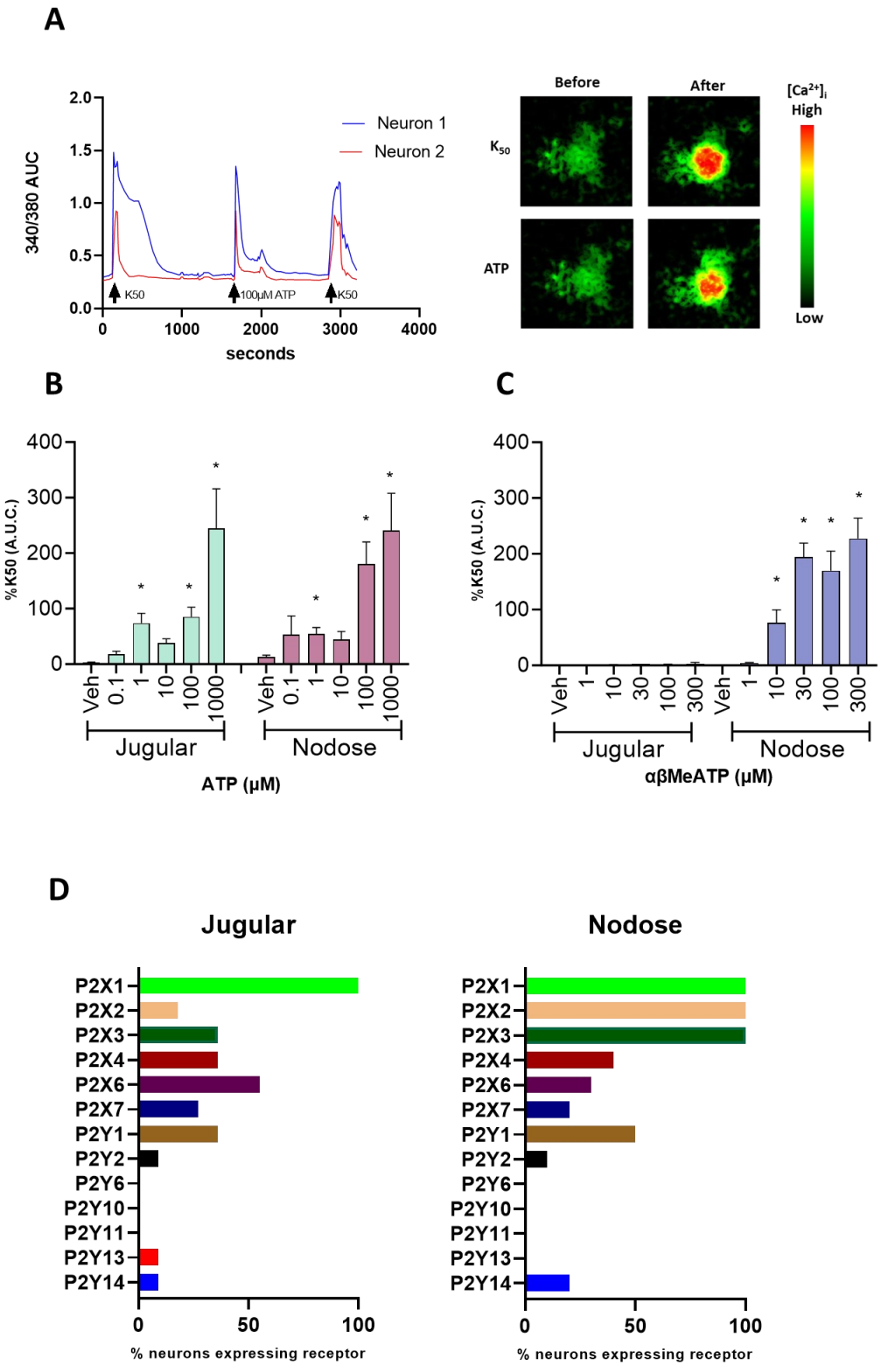


Figure 4. 2 Effect of ATP and αßMe-ATP concentration response on intracellular calcium levels in guinea pig jugular and nodose airway neurons and purinergic receptor expression.

(A) Example trace and image of intracellular calcium responses in two isolated airway-specific nodose neurons. Traces show the ratio of the light intensity emitted by calcium-bound/unbound Fura2 by

*sequentially exposing neurons to λ = 340nm and λ = 380nm and respectively measuring the light emitted at λ = 520nm. Neurons were exposed to K_{50} followed by ATP (100μM) and a final K_{50} response to ensure cell viability. Summary data of $[Ca^{2+}]_i$ increases induced by vehicle (0.1% dH_2O) or (B) ATP (0.1 – 1000μM) N=3-8 or (C) αβMe-ATP (1-300μM) N=3-4 in jugular and nodose neurons measured as area under curve (A.U.C) and normalised as a percentage of the response to K_{50} (%K_{50}). Data shown as mean ± SEM. * indicates statistical significance at p<0.05 using Kruskal Wallis test and Dunns post-test comparing responses to vehicle. (D) Single cell purinergic receptor expression data from 11 jugular and 10 nodose neurons from a naïve male Dunkin-Hartley guinea pig N=1. Data presented a % neurons expressing a receptor.*

4.3.2. Effects of ATP concentration response on guinea pig vagus nerve

Having shown that ATP activates airway terminating vagal neurons, the effects of ATP on whole vagus nerve segments was assessed using the *in vitro* isolated vagus nerve recording technique performed using vagus nerves from naïve guinea pigs. This technique was used to determine the effect of ATP on all the nerve fibres contained within the vagus nerve (not just airway-terminating nerves) but is amenable to higher throughput pharmacological investigation.

A vehicle response (0.1% dH_2O) and an ATP concentration response (10μM – 1mM) was performed and showed that ATP caused depolarisation of vagal sensory afferent nerve fibres in a concentration-dependent manner (Figure 4.3). A similar concentration-dependent increase in depolarisation was seen with αβMe-ATP and the TRPV4 agonist GSK101 (Bonvini et al., 2016).

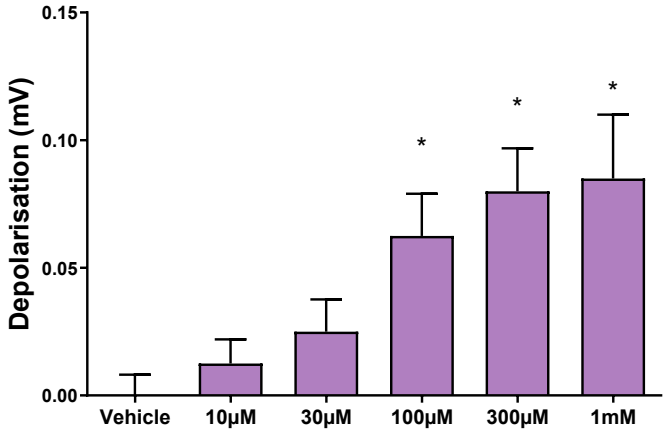


Figure 4. 3 Effect of ATP concentration response on guinea pig vagal nerve depolarisation.

*Effect of vehicle (0.1% dH_2O) and an ATP concentration response (10μM – 1mM) on depolarisation of guinea pig vagus nerve, N=4, data shown as mean ± SEM. * indicates statistical significance at p<0.05 using Kruskal Wallis test and Dunns post-test comparing responses to vehicle.*

4.3.3 Effects of ATP on guinea pig recurrent laryngeal nerve

In addition to measuring activation of receptors expressed on airway-specific neurons and the neuronal axon of the vagus nerve, the *ex vivo* electrophysiological tracheal recording (eTRec) system can be used to measure effects of ATP on nerve terminals. eTRec measures the activation of a branch of the vagus, the recurrent laryngeal nerve (RLN) which innervate the upper airways. This trachea-attached nerve recording technique has the advantage of being able to measure nerve activity following activation of receptors on the peripheral nerve termini within the tracheal lumen as drugs are perfused through the trachea.

Having shown that ATP can directly cause activation of isolated airway-specific neurons, and isolated vagus nerves, this technique was used to examine whether the endogenous ligand ATP administered to the peripheral nerve terminals in the trachea could elicit activation of airway sensory nerves of the recurrent laryngeal nerve (RLN). ATP did cause a concentration-dependent increase in neuronal mass activity in this system, demonstrating that the endogenous ligand ATP can elicit airway sensory nerve firing when administered to the nerve terminals in the trachea (Figure 4.4A-B). The effects of αβMe-ATP were also assessed as a comparator and caused activation of RLN airway nerves as expected (Figure 4.4C).

Previous publications from the group have also shown that the TRPV4 agonist GSK101 causes depolarisation of the vagus nerve in a concentration-dependent manner via the release of ATP and subsequent activation of P2X3, known as the TRPV4-ATP-P2X3 axis (Bonvini et al., 2016). Using the eTRec system, the effects of the TRPV4 agonist GSK101 were also examined. The activation of TRPV4 by GSK101 caused activation of RLN airway nerves, similar to the direct application of ATP (Figure 4.4D).

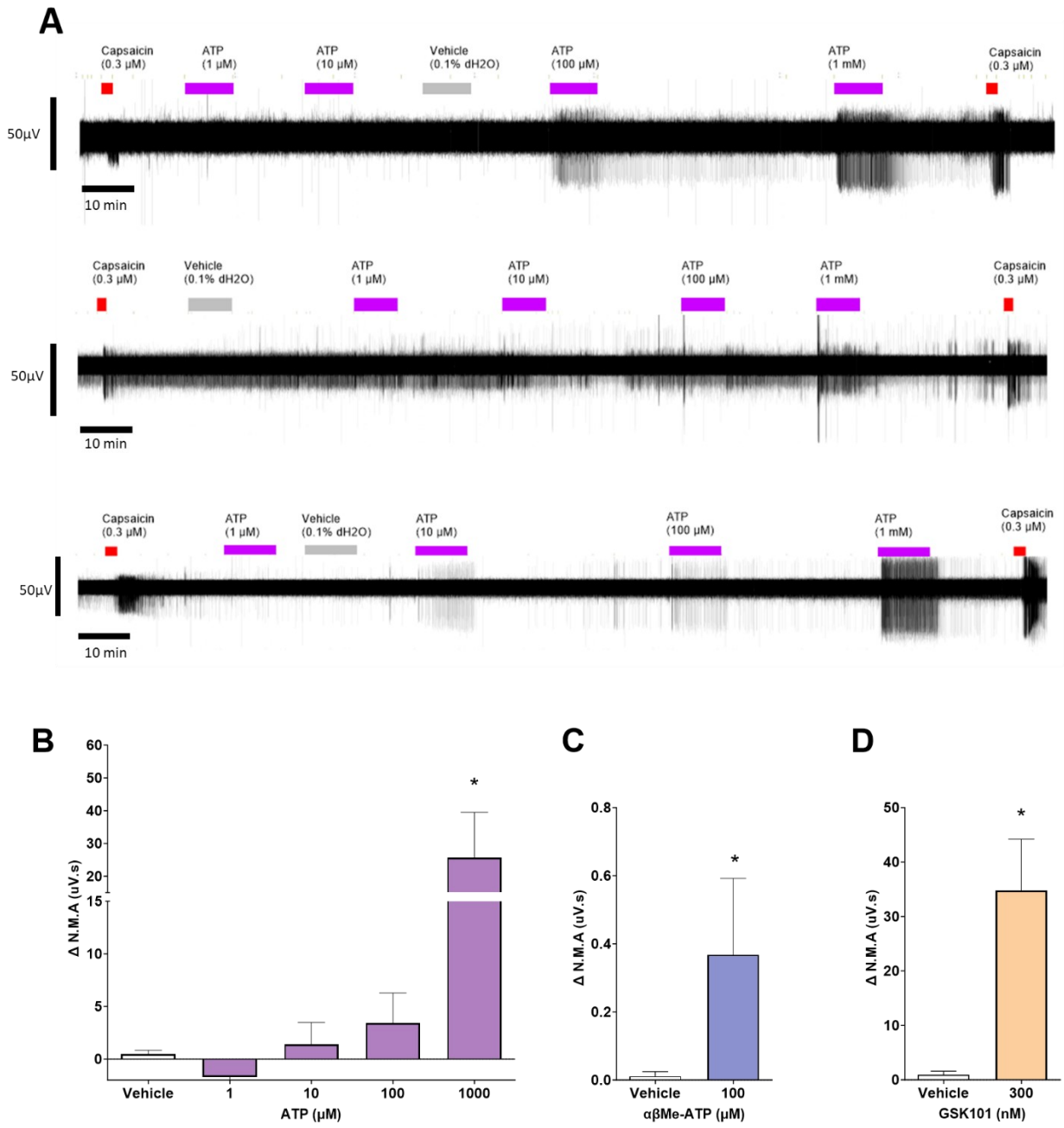


Figure 4. 4 Effect of ATP, αβMe-ATP and GSK1016790A on guinea pig RLN activity.

*(A) Example traces of ATP concentration response (10μM – 1mM ATP), and summary graphs showing the effect of (B) vehicle (0.1% dH_2O) or ATP (1μM – 1mM ATP), (C) vehicle (0.1% dH_2O) or αβMe-ATP (100μM), (D) vehicle (0.1% DMSO) or GSK101 (300nM) on trachea-attached guinea pig recurrent laryngeal nerve. Data presented as delta nerve mass activity where background activity is recorded prior to the addition of drug for the same amount of time and subtracted from drug responses. N=3, data shown as mean ± SEM. * indicates statistical significance at p<0.05 using Kruskal Wallis test and Dunns post-test comparing responses to vehicle.*

4.3.4 Effects of P2X3 antagonists on direct and indirect ATP-induced guinea pig vagus nerve depolarisation

Having shown that ATP causes depolarisation and firing of airway sensory nerves using 3 different techniques, the effects of a pre-clinical and a clinical P2X3 antagonist against direct ATP-induced vagus nerve depolarisation were examined to confirm that the depolarisation observed was via the sensory nerve receptors for ATP. Additionally, the effect of the P2X3 antagonists on TRPV4 agonist-induced depolarisation were examined, to compare the effects of the pre-clinical and clinical antagonist on the endogenously released ATP following activation of TRPV4.

The effect of vehicle (0.1% DMSO) or increasing concentrations (0.01-10µM) of the non-selective P2X3 antagonists Gefapixant and AF-353 (analogue of Gefapixant) on depolarisation induced by a sub-maximal concentration of 100µM ATP or 300nM GSK101 were examined. Concentration-dependent inhibition of both TRPV4 and ATP-induced vagus nerve depolarisation were observed with both P2X3 antagonists (Figure 4.5).

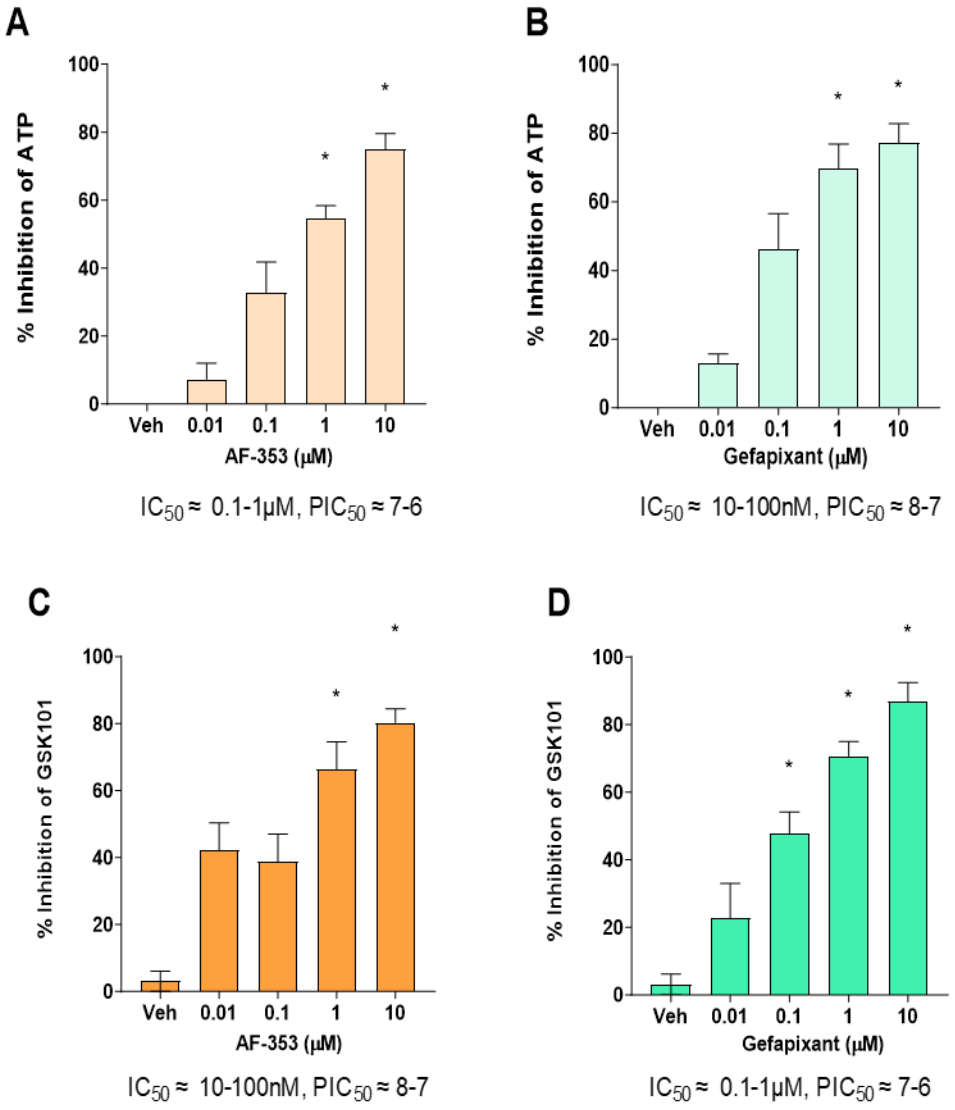


Figure 4. 5 Effect of P2X3 antagonists on direct and indirect ATP-induced vagus nerve depolarisation in the guinea pig.

*ATP (100μM) and GSK101 (300nM) were used on the following P2X3 antagonist concentration responses (0.01μM -10μM); AF-353 and Gefapixant. (A-B) P2X3 antagonists against 100μM ATP-induced depolarisation and (C-D) P2X3 antagonists against 300nM GSK101-induced depolarisation. N=4-6, data shown as mean ± SEM. * indicates statistical significance at p<0.05 using Kruskal Wallis test and Dunns post-test comparing responses to vehicle.*

The table below compares the different pIC_{50} values observed in the literature for human and rat P2X3 and P2X2/3 expressed in cells lines (Table 4.1). PIC_{50} is equivalent to the -log(IC50) where the larger the PIC_{50} value, the more potent the compound. From the effect of various concentrations of P2X3 antagonist on ATP- and GSK101-induced depolarisation, a crude estimate of IC50 was obtained (as

illustrated in Figure 4.5 above). The approximate potencies of AF-353 and Gefapixant in guinea pig isolated vagus nerve were broadly similar to the potencies reported against heterologously expressed human and rat P2X3 in cell lines. According to the literature, Gefapixant does not look to be as potent as BLU-5937 which is more selective for P2X3 which may explain why it is more effective in the clinic and has a lower incidence of taste disturbance effects (Birring et al., 2022).

Compound	pIC_{50} $P2X_3$		pIC_{50} $P2X_{2/3}$
	Human	Rat	Human
AF-353 (Carter et al., 2009)	8.1	8.1	7.4
Gefapixant (Richards et al., 2019)	6.8		6.7
BLU-5937 (Garceau and Chauret, 2019)	7.6	7.0	<4.6[3]

Table 4. 1 Table of pIC50 of P2X3 antagonists on P2X3 and P2X2/3 receptors from the literature.

4.3.5 Effects of P2X3 antagonists on direct and indirect ATP-induced firing of the recurrent laryngeal nerve

Using the eTRec system it was shown that direct ATP and indirect ATP (through the activation of TRPV4) causes firing of the RLN when stimuli are applied to the peripheral nerve terminals *in situ* in the trachea. In isolated whole vagus nerves ATP and GSK101-induced depolarisation could be blocked by AF-353, therefore the effect of AF-353 against ATP and GSK101-induced activation of airway nerves was examined in the eTrec system.

A sub-maximal concentration of 100µM ATP and 300nM GSK101 were used for these experiments. 10µM AF-353 blocked ATP and GSK101-induced firing of the RLN which suggests that blocking P2X3 receptors on airway nerve peripheral terminals inhibits both directly applied ATP and also indirect indigenously released ATP (Figure 4.6).

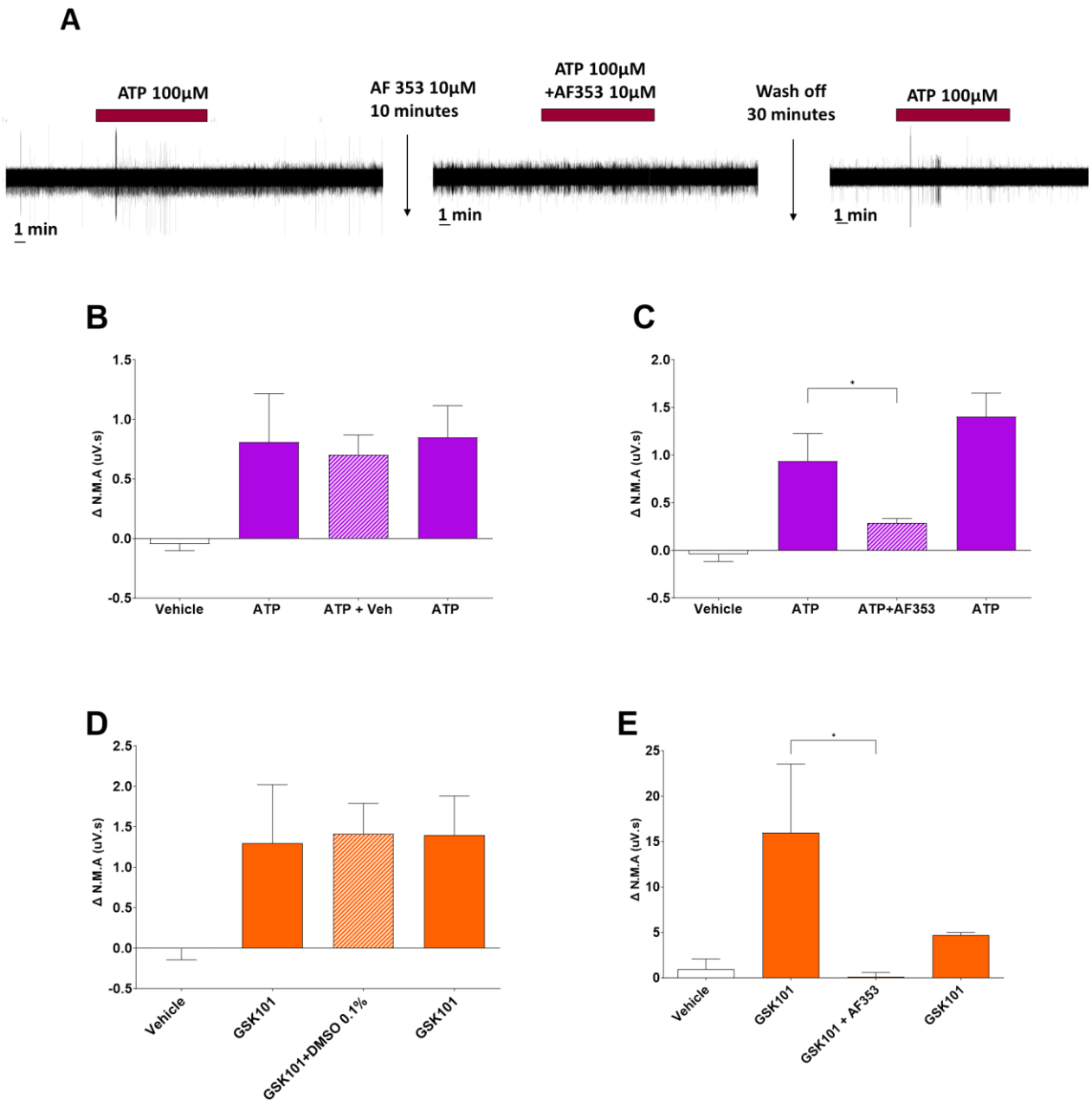


Figure 4. 6 Effect of P2X3 antagonist AF-353 against direct and indirect ATP-induced activation of the recurrent laryngeal nerve.

ATP (100µM) or GSK101 (300nM) were perfused into the tracheal lumen for 10 minutes twice to elicit control nerve responses. Vehicle (0.1% DMSO) or AF-353 (10µM) were then administered alone for 10 minutes prior to another stimulation with either ATP or GSK101 in the presence of vehicle/AF-353 for 10 minutes. All drugs were washed off for 30 minutes prior to a finial stimulation with ATP or GSK101 to confirm viability. (A) Example trace of ATP responses prior to, in the presence of, and following wash-out of AF-353. Bar graphs presented as Δ nerve mass activity showing effect of (B) vehicle or (C) AF-353 on ATP responses, and (D) vehicle or (E) AF-353 on GSK101 responses. Background activity is

*recorded prior to the addition of drug for the same amount of time and subtracted from drug responses. N=3 per group, data shown as mean ± SEM. * indicates statistical significance at p<0.05 using paired t test comparing responses before and after addition of antagonist.*

4.3.6 Effects of P2X3 antagonists on direct and indirect ATP-induced human vagus nerve depolarisation

An additional advantage of the *in vitro* isolated vagus nerve recording system is that it can be used to obtain translational data using human donor tissues. Having shown the effects of ATP on airway sensory nerves in the guinea pig, it was important to see if these effects could be translated to and reproduced in human donor tissues.

The effects of P2X3 antagonists on ATP and TRPV4 induced depolarisation of human vagus nerve were investigated using human vagus from a deceased 65-year-old female COPD patient. AF-353 and Gefapixant caused a concentration-dependent inhibition of ATP-induced vagus nerve depolarisation (Figure 4.7A-C) and could also inhibit TRPV4-induced vagus nerve depolarisation (Figure 4.7C).

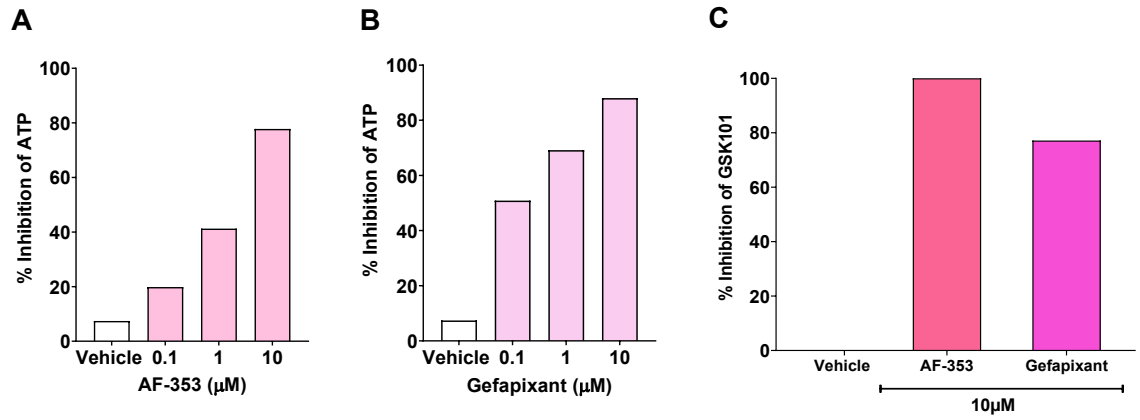


Figure 4. 7 Effect of P2X3 antagonists on- direct and indirect ATP-induced depolarisation of human vagus nerve.

P2X3 antagonist concentration responses (0.1μM -10μM); (A) AF-353 and (B) Gefapixant were tested against ATP (100μM) induced vagus nerve depolarisation. These P2X3 antagonists (10μM) were also tested against GSK101 (300nM) induced depolarisation (C). Due to limited availability of human tissues, N=1.

Table 4.1 in section 4.3.4 compares the pIC_{50} values in the literature for P2X3 and P2X2/3 receptors against human and rat P2X3 and P2X2/3 expressed in cell lines. The potency of the same ligands on ATP-induced human vagus nerve depolarisation (Figure 4.7) appeared to be broadly similar. However,

Due to limited availability of human tissues this was only from N=1 and more N numbers (N = 3-5) are required for statistical analysis to confirm these findings.

4.4 Discussion

The aims within this chapter were to demonstrate the activation of airway sensory nerves by endogenous ATP in preclinical models.

Previous studies have investigated the metabolically stable analogue of ATP, αβMeATP on airway sensory nerves (Bonvini et al., 2016). AβMeATP is more selective for P2X1 and P2X3 purinergic receptors. However, less is known about the pharmacological effects of the endogenous ATP ligand in airway afferents. The data gathered in this chapter utilised different techniques including calcium imaging of airway specific ganglia neurons, isolated vagus nerve recording, and electrophysiological tracheal-attached recordings (eTRec) of the recurrent laryngeal nerve (RLN) to investigate the pharmacological effects of endogenous ATP on airway sensory nerves. Guinea pig tissues were used as they have a cough reflex similar to that of humans.

Calcium imaging of airway sensory nerves is a useful technique that can measure the influx of calcium into airway-specific neurons as an indication of nerve activation. This enables investigation of the effect of compounds on receptors present on airway terminating vagal neurons. Using this system, it was found that ATP caused concentration-dependent increases in intracellular calcium levels in both airway specific nodose and jugular neurons (Figure 4.2).

Next, the effects of ATP on sections of the whole vagus nerve trunk were investigated. In vitro isolated vagus nerve recording were used to investigate the effects of ATP following activation of receptors expressed on the neuronal axon of the vagus nerve. An advantage of this technique is that it is relatively high-throughput and can also be used on human donor tissues. Similar to findings using calcium imaging, ATP caused concentration-dependent depolarisation of the vagus nerve (Figure 4.3).

Having measured activation of receptors expressed on airway-specific neurons and the neuronal axon of the vagus nerve, the *ex vivo* electrophysiological tracheal recording (eTRec) system was used to measure the effects of ATP on nerve terminals. eTRec measures a branch of the vagus, the recurrent laryngeal nerve (RLN) which innervates the upper airways. This technique uses a more physiologically relevant way of causing nerve activation as it measures nerve activity following activation of receptors on the nerve termini within the tracheal lumen as drugs are perfused through the trachea. ATP perfused through the trachea caused increasing firing of compound action potentials (CAP) of airway sensory nerve endings within the RLN of guinea pigs (Figure 4.4).

In order to understand the pharmacology of ATP in airway sensory nerves, the effects of blocking ATP-activated P2X3 receptors was examined. P2X3 receptors are ion channels which consist of 3 subunits; these may be identical P2X3 subunits (homotrimeric) or may contain a single P2X2 subunit, known as P2X2/3 heterotrimeric channels.

Gefapixant is a non-selective P2X2/3 antagonist which was one of the first drugs to show antitussive efficacy in phase 2 clinical trials in refractory chronic cough patients. Data from the most recent Gefapixant phase 3 clinical trial found that Gefapixant dosed at 45mg twice per day showed significant reduction in 24 hour cough frequency compared to placebo at week 12 (18.5% reduction) and at week 24 (14.6% reduction) (McGarvey et al., 2022, Smith et al., 2020b). Given the efficacy of Gefapixant in large scale clinical trials, it is currently in the process of FDA and MHRA approval. However, the most common adverse effect of Gefapixant was taste disturbances which is thought to be related to its impact on P2X2 and P2X2/3 heterotrimeric receptors which are thought to be involved in taste signal transduction. The development of more a selective P2X3 antagonist which blocks P2X3 homotrimeric channels rather than the heteromeric P2X2/3 channels could potentially overcome taste disturbance side effects whilst maintaining antitussive efficacy.

Bellus Health have developed a selective and non-competitive homotrimeric P2X3 antagonist, BLU-5937 (Camlipixant). Pre-clinical studies had shown that this compound had antitussive efficacy in a guinea pig cough model, but – in point of difference from Gefapixant – did not alter taste perception in a rat behavioural taste model (Garceau and Chauret, 2019). This compound was taken forward to clinical trials and in their most recent phase 2b trial (SOOTHE trial) BLU-5937 caused significant reductions in 24-hour cough frequency compared to placebo at week 4 when dosed twice daily in refractory chronic cough patients; 21.1% reduction at 12.5mg , 34.4% reduction at 50mg and 34.2% reduction at 200mg (Smith et al., 2022). This efficacy was observed in patients with a higher cough rate. Importantly, a lower and milder incidence of taste disturbance adverse events was recorded compared to those seen with Gefapixant. Camlipixant is now in phase 3 clinical trials evaluating the efficacy, safety, and tolerability of the compound in refractory chronic cough patients with results expected in 2024/2025. These phase 2 clinical trial data suggest that Camlipixant may be more effective at reducing cough frequency compared to Gefapixant with fewer adverse taste effects, though phase 3 clinical trial data is required to make these comparisons. The promising potential of these P2X3 receptor antagonists for the treatment of refractory chronic cough has led to the development of other novel selective P2X3 antagonists as outlined in section 1.3.8. (Friedrich et al., 2023, Niimi et al., 2022).

The pre-clinical data presented here is therefore in line with what is observed in the clinic as Gefapixant and its pre-clinical analogue AF-353 were capable of blocking ATP-induced vagus nerve depolarisation in guinea pig tissues (Figure 4.5). In addition to demonstrating that P2X3 receptor antagonism can block ATP in segments of isolated vagus nerve, it was also shown that AF-353 can inhibit ATP-induced firing of the airway nerve terminals in the RLN of the guinea pig (Figure 4.6).

Having shown that P2X3 antagonists can block airway sensory nerve activation through the endogenous ATP ligand, it was also important to examine whether it could also block indirect endogenously released ATP driven through the activation of TRPV4. Previous publications have shown that the TRPV4 agonist GSK1016790A (GSK101) causes depolarisation of guinea pig vagus nerve in a concentration-dependent manner which is thought to be through the release of ATP and subsequent activation of P2X3, known as the TRPV4-ATP-P2X3 axis (Bonvini et al., 2016). The data presented in this chapter demonstrates that P2X3 antagonists were able to block TRPV4- induced activation in both isolated guinea pig vagus nerve tissues and in tracheal-attached guinea pig RLN.

This pre-clinical data therefore supports the clinical findings of reduced cough frequency in refractory chronic cough patients in response to Gefapixant and BLU-5937. Importantly, translational studies using human donor tissues demonstrated that ATP-induced depolarisation (both directly applied ATP and ATP released via TRPV4 activation) of human vagus nerve was inhibited by Gefapixant and AF-353 (Figure 4.7), supporting a role for ATP in cough.

When comparing the rank potency of these compounds in the literature (Table 4.1), AF-353 is reported to be the most potent in both human P2X3 and rat P2X3 expressing cells, however the relative differences in potencies are not large. In isolated vagus nerves from both humans and guinea pig, the 2 antagonists examined appeared to be broadly similar in terms of their potency, however only rough IC_{50} values can be obtained with the data from this system. Any slight differences in potencies are likely due to differences in receptor expression in the vagus nerve which is a more physiologically relevant setting for investigating these antagonists on airway sensory nerves. The main finding therefore is that both P2X3 antagonists tested inhibited the depolarisation caused by both directly applying ATP and inducing ATP release provoked by a TRPV4 agonist.

In summary, these data support the hypothesis that the endogenous ATP ligand can cause activation of airway sensory nerves, which can be blocked using P2X3 antagonists. The pharmacology of P2X3 antagonists in pre-clinical primary tissues lines up with the effectiveness of P2X3 antagonists in chronic cough patients in clinical trials. Thus far, clinical trials have shown that blocking the action of ATP on

sensory nerves is an effective way to reduce cough, however an alternative strategy for therapy could be to reduce the amount of ATP in the extracellular space. The next aim will be to investigate the effects of breaking down this ATP using CD39, an ecto-nucleotidase enzyme that rapidly metabolises ATP to AMP. This next chapter will gather data to explore the potential use of CD39 as a therapy for airway disease conditions, where lung eATP is elevated, through investigating the effects of CD39 on airway sensory nerves.

Chapter 5: Investigating the Effects of Ecto-nucleotidases on ATP-Induced Activation of Airway Sensory Nerves

5.1 Rationale

In the previous chapter ATP was shown to cause activation of airway sensory nerves in pre-clinical primary tissues through activation of P2X3 purinergic receptors. This was directly through the addition of ATP or through indirect release of ATP via activation of the TRPV4 receptor. This activation could be blocked using P2X3 receptor antagonists which is in line with the efficacy of P2X3 antagonists in refractory chronic cough patients in clinical trials (Smith et al., 2020b, McGarvey et al., 2022). However, blocking these purinergic receptors have only demonstrated partial reduction in cough compared to placebo and are associated with taste-disturbance side effects (McGarvey et al., 2022). Therefore, a better therapeutic approach may be to target extracellular ATP (eATP) upstream of P2X3 purinergic signalling by reducing the amount of eATP present in the extracellular space through increased breakdown of ATP.

Under normal conditions, ATP is highly regulated and broken down in the extracellular space by ecto-nucleotidases including CD39 and CD73 (Figure 5.1), which rapidly metabolises ATP to AMP and AMP to adenosine respectively (Zimmermann et al., 2012). However, increased eATP in the lungs contributes to the pathogenesis and symptoms of chronic lung diseases which could be through increased release of ATP via activation of receptors such as TRPV4 and/or dysregulation in the breakdown of eATP. This is supported by a study which showed an attenuation of CD39 expression in the lung tissue of patients with COPD, which could be responsible for pulmonary ATP accumulation (Aliagas et al., 2018). Therefore, increasing breakdown of eATP using enzymes such as CD39 could be a potential therapy strategy for airway disease conditions where lung eATP is elevated.

In order to test this, two versions of the CD39 enzyme, CD39-His (WT CD39) and CD39-analogue (an engineered version of CD39-His) will be investigated to determine their effects on ATP-induced activation of airway sensory nerves. An inactivate mutant version of CD39 (CD39-Mut) will also be tested as a negative control. These results could indicate whether increasing ATP breakdown could be a potential additional strategy for the treatment of chronic cough.

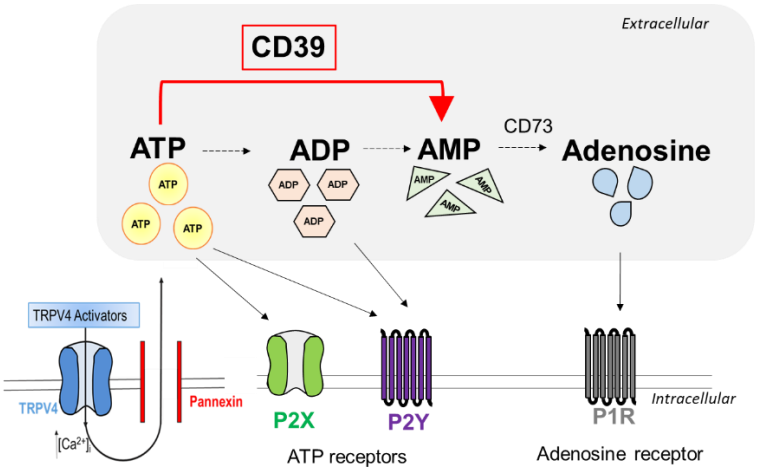


Figure 5. 1 Schematic demonstrating ATP breakdown in the extracellular space by ecto-nucleotidase enzymes. CD39 metabolises ATP to AMP which is then further metabolised by CD73 to adenosine.

5.1.1 Chapter hypothesis

The activation of airway sensory nerves by ATP can be reduced by breaking down ATP present in the extracellular space using the ecto-nucleotidase enzyme CD39.

5.1.2 Aims

- Determine the effects of ATP breakdown on direct ATP and indirect TRPV4 induced depolarisation of isolated guinea pig vagus nerves.
- Determine the effects of ATP breakdown on TRPV4 induced firing of single afferent Aδ- fibres.
- Determine the effects of ATP breakdown on TRPV4 induced cough in a conscious guinea pig cough model and its impact on eATP in biological samples.

5.2 Methods

CD39 tools were provided by collaborators in the Biologics engineering team at AstraZeneca, Sweden. CD39-His was comprised of WT CD39 followed by a 6x Histidine tag. CD39-analogue was an engineered version of CD39-His and CD39-Mut was the lower activity variant of CD39-His which contained four mutations targeted to the enzymatic active site and were shown by the Biologics engineering team at AstraZeneca to be approximately 65-fold lower in enzymatic ATP hydrolysis activity compared to WT CD39-His.

5.2.1 Cell Titer Glo assay

The enzymatic activity of two CD39 enzymes; CD39-His and CD39-analogue were investigated using the commercially available Cell Titer Glo assay (Promega, USA) as per the manufacturer's protocol. Briefly, changes in relative light units (RLU) in plates spiked with 100µM ATP were assessed with increasing concentrations of CD39 variants (0.001nM – 10nM).

5.2.2 *In vitro* isolated vagus nerve recordings

Male guinea pig vagal nerve trunks were dissected and placed in a grease-gap recording chamber as previously described in section 2.4.1. Sub-maximal concentrations of agonists were previously determined from agonist concentration response curves previously carried out in this system.

5.2.2.1 Enzyme concentration response curves

A concentration response between 1-300nM of CD39-His and 0.1-300nM CD39-analogue were measured against the previously determined submaximal concentrations of ATP (100µM) and TRPV4 agonist GSK1016790A (GSK101, 300nM) induced depolarisation based on previous literature (Bonvini et al., 2016). A mutant version of CD39 (CD39-Mut) was also tested as a negative control.

A classical pharmacological approach was taken where two reproducible agonist responses were established, followed by incubation with a single concentration of enzyme for 10 minutes and then restimulation of the nerve with agonist in the presence of the enzyme to determine inhibition of the response. Nerves were then washed with Krebs until baseline was reached, followed by a final agonist response to ensure the nerve was still viable.

5.2.2.2 Data Analysis

Nerve depolarisation was assessed by measuring the peak amplitude of the response in millivolts (mV). The approximate IC_{50} and PIC_{50} values were determined for each agonist response. All data are presented as mean ± S.E.M, with statistical significance set at $P < 0.05$.

5.2.3 *In vivo* single fibre recordings

This technique enables the investigation of compounds on the firing rate of individual airway sensory nerve fibres in anaesthetised guinea pigs. This involves cutting the left and right vagus nerves at the central end to prevent the generation of centrally-mediated reflexes and the left vagus nerve is then teased down to individual fibres which impulses are measured from. This technique has the advantage of measuring compounds on the nerve termini with an end point of nerve firing and therefore is more physiologically relevant than *in vitro* isolated vagus nerve recordings.

5.2.3.1 Surgery

Male Dunkin Hartley guinea pigs (400 – 750g) were anaesthetised through intraperitoneal administration of urethane (1.5g/kg) with additional anaesthetic administered as required. The right jugular artery was cannulated for the administration of drugs. The neuromuscular blocker vecuronium bromide was used to paralyse the animal with an initial dose of 0.1mg/kg intravenously followed by 0.05mg/kg every 20 minutes thereafter. Levels of anaesthesia were constantly monitored throughout the procedure. Guinea pigs were then prepared as detailed in (Adcock et al., 2003).

Briefly, the trachea was cannulated and blood gas and pH were maintained at physiological levels using a ventilator (Ugo Basile; Gemonio, Italy) set at a rate of 50 – 60 breaths per minute with a tidal volume of 10ml/kg. The ventilator was connected to an Aerogen nebuliser (DSI; Minnesota, US) to enable aerosolization of compounds into the airways. The right carotid artery was cannulated to measure systemic arterial blood pressure and heart rate which were monitored using a transducer (Gould P2X3L, MEMSCAP SP 844; Crolles, France). Temperature was monitored with a rectal thermometer and maintained at 37°C using a heated blanket and control unit (Harvard Apparatus; Massachusetts, US). Tracheal pressure was also recorded using an air pressure transducer (SenSymb647, MEMSCAP SP 844; Crolles, France) attached to the side arm of the tracheal cannula.

Both cervical vagal nerves were cut at the central end and dissected free from the carotid artery, sympathetic and aortic nerves. The left vagus nerve was further cleared of surrounding tissues and fascia. The skin and muscles surrounding the cervical incision were tied to a metal ring, the centre of which was filled with mineral oil to create a non-conductive well. Actional potentials were recorded using Bipolar Teflon coated platinum electrodes which were exposed at the tips. Using a binocular microscope, thin filaments were teased from the vagus nerve and placed on a recording electrode until a single active unit of no more than 2 or 3 fibres were obtained. A reference electrode was placed on the nerve fascia. These electrodes were connected to a preamplifier headstage (NL100k Digitimer. The signal was then amplified (NL104 Digitimer), filtered (NL125 Digitimer), and passed through a 'Humbug' to remove 50-60hz mains electrical noise (Digitimer). All signals (including arterial blood

pressure, tracheal pressure and heart rate) were recorded using Spike 2 data acquisition software. The input signal was also monitored in real-time using a digital storage oscilloscope (DPO 2012, 75 Tektronix; OR, USA) which was fed through an audio amplifier to a loudspeaker. Guinea pigs were euthanised through an overdose of pentobarbitone at the end of the experiment.

5.2.3.2 Nerve fibre identification

Single vagus nerve fibres were identified as originating from the family of slowly adapting stretch receptors (SARs), rapidly adapting stretch receptors (RARs) or chemosensitive C-fibres using a set of criteria previously outlined in (Adcock et al., 2003). These criteria would include patterns of spontaneous activity of the fibre, responses to hyperinflation or deflation, conduction velocity and responses to capsaicin and citric acid. Fibres that lacked spontaneous activity, a response to hyperinflation and deflation but did respond to capsaicin, were assumed to be a C-fibres. Conversely, fibres with a set pattern of spontaneous activity and responded to hyperinflation, deflation and to citric acid aerosol were categorised as Aδ-fibres (RARs). Following the experiment, conduction velocity was measured as a final means of verification, as non-myelinated C-fibres are slower than myelinated Aδ-fibres as outlined in (Adcock et al., 2003).

5.2.3.3 Experimental protocol

The following experimental protocol was carried out to investigate the effects of CD39-analogue and the mutant control CD39-Mut on GSK1016790a (GSK101) induced firing of Aδ-fibres. Once identified as an Aδ-fibre, control responses were obtained to aerosolised GSK1016790a (100 ng mL^{-1}, 1 min). After a 30-minute interval, either the control peptide (CD39-Mut, 30nM in 200µL) or CD39-analogue (30nM in 200µL) was administered via aerosol. An aerosol of GSK101 (100 ng mL^{-1}, 1 min) was then repeated after administration of either the control peptide or CD39-analogue. Changes in fibre activity, intratracheal pressure and blood pressure were continuously recorded throughout. Data were expressed as mean ± SEM of total action potential impulse firing before and after addition of each drug.

5.2.4 Aerosol-induced conscious guinea pig cough model

This technique allows the investigation of tussive and antitussive stimuli in conscious, naïve guinea pigs which unlike mice or rats, have a similar cough response to that of humans (Maher et al., 2009). The TRPV4 agonist GSK101 is a known tussive stimuli that causes cough in guinea pigs (Bonvini et al., 2016).

Conscious unrestrained male Dunkin Hartley guinea pigs were placed in individual transparent perspex plethysmography chambers (DSI; Minessota, US). A total of 8 chambers were run concurrently and

each individually connected to an Aerogen nebuliser (DSI). 8 guinea pigs were exposed to a tussive stimuli at once. Coughs were recorded through the use of CCTV bird box cameras and microphones (Spy Camera CCTV; Bristol, UK). Flow data were also recorded and analysed using DSI software. Cough was retrospectively quantified by observing changes in pressure, sound and posture of the animal by two trained observers.

5.2.4.1 Experimental protocol

Animals were anaesthetised with 4% isoflurane and intratracheally dosed with CD39-His 0.3mg/kg-10mg/kg, vehicle (0.1% DMSO in 0.9% saline) or a mutant control (CD39-Mut 1mg/kg) 30 minutes prior to challenge with the TRPV4 agonist, GSK101. Guinea pigs were placed in individual perspex plethysmography chambers where they were exposed to aerosolised GSK101 30µg/mL for 5 minutes, and cough counted for ten minutes. Cough counts were performed by analysing airflow patterns along with manual observation by trained observers as previously described (Birrell et al., 2009, Maher et al., 2009, Bonvini et al., 2016). BALF and plasma samples were collected in 6mM EDTA and ATP levels were assessed using the Cayman ATP detection assay (see section 2.3.2)

5.2.4.2 Data analysis

All data are presented as mean ± S.E.M, with statistical significance set at $P < 0.05$.

5.3 Results

5.3.1. Concentration response of CD39 variants on 100µM ATP using a plate-based luminescent assay

To determine the enzymatic activity of the two CD39 variants being investigated; CD39-His and CD39-analogue, a concentration response curve of both enzymes (0.001-10nM) were assessed against 100µM spiked ATP using the Cell Titer Glo ATP assay. Both enzymes caused a concentration-dependent decrease in luminescence with increasing concentrations of enzyme and the CD39-analogue was more potent compared to CD39-His (Figure 5.2).

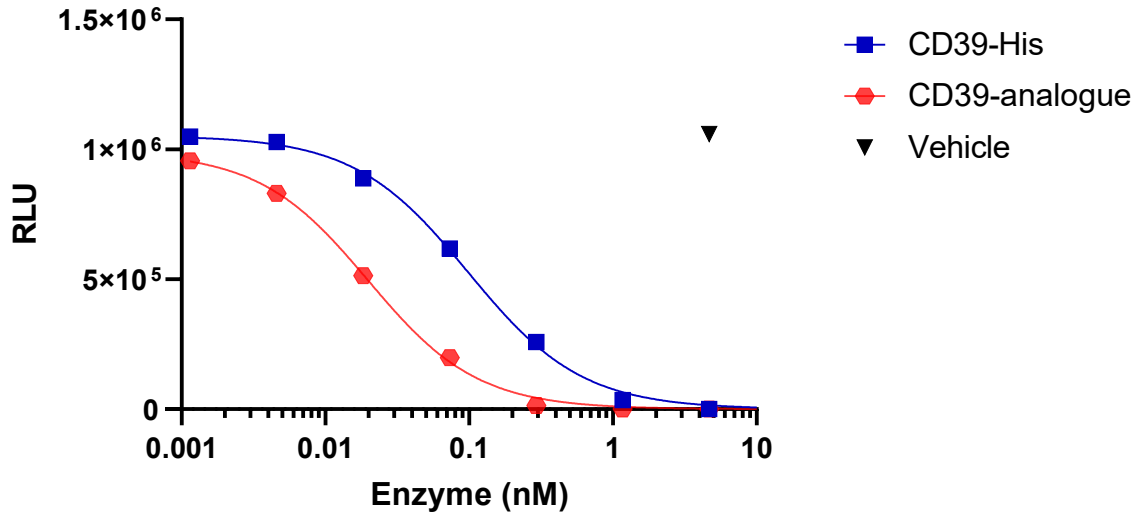


Figure 5. 2 Concentration response of CD39 enzymes on 100µM ATP.

A concentration response (0.001nM – 10nM) of CD39-His and CD39-analogue were added to 100µM spiked ATP and relative light units (RLU) measured using the Cell Titer Glo ATP assay.

5.3.2. Effects of CD39-His concentration response on ATP and GSK101 induced depolarisation of guinea pig vagus nerve

Having previously shown that ATP causes depolarisation of airway sensory nerves using *in vitro* isolated nerve recordings, the effects of CD39-His were assessed on direct-ATP-induced nerve depolarisation to determine the impact of ATP breakdown. Additionally, the effect of CD39-His on TRPV4 agonist induced depolarisation was examined as activation of TRPV4 has been shown to cause ATP release and subsequent activation of airway sensory afferent nerves (Bonvini et al., 2016). The effect of a mutant variant of CD39-His referred to as CD39-Mut was also tested as a negative control.

The effect of vehicle (0.1% DMSO), CD39-Mut (300nM) and CD39-His (1-300nM) were examined on depolarisation induced by sub-maximal concentrations of 100µM ATP or 300nM GSK101. Concentration-dependent inhibition of both TRPV4 and ATP-induced vagus nerve depolarisation were observed with CD39-His (Figure 5.3).

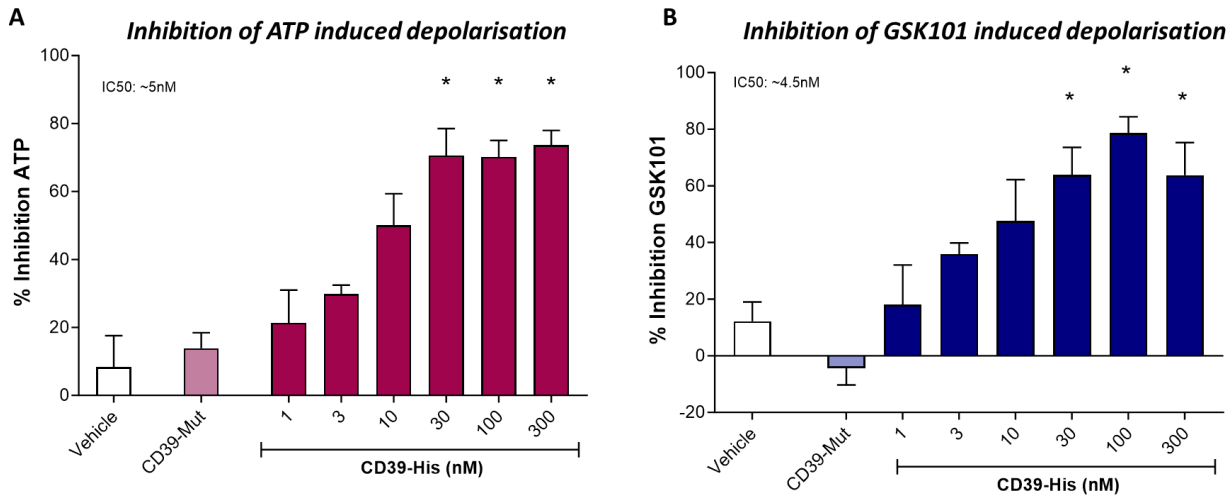


Figure 5. 3 Concentration response of CD39-His on ATP and GSK101 induced depolarisation of guinea pig vagus nerve.

*Concentration-dependent dose response of CD39-His (1nM -300nM) on (A) 100µM ATP-induced depolarisation of guinea pig vagus nerve, N=4 and (B) 300nM GSK101 induced depolarisation of guinea pig vagus nerve N=3-4. Data shown as mean ± SEM. * indicates statistical significance at p<0.05 using Kruskal Wallis test and Dunns post-test comparing responses to vehicle.*

5.3.3. Effects of CD39-analogue concentration response on ATP and GSK101-induced depolarisation of guinea pig vagus nerve

The effects of another CD39 variant; CD39-analogue which appeared to be more potent using a plate-based assay (see section 5.3.1) was also assessed on direct-ATP and indirect TRPV4 induced nerve depolarisation to determine the impact of ATP breakdown.

The effect of vehicle (0.1% DMSO), CD39-Mut (300nM) and CD39-analogue (0.1-300nM) were examined on depolarisation induced by sub-maximal concentrations of 100µM ATP or 300nM GSK101. Concentration-dependent inhibition of both TRPV4 and ATP-induced vagus nerve depolarisation were observed with increasing concentrations of CD39-analogue (Figure 5.4).

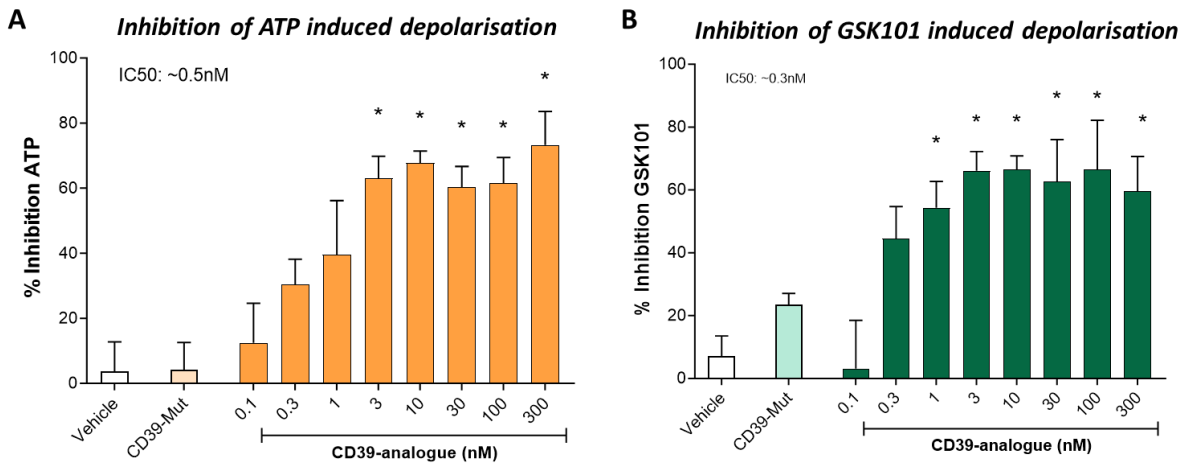


Figure 5. 4 Concentration response of CD39-analogue on ATP and GSK101 induced depolarisation of guinea pig vagus nerve.

Concentration-dependent response of CD39-analogue (0.1nM -300nM) on (A) 100µM ATP-induced depolarisation of guinea pig vagus nerve, N=3-4 and (B) 300nM GSK101 induced depolarisation of guinea pig vagus nerve N=3-4. Data shown as mean ± SEM. indicates statistical significance at p<0.05 using Kruskal Wallis test and Dunns post-test comparing responses to vehicle.*

5.3.4. Effects of CD39-analogue on single fibre firing in guinea pig Aδ- fibres

Having observed the effects of CD39 tools using isolated vagus nerve recordings, the next step was to see whether these effects extend and translate in an *in vivo* model. Whole animal single afferent fibre recording is a more airway relevant model that measures action potential firing in specific subtypes of nerves. Previous publications using this technique have shown that aerosol administration of GSK101 causes a marked prolonged stimulation of Aδ- fibres (Bonvini et al., 2016). Therefore, the effect of the more potent CD39-analogue and the mutant version CD39-Mut on TRPV4 induced Aδ- fibre firing was investigated.

The Aδ- fibre was identified from other fibre subtypes by confirming its response to citric acid and other criteria outlined in section 5.2.3. The mutant version of CD39 had no effect on GSK101 induced Aδ- fibre firing, however a marked reduction was observed with the CD39-analogue compound (Figure 5.5).

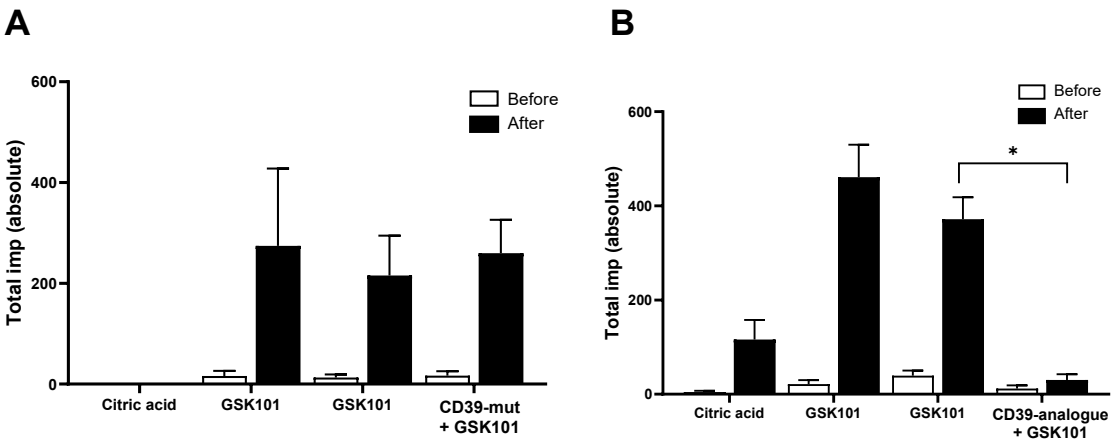


Figure 5. 5 Effect of CD39 tools on TRPV4 induced Aδ-fibre firing in guinea pigs.

*Following identification of Aδ-fibres based on their response to 0.3M citric acid aerosol for 1 minute, two control responses were obtained to aerosolised GSK101 (100 ng mL-1, 1 min). After a 10-minute interval, either (A) CD39-Mut (30nM) or (B) CD39-analogue (30nM) was administered via aerosol for 30 minutes. An aerosol of GSK101 (100 ng mL-1, 1 min) and either CD39-Mut (30nM) or CD39-analogue (30nM) was then repeated N=3. Data shown as mean ± SEM of total action potential impulse firing before and after addition of each compound. *indicates statistical significance ($p < 0.05$), paired t test comparing responses before and after aerosol administration of enzyme.*

5.3.5. Effects of CD39-His on GSK101 induced cough in guinea pigs

The effects of CD39 tools at reducing ATP-induced depolarisation has been demonstrated in isolated vagus nerve recordings and single-fibre firing of Aδ-fibres. However, the effects of CD39 tools on the cough response in a whole animal *in vivo* is yet to be determined. Therefore, the next step was to assess the effects of CD39 tools on the cough reflex in a conscious whole animal system. Previous publications have shown that 30µg/mL aerosolised GSK101 induces cough in a guinea pig conscious cough model. Importantly, cough could be reduced using a P2X3 receptor antagonist further implicating the role of ATP in cough (Bonvini et al., 2016). Using this system, initially the effects of intratracheally dosed CD39-mut (1mg/kg) and CD39-His (0.3 – 3 mg/kg) were investigated. At 3mg/kg there appeared to be a trend towards decreased cough, although this was not statistically significant (p=0.0699) (Figure 5.6). Future work will assess the impact of CD39-analogue in this model which was shown to be more potent *in vitro*.

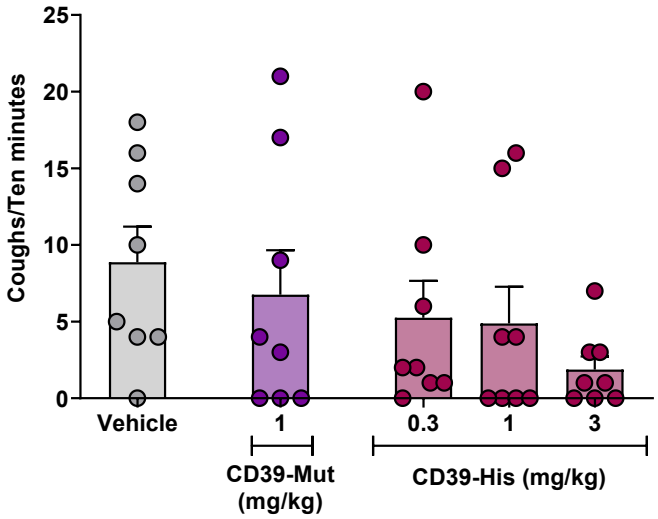


Figure 5. 6 Investigating the effect of CD39-His on GSK101 induced cough in guinea pigs.

Number of coughs were measured over 10 minutes following challenge with aerosolised GSK1016790a (30µg/ml) N=8 per treatment group. Data shown are mean ± SEM. At 3mg/kg CD39-His p = 0.0699, Kruskal-Wallis with Dunn's multiple comparison test.

5.3.6. Effects of CD39-His on BALF eATP levels in a conscious guinea pig cough model

Levels of eATP in BALF samples from the guinea pig cough study were assessed using the ATP detection assay. These measurements were used to determine whether there was target engagement of CD39-His in the lungs and whether reduction in cough observed at the highest dose of CD39-His could be attributed to reduced levels of eATP in the lungs.

CD39-His significantly reduced levels of eATP in BALF at all concentrations tested, with a small effect of the mutant control. This could be explained as the mutant control was only 100x less potent than CD39-His and so will elicit lesser rather than no inhibitory activity.

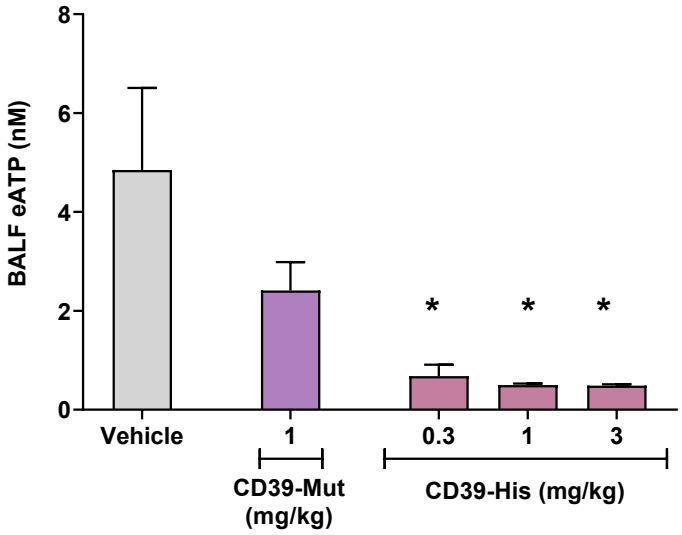


Figure 5. 7 Investigating the effect of CD39-His on eATP in BALF from GSK101 induced cough in guinea pigs.

*eATP measured using the ATP detection assay in BALF samples from guinea pigs dosed with CD39-His and challenged with aerosolised GSK1016790a (30µg/ml) N=8 per treatment group. Data shown are mean ± SEM. *indicates statistical significance (p=0.0052, 0.0091, 0.0052, respectively), analysed with Kruskal-Wallis test followed by Dunn's multiple comparison test.*

5.3.7. Effects of CD39-His on plasma eATP levels in a conscious guinea pig cough model

Animals from this study were dosed intratracheally to ensure CD39-His was present in the lungs. However, the effect of CD39-His on systemic levels of eATP were also assessed in plasma samples to determine whether CD39-His reached the systemic circulation and was still active as this may be indicative of potential systemic effects. CD39-His significantly inhibited systemic ATP in the plasma at doses above 1mg/kg, with no effect of the mutant control (Figure 5.8). These data suggest that systemic eATP can be broken down *in vivo* by CD39-His, and positively suggests that eATP can be accurately detected in biological samples from animals treated with ATP intervention therapies.

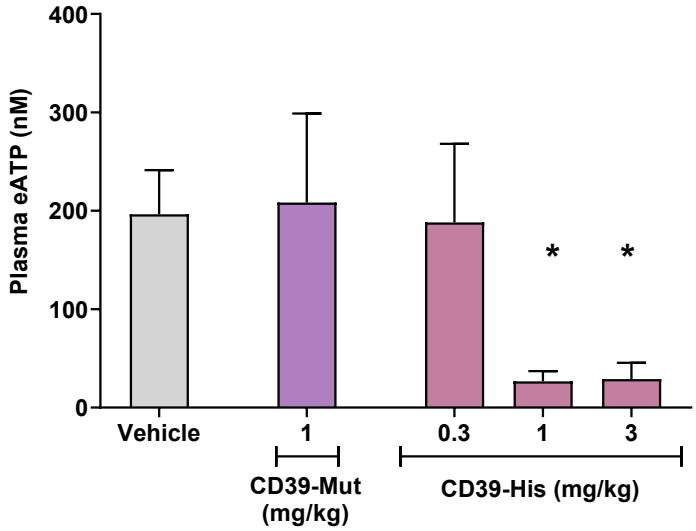


Figure 5. 8 Investigating the effect of CD39-His on eATP in plasma from GSK101 induced cough in guinea pigs.

*eATP measured using the ATP detection assay in plasma samples from guinea pigs dosed with CD39-His and challenged with aerosolised GSK1016790a (30µg/ml) N=8 per treatment group. Data shown are mean ± SEM. *indicates statistical significance (p=0.0084 and 0.0143, respectively), analysed with Kruskal-Wallis test followed by Dunn's multiple comparison test.*

5.4 Discussion

The aim of this chapter was to assess the effects of ATP breakdown on ATP-induced activation of airway sensory nerves. In order to test this, two CD39 enzymes; CD39-His and its analogue; CD39-analogue were investigated to determine their effects on ATP-induced activation of airway sensory nerves. A mutant version of these enzymes; CD39-Mut was also tested as a negative control. Initially, these enzymes were investigated using *in vitro* isolated vagus nerve recordings to investigate their effects on ATP-induced depolarisation. The advantage of this technique is that it is relatively high-throughput and using this technique both CD39-His and CD39-analogue caused concentration-dependent decreases in direct ATP-induced vagus nerve depolarisation and in direct TRPV4 induced ATP release in the guinea pig supporting the chapter hypothesis (Figure 5.3 and Figure 5.4).

The effects of these enzymes were then tested in whole animal single afferent fibre recordings which is a more physiologically relevant technique that has the advantage of measuring the effects of drugs on the nerve termini with an end point of action potential firing in specific subtypes of nerves. Nonetheless, the procedures entailed within this technique are relatively complex and can only be performed by highly skilled and trained personnel and is therefore not as high throughput as other techniques such as isolated vagus nerve recordings. Based on this, the more potent CD39 tool; CD39-analogue was tested in this system against the TRPV4 agonist GK101 induced firing of Aδ- fibres. This was selected instead of direct ATP-induced activation as the submaximal concentration of ATP had not yet been determined in this model. However, previous studies had already shown that aerosol administration of GSK101 (100 ng mL-1, 1 min) causes a marked prolonged stimulation of Aδ- fibres through the release of ATP which could be blocked using P2X3 receptor antagonists (Bonvini et al., 2016) and was therefore selected for testing the effects of CD39-analogue in this model. Although this technique is typically used to investigate pharmacological intervention using small molecules to block receptors, aerosolisation of the CD39-analogue enzyme was shown to reduce GSK101 induced stimulation of Aδ- fibres with no effect observed with the mutant control which supports the chapter hypothesis (Figure 5.5).

The final method used to assess the role of ATP breakdown on complete cough reflex events was through investigating the effects of CD39-His on GSK101 induced cough in a guinea pig conscious cough model. The key advantage of this technique is that the effects of drugs on cough can be assessed in conscious whole animals which provides translational data as the tussive responses induced in guinea pigs are similar to those observed in the clinic (Birrell et al., 2009). Using this model, a trend towards decreased cough was observed at the highest dose 3mg/kg which despite not being statistically significant ($p = 0.0699$), is still promising given the reduction in cough observed relative to

control groups (Figure 5.6). Similar to the previous techniques used in this chapter, these models are typically used to assess pharmacological intervention using small molecules to block receptors by challenging animals with receptor specific agonists. However, in this experiment, the effect of an enzyme on inhibition of cough was assessed and may therefore require increased n numbers to increase the statistical power of the data. Future work will investigate the antitussive effects of the CD39-anaolgue in this model which is shown to be more potent *in vitro.* Target engagement of CD39-His was evident in this model as CD39-His significantly reduced eATP in BALF at all concentrations tested (Figure 5.7) and significantly reduced systemic eATP in the plasma at doses above 1mg/kg (Figure 5.8).

Although P2X3 antagonists are currently the most promising antitussive therapies in development, blocking these purinergic receptors have only demonstrated partial reduction in cough in the clinic compared to placebo and are associated with taste-disturbance side effects (McGarvey et al., 2022). Preliminary data from this chapter suggests that increasing breakdown of eATP using CD39 enzymes reduces activation of airway sensory nerves and has potential to reduce cough in an aerosol-induced conscious guinea pig cough model. Changes in eATP can also be accurately detected in biological samples to determine target engagement of these ATP intervention therapies. Therefore, targeting eATP upstream of P2X3 purinergic signalling by reducing eATP levels through increased breakdown, may be a promising alternative treatment strategy where eATP could also be acting on other purinoreceptors to evoke cough. Although more research is required, breakdown of eATP using CD39 enzymes could potentially be used in combination or as an alternative strategy to P2X3 receptor antagonists which may be more efficacious with fewer adverse effects. Therefore, the use of CD39 tools for the breakdown of ATP could be a potential therapy strategy for chronic cough and other airway disease conditions where lung eATP in elevated.

Nonetheless, it is important to note that CD39 can lead to increased levels of extracellular adenosine as CD39 metabolises ATP to AMP which are further broken down into adenosine by CD73. This increase in adenosine through activation of P1 receptors can have many downstream effects such as inducing neurogenic mediated bronchospasm and modulating the release of inflammatory mediators by mast cells (Ramsdell, 2003, Spicuzza et al., 2006). Increased levels of adenosine in the systemic circulation are also associated with increased bleeding risk as adenosine is a strong vasodilator involved in the signalling cascade that inhibits platelet activation which may prevent blood clotting following tissue damage (Johnston-Cox et al., 2011). Therefore, more work is required to determine whether there are any therapeutic benefits of using CD39 which outweigh any risks *in vivo*. The next chapter will investigate the use of these CD39 tools in well-established inflammatory disease models in order to assess its impact on eATP and other disease markers.

Chapter 6: Investigating Extracellular ATP in Animal Models of Respiratory Disease

6.1 Rationale

There is a growing amount of research to suggest that increased extracellular adenosine triphosphate (eATP) in the airways contributes to the pathogenesis and symptoms of chronic respiratory diseases. Having developed a reproducible and reliable methodology for the retrieval and assessment of eATP in biological samples, this was investigated in animal models of respiratory disease. Increased eATP in the lungs of these animal models is hypothesised to be a driver in the pathophysiological mechanisms driving disease.

Cigarette smoke (CS) exposure is commonly used in the development of inflammatory airway disease models such as Chronic Obstructive Pulmonary Disease (COPD) as it is thought to be the primary causative factor in the pathogenesis of COPD with the majority of patients either current or former smokers (Hlapčić et al., 2019). CS exposure results in a dysregulated inflammatory response in the airways characterised by an increase in inflammatory cells and the release of pro-inflammatory mediators (Vandivier and Ghosh, 2017). Importantly, increased levels of eATP have been reported in models of CS-induced inflammation and in the lungs of COPD patients where they correlate with disease severity (Mortaz et al., 2009, Cicko et al., 2010, Baxter et al., 2014, Lommatzsch et al., 2010, Eltom et al., 2014). This increase in ATP is thought to be involved in the recruitment and activation of inflammatory cells such as neutrophils through activation of P2Y receptors (Cicko et al., 2010, Mortaz et al., 2010). Additionally, several studies have shown that increased eATP can drive inflammation in these models through P2X7-induced activation of the NLRP3 inflammasome, a multi-meric protein complex that leads to the release of two potent pro-inflammatory cytokines interleukin-1β (IL-1β) and interleukin-18 (IL-18). These cytokines serve as signalling molecules that play a key role in the pathogenesis of CS-induced inflammation in the lungs and have been shown to be upregulated in COPD patients and CS exposed mouse models (Ekberg-Jansson et al., 2001, Petersen et al., 2007, Lucey et al., 2002, Kang et al., 2007, Churg et al., 2009, Baxter et al., 2014).

Given that ATP has been previously shown to be upregulated in CS exposed mouse models and also plays a role in activation of the NLRP3 inflammasome and subsequent release of pro-inflammatory cytokines, eATP levels are hypothesised to be elevated in this model which can be tested using CD39 tools. In the previous chapter, *in vitro* studies demonstrated the use of CD39 tools which cause degradation of ATP to reduce activation of airway sensory nerves. An aerosol-induced conscious guinea pig cough model was also used to demonstrate the *in vivo* effects of CD39-His in a whole animal

and its potential to reduce evoked cough and eATP levels in biological samples. However, these experiments and tissues were taken from naïve animals. Therefore, the next steps would be to investigate eATP levels and the potential impact of ATP degradation in an acute CS-exposure animal model of respiratory disease. However, prior to this, it is first necessary to characterise the pharmacodynamic and pharmacokinetic properties of CD39-His *in vivo* in the naïve mouse. Preliminary experiments will involve several dose-ranging and timecourse studies to determine the appropriate dose, route of administration and dosing frequency of CD39-His. Once this has been established, the effects of CD39-His can be investigated in a CS mouse model.

Ozone is another major pollutant which is associated with airway inflammation and is used to develop respiratory disease models (Sokolowska et al., 2019). Studies have shown that human lung epithelial cells release eATP during ozone exposure (Kong et al., 2021). Mouse *in vivo* studies have also shown that ozone exposure induces airway hyperreactivity and neutrophilic inflammation in the lungs where increased eATP levels have been reported (Kong et al., 2021). It is hypothesised that ozone induces increased lung eATP which drives airway inflammation which will be further investigated in an acute ozone exposure model.

Respiratory viruses are also a major cause of COPD development and exacerbations. Polyinosinic:polycytidylic acid (Poly I:C) is a synthetic analogue of dsRNA and a toll-like receptor 3 (TLR3) agonist commonly used to mimic viral infection. TLR3 is a member of the toll-like receptor family of pattern recognition receptors involved in activating the innate immune system. Pre-clinical studies have shown that Poly I:C causes increased eATP release and mucus release from human bronchial epithelial cells (Shishikura et al., 2016). Poly I:C has also been shown to exacerbate airway inflammation and remodelling in CS exposed mice (Mei et al., 2022). Therefore, eATP levels with also be investigated in a Poly I:C model.

These results could confirm whether eATP is upregulated across a range of different respiratory disease models. Animal models which recapitulate increased eATP observed in human airway disease are required to determine the impact of CD39 in reducing eATP as a potential strategy for the treatment of chronic respiratory diseases where increased pulmonary eATP is involved in driving disease pathogenesis.

6.1.1 Chapter hypothesis

eATP is elevated in pre-clinical models of chronic respiratory disease and is involved in driving disease pathogenesis. *In vivo* delivery of CD39-His can reduce lung levels of eATP and other airway disease markers in these models.

6.1.2 Aims

- Determine the dose-response of CD39-His *in vivo.*
- Determine the duration of action of CD39-His *in vivo.*
- Investigate different routes of administration of CD39-His.
- Investigate the effects of CD39-His in an acute 3 day cigarette smoke mouse model.
- Investigate eATP levels in acute 3 day and chronic 2 and 4 month cigarette smoke mouse models.
- Investigate eATP levels in an acute ozone exposure model.
- Investigate eATP levels in a Poly I:C challenge model.

6.2 Methods

The dose-ranging, timecourse and cigarette smoke (CS) *in vivo* studies described in this section were run by collaborators in the 'Bioscience In Vivo' team at AstraZeneca, Sweden. Samples were shipped to Imperial College London for analysis.

6.2.1 *In vivo* dose-ranging and timecourse experiments

Female C57/BL6J mice (20g ± 10%) were purchased from Charles River Laboratories, Germany. Animals were housed in groups within temperature controlled (21°C) individually ventilated cages with access to food and water. All animals were acclimatised to their environment for at least one week prior to experimentation.

6.2.1.1 Experimental protocol for intratracheal dose-ranging study

Mice were anaesthetised with isoflurane mixture (air/oxygen and 3.5% isoflurane), placed in a supine position at a 30-40˚ angle and instilled with vehicle (PBS) or CD39-His. CD39-His doses used were 0.003, 0.01, 0.03, 0.1, 0.3, 1.0, 3.0 mg/kg. Topical instillation of the enzyme was performed by using a modified curved metal cannula with a bolus-bulb attached to the end. The syringe was prefilled with 0.15ml air and the dose volume was put in the opening of the syringe with a pipette prior to placing it on the cannula. Following dosing, mice were placed in cages in a supine position until consciousness was regained. The instillation volume used was ≈ 2 ml/kg, 40 µL/mouse. 30 minutes after intratracheal (i.t.) dosing, mice were euthanised by a single intraperitoneal injection of 0.2ml pentobarbital (100 mg/mL). BALF and plasma samples were collected in 6mM EDTA and ATP levels assessed using the Cayman ATP detection assay (see section 2.1.2 and section 2.3.2).

6.2.1.2 Experimental protocol for timecourse study

Mice were anaesthetised and intratracheally dosed with vehicle, 0.03mg/kg or 0.1mg/kg CD39-His as previously described (see section 6.2.1.1). The effect of CD39-His over 48 hours was assessed by euthanising animals across a range of 7 timepoints at 0.5, 2, 4, 8, 16, 24 and 48 hours by a single intraperitoneal injection of 0.2ml pentobarbital (100 mg/mL). BALF and plasma samples were collected in 6mM EDTA and ATP levels assessed using the Cayman ATP detection assay (see section 2.1.2 and section 2.3.2).

6.2.1.3 Experimental protocol for intranasal dose-ranging study

Mice were anaesthetised with isoflurane mixture (air/oxygen and 3.5% isoflurane). Mice were then given 40µl of CD39-His or vehicle (PBS) in the left nostril. CD39-His doses used were 0.03, 0.1, 0.3, 1.0 mg/kg. Following instillation, mice were placed back in the cages in a supine position until they regained consciousness. 24 hours post-dose, mice were euthanised by a single intraperitoneal

injection of 0.2ml pentobarbital (100 mg/mL). BALF and plasma samples were collected in 6mM EDTA and ATP levels assessed using the Cayman ATP detection assay (see section 2.1.2 and section 2.2.2).

6.2.1.4 Data analysis

All data are presented as mean ± S.E.M and analysed using Kruskal-Wallis with Dunn's multiple comparison test.

6.2.2 Mouse cigarette smoke models

6.2.2.1 CD39-His in a mouse 3-day cigarette smoke model

Mice were randomly assigned treatment groups and weighed prior to dosing. Mice were dosed i.n. with vehicle or CD39-His (0.03 - 1mg/kg) 24 hours prior to the first smoke exposure and daily throughout the study. The positive control compound Kineret (Anakinra), an IL-1 receptor antagonist, was delivered via an implanted osmotic pump (Azlet 1007D, reservoir 100ul, Rate 0.5µl/h) and diluted in saline to a final concentration of 44.8 mg/ml. The mini-pumps were prepared according to the manufacturer's instructions (Alzet osmotic pumps, CA, USA).

Mice were exposed to cigarette smoke twice daily in a SIU24 smoke machine (PromechLab AB, Vintrie, Sweden; 3R4F cigarettes from The Tobacco and Health Research Institute, University of Kentucky) for 3 days. Each challenge procedure duration was approximately 50 minutes with 4 hours between the end of the first exposure and start of the second exposure. The smoke machine was set at a constant flow of approximately 1.7L.min^{-1} and a smoke stream of 10 seconds followed by an air stream of 20 seconds. A total of 10 puffs and 10 cigarettes were used per exposure session.

During CS exposure animals were housed in wire mesh cages. The individual groups were positioned in a randomised way in the exposure chamber for every smoke exposure session, with a maximum of 8 mice per compartment. Mice from air groups were exposed to room air only, using the same strategy. 18 hours after the last CS exposure, mice were euthanised by a single intraperitoneal injection of 0.2ml pentobarbital (100 mg/mL).

BALF and plasma samples were collected in 6mM EDTA and ATP levels assessed using the Cayman ATP detection assay (see section 2.1.2 and section 2.3.2). BALF cells were isolated and resuspended in RPMI media. Total white blood cell numbers were determined using an automated cell counter Sysmex XP-300 (Sysmex Ltd, UK). BALF cells were then mounted onto slides and spun at 800g for 5 minutes at room temperature in a cytospin centrifuge (Shandon, Runcom, UK). Slides were stained with a Hematek modified Wright stain (Siemens Heathineers, Germany) using a Hematek 2000 automated slide strainer (Ames Co., Elkhart, USA). Cytospins were used for neutrophil counts by counting 200 cells per slide under 40-times magnification on a light microscope by a blinded operator

based on morphological criteria. BALF supernatant were used for the analysis of inflammatory mediators. The concentrations of IL-1β (mouse IL-1β ELISA kit, Invitrogen) and of IL-18 (mouse IL-18 ELISA kit, Invitrogen) in BALF were measured by ELISA as per the manufacturers' instructions.

6.2.2.2 Mouse 3-day CS timecourse

Mice were exposed to CS over 3-days as described in section 6.2.2.1. Mice were culled with a single intraperitoneal injection of 0.2ml pentobarbital (100 mg/mL) at the following time points after the last exposure; 0, 0.5, 1, 2, 6 and 24 hours. BALF samples were collected in 6mM EDTA and ATP levels assessed using the Cayman ATP detection assay (see section 2.1.2 and section 2.32).

6.2.2.3 Chronic mouse CS experiments

Mice were chronically exposed to CS smoke as described in section 6.2.2.1 over the course of 2 and 4 months. BALF and plasma samples were collected in 6mM EDTA and ATP levels assessed using the Cayman ATP detection assay (see section 2.1.2 and section 2.3.2).

6.2.3 Acute Ozone exposure model

Female C57BL/6J mice were randomly assigned and exposed once for 3 hours, to either room air or ozone at 3ppm in clear perspex chambers. Mice were monitored continuously throughout the exposure. An Ozonetech ACT-3000P ozone generator was used with two positive pressure systems (flow rate 8-24 L/min). The first pumped air through the ozone generator (8 – 12 L/min) and the second pumped air into a mixing chamber (0 – 12 L/min), in which it was mixed with ozone coming out of the ozone generator. This was to allow better control of the ozone levels entering the animal chambers, which were maintained at 3ppm. Ozone levels were assessed every 2 minutes, by having two aeroqual Series 500 - Portable Ozone Monitors in the chamber. Following the last ozone exposure, mice were euthanised at different time points between 0 – 24 hours by a single intraperitoneal injection of 0.2ml pentobarbital (100 mg/mL).

BALF and plasma samples were collected in 6mM EDTA and ATP levels assessed using the Cayman ATP detection assay (see section 2.1.2 and section 2.3.2). BALF cells were isolated and total white blood cells and neutrophil counts were determined as described in section 6.2.2.1.

6.2.3 Poly I:C model

Female C57Bl/6 mice were weighed and challenged intranasally (i.n) with poly I:C (tlr-pic; InvivoGen) at 3 µg/mouse or sham challenged i.n. with saline. Post challenge, mice were euthanised at different time points between 2 – 172 hours by a single intraperitoneal injection of 0.2ml pentobarbital (100 mg/mL). BALF and plasma samples were collected in 6mM EDTA and ATP levels assessed using the

Cayman ATP detection assay (see section 2.1.2 and section 2.3.2). BALF cells were isolated and total white blood cells and neutrophil counts were determined as described in section 6.2.2.1.

6.3 Results

6.3.1. Effects of intratracheal dose-response of CD39-His on BALF eATP levels in naïve mice

Dose-ranging studies are important preliminary studies used to determine the efficacy and potency of a novel drug *in vivo*. Prior to testing the effects of CD39-His in a CS mouse model, it was first necessary to determine which concentration of CD39-His effectively reduced levels of eATP in naïve animals. To determine the dose-response of CD39-His *in vivo*, preliminary studies using naïve mice were performed where animal were dosed intratracheally (i.t.) with a single dose of CD39-His between 0.003 – 3mg/kg. This route of administration was used to ensure that the enzyme was present in the lungs and airways as this is where eATP is thought to be elevated in chronic lung diseases. CD39-His dosed i.t. caused a significant dose-dependent reduction of endogenous eATP levels in the BALF (Figure 6.1A). BALF samples were also exogenously spiked with 100nM ATP and this was dose-dependently reduced indicating target engagement of the enzyme as active CD39-His was present in the airway lumen (Figure 6.2B).

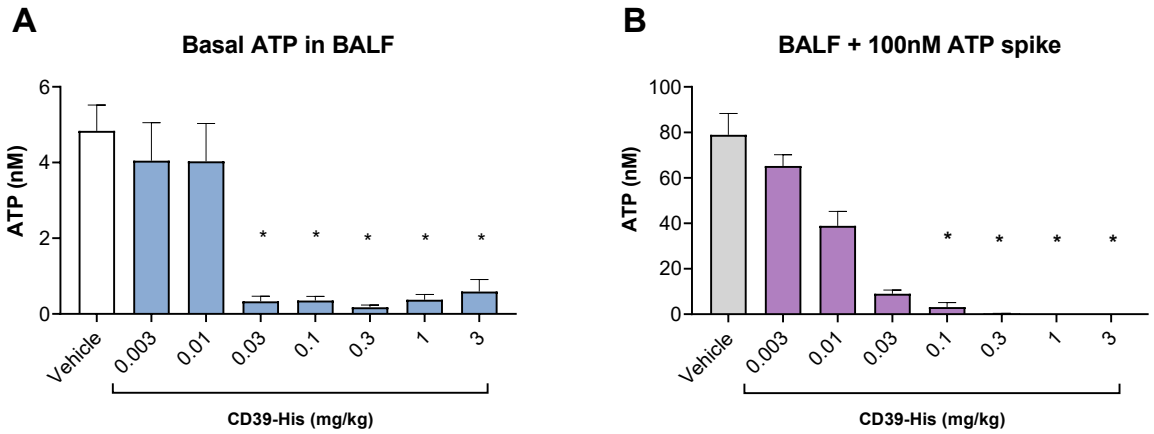


Figure 6. 1 Effect of CD39-His dose-response on BALF eATP levels in naïve mice.

*Vehicle or CD39-His (0.003 – 3mg/kg) were dosed intratracheally (i.t.) to naïve C57BL/6 mice. 30 minutes post dose, animals were culled and bronchoalveolar lavage fluid (BALF) was collected for ATP analysis using the ATP detection assay. eATP levels were measured in (A) neat BALF samples and (B) neat BALF samples exogenously spiked with 100nM ATP. N=6 per treatment group. Data shown are mean ± SEM. * indicates statistical significance ($p < 0.05$), Kruskal Wallis with Dunn's Post Test.*

6.3.2. Effects of intratracheal dose-response of CD39-His on plasma eATP levels in naïve mice

Animals from this study were dosed intratracheally to ensure CD39-His was present in the lungs. However, the effect of CD39-His on systemic levels of eATP were also assessed in plasma samples to determine whether CD39-His reached the systemic circulation and was still active as this may be indicative of potential off-target effects. CD39-His impacted on plasma eATP levels only at the highest doses used (1mg/kg and 3mg/kg) suggesting that lower doses used may prevent any possible unwanted systemic effects such as increased bleeding risk (Figure 6.2).

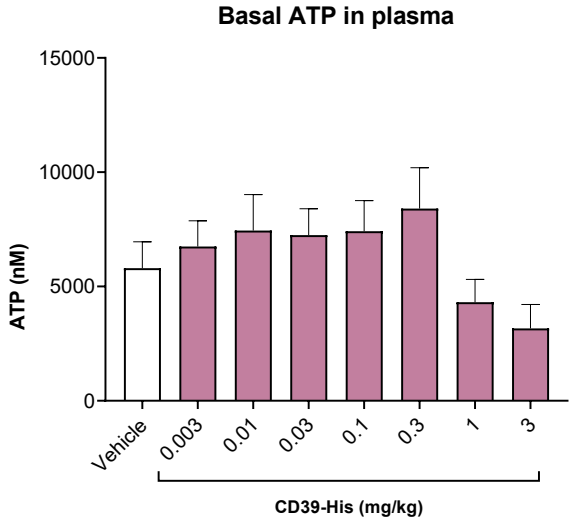


Figure 6. 2 Effect of CD39 dose-response on plasma eATP levels in naïve mice.

*Vehicle or CD39-His (0.003 – 3mg/kg) were dosed intratracheally (i.t.) to naïve C57BL/6 mice. 30 minutes post dose, animals were culled, and plasma samples were collected for ATP analysis using the ATP detection assay. N=6 per treatment group. Data shown are mean ± SEM. * indicates statistical significance ($p < 0.05$), Kruskal Wallis with Dunn's Post Test.*

6.3.3. Effects of intratracheal timecourse of CD39-His on BALF eATP levels in naïve mice

Having established an effective dose-response, the lowest 2 concentrations which impacted lung levels of eATP; 0.03mg/kg and 0.1mg/kg were used in a timecourse study to determine the duration of action of CD39-His. This was required to determine how long the effects of CD39-His lasted following initial dosing which can be used determine how frequently animals need to be dosed in more disease relevant models in order to see an effect.

The effect of both concentrations of CD39-His over 48 hours was monitored across a range of 7 timepoints at 0.5, 2, 4, 8, 16, 24 and 48 hours. The effects of CD39-His at 0.03mg/kg and 0.1mg/kg on

basal and spiked levels of eATP lasted for up to 24 hours post dose which suggests that animals can be dosed once a day (Figure 6.3).

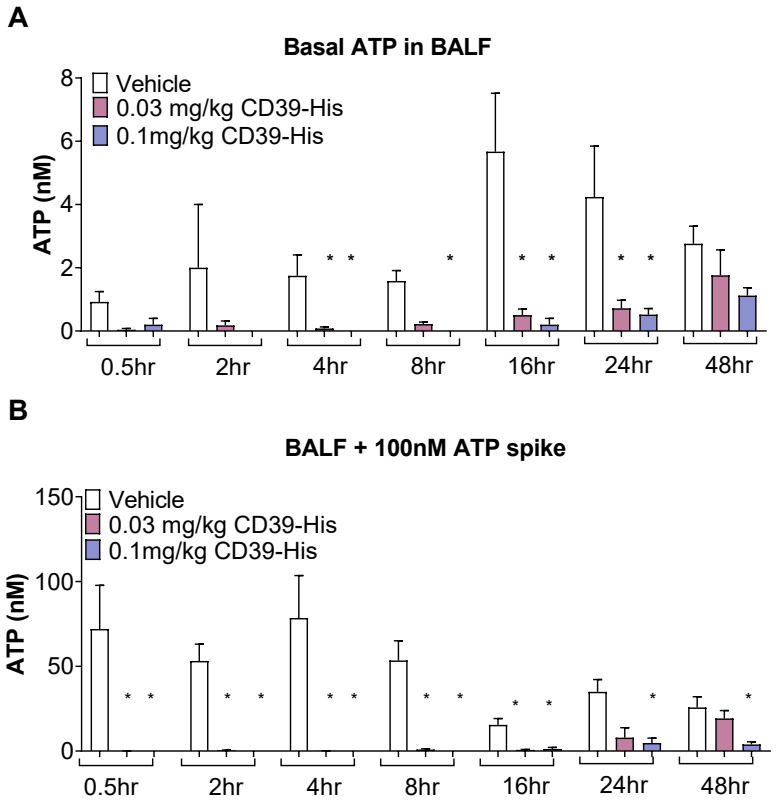


Figure 6. 3 Effect of CD39 timecourse on BALF eATP levels in naïve mice.

*Vehicle or CD39-His (0.03 and 0.1mg/kg) were dosed i.t to naïve C57BL/6 mice and 0.5 – 48 hours post dose animals were culled and BALF samples were collected for ATP analysis using the ATP detection assay. eATP levels were measured in (A) neat BALF samples and (B) neat BALF samples exogenously spiked with 100nM ATP, N=6 per group. Data shown are mean ± SEM. * indicates statistical significance ($p < 0.05$), Kruskal Wallis with Dunn's Post Test.*

6.3.4. Effects of intranasal dose-response of CD39 on BALF eATP levels in naïve mice

Having shown that CD39-His was effective against endogenous ATP levels for up to 24 hours following i.t. dosing, the effects of intranasal (i.n.) dosing was assessed at 24 hours. This was investigated as the i.t. route of administration is an invasive technique which requires the insertion of a cannula into the trachea which may lead to increased inflammation, particularly if repeated dosing is required. However, the i.n. route of administration is less invasive and would be preferrable as it would avoid the risk of extraneous inflammation in mouse disease models such as the 3-day CS model and is more amenable to repeat dosing.

Mice were dosed i.n. with vehicle or 0.03mg/kg – 1mg/kg CD39-His which caused a dose-dependent reduction of endogenous eATP levels in the BALF (Figure 6.4A). Samples were also exogenously spiked with 100nM ATP, and this was dose-dependently reduced (Figure 6.4B) suggesting active CD39-His was present in the airway lumen when dosed intranasally and can therefore be used as a route of administration when investigating the effects of CD39-His in mouse disease models. As a comparison, one of the treatments groups were dosed i.t. with vehicle or 0.1mg/kg CD39-His which significantly reduced levels of endogenous eATP as previously shown.

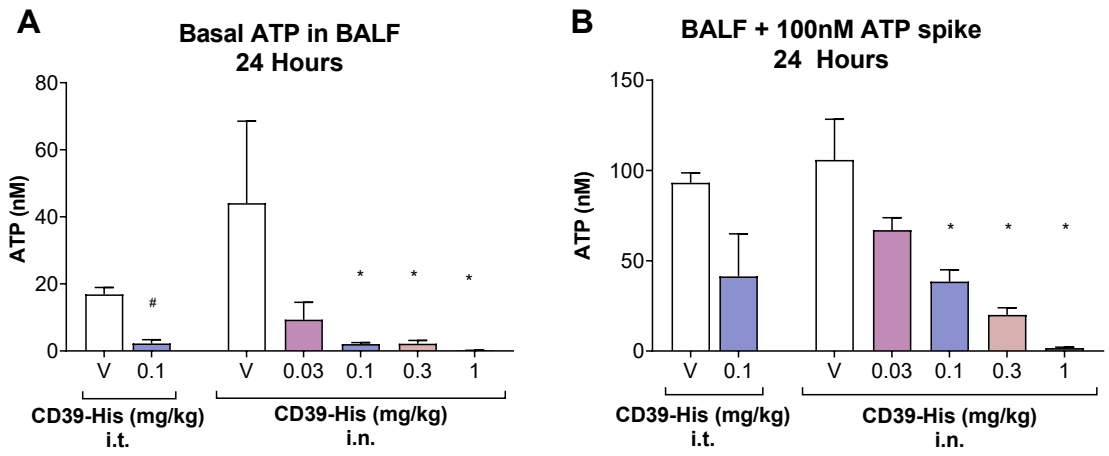


Figure 6. 4 Effect of CD39-His dosed intranasally and intratracheally on BALF eATP levels in naïve mice.

*Vehicle or CD39-His (1mg/kg) were dosed i.t. to naïve C57BL/6 mice. Vehicle or CD39-His (0.03 – 1mg/kg) were dosed i.n. to naïve C57BL/6 mice. 24 hours post dose animals were culled and BALF was collected for ATP analysis using the ATP detection assay. eATP levels were measured in (A) neat BALF samples and (B) neat BALF samples exogenously spiked with 100nM ATP, N=6 per group. Data shown are mean ± SEM. * indicates statistical significance ($p < 0.05$), kruskal Wallis with Dunn's Post Test, # ($p < 0.05$) Mann Whitney U Test.*

6.3.5. Investigating effects of CD39-His in an acute 3-day cigarette smoke mouse model

Having determined the efficacy of CD39-His dosed i.n. against both basal and spiked ATP in BALF, CD39-His was tested in a 3-day CS model to assess whether it was able to reduce eATP in the lungs. CD39-His was dosed i.n. (0.03 – 1mg/kg) 24 hours prior to the first smoke exposure and daily throughout the study.

CD39-His caused a dose-dependent inhibition of both basal and spiked ATP in BALF which suggests that functional CD39-His was present in the lungs (Figure 6.5A-B). However, when comparing the

vehicle groups in the air exposed animals to smoke exposed animals, there was no increase in eATP following smoke exposure.

To confirm that CS induced inflammation in this model, neutrophils and total white blood cells were measured in the BALF samples (Figure 6.5C-D). Both neutrophils and total white blood cells were elevated in smoke exposed animals compared to air controls suggesting CS-induced inflammation in these animals. Kineret, an interleukin-1 receptor antagonist was used as a positive control as it is known to reduce airway neutrophilia in models of lung inflammation (Hernandez et al., 2015). In CS exposed animals dosed with Kineret, there was a significant reduction in neutrophils compared to vehicle controls which further supports that CS exposure induced airway inflammation in this model.

Levels of the ATP driven pro-inflammatory cytokines IL1-β and IL-18 were also measured and shown to be elevated in BALF samples from CS exposed animals (Figure 6.5E-F). Interestingly, the top doses of CD39-His appeared to reduce IL1-β levels similar to that observed in air exposed animals. However, although CS exposure induced inflammation in this model, CD39-His appeared to have no functional effect on leukocytes or IL-18 levels. Given that levels of eATP measured were not elevated in CS exposed animals compared to air controls, an alternative model of airway disease such as the mouse bleomycin model of lung fibrosis (IPF) where increased eATP is observed may be required to assess the impact of CD39-His on eATP and other ATP driven disease markers.

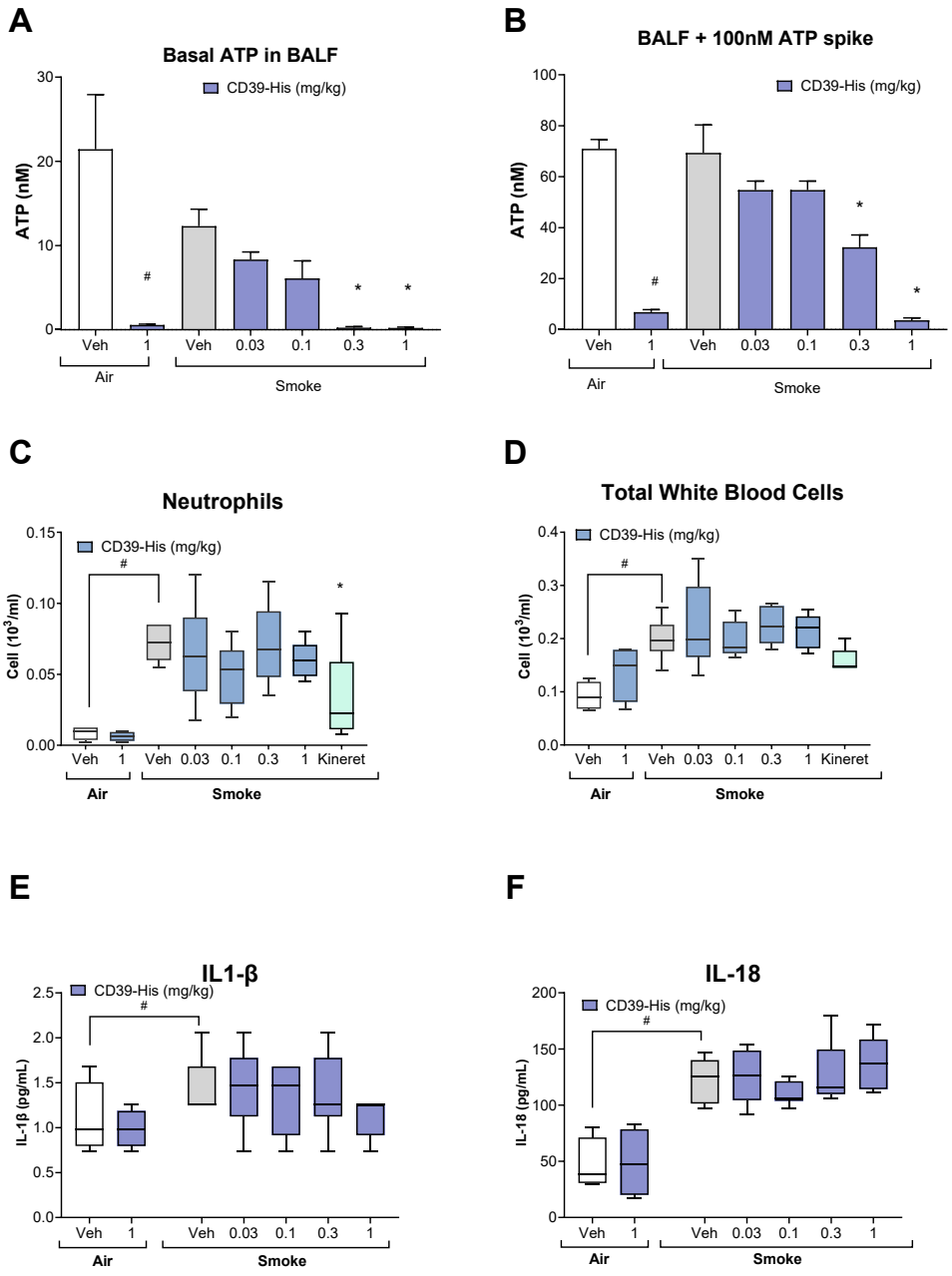


Figure 6. 5 Effect of CD39-His on BALF eATP levels and inflammatory markers in a 3-day CS mouse model.

*Mice were dosed i.n. with vehicle or CD39-His (0.03 - 1mg/kg) 24 hours prior to the first smoke exposure and daily throughout the study. Mice were exposed to air or cigarette smoke for 50 minutes twice daily for 3 days. BALF samples were collected for ATP analysis using the ATP detection assay. eATP levels were measured in (A) neat BALF samples and (B) neat BALF samples exogenously spiked with 100nM ATP. Other inflammatory disease markers including (C) neutrophils, (D) total white blood cells, (E) IL-1β and (F) IL-18 were measured in BALF. N=4 in air exposed groups and N=6 in smoke exposed groups. Data shown are mean ± SEM. * indicates statistical significance ($p < 0.05$), Kruskal Wallis with Dunn's Post Test, # ($p < 0.05$) Mann Whitney U Test.*

6.3.6. eATP levels in acute and chronic mouse CS models

When investigating the effects of CD39-His in the 3-day CS model, there was no increased eATP found in the BALF of smoke exposed animals compared to air exposed animals treated with vehicle 18 hours after the last smoke exposure. A potential hypothesis for this could be that eATP levels are increased at an earlier timepoint. To investigate this, a timecourse experiment was performed to see how eATP levels differed between air and smoke exposed animals at various time points up to 24 hours after the last CS exposure. Across all timepoints measured, eATP was reduced in smoke exposed animals (Figure 6.6).

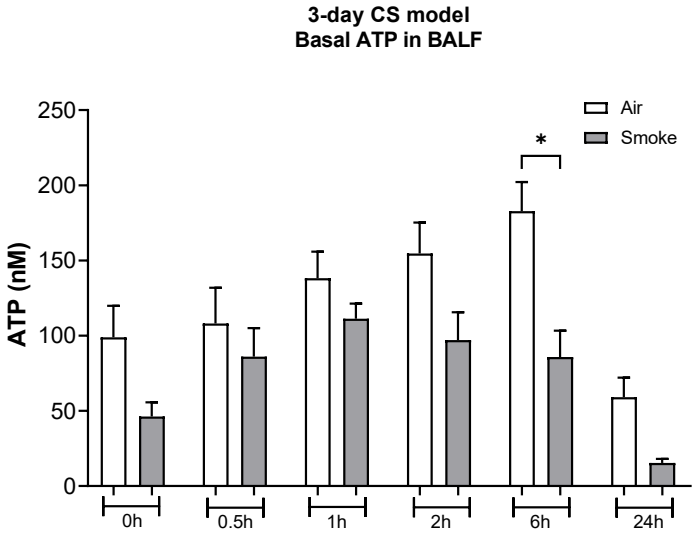


Figure 6. 6 eATP levels in an acute 3-day cigarette smoke mouse model.

*Mice were exposed to air or cigarette smoke for 50 minutes twice daily for 3 days. BALF was collected for ATP analysis using the ATP detection assay. N=8 per group. Data shown are mean ± SEM. * indicates statistical significance ($p < 0.05$), Kruskal Wallis with Dunn's Post Test.*

Based on this data, it was hypothesised that chronic exposure of CS is required to see increased levels of eATP compared to air controls. This was measured in two strains of mice; Balb/c and C57BL/6 mice exposed to either 2 months or 6 months of CS. None of the groups measured had significantly increased levels of eATP in smoke exposed compared to air exposed animals (Figure 6.7). As a result, future work will involve identifying alternative respiratory disease models such as a mouse bleomycin model of lung fibrosis (IPF) where there is elevated eATP to investigate the therapeutic potential of CD39-His in reducing eATP and other ATP driven endpoints.

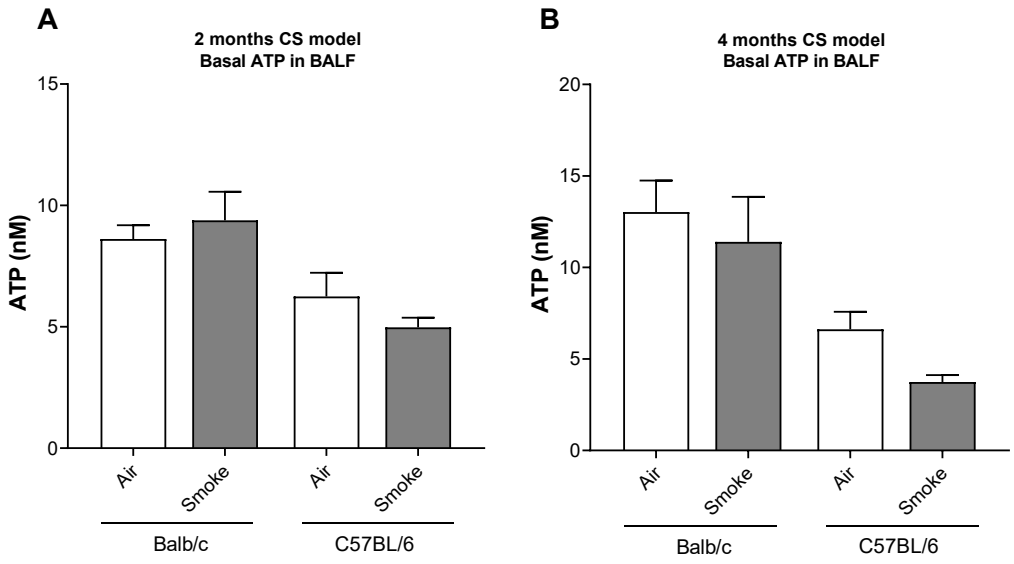


Figure 6. 7 eATP levels in chronic cigarette smoke mouse models.

*Mice were exposed to air or cigarette smoke for 50 minutes twice daily over the course of (A) 2 months and (B) 4 months. BALF samples were collected for ATP analysis using the ATP detection assay. N=8 per group. Data shown are mean ± SEM. * indicates statistical significance ($p < 0.05$), Kruskal Wallis with Dunn's Post Test.*

6.3.7. eATP levels in an acute ozone exposure model

When investigating the effects of CD39-His in the acute and chronic CS model, there was no increased eATP found in the BALF of CS exposed animals compared to air exposed animals. A potential hypothesis for this could be that pulmonary eATP levels are not elevated in this particular model. In order to test the effects of CD39 on lowering ATP and inhibiting ATP-driven disease, an animal model which recapitulates increased eATP observed in humans was required. Therefore, eATP levels were assessed in an alternative inflammatory airway disease model induced by 3 hours of ozone exposure. A timecourse experiment was performed to see how eATP levels differed between air and ozone exposed animals at various time points up to 24 hours post exposure. Across all timepoints measured, there was a decreasing trend in BALF eATP following ozone exposure. However, an inflammatory disease phenotype was still induced by ozone exposure as neutrophil counts were elevated and significantly higher 6 hours and 24 hours post exposure (Figure 6.8).

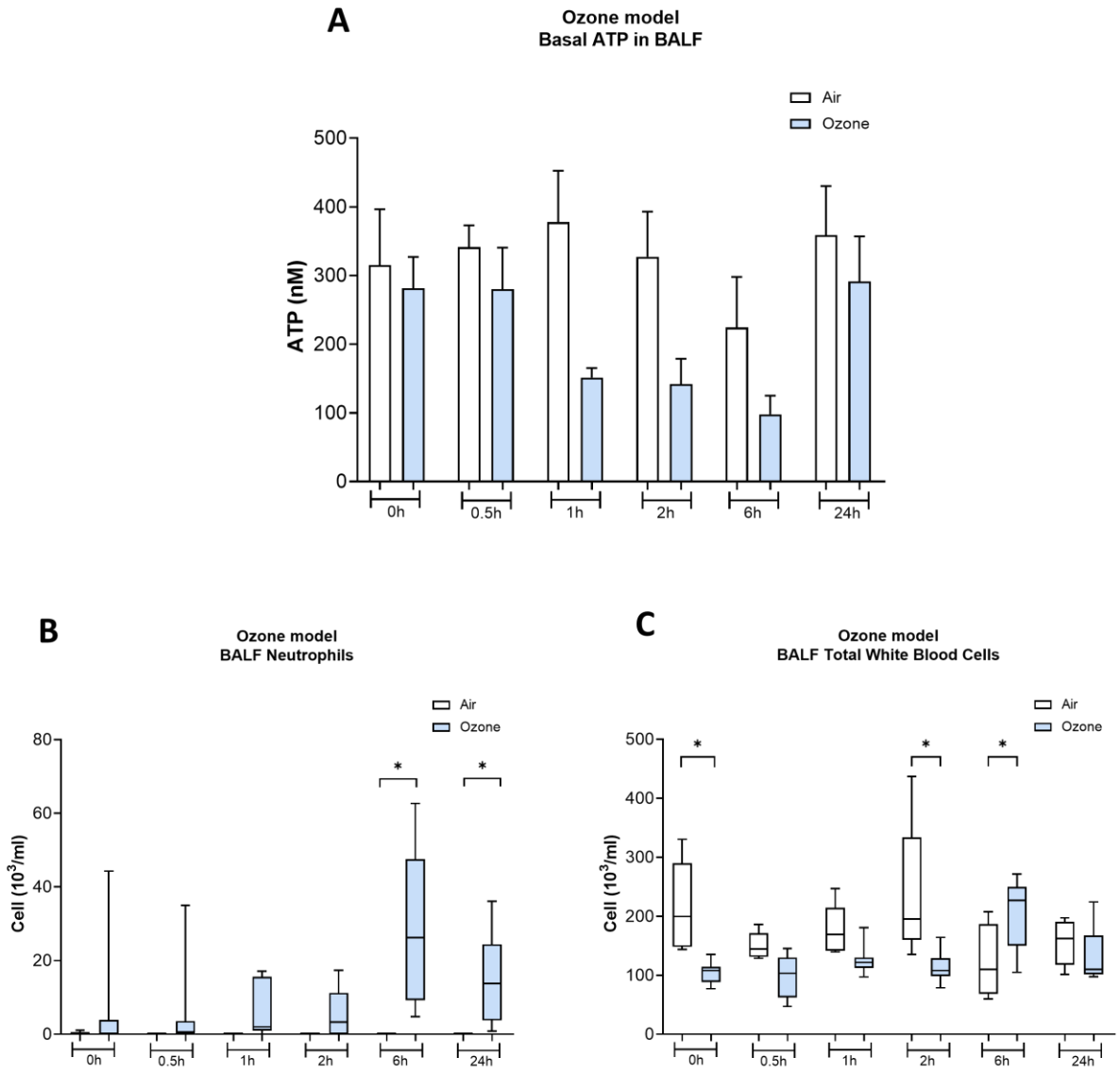


Figure 6. 8 eATP levels and inflammatory markers in an acute 3-hour ozone exposure model.

*Animals were exposed to air or ozone (3 ppm) once for 3 hours and 0 – 24 hours post exposure animals were culled. BALF samples were collected and analysed for (A) basal eATP, (B) neutrophils and (C) total white blood cells, N=8 per group. Data shown as mean ± SEM. * indicates statistical significance ($p < 0.05$), Kruskal Wallis with Dunn's Post Test.*

6.3.8. eATP levels in a Poly I:C model

As the previous models did not show elevated eATP levels despite inducing an inflammatory phenotype, eATP levels were investigated in an alternative Poly I:C model of airway inflammation. A timecourse experiment was performed to see how eATP levels differed between animals given a single dose of saline vehicle or 30µg Poly I:C at various time points between 2 – 168 hours post challenge. Across most timepoints measured, there was a decreasing trend in BALF eATP following Poly I:C challenge which were significantly reduced 24 hours, 48 hours and 72 hours post challenge. Despite this, an inflammatory disease phenotype was still induced by Poly I:C challenge as neutrophil counts were elevated and significantly higher than vehicle challenged animals at 24 – 96 hours post challenge (Figure 6.9).

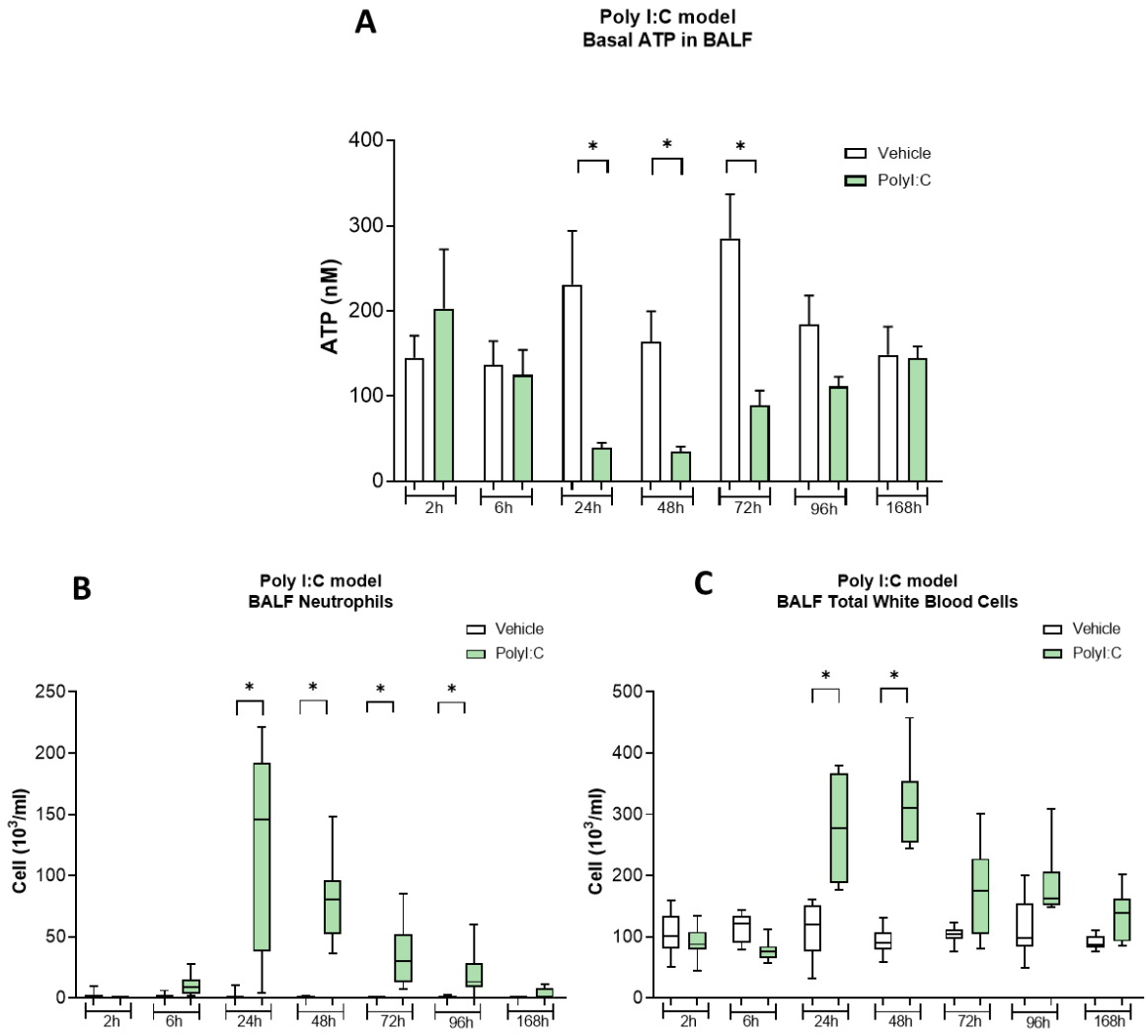


Figure 6. 9 eATP levels and inflammatory markers in a poly I:C exposure mouse model.

*Mice were exposed to vehicle or poly I:C 30µg i.n. once and 2 – 168 hours post exposure animals were culled. BALF samples were collected and analysed for (A) basal eATP, (B) neutrophils and (C) total white blood cells, N=8 per group. Data shown as mean ± SEM. * indicates statistical significance ($p < 0.05$), Kruskal Wallis with Dunn's Post Test.*

6.4 Discussion

Having developed reliable and reproducible methods for the retrieval and assessment of eATP in biological samples, the aim of this chapter was to investigate eATP levels in animal models of respiratory disease. It was hypothesised that lung eATP levels would be increased across several respiratory disease models as it is thought to be a key driver in the pathogenesis of airway disease.

Prior to investigating CD39-His in a 3-day mouse CS smoke model, it was first necessary to determine a dose-response in naïve mice. Dose-ranging studies are performed to identify the most effective dose of a novel drug and can also be used to identify toxic or lethal doses of a novel drug. Half-log concentrations were used as this provides a wide enough range of concentrations to identify the no-effect, mean effective and maximal effective doses of a compound. Naïve mice were dosed i.t. between 0.003-3mg/kg CD39-His. This route of administration was used to ensure that the compound was present in the lungs and airways as this is where eATP is elevated in chronic lung diseases. Following intratracheal lung delivery, CD39-His caused a dose-related reduction in endogenous eATP levels in BALF and in BALF spiked with 100nM ATP which suggested that active CD39-His was present in the airway lumen (Figure 6.1). the lowest 2 concentrations which caused a significant reduction in endogenous ATP in BALF; 0.03mg/kg and 0.1mg/kg were used for future experiments.

The effect of CD39-His was also investigated in plasma samples to determine whether it had an impact on systemic eATP levels as this could be indicative of increased bleeding risk as studies have shown that CD39 on the surface of platelets are involved in limiting thrombotic events following endothelial damage (Morello et al., 2021). The breakdown of ATP by CD39-His could also lead to increased levels of adenosine in the systemic circulation as CD39 metabolises ATP to AMP which is further broken down by the enzyme CD73 into adenosine (Zimmermann et al., 2012). Studies have shown that increased levels of adenosine in the systemic circulation is also associated with increased bleeding risk as adenosine is a strong vasodilator involved in the signalling cascade that inhibits platelet activation which may prevent blood clotting following tissue damage (Johnston-Cox and Ravid, 2011). At the lowest concentrations of CD39-His that effectively reduced eATP in BALF, 0.03mg/kg and 0.1mg/kg, CD39-His did not impact eATP levels which indicates that dosing at this concentration prevents CD39-His reaching the systemic circulation and may therefore prevent increased bleeding risk (Figure 6.2).

Having established a dose-response of CD39-His in naïve mice, the next step was to determine how long the effects of CD39-His lasted on reducing eATP levels in biological samples. These are known as duration of action experiments where the effects of a drug are measured at different time points to determine how long these effects last following a single dose. This data is used to determine how frequently animals need to be re-dosed with a drug for it to continue having the desired effect, which

in this case was a reduction in eATP levels in BALF samples. Animals were dosed with either vehicle, 0.03mg/kg or 0.1mg/kg CD39-His as these were the lowest 2 concentrations which reduced lung levels of eATP. The effects of these doses at reducing eATP levels in BALF samples were monitored across 7 timepoints at 0.5, 2, 4, 8, 16, 24 and 48 hours. The effects of CD39-His at reducing basal eATP in BALF were shown to last up to 24 hours and by 48 hours there were no significant reductions in basal eATP (Figure 6.3). Based on this, in order for CD39-His to continue to reduce lung levels of eATP over the course of the experiment, animals would need to be dosed with CD39-His once daily.

Given that CD39-His was to be investigated in an inflammatory CS model, intratracheal (i.t.) dosing could lead to increased inflammation unrelated to smoke exposure as this route of administration is invasive and requires the insertion of a cannula into the trachea which would need to be repeated daily. An alternative less invasive route of administration would be intranasal (i.n.) dosing as it does not require the insertion of any equipment into the trachea which reduces the risk of extraneous inflammation in animal models and is more amenable to repeat dosing. However, previous in-house data has shown that when animals are dosed i.n. a higher concentration of drug is required as dosing via the nasal passage often means animals may swallow part of the dose causing a lower concentration of drug to reach the lungs. Therefore, the effects of intranasal dosing on endogenous ATP levels in naïve mice were also tested at a higher concentration range of 0.03mg/kg – 1mg/kg CD39-His. As the effects of CD39-His were previously shown to last for at least 24 hours, animals were culled 24 hours post-dose following i.n. dosing. Similar to what was observed in mice i.t. dosed with CD39-His, i.n. dosing of CD39-His also caused a dose-dependent reduction in endogenous eATP levels in BALF and in BALF exogenously spiked with ATP (Figure 6.4). A higher concentration of 0.1mg/kg was required to see a statistically significant decrease in basal ATP in BALF compared to i.t. dosing, likely due to animals swallowing part of the dose. Despite this, the data suggests that i.n. dosing can be used going forward as the data suggests active CD39-His was present in the airway lumen using this route of administration.

Having established the appropriate concentration-range, dosing frequency and route of administration of CD39-His *in vivo* using naïve mice, this was investigated in a 3-day CS exposure model. Animals in this model were i.n. dosed once daily with vehicle or the same dose range of 0.03mg/kg – 1mg/kg CD39-His as this concentration range showed a concentration-dependent decrease in basal eATP in naïve mice. Air control animals were also dosed with either vehicle or 1mg/kg CD39-His as this concentration of CD39-His was shown to significantly reduce BALF eATP in naïve mice. As previously shown in naïve mice, air exposed mice dosed with CD39-His had significant reductions in basal eATP and exogenously spiked ATP compared to vehicle controls. Similarly, a dose-

dependent reduction in eATP was also observed in basal BALF and BALF exogenously spiked with ATP in mice exposed to CS with significant reductions in eATP at the top doses of 0.3mg/kg and 1mg/kg compared to vehicle which suggests functional CD39-His was present in the lungs (Figure 6.5A-B).

However, when comparing basal eATP levels in BALF from vehicle treated animals in the air exposed group to the CS exposed group, there were no increase in eATP following CS exposure. This was not as expected as previous publications have reported increased levels of eATP in 3-day CS exposed animals compared to air controls (Baxter et al., 2014, Cicko et al., 2010). A potential reason could be that CS exposure did not induce inflammation in this model. To investigate this, total white blood cells and neutrophils were measure in the BALF (Figure 6.5C-D). In line with previous publications, CS exposure in these animals did cause an increase in neutrophils and total white blood cells which suggests that inflammation was induced in this model (Cicko et al., 2010, Eltom et al., 2014, Baxter et al., 2014, Eltom et al., 2011). The interleukin-1 receptor antagonist, Kineret, was also used as a positive control in this model as it is known to reduce airway neutrophilia in models of lung inflammation and significantly reduced neutrophil counts in CS exposed animals in this model (Hernandez et al., 2015). When measuring the pro-inflammatory cytokines in BALF samples from this model, IL1-β and IL-18 were also increased following CS exposure compared to air controls which further suggests that CS exposure induced inflammation in this model.

Based on this, it was hypothesised that increased eATP was not measured in the BALF of CS exposed animals as the 18-hour timepoint at which animals were culled following the last CS exposure may have been too late to see a window of increased eATP in CS exposed animals. Therefore, a timecourse experiment was performed where animals were culled at various timepoints up to 24 hours after the last CS exposure in the 3-day CS model. Across the various timepoints, eATP was not increased in smoke exposed animals compared to air controls (Figure 6.6). Given that in humans the development of COPD is associated with chronic cigarette smoking, it was hypothesised that acute 3-day CS exposure may not be sufficient to see increases in lung eATP. To test this hypothesis, samples from chronic CS exposure models run by AstraZeneca collaborators were sent for analysis. In these models, Balb/c and C57BL/6 mice were exposed to CS for 2 months or 4 months. Neither of these chronic CS exposure models had significantly increased levels of eATP in smoke exposed compared to air exposed animals (Figure 6.7). As the animals used in these CS models were young and healthy prior to CS exposure, a potential hypothesis could be that these animals have a compensatory mechanism such as increased ecto-nucleotidase activity to counteract any CS induced eATP increases (Zimmermann et al., 2012).

Although the disease phenotype, characteristic of inflammation such as increased total white blood cells, neutrophils and cytokines were observed in the 3-day CS model, at the concentrations tested CD39-His did not have an impact on all of these markers (6.5E-F). Only the top doses of CD39-His appeared to reduce IL1-β levels similar to that observed in air exposed animals. However, there was no clear concentration-dependent trend in this decrease. Despite the eATP data which suggests there was active CD39-His present in the lungs of CS exposed animals which caused a concentration-dependent decrease in eATP, aside from the effect of high doses on CD39-His on IL-1β, CD39-His did not appear to have any functional effect on other inflammatory markers measured in this model. This could also suggest that other inflammatory signalling pathways aside from ATP may be key in driving inflammation in these models.

For instance, the inflammasome can be activated by other danger signals produced by cells known as danger associated molecular patterns (DAMPs). DAMPs are released in response to cellular and tissue damage, conditions of stress and modification of host proteins by pathogens. Although ATP is known to function as a DAMP, other molecules such as monosodium urate crystals and hyaluronic acid are believed to function as DAMPs which may be involved in CS induced inflammation (Birrell and Eltom, 2011). The NLRP3 inflammasome can also be triggered by the activation of receptors that detect the presence of pathogens through pathogen associated molecular patterns (PAMPs). This includes Toll-like receptors (TLRs) such as TLR4, a receptor for bacterial endotoxins (Birrell and Eltom, 2011). CS exposure leads to several endogenous and exogenous ligands that bind to TLR4 such as heat shock proteins and breakdown products of the extracellular matrix. A study found that mice genetically altered to have non-functional TLR4 failed to develop inflammation after CS challenge which suggests that this pathway may also be important in driving inflammation in CS exposure models (Maes et al., 2006). Studies have also shown that CS-induces release of reactive oxygen species is also involved in activation of the NLRP3 inflammasome (Zhou et al., 2011). These data suggest that CD39-His may not have any functional effect on inflammation in this model as reducing eATP may not have an impact on other signalling pathways involved in driving the inflammatory phenotype present in this model.

Although increased levels of eATP are reported in the BALF of COPD patients, it is also important to note that COPD develops slowly over decades and therefore murine CS exposure models, despite being the most utilised animal models of COPD, may not be able to recapitulate all the mechanisms and pathways involved in the pathogenesis of COPD (Lommatzsch et al., 2010, Vandivier and Ghosh, 2017). For instance, certain characteristics of disease observed in patients with COPD such as excess mucus production, mucus cell metaplasia or periodic exacerbations is not found in CS exposed animal models (Vandivier and Ghosh, 2017).

Given that increased eATP was not observed in animal models following CS exposure, eATP levels were investigated in an acute ozone exposure model. Previous publications have shown that ozone exposure leads to airway inflammation and the upregulation of several inflammatory cytokines including IL-1β and IL-18 which are thought to be driven by ATP-induced activation of the NLRP3 inflammasome (Sokolowska et al., 2019). Another study also showed that BALF eATP levels were elevated in animals exposed to ozone (2ppm) for 3 hours (Kong et al., 2021). Based on these findings, it was hypothesised that 3-hour ozone exposure would result in increased lung eATP. Total white blood cells and neutrophil counts were also measured to ensure that ozone exposure induced an inflammatory phenotype. Similar to the CS model there was no significant increase in eATP and across all time points there was a trend towards decreased eATP in ozone exposed compared to air exposed animals. However, an inflammatory phenotype was still observed as there were increases in neutrophils and total white blood cells following ozone exposure (Figure 6.8). This suggests that eATP may not be driving the inflammatory phenotype observed in this model which is supported by studies which show that ozone triggers a wide range of interactive signalling pathways that lead to inflammatory responses including the activation of membrane receptors such as TLRs, intracellular kinases and phosphatases and transcriptional factors that regulate inflammatory genes (Yan et al., 2016).

In both the CS and ozone respiratory disease models an unexpected decrease in eATP was observed. The next step was to investigate eATP levels in a Poly I:C model of airway inflammation. Poly I:C is a TLR3 agonist which mimics viral infection which has been shown to induce inflammation and impair lung function in mice (Stowell et al., 2009). *In vitro* studies have also shown that Poly I:C induces eATP release and mucus release from human bronchial epithelial cells (Shishikura et al., 2016). *In vivo* Poly I:C exposure was also shown to exacerbate airway inflammation and remodelling in CS exposed mice (Mei et al., 2022). Therefore, BALF eATP levels were investigated in a Poly I:C exposed model to see if it was elevated. Similar to the CS and ozone exposure models, there was a trend towards decreased eATP following dosing which was significantly reduced 24 – 72 hours post dose. However, neutrophils and total white blood cells were elevated which suggests that Poly I:C exposure induced an inflammatory phenotype. This could suggest that other non-ATP driven mechanisms are involved in activation of inflammatory pathways. For instance, Poly I:C which directly activates TLR3 induces the upregulation of IL-8 and IL-6 which are known to amplify inflammatory responses and exacerbate conditions of COPD and asthma (Lever et al., 2015, Bérubé et al., 2009).

Having observed a decreasing trend in eATP levels across three inflammatory airway disease models, another potential reasons as to why decreased eATP following challenge is observed could be because

the mice used in these models were healthy prior to exposure and perhaps there is increased ATP breakdown activity as a compensatory mechanism. If so, eATP levels could be elevated following exposure to either CS, ozone or Poly I:C but may be rapidly degraded as a compensatory mechanism prior to the collection of BALF which means this rise in eATP is not captured in the sample.

To address this hypothesis future work will investigate whether there is increased ecto-nucleotidase expression and activity in the lungs of these animal models. Preliminary work to develop an assay to measure ecto-nucleotidase activity in BALF samples using the ATP detection assay is described in chapter 8, (see section 8.3.4). This activity assay could be used to investigate whether CS, ozone or Poly I:C challenge triggers an upregulation in ATP breakdown which may explain why an increase in eATP is not observed in these disease models. If this is the case, perhaps BALF may not be an ideal measure of pulmonary eATP levels. Future work could explore the use of visualising ATP release from individual cells in real-time using microscopy as details in chapter 8, (see section 8.3.3).

In summary, across all 3 respiratory disease models an unexpected decrease in lung eATP was observed and therefore the hypothesis that lung eATP is elevated in these disease models is rejected. Further work is required to determine whether this can be attributed to increased ATP breakdown as a compensatory mechanism given that the animals used in these models were relatively young and healthy. Alternatively, eATP may not be key in driving the pathophysiology observed in these inflammatory disease models. As a result, alternative airway disease models where eATP is elevated and shown to be driving disease pathogenesis is required to investigate the therapeutic potential of tools such as CD39-His in reducing eATP and other ATP driven endpoints.

Although eATP is elevated in clinical samples from asthma, COPD and IPF patients, it is important to note that pre-clinical animal models are not able to completely recapitulate the exact pathophysiological mechanisms and pathways characteristic of these conditions. In previous chapters, eATP has been shown to activate airway sensory nerves which can be reduced by CD39 induced ATP breakdown and by blocking ATP-induced purinergic P2X3 receptors (Drake et al., 2023). Given that eATP levels from chronic cough patients have not been reported in the literature, the next chapter aims to investigate the hypothesis that eATP levels are elevated in chronic cough patients and is a key driver in the pathophysiological mechanism underlying chronic cough.

Chapter 7: Measuring Extracellular ATP in Refractory and Unexplained Chronic Cough Patient Samples

7.1 Rationale

There is growing body of research implicating extracellular ATP (eATP) in driving disease pathogenesis and symptoms in a range of chronic respiratory diseases. This is supported by studies which have reported elevated eATP in the lungs of patients with COPD, asthma and IPF (Lommatzsch et al., 2010, Idzko et al., 2007, Riteau et al., 2010, Hlapčić et al., 2019). A common symptom across these diseases is chronic cough (CC), which is defined as excessive and/or inappropriately activated cough occurring for more than 8 weeks. As well as occurring as a symptom of respiratory disease, CC can also be idiopathic in nature, known as Unexplained Chronic Cough (UCC). CC that persists despite treatments targeting those with underlying respiratory disease is described as Refractory Chronic Cough (RCC). ATP is thought to play a key role in driving CC as antagonists of purinergic P2X3 receptors present on sensory afferent nerves have shown antitussive efficacy in refractory and unexplained chronic cough (RUCC) patients in clinical trials (McGarvey et al., 2022, Drake et al., 2023). However, eATP levels in the airways or systemic circulation of CC patients are yet to be determined. Therefore, the aim of this chapter is to investigate eATP levels in refractory and unexplained chronic cough (RUCC) patient samples to see if eATP levels are increased in the lungs compared to that of healthy volunteers (HV), utilising the ATP assays characterised in Chapter 3. Throughout this chapter CC will be used to refer to RUCC patients. Bronchoalveolar lavage fluid (BALF) measurements will be used to indicate lung levels of eATP and plasma samples to indicate systemic levels of eATP.

7.1.1 Chapter hypothesis

Extracellular ATP (eATP) is elevated systemically and in the lungs, specifically the lung secretions, of refractory and unexplained chronic cough (RUCC) patients.

7.1.2 Aims

- Measure eATP in plasma samples from patients with RUCC and HV.
- Measure eATP in BALF samples from patients with RUCC and HV.
- Determine whether there are any correlations between eATP levels and cough counts.
- Determine whether the ATP detection assay and Hygiena device produce similar results.

7.2 Methods

Human plasma and BALF samples were obtained from clinical collaborators; professor Jacky Smith and her team at the University Hospital of South Manchester, UK. These studies were approved by the London-Dulwich Research Ethics Committee (REC reference: 21/PR/1233 and 18/NW/0254).

7.2.1 Cough Central clinical study

The cough central study was a UK-based study launched in 2020 by Manchester University NHS Foundation Trust (MFT). The primary objective of this study was to investigate resting-state functional connectivity in the central nervous system in refractory and unexplained chronic cough (RUCC) patients compared to healthy controls. However, for the purpose of this thesis the aim was to investigate plasma levels of eATP in RUCC patients compared to healthy controls.

RUCC patients attended three study visits where they were screened for eligibility and blood samples were collected. Subjects were then fitted with a VitaloJak cough monitoring device and at least 24 hours following the start of cough monitoring they attended the clinic a second time for a cough challenge study. HV completed the cough challenge immediately after the screening visit and were not fitted with a VitaloJak cough monitoring device.

For the cough challenge, subjects were asked to inhale hypotonic saline solutions with decreasing osmolarity up to the maximum tolerated dose. A 0.9% saline placebo dose was also included in the study. Several endpoints were measured including forced expiratory volume in 1 second (FEV_1).

Following the cough challenge visit, subjects were asked to come in for a final visit to perform a functional Magnetic Resonance Imaging (fMRI) scan and several parameters were measured. 20 HV and 50 RCC patients were recruited for this study.

Recruitment criteria for the study is outlined in table 2.1. All RCC patients were recruited from the Wythenshawe tertiary cough clinic at MFT. HV were recruited through advertising in the hospital and university (MFT) and through a database of subjects previously expressing an interest in participating in clinical trials. Prior to being consented for the study, all subjects received a copy of the patient information sheet and were given adequate time to decide whether they wanted to partake in the study. The Cough Central study was approved by the London-Dulwich Research Ethics Committee (REC reference: 18/NW/0254).

Cough Central Subjects Inclusion Criteria	Cough Central Subjects Exclusion Criteria
• Male and female CC patients and HV between 18-80 years inclusive. • Participants must have capacity to consent. • Participants must be non-smokers; ex-smokers <20 pack years, >6 months abstinence. • HV must have no clinically relevant abnormalities based on their medical history, physical examination, vital signs, or significant past respiratory disease, and must have spirometry within normal limits. • CC patients must have a diagnosis of refractory CC as defined by the British Thoracic Society (BTS) guidelines. • CC patients must not have evidence of asthma and have an FEV_1 > 70% predicted value.	• Participants with asthma. • Routine contraindications to fMRI scanning e.g. certain metal implants, recent surgery, extreme claustrophobia etc. • Participants who have received any medications likely to modulate cough within 2 weeks of enrolment. • Participants currently taking ACE inhibitors. • Participants on anticoagulants and unable to safely come off these. • Participants with any condition that may increase circulating levels of ATP/ATP metabolites e.g., chronic cardiac failure, chronic hypoxia, vigorous exercise in the last 48 hrs, or regular vigorous exercise, such as professional sports or competitive training. • Participants who are pregnant or breastfeeding. • Participants with FEV1 <70% predicted (CC) or <80% predicted (HV). • Participants with recent history of upper or lower respiratory tract infection or significant changes in pulmonary status within 4 weeks prior to enrolment. • Participants with other severe, acute, or chronic medical or psychiatric conditions that may increase the risk associated with trial participation or may interfere with the interpretation of trial results.

Table 7. 1 Recruitment criteria for Cough Central study.

7.2.2 ANTHEM Clinical study

The ANTHEM clinical study (ATP in the Airways and Blood in Chronic Cough) was a UK-based clinical study launched in 2021 by Manchester University NHS Foundation Trust (MFT). Enrolled subjects underwent clinical assessment followed by blood and BALF sample collection. Recruitment criteria for the study are outlined in table 2.2. All RUCC patients were recruited from the Wythenshawe tertiary cough clinic at MFT. HV were recruited through MFT's Medicines Evaluation Unit (MEU). Prior to being consented for the study, all subjects received a copy of the patient information sheet and were given adequate time to decide whether they wanted to partake in the study. The ANTHEM study was approved by the London-Dulwich Research Ethics Committee (REC reference: 21/PR/1233).

ANTHEM Subjects Inclusion Criteria	ANTHEM Subjects Exclusion Criteria
• Male and female CC patients and HV between 18-80 years inclusive. • Participants must have capacity to consent. • Participants must be non-smokers; ex-smokers ≤10 pack years, >6 months abstinence. • HV must have no clinically relevant abnormalities based on their medical history, physical examination, vital signs, or significant past respiratory disease, and must have spirometry within normal limits. • CC patients must have a diagnosis of RCC as defined by the European Respiratory Society (ERS) / American College of Clinical Pharmacy (ACCP) guidelines.	• Participants who have received any medications likely to modulate cough within 2 weeks of enrolment. • Participants currently taking ACE inhibitors. • Participants on anticoagulants and unable to safely come off these. • Participants with any condition that may increase circulating levels of ATP/ATP metabolites e.g., chronic cardiac failure, chronic hypoxia, vigorous exercise in the last 48 hrs, or regular vigorous exercise, such as professional sports or competitive training. • Participants who are pregnant or breastfeeding. • Participants with FEV1 <70% predicted (CC) or <80% predicted (HV). • Participants with recent history of upper or lower respiratory tract infection or significant changes in pulmonary status within 4 weeks prior to enrolment. • Participants with other severe, acute, or chronic medical or psychiatric conditions that may increase the risk associated with trial participation or may interfere with the interpretation of trial results.

Table 7. 2 Recruitment criteria for ANTHEM study.

7.2.3 Human sample collection and processing

The addition of EDTA to the collection protocol of biological fluids was shown to allow reliable and reproducible detection of ATP levels (see chapter 3, section 3.3.4 and 3.3.5), this methodology was fed back to our clinical collaborators. They were able to use this information to inform clinical sample collection allowing investigation into eATP levels in RCC patients. BALF and plasma samples were taken with specified concentrations of EDTA solution, to ensure all samples contained approximately 6mM EDTA.

7.2.3.1 Human Plasma

Plasma samples were drawn from the median cubital or cephalic vein in the arms of subjects and collected into K2E K2EDTA blood collection tubes (Avantor, USA) and immediately placed on ice. Blood samples were then centrifuged (1200g, 10min, 4°C) to separate cells from the plasma supernatant and the plasma was aliquoted and stored at -80°C until further analysis.

7.2.3.2 Human Bronchoalveolar lavage fluid (BALF)

Fibreoptic bronchoscopy was performed under conscious sedation and BALF was collected according to the ATS guidelines (Meyer et al., 2012) at a specialist cough clinic at the University Hospital of South Manchester, UK as previously described (West et al., 2012). BALF was combined into K2E K2EDTA blood collection tubes (Avantor, USA). All BALF samples were centrifuged (800g, 10min, 4°C) to

separate cells from the supernatant. The supernatant BALF was aliquoted and stored at -80°C until further analysis.

7.2.4 ATP measurements

7.2.4.1 ATP detection assay

The ATP Detection Assay kit- Luminescence assay (Cayman chemical, USA) referred to as the ATP detection assay was performed as per the manufacturer's protocol with modifications detailed in section 2.3.2.

Briefly, samples were thawed on ice. An ATP standard was prepared by serially diluting the standard in sterile water ranging between 100pM – 100µM. 10µl of standard was added to the relevant wells of a black ½ area 96-well optiplate and 10µl of sterile water was added to remaining wells. This was followed by 10µl of medium (saline with EDTA) to the standard wells and 10µl of sample to sample wells. Finally, the reaction mix was prepared using the reagents provided in the kit and 100µl of reaction mix was added to all wells. The plate was then dark adapted for 20 minutes at room temperature prior to being read in the SpectraMax iD5 multi-mode microplate reader.

7.2.4.2 Hygiena Device

The Hygiena ensure touch luminometer (Hygiena, USA) referred to as the hygiena device was used as described in section 2.3.3.

Briefly, 15µl of sample was placed in a 2ml Eppendorf tube and measurements were taken by using the hygiena Ultrasnap swab. The swab was placed into the sample and rotated round 5 times and then placed back into its casing. The top of the swab was then snapped to release the liquid reagent to the bottom of the swab. The casing was then shaken for a few seconds before being placed into the luminometer which provided relative light unit (RLU) measurements from the samples.

7.2.4.3 SystemSure Plus ATP monitor

Immediate ATP measurements were performed by the clinical collaborators during blood sample collection for the Cough Central study. Plasma samples were collected on a SureSnap ATP detection swab housed inside the SystemSure Plus ATP monitor to give an immediate reading of RLU measurements from the samples which are directly proportional to ATP levels.

7.2.4.4 Data analysis

For experiments whereby an ATP standard curve was performed, ATP concentrations were interpolated from the ATP standard curve (100pM – 100µM) which was run in duplicate by linearly plotting log (concentration) in the x axis and average relative light units (RLU) in the y axis. In samples

that had been diluted, the dilution factor was considered when interpolating ATP concentrations. All data are presented as mean ± S.E.M and statistical analysis performed used Welch's t test.

7.3 Results

7.3.1 eATP measurements in Cough Central plasma samples

Plasma samples from the Cough Central study were measured by clinical collaborators using this SystemSure ATP monitor device. This provided immediate readouts which were performed to give an insight into the possibility of using this technique for future point-of-care use whereby these measurements could be used as a biomarker to identify patients likely to respond to ATP-targeted therapies. An additional advantage of this technique is that immediate read out of samples reduces the need to freeze-thaw samples for plate assay analysis and therefore may reduce the likelihood of rapid ATP degradation. Plasma samples were also stored on ice and shipped to Imperial College London for analysis using the ATP detection assay. Data from both assays are presented as relative light units for comparison as an ATP standard curve was not performed during the SystemSure ATP measurements. A similar trend was observed between both techniques whereby there were no significant differences in plasma eATP between HV and CC patient samples. However, the raw RLUs measured using the Cayman ATP detection assay were approximately 1000 times higher than that using the SystemSure ATP monitor (Figure 7.1).

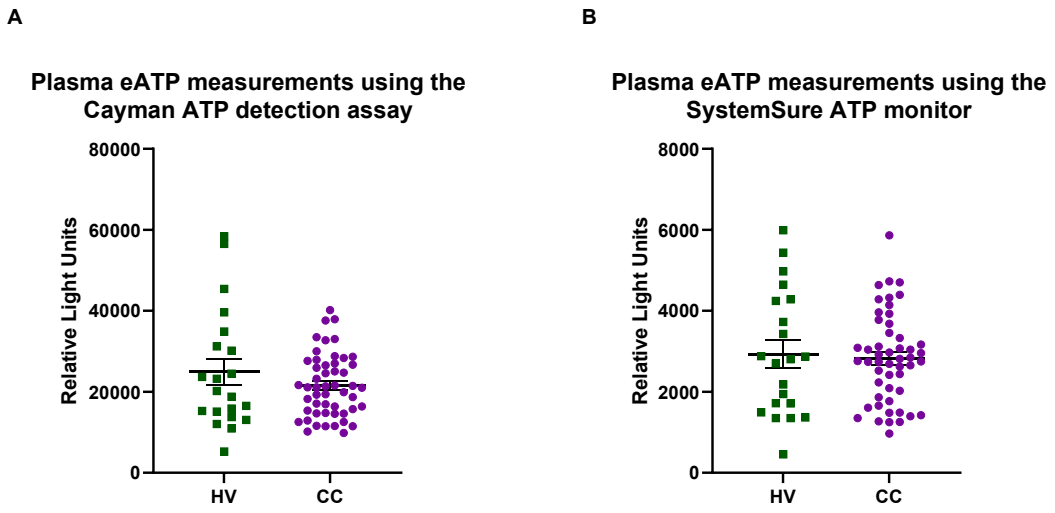


Figure 7. 1 Cough Central plasma eATP measurements.

Measurements were taken from chronic cough (CC) patient samples n=51 and healthy volunteers (HV) n=21. (A) eATP measurements using Cayman ATP detection assay. (B) eATP measurements using the SystemSure ATP monitor. Data presented as RLUs mean ± S.E.M.

7.3.2 eATP measurements in male versus female Cough Central samples

CC is more prevalent in females compared to males and several studies have shown sex-related differences in cough hypersensitivity. For instance, cough challenge studies have shown that women with and without CC have a heightened sensitivity to tussive stimuli compared to men (Varechova et al., 2008, Morice et al., 2014a). Observational studies also show a higher prevalence of CC in females relative to males. For example, a survey of 10032 adults found that two thirds of patients with CC were female (Morice et al., 2014a).

Based on these findings, although there were no significant differences between CC patients and HV, the data was grouped by gender to see if there were any differences. No trends or significant differences were seen between genders in the CC and HV groups (Figure 7.2).

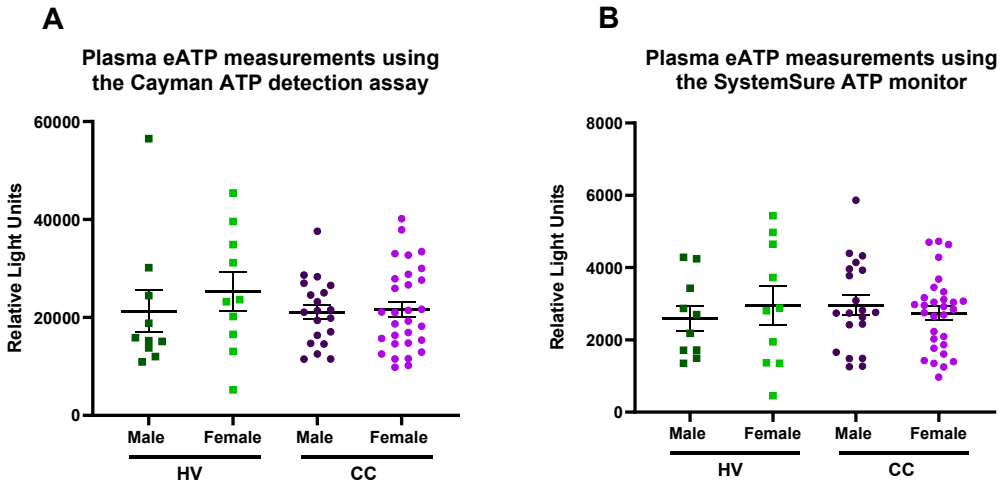


Figure 7. 2 Cough Central plasma eATP measurements in males versus females.

Measurements were taken from chronic cough (CC) patient samples; male n=20, female n=29 and healthy volunteers (HV); male n=10, female n=10. (A) eATP measurements using Cayman ATP detection assay. (B) eATP measurements using the SystemSure ATP monitor. Data presented as RLUs mean ± S.E.M.

7.3.3 Correlations between eATP measurements and cough counts in Cough Central

During the Cough Central study, CC patients were fitted with a VitaloJak cough monitoring device during their first visit. This was used to measure total cough counts over 24 hours prior to the cough challenge studies. Although there were no significant differences between eATP measurements in plasma samples from CC patients and HV, correlations between cough counts and eATP plasma measurements from CC patients were analysed. There were no clear correlations observed between

cough counts and eATP measurements from individual CC patients. However, a very weak positive trend was observed with the Cayman measurements compared to the SystemSure measurements (Figure 7.3).

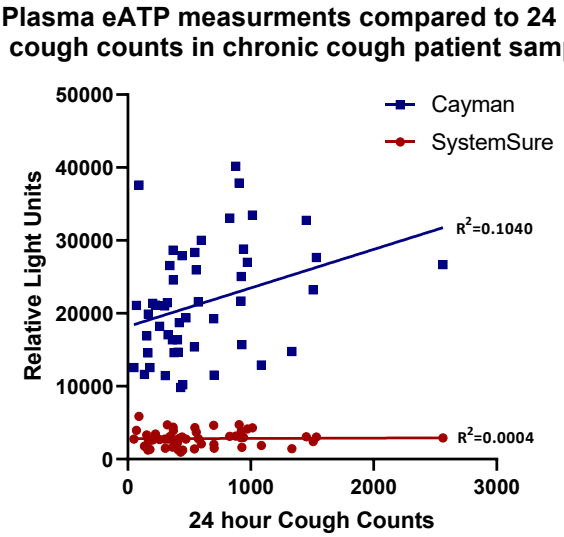


Figure 7. 3 Correlations between Cough Central plasma eATP measurements and 24 hour cough counts in chronic cough patient samples.

24 hour Cough counts were measured in chronic cough (CC) patients n=50 and plasma eATP levels were measured in these patients using the Cayman ATP detection assay and the SystemSure ATP monitor. Data presented as RLUs and linear regression used to fit the data whereby R^2=1 would indicate that the data perfectly fits a linear model.

7.3.4 eATP measurements in ANTHEM BALF samples

Given that there were no differences in plasma eATP measurements between CC patients and HV, the next step was to investigate lung levels of eATP by measuring eATP in BALF samples.

During the ANTHEM study, BALF samples were collected and stored on ice and shipped to Imperial College London for analysis using both the ATP detection assay and the Hygiena device. Unlike the Cough Central study whereby immediate ATP measurements were taken using the SystemSure ATP monitor, sample analysis from the ANTHEM study required samples to be freeze-thawed for analysis.

Neat BALF samples were measured against an ATP standard curve to enable extrapolation of ATP concentrations using both the Cayman ATP detection assay and the Hygiena device which were measured on the same samples in parallel. Using both techniques there were significant reductions in BALF eATP in CC patient samples compared to HV, although the hygiena device ATP values were

approximately 3 times lower than that measured with the plate-based Cayman ATP detection assay. This data was also grouped by gender but no significant differences were observed (Figure 7.4).

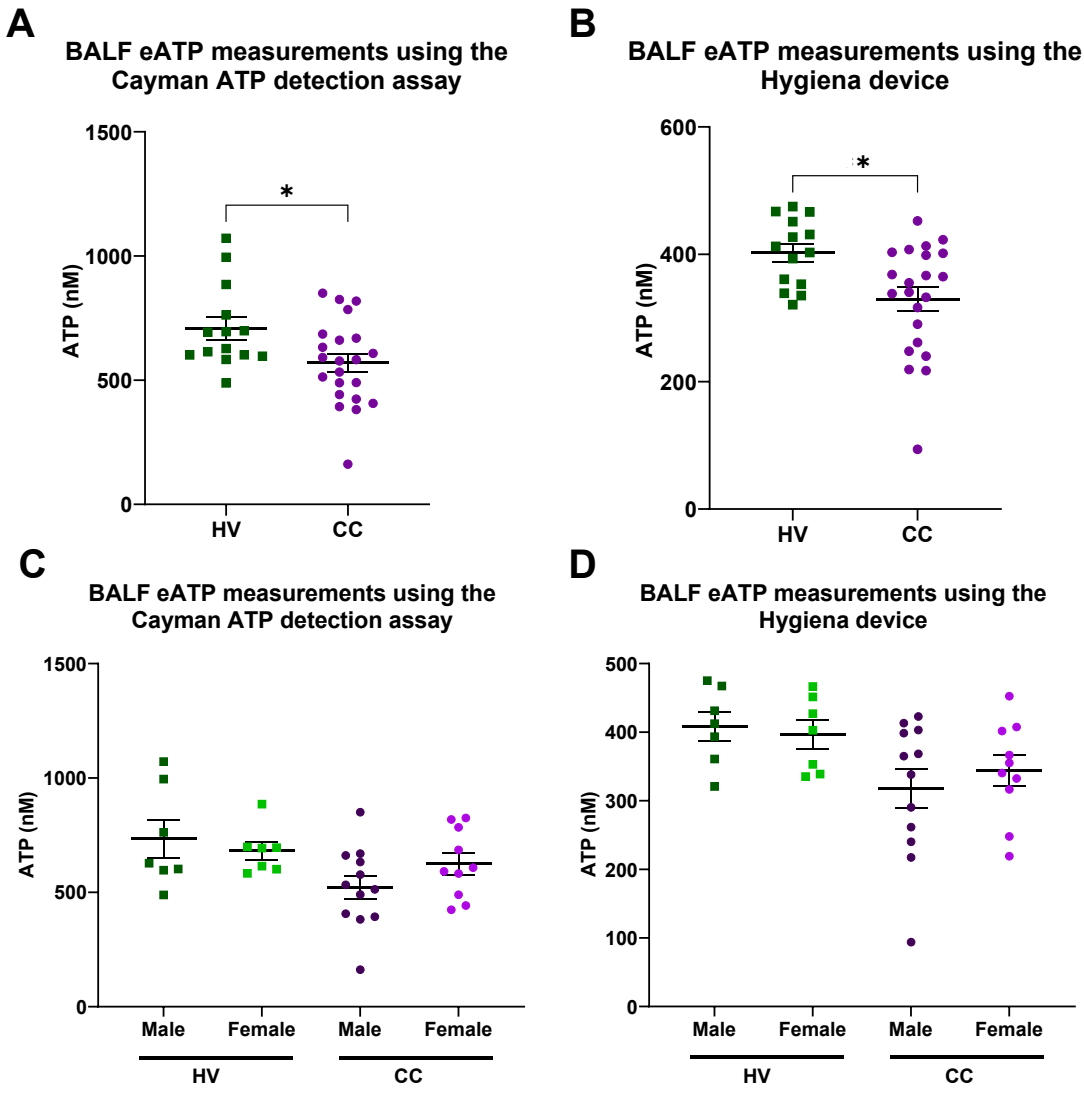


Figure 7. 4 ANTHEM BALF eATP measurements.

*Measurements were taken from chronic cough (CC) patient samples n=14 (n=7 male, n=7 female) and healthy volunteers (HV) n=22 (n=12 male, n=10 female). (A) eATP measurements using Cayman ATP detection assay comparing total CC and HV and (C) grouped by gender. (B) eATP measurements using the Hygiena device comparing total CC and HV and (D) grouped by gender. Data shown are mean ± SEM. * indicates statistical significance Welch's t test (p=0.0222 and 0.0037, respectively).*

7.3.5 eATP measurements in ANTHEM plasma samples

Plasma samples were also collected during the ANTHEM study and eATP measured as an indication of systemic eATP levels. Neat samples were measured using the Cayman ATP detection assay. However,

plasma samples were diluted 8x in PBS as this device has a reduced range of ATP detection as detailed in chapter 3 (section 3.3.3). This protocol will also be followed by clinical collaborators for SystemSure ATP measurements of plasma. A significant increase in plasma eATP measurements were observed in CC patient samples compared the HV using both techniques. Interestingly, these were significantly increased in female CC patients compared to male CC patients (Figure 7.5).

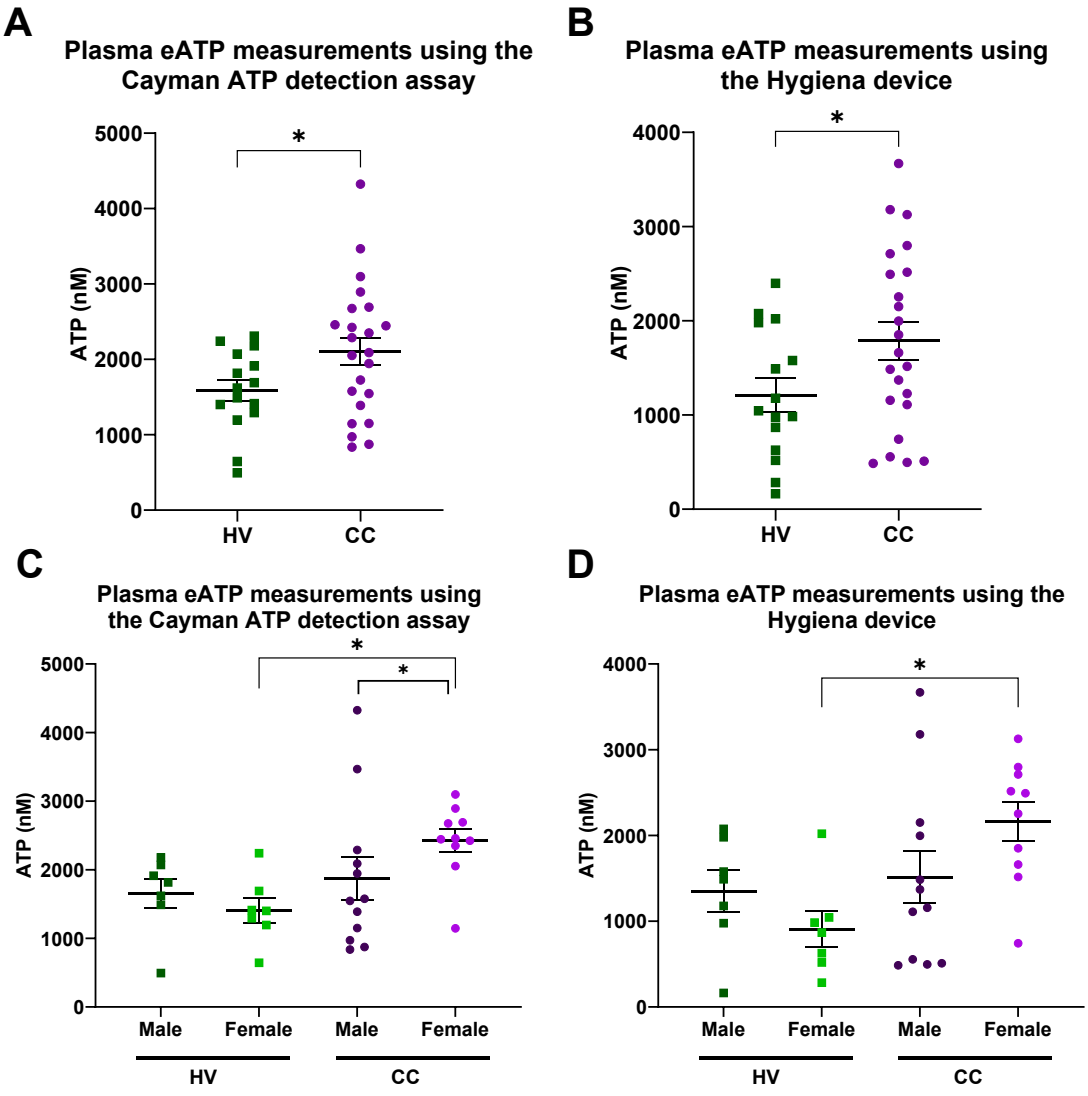


Figure 7. 5 ANTHEM plasma eATP measurements.

*Measurements were taken from chronic cough (CC) patient samples n=14 (n=7 male, n=7 female) and healthy volunteers (HV) n=22 (n=12 male, n=10 female). (A) eATP measurements using Cayman ATP detection assay comparing total CC and HV and (C) grouped by gender. (B) eATP measurements using the Hygiena device comparing total CC and HV and (D) grouped by gender. Data shown are mean ± SEM. * indicates statistical significance Welch's t test (A: p=0.03, B: p=0.0379, C: p=0.0145 and 0.0751, respectively, D: p=0.0128).*

7.3.6 Comparing eATP measurements using the Cayman assay and Hygiena device

The same samples were measured in parallel using the Cayman assay and Hygiena device which enable measurement comparisons to be made between the two techniques. The same ATP standards were also used to produce a standard curve to allow extrapolation of ATP concentrations which were also dilution-adjusted. In general, there was a good correlation between the Cayman assay and Hygiena device. An increase in divergence between plasma measurements between the two techniques with higher ATP concentrations was observed (Figure 7.6).

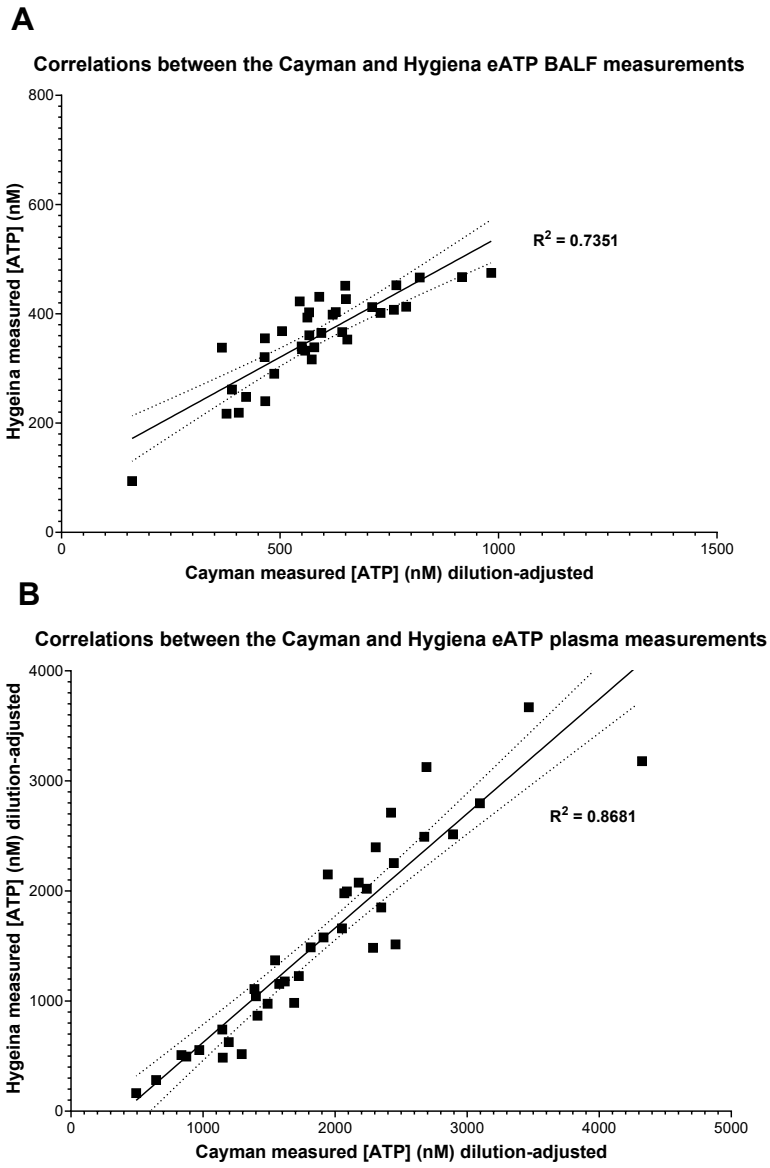


Figure 7. 6 Correlations between eATP measurements using the Cayman assay and Hygiena device.

Correlations between all samples measured n=38 between the plate-based Cayman assay and the hand-held Hygiena device were investigated in (A) BALF and (B) plasma samples where all samples

were dilution-adjusted. Linear regression used to fit the data whereby R^2=1 would indicate that the data perfectly fits a linear model.

7.3.7 Correlations between eATP measurements and cough counts in the ANTHEM study

During the ANTHEM study, CC patients were also fitted with a VitaloJak cough monitoring device during their first visit. This was used to measure average daily cough counts. Although there were significant differences between eATP measurements in plasma samples from CC patients and HV, there were no correlations observed between cough counts and eATP plasma measurements from CC patients. A trend towards a weak positive correlation was observed in BALF eATP measurements and cough counts, though this was not significant (Figure 7.7).

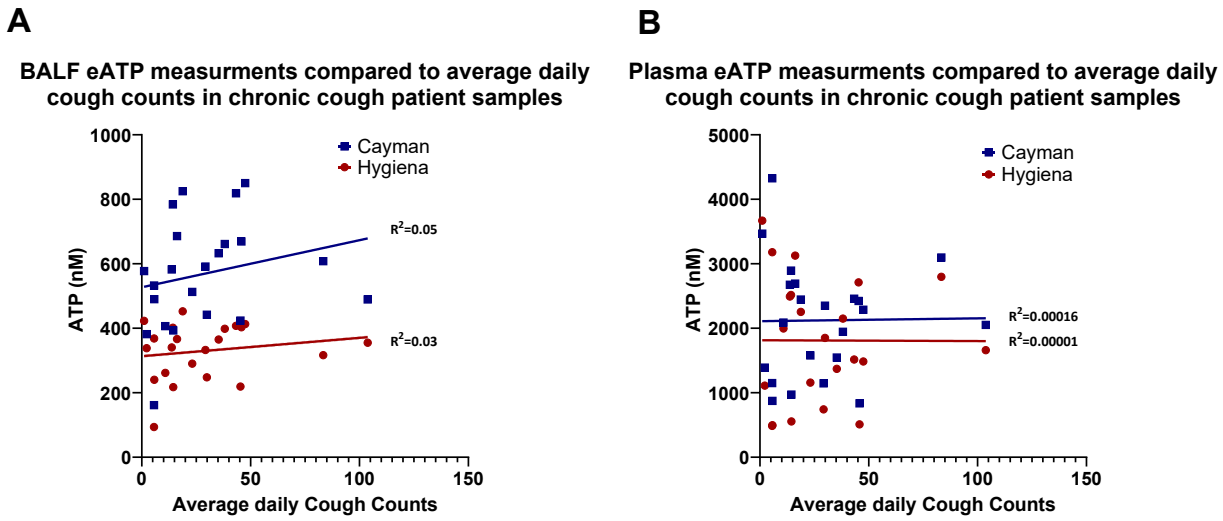


Figure 7. 7 Correlations between ANTHEM eATP measurements and average daily cough counts in chronic cough patient samples.

Average daily counts were measured in chronic cough (CC) patients n=22 and this was correlated against (A) BALF eATP levels and (B) plasma eATP levels measured in these patients using the Cayman ATP detection assay and the Hygiena device. Linear regression used to fit the data whereby R^2=1 would indicate that the data perfectly fits a linear model.

7.4 Discussion

There is increasing evidence for the role of eATP in driving chronic respiratory diseases, based on studies which report elevated eATP in patients with COPD, asthma and IPF (Lommatzsch et al., 2010, Idzko et al., 2007, Riteau et al., 2010, Hlapčić et al., 2019). However, to date there is no literature to suggest that eATP is also elevated in patients with refractory or unexplained chronic cough (RUCC).

Therefore, the aim of this chapter was to investigate eATP measurements in both BALF and plasma samples from RUCC patients compared to healthy controls. These samples were collected using the protocol developed as described in chapter 3 (see section 3.3.4 and 3.3.5) whereby the collection of samples with a final volume of 6mM EDTA was shown to prevent rapid degradation of eATP. This protocol was used during collection of biological samples by clinical collaborators. eATP measurements were performed using the plate-based Cayman ATP detection assay characterised in chapter 3, which was shown to be the most sensitive assay tested. Measurements were also performed using the SystemSure ATP monitor and Hygiena device which are similar hand-held devices which require samples to be swabbed and placed in the hand-held device for measurements. Although less sensitive than the Cayman assay, both these devices provide immediate RLU read-outs which has the advantage of being used for bedside monitoring of ATP levels and could be more readily utilised in a clinical setting. Furthermore, the Cayman assay requires trained individuals to perform the measurements in a laboratory environment where additional equipment such as a plate reader is required, whereas the hand-held devices do not require a trained individual or any additional laboratory equipment for measurements.

Plasma measurements from the Cough Central study suggest there were no differences between HV and CC patients using the Cayman assay and SystemSure ATP monitor. RLU values were presented for both techniques as an ATP standard curve was not run with the SystemSure ATP monitor. RLU values appeared to be approximately 1000 times higher using the SystemSure device compared to the Cayman ATP detection assay though a standard curve and extrapolation of ATP concentrations is required to assess differences between techniques. Based on this data it suggests that there are no differences in systemic levels of eATP between CC patients and HV (Figure 7.1). Observational studies show that CC is more prevalent in females compared to males, and women are overrepresented in cough clinics. In addition to this, sex-related differences in cough hypersensitivity have also been identified with females found to be more sensitive to tussive stimuli compared to males in cough challenge studies and also have an increased 24 hour cough frequency (Varechova et al., 2008, Morice et al., 2014a, Kelsall et al., 2009, Satia et al., 2017). Therefore, eATP measurements between CC

patients and HV were also grouped by gender, however no significant differences were observed between the groups (Figure 7.2).

During the Cough Central study, patients with CC were also fitted with a VitaloJak cough monitoring device. This was able to measure baseline 24-hour cough counts prior to the cough challenge studies. An XY plot was used to determine whether there were any correlations between cough counts and plasma eATP levels. There were no clear significant trends between the two variables although a very weak positive trend was observed in Cayman ATP detection assay measurements compared to the SystemSure monitor measurements (Figure 7.3). Overall, these data suggests no clear correlations can be made between cough counts and plasma eATP levels.

Given that eATP is hypothesised to be driving the pathogenesis and symptoms of chronic respiratory diseases, perhaps it is only lung levels of eATP that are elevated in CC. In order to investigate this, eATP levels were measured in BALF samples from CC patients and HV from another clinical study called ANTHEM as BALF samples were not collected in the Cough Central study. These were also grouped by gender to see if there were any differences between eATP levels (Figure 7.4). These samples were frozen and shipped to Imperial College London for analysis. Surprisingly, eATP levels were significantly reduced in CC patient samples compared with HV. Although this data goes against the hypothesis of increased eATP levels in the BALF of CC patients, it is in line with what was previously observed in the present study of 3 different respiratory disease animal models (Chapter 6, sections 6.3.6, 6.3.7 and 6.3.8). However, it was hypothesised that the reduction of eATP that was observed in the animal models was because they may not be able to completely recapitulate all the mechanisms and pathways involved in chronic respiratory diseases in humans.

Another potential hypothesis for these observations is that eATP levels could be elevated but may be rapidly degraded as a compensatory mechanism prior to the collection of BALF which means increased eATP is not captured in the sample which could potentially explain why significantly less eATP is measured in BALF samples from CC patients. To investigate this, future work is required to investigate whether there is increased ecto-nucleotidase expression and activity in the lungs. Preliminary work to develop an assay to measure ecto-nucleotidase activity in BALF samples using the ATP detection assay is described in chapter 8 (see section 8.3.4). This activity assay could be used to investigate whether there is a compensatory upregulation in ATP breakdown in CC patients which may explain why an increase in eATP is not observed. If this is the case, perhaps BALF may not be an ideal measure of pulmonary eATP levels. It is also important to note that eATP is thought to be released locally by cells and act on purinergic receptors expressed on cells within close proximity. Using human BALF sample collection, samples are taken from a specified, relatively small, region of the lungs and are heavily

diluted and therefore may not be reflective of localised release of eATP from cells. Furthermore, volumes of BALF recovered vary from patient to patient. Although the data collected in this chapter suggest BALF eATP is not elevated in CC patients, alternative techniques for the measurement of eATP in the lungs could be explored, such as bronchosorption which involves the use of synthetic absorptive matrices (SAM). Briefly, this involves the use of a bronchosorption catheter which is passed down the operating port of a bronchoscope and has an inner SAM probe that is extruded under direct vision from the catheter using a handpiece. The main benefit of this technique is that it reduces analyte dilution associated with bronchoalveolar lavage and can also ensure sampling from nerve terminals. Several studies using the bronchosorption technique suggested that higher levels of cytokines were recorded in lavage samples and no safety concerns were reported (Hansel et al., 2017, Sadiq et al., 2021, Jackson et al., 2014, Farne et al., 2018). This technique may therefore reduce variability between samples as there are less variations in the volume of samples recovered.

Plasma eATP levels were also measured from the ANTHEM study and interestingly there was a significant increase in eATP levels in CC patients compared to HV using both techniques. Although this was not observed in plasma samples from the Cough Central study, the data from the ANTHEM study supports the hypothesis that eATP plays a role in the pathogenesis and symptoms of CC. Interestingly, there was a significant increase in plasma eATP in female compared to male CC patients measured using the more sensitive Cayman ATP detection assay. Significant increases were also observed in female CC patients compared to female HV using both assays (Figure 7.5). This is in line with the observation that CC is more prevalent in females compared to males and this difference could potentially be attributed to increased eATP in females compared to males. This suggests that systemic eATP levels measured in the plasma are elevated in CC patients. However, given that this was not observed in the Cough Central study, increase n numbers are required to confirm this observation. It is also important to note that patients with asthma were excluded from the Cough Central study which may account for this difference. Taken together, the hypothesis that BALF eATP is elevated in CC patients cannot be accepted.

As the samples were measured in parallel using the Cayman assay and Hygiena device, correlations between the two techniques were investigated. In general, there was a positive correlation between both techniques with a slight increase in divergence between plasma measurements at higher ATP concentrations. Nonetheless, given that a positive trend was observed with both plasma and BALF samples, it suggests that both techniques give reliable eATP readouts (Figure 7.6). Although the hygiena device is not as sensitive as the ATP detection assay, it does not require the use of laboratory equipment and provides fast RLU readouts and therefore may be useful with regards to point-of-care use in a clinical setting.

During the ANTHEM study, CC patients were fitted with a VitaloJak cough monitoring device which provided a measure of average daily coughs. This was plotted against eATP measurements to see if there were any correlations between the two variables. Although eATP was significantly increased in plasma samples from CC patients compared to HV, there were no correlations between this and average daily cough counts in these patients. A weak positive trend was observed between these cough counts and BALF eATP measurements but were not significant (Figure 7.7). These data suggest that eATP levels may not correlate with cough counts in this patient group. There are on-going clinical studies in Professor Jacky Smith's team at the University Hospital of South Manchester to determine whether patients with different disease backgrounds have different cough responses to different cough stimuli and whether eATP may be elevated in specific patient populations.

Samples collected from these studies will also be sent to collaborators in the Dynamic Omics team at AstraZeneca for future analysis using mass spectrometry. This technique has the advantage of direct eATP measurements as well as measuring ATP metabolites.

The data from this chapter suggests that plasma eATP is elevated in a subset of CC patients compared to HV, though more data is required to confirm this. With regards to BALF, eATP levels were lower in CC patients compared to HV which suggests that BALF may not be ideal for assessing eATP levels and perhaps alternative techniques such as bronchosorption should be explored. Overall, the plasma eATP measurements in the ANTHEM study are promising and support the potential use of plasma eATP as a biomarker to allow a precision medicine approach to be taken. The increased eATP measured in females compared to males supports observations in the clinic of increased incidence of CC in females. These measurements could therefore be utilised in patients with CC, to identify patient populations with elevated eATP who are thought to be more likely to respond to ATP-targeted therapies.

Chapter 8: Summary and Future Studies

8.1 Summary of thesis

There is an increasing amount of research which implicates extracellular ATP (eATP) in the pathogenesis and symptoms in a range of chronic respiratory diseases. This is supported by studies which report elevated levels of eATP in patients with asthma (Idzko et al., 2007), Chronic Obstructive Pulmonary Disease (COPD) (Lommatzsch et al., 2010) and Idiopathic Pulmonary Fibrosis (IPF) (Riteau et al., 2010). Pre-clinical research suggests this eATP is released from several cell types in the lungs leading to the activation of purinergic receptors and subsequent activation of inflammatory and neuronal pathways involved in disease pathogenesis (Bonvini et al., 2020, Rahman et al., 2018, Baxter et al., 2014, Robinson et al., 2016, Burnstock, 2018).

Pre-clinical data have also highlighted the role of ATP and its activation of purinergic P2X3 receptors present on sensory afferent nerves in chronic cough (Bonvini et al., 2016). Chronic cough can be idiopathic in nature, known as Unexplained Chronic Cough (UCC) or can persist despite treatments targeting those with underlying respiratory disease which is described as Refractory Chronic Cough (RCC). Antagonists of the P2X3 receptor have shown antitussive efficacy in refractory and unexplained chronic cough (RUCC) patients in several clinical trials. Original phase 2 studies with the P2X3 Gefapixant were originally in UCC patients. However, Phase 2b and phase 3 studies included patients with RCC. The P2X3 antagonist Gefapixant was recently approved for use in Europe, Switzerland and Japan for RUCC (McGarvey et al., 2022, Drake et al., 2023). However, it remains unclear whether eATP is elevated in the airways of chronic cough patients.

Although there is literature investigating eATP in other airway diseases, levels of eATP measured vary from study to study often ranging from picomolar to micromolar concentrations. Furthermore, different techniques, methodology and chelating agents are often used for the retrieval and assessment of eATP in biological samples which means they are not always reproducible and vary in sensitivity and reliability. In addition to this, eATP is tightly regulated in the extracellular space by ecto-nucleotidases such as CD39 which rapidly break down eATP. Therefore, levels of eATP detected in biological samples are often below the limit of detection and/or are not reflective of true eATP levels. One aim of this thesis was to develop a more standardised technique for the retrieval and assessment of eATP in biological samples which was both reliable and reproducible. This was required to assess levels of eATP in pre-clinical airway disease models and chronic cough patient samples. These measurements could also contribute to the use of eATP as a biomarker to determine target

engagement of compounds which impact eATP and help identify patients with elevated levels of eATP enabling a precision medicine approach to be taken for ATP-targeted treatments.

The primary aim of **Chapter 3** was to optimise the methodology for the retrieval and assessment of eATP in biological samples. Two different plate-based luminescence assays, the PerkinElmer ATPlite assay and Cayman ATP detection assay, were compared to determine which assay was more sensitive at detecting eATP levels. During testing it was found that the white 96-well plates provided with the kits increased cross-talk between wells. Therefore, different plate types were also tested, and it was found that black ½ area 96-well plates had the least amount of cross-talk; consequently this was used in future experiments. The Cayman ATP detection assay was found to be more sensitive with a lower limit of detection of 0.1nM compared to 10nM with the ATPlite assay. A further advantage of the ATP detection assay was that it only required 10µl of sample whereas the ATPlite assay required 100µl of sample. This is useful as the volume of samples obtained particularly from murine models are relatively low. The use of the hand-held hygiena device was also investigated. Although it was less sensitive than the ATP detection assay with a LLOD of 10nM, this device had the advantage of immediate sample measurements which may be useful for immediate readings in a clinical setting.

The rapid breakdown of eATP in biological samples is another challenge when measuring eATP. The use of EDTA, a chelating agent which binds metal ions such as calcium was investigated in reducing this rapid eATP breakdown. It was found that a final concentration of 6mM EDTA in plasma and bronchoalveolar lavage fluid (BALF) samples reduced rapid breakdown of eATP. The CD39 enzyme which can break down ATP was also used to confirm that the luminescence detected with the ATP detection assay was reflective of eATP levels in biological samples from mice, rats and guinea pigs. Preliminary data from collaborators in the Dynamic Omics team at AstraZeneca suggested that eATP breakdown products could also be measured in these samples. In this chapter, a more reliable and reproducible methodology for the assessment of eATP in biological samples was developed and used for future assessment of eATP in pre-clinical and clinical samples.

In addition to assessing levels of eATP in these samples, **Chapter 4** aimed to provide complimentary evidence for the role of endogenous ATP in activating airway sensory nerves that lead to the cough reflex. Chronic cough is a common symptom of a range of chronic respiratory diseases or can be idiopathic in nature. The antitussive effects of drugs such as the purinergic P2X3 antagonist Gefapixant supports the role of ATP in driving cough (McGarvey et al., 2022). Pre-clinical studies have investigated the role of ATP analogues such as αβMe-ATP which is more stable than ATP and more selective for

P2X1 and P2X3 purinergic receptors. However, more research was needed to demonstrate the ability of ATP, rather than analogues in the activation of airway sensory nerves. The aim of Chapter 4 was to investigate ATP in airway sensory nerves using a variety of electrophysiological techniques in order to improve understanding of the pharmacological effects of endogenous ATP and its role in the cough reflex. Calcium imaging of airway specific guinea pig ganglia showed that ATP caused a concentration-dependent increase in intracellular calcium levels in both airway specific nodose and jugular ganglia.

Activation of airway sensory nerves by endogenous ATP was also observed using *in vitro* vagus nerve recordings on sections of the whole vagus nerve; endogenous ATP was then studied in an *ex vivo* electrophysiological tracheal recording (eTRec) system, which showed increased nerve activity in a branch of the vagus known as the recurrent laryngeal nerve (RLN) which innervates the upper airways. The advantage of eTRec was that it is a more physiologically relevant way of causing nerve activation as it measured the effects of ATP on nerve terminals within the intact tracheal lumen.

The pharmacology of ATP on airway sensory nerves was also explored by blocking ATP activated P2X3 receptors. Gefapixant and its pre-clinical analogue AF-353 were able to block ATP-induced vagus nerve depolarisation in guinea pigs. AF-353 was also shown to inhibit-ATP-induced firing of the airway nerve terminals in the RLN of the guinea pig. Having shown that P2X3 antagonists could block airway sensory nerve activation through the endogenous ATP ligand, the next step was to examine whether it could also block indirect endogenously released ATP through activation of TRPV4 as illustrated in Figure 8.1. Previous publications have demonstrated the ability of the TRPV4 agonist GSK1016790A (GSK101) to cause depolarisation of guinea pig vagus nerve through the indirect release of eATP and subsequent activation of P2X3 referred to as the TRPV4-ATP-P2X3 axis (Bonvini et al., 2016).

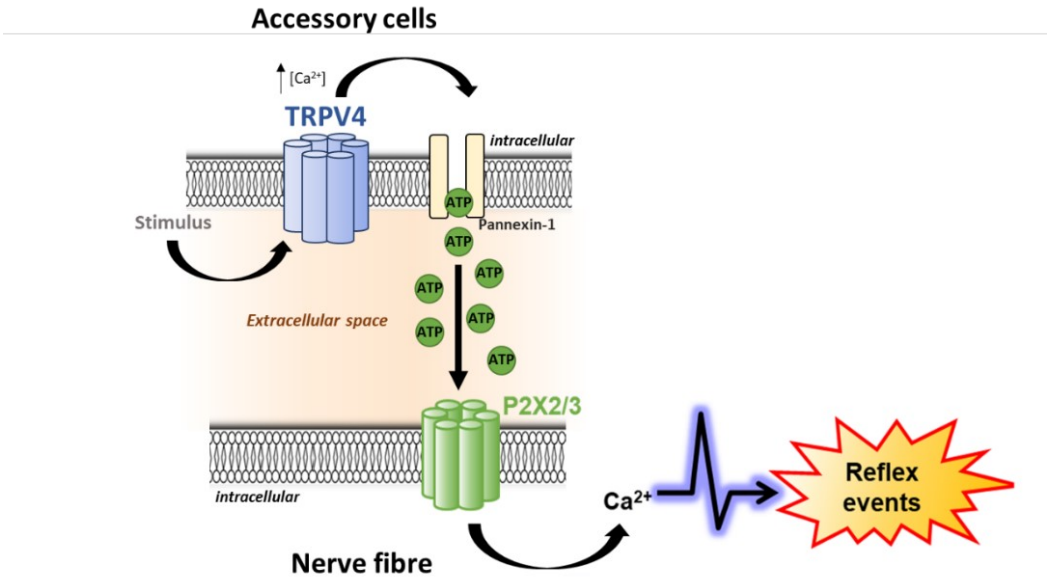


Figure 8. 1 Schematic illustrating TRPV4 induced release of eATP activating P2X2/3 receptors.

Activation of TRPV4 leads to the release of ATP through pannexin-1 channels which stimulates P2X2/3 receptors on airway sensory nerves causing action potential firing. This can occur in the same cell (autocrine signalling) or between neighbouring cells (paracrine signalling). Figure adapted from (Grace et al., 2017).

P2X3 antagonists were able to block TRPV4-induced activation in both isolated guinea pig vagus nerve tissues and in tracheal attached guinea pig RLN. Importantly, translational studies were also performed on human donor tissue and demonstrated that ATP-induced depolarisation (both directly applied ATP and ATP released via TRPV4 activation) of human vagus nerve was inhibited by Gefapixant and AF-353. The data in this chapter demonstrated the ability of the endogenous ATP ligand to activate airway sensory nerves and the pharmacology of P2X3 antagonists in pre-clinical primary tissues were in line with the efficacy of P2X3 antagonists in the clinic. Thus far, clinical trials have focused on blocking the action of ATP on sensory nerves. However, this can be associated with off-target effects such as taste disturbances commonly reported with P2X3 antagonists such as Gefapixant (McGarvey et al., 2022). It is hypothesised that these taste disturbances are likely due to drugs also blocking P2X2/3 receptors innervating taste buds as more selective P2X3 antagonists such as Camlipixant, have a lower incidence of taste disturbances (Birring et al., 2022, Garceau and Chauret, 2019). An alternative approach to treating chronic cough could be to reduce the amount of eATP in the extracellular space by increasing eATP breakdown.

The aim of **Chapter 5** was to investigate the effects of breaking down ATP using ecto-nucleotidases such as CD39 on ATP-induced activation of airway sensory nerves. In order to investigate this, two

CD39 enzymes, CD39-His and its analogue, and CD39-analogue were investigated. A mutant version of these enzymes, CD39-Mut was also tested as a negative control. *In vitro* isolated vagus nerve recordings in the guinea pig showed that both CD39 enzymes caused a concentration-dependent decrease in direct ATP-induced and indirect TRPV4 induced depolarisation of the vagus nerves. The CD39-analogue was found to be more potent than CD39-His. CD39 was also investigated using whole animal single afferent fibre recordings; this is a more physiologically relevant technique with the advantage of measuring the effects of drugs on the nerve termini with an end point of action potential firing in specific subtypes of nerves. As this technique was relatively low-throughput and required highly skilled and trained personnel to perform the experiment, only the more potent CD39 tool, CD39-analogue, was tested in this system; thus, the enzyme was tested following TRPV4 induced prolonged firing of Aδ- fibres, which was previously shown to be blocked by P2X3 receptor antagonists (Bonvini et al., 2016). Intratracheal administration of the CD39-analogue enzyme was shown to reduce GSK101 induced stimulation of Aδ- fibres, whereas the mutant control had no effect. The final method used to assess ATP activation of the cough reflex events was through investigating the effects of CD39-His on a TRPV4 induced guinea pig conscious cough model. A key advantage of this model is that it allows the investigation of drugs directly on cough in the whole animal which can provide translational data as the tussive responses induced in guinea pigs are similar to those observed in humans (Birrell et al., 2009). Using this model, a trend towards decreased cough was observed at the highest dose of 3 mg/kg CD39-His which despite not being statistically significant P=0.0699, is still promising given the reduction in cough observed relative to control groups. Target engagement of CD39-His was evident in this model as CD39-His significantly reduced eATP in BALF at all concentrations tested and significantly reduced systemic eATP in the plasma at doses above 1mg/kg. The data gathered in this chapter were from naïve animals. Therefore, the next step was to investigate eATP in animal models of chronic respiratory diseases and determine whether CD39 tools are able to reduce eATP as well as other disease markers in these models.

Having previously determined a reliable and reproducible method for the retrieval and assessment of eATP in biological samples, the aim of **Chapter 6** was to investigate eATP in animal models of respiratory disease and determine whether CD39-His could impact eATP and other airway disease markers. This included both acute and chronic cigarette smoke exposure models, an acute ozone exposure model and a Poly I:C model. These animal models are commonly used to model characteristics of inflammatory airway diseases such as chronic obstructive pulmonary disease (COPD) and asthma. Interestingly across all these airway disease models, a decrease in eATP was found in BALF samples from diseased animals compared to healthy controls despite an inflammatory

phenotype induced in the diseased animals. Several hypotheses were proposed as to why this was observed including an increase in ecto-nucleotidase activity in these animals in response to the induction of a disease phenotype as a compensatory mechanism. This could be investigated further as discussed in section 8.3.4. Additionally, these were only models of human airway disease and do not completely recapitulate the pathophysiological mechanisms observed in human airway diseases. Alternatively, eATP may only be a key mediator in driving cough and not chronic inflammation observed in these disease models.

CD39-His was also investigated in the acute cigarette smoke exposure model and despite a reduction in eATP in the BALF and plasma of animals, CD39-His did not have an impact on inflammation with regards to lowering levels of leukocytes and ATP driven cytokines such as IL-18. A slight reduction in another ATP driven cytokine, IL-1β, was observed at the top doses of CD39-His similar to levels present in air exposed controls, however this was not significant. Based on these findings, an alternative animal model where eATP levels are elevated in diseased lungs such as IPF animal models is required to determine the impact of CD39-His on airway disease markers (see section 8.3.6).

Although eATP is elevated in clinical samples from asthma, COPD and IPF patients, to date there are no publications investigating eATP in chronic cough patient samples. Given the efficacy of purinergic P2X3 receptor antagonists in the clinic, the aim of **Chapter 7** was to determine whether eATP is elevated in refractory and unexplained chronic cough (RUCC) patient samples which would support the hypothesis that eATP is a key driver in cough. Surprisingly, similar results to those observed in the animal disease models were found in the BALF of RUCC patients taking part in the ANTHEM clinical study, whereby eATP levels were significantly lower in RUCC patients compared to healthy controls. Although this was unexpected, a potential hypothesis was that there could be increased ecto-nucleotidase activity in these patients. Although eATP levels in BALF was not increased compared to healthy controls, BALF may not necessarily be reflective of localised eATP release from cells within the lungs as lavaging the lungs heavily dilutes any analytes present in the sample. Future work could explore alternative methods for measure lung eATP such as bronchosorption as described in section 8.3.6.

eATP was also measured in plasma samples from two different clinical trial studies, the Cough Central study and the ANTHEM study. The Cayman ATP detection assay was used for these measurements from both studies. The Cough Central samples were also analysed by collaborators using the SystemSure ATP device and the ANTHEM samples were also measured using the Hygiena device. These

types of measurements may be useful for point-of-care use as it provides immediate read outs. In the Cough Central patient samples, there were no differences observed between plasma from RUCC patients or healthy controls. However, in the ANTHEM study there was a significant increase in plasma eATP levels in RUCC patients compared to healthy controls. Interestingly in the RUCC patient group, females had significantly increased eATP levels compared to males. This is in line with observational studies which show that chronic cough is more prevalent in females compared to males. For instance, a survey of 10032 adults found that two thirds of chronic cough patients were female (Morice et al., 2014). This data suggests that systemic eATP levels measured in the plasma is elevated in chronic cough patients. However, given that this was not observed in the Cough Central study, the analysis of additional samples once collected are required to confirm this observation. It is also important to note that patients with asthma were excluded from the Cough Central study which may account for this difference.

As the same samples were measured in parallel using both the ATP detection assay and the hygiena device, correlations were made between the two techniques and in general there was a positive correlation between the two. Cough counts were also measured in these studies and correlated with plasma and BALF eATP levels. No significant trends were observed although there was a weak positive correlation between BALF eATP levels and cough counts in RUCC patients from the ANTHEM study. More data is required to determine whether these findings are observed across a wider range of chronic cough patients. The increase in plasma eATP in RUCC patients compared to healthy controls in the ANTHEM study looks promising and supports the potential use of plasma eATP as a biomarker. This could potentially be used in the future to identify patients with high levels of eATP who may be more likely to respond to ATP targeted therapies such as P2X3 antagonists.

8.2 Limitations of this research and experimental challenges

There are several limitations to the techniques used within this thesis which have been previously outlined in the relevant chapters. Although luminescence-based assays are commonly used to measure ATP in samples, they indirectly measure ATP through the release of light in the ATP driven chemical reaction which converts luciferin to oxyluciferin and light through activity of the luciferase enzyme. Mass spectrometry is a more accurate technique which directly measures ATP metabolites (see section 8.3.1). However, this technique is very costly and requires samples to be shipped to collaborators for analysis.

The isolated vagus nerve recording technique is high throughput and readily amenable to pharmacological investigation using specific antagonists or ecto-nucleotidases. However, it is not completely physiologically relevant given that drugs are applied directly onto the nerve axon rather than the nerve endings and is not a true measure of what occurs in an *in vivo* setting. Furthermore, it is a measure of activation of receptors and ion channels present on the nerve trunk which may not be present in the same conformation as those found on nerve terminals. The majority of experiments using this technique were performed on guinea pig tissues which may differ to those found in humans. The vagus nerve also innervates a range of midline organs and tissues aside from the lungs and therefore activation cannot be attributed to the activation of airway specific nerve fibres alone. This technique could also have been used using human donor tissues which would have provided translational data. However, the availability of these tissues were limited particularly due to the COVID-19 pandemic.

To overcome these limitations, responses were repeated in the more physiologically relevant eTRec system which measured the effects of compounds present on nerve terminals within the tracheal lumen. This was also repeated in airway terminating single fibres in guinea pigs which has other limitations as it is both labour intensive and costly given that only one fibre can be used at a time. The role of CD39 tools in these systems were also investigated as well as in an *in vivo* conscious guinea pig cough model, where responses were more reflective of what happens in a whole animal as interactions occurred at the nerve terminals following aerosolisation of a tussive stimuli and was therefore more indicative of the cough reflex itself. Nonetheless, this was a model of evoked cough and not of spontaneous cough which is more difficult to model and is not as well established.

The COVID-19 pandemic also meant that there were delays in obtaining clinical samples as all clinical trials were stopped during the pandemic. Measuring BALF eATP levels as an indicator of lung levels of eATP also has its limitations as this method of sampling heavily dilutes any metabolites present in the samples. To overcome this, future work could explore other alternatives to assessing eATP in the lungs

such as bronchosorption (section 8.3.6) or the use of luciferase-based cell lines to try to image the release of eATP in real-time (section 8.3.3) (Cicko et al., 2018).

8.3 Future work

8.3.1 Mass spectrometry analysis of eATP and metabolites in biological samples

The eATP data gathered in this thesis were predominantly measured using luminescence-based assays. However, preliminary data collected in collaboration with the Dynamic Omics team at AstraZeneca, Gaithersburg, suggested that eATP breakdown products could also be measured in these samples. Although costly, this technique has the capacity to accurately and directly detect and quantify numerous molecules and can be automated allowing for large-scale analysis. Clinical samples from refractory and unexplained chronic cough patients and healthy volunteers are being sent for mass spectrometry analysis which has the key advantage of accurately determine levels of eATP metabolites such as adenosine diphosphate (ADP), adenosine monophosphate (AMP) and adenosine which could give an indication of eATP breakdown in these samples.

8.3.2 Real-time imaging of ATP release *in vitro*

The pharmacological studies performed in **Chapter 4** suggest that TRPV4 activation can lead to the release of eATP in airway-specific ganglia. However, this is yet to be imaged in real-time. Future work could involve the isolation of nodose and jugular ganglia which could be incubated in medium containing the reagents required for the luminescence-based luciferase-luciferin chemical reaction. These cells could then be visualised under a microscope and following stimulation with the TRPV4 agonist, GSK101, quantification of luminescence and its release could potentially be imaged in real-time to provide dynamic evaluation of cellular ATP induction and extracellular relocation. Other publications have utilised a similar technique whereby ATP release induced by mechanical stretch in human airway smooth muscles were shown in real-time (Takahara et al., 2014).

8.3.3 Real-time imaging of ATP release *in vivo*

Despite elevated eATP levels being found in biological samples from a range of chronic lung diseases (Riteau et al., 2010), this eATP release in the lungs has not been visualised *in vivo*. Future work could aim to develop a technique that could be used to measure ATP release *in vivo* utilising luciferase-based cell lines. These cell lines would contain a luciferase probe that can be administered to animals in order to observe ATP release in the lungs (Morciano et al., 2017). Preliminary proof-of-concept experiments involving an ATP concentration response could initially be performed in cell culture and assessed using a luminescence plate reader. The end goal would be to administer these cell lines into

animal models to visualise ATP release in the lungs *in vivo*. This could enable confirmation of elevated eATP levels and relocation/metabolism in models of disease, allowing further investigation into tools such as TRPV4 antagonists and CD39 in reducing eATP levels *in vivo*. A similar approach was used by Cicko et al, to demonstrate eATP release in a murine model of lipopolysaccharide (LPS) induced inflammation (Cicko et al., 2018).

8.3.4 Assessing ecto-nucleotidase activity in biological samples

Preliminary work was performed to develop an assay to measure ecto-nucleotidase activity in biological samples using the ATP detection assay. Initial experiments involved measuring the rate of ATP decrease in standard medium over time. Providing samples contained 0.1 - 1µM ATP, total ecto-nucleotidase activity equivalent to known concentrations of CD39 activity (0.01nM – 1nM) could be estimated in the medium (Figure 8.2).

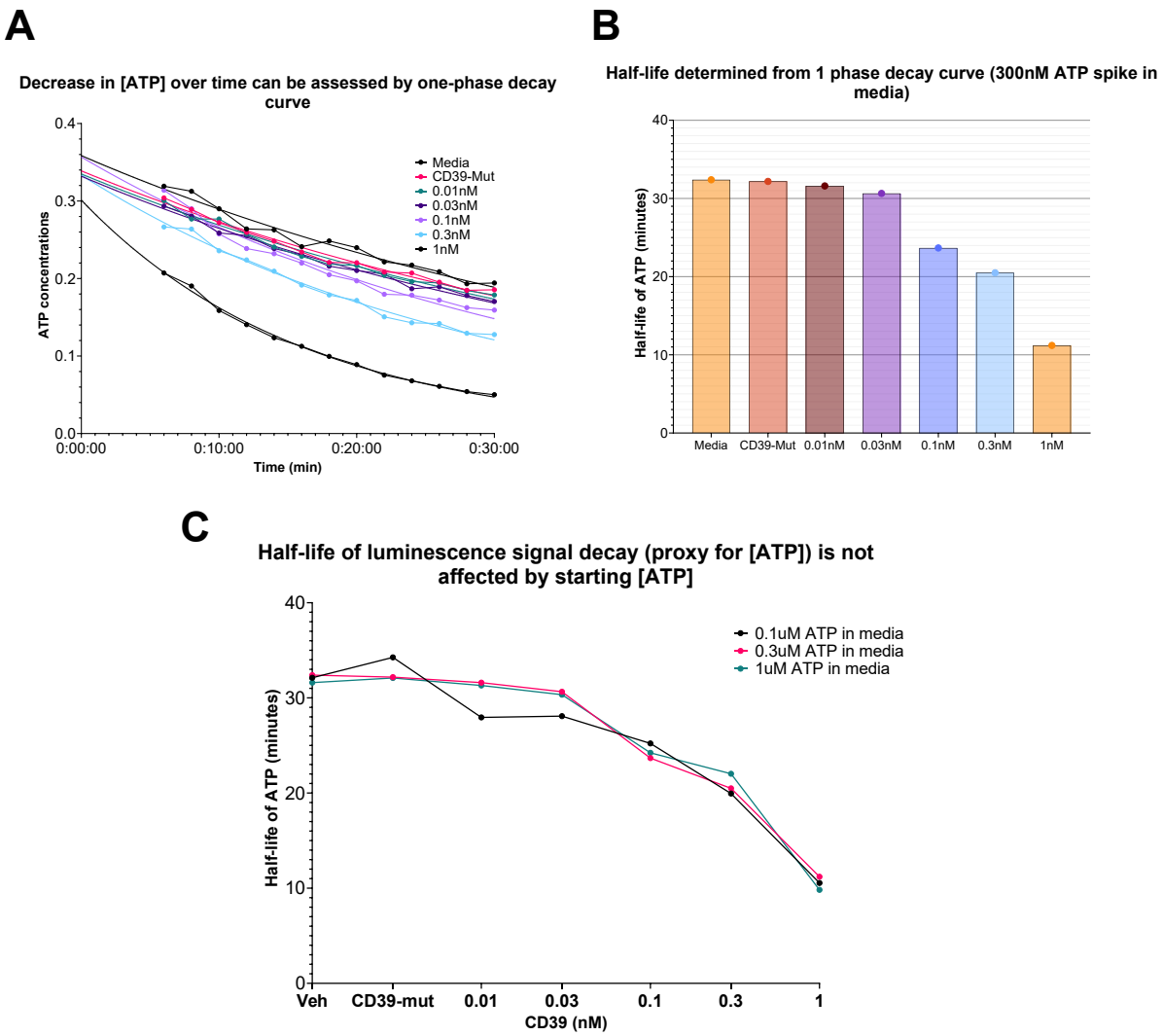


Figure 8. 2 Assessing ATP breakdown over time using the Cayman ATP detection assay.

(A) One-phase decay curve of medium (saline) alone, spiked with CD39-Mut or CD39 (0.01nM – 1nM) over 30 minutes. (B) Half-life of the 300nM ATP spike in medium. (C) Half-life of 0.1µM, 0.3µM and 1µM ATP saline solutions, spiked with vehicle, CD39-mut or CD39 (0.01nM – 1nM).

The next step was to use this technique to assess ecto-nucleotidase activity in BALF samples from naïve mice. BALF samples with less than 300nM endogenous eATP were spiked with 300nM exogenous ATP to determine the half-life of ATP. CD39 concentrations were used as a metric for estimating total ecto-nucleotidase activity in samples whereby a standard curve was produced with increasing concentrations of CD39 were added to saline controls spiked with 300nM ATP. Total ecto-nucleotidase activity in naïve mouse BALF (N=3) were equivalent to approximately 0 – 0.1nM CD39 (Figure 8.3).

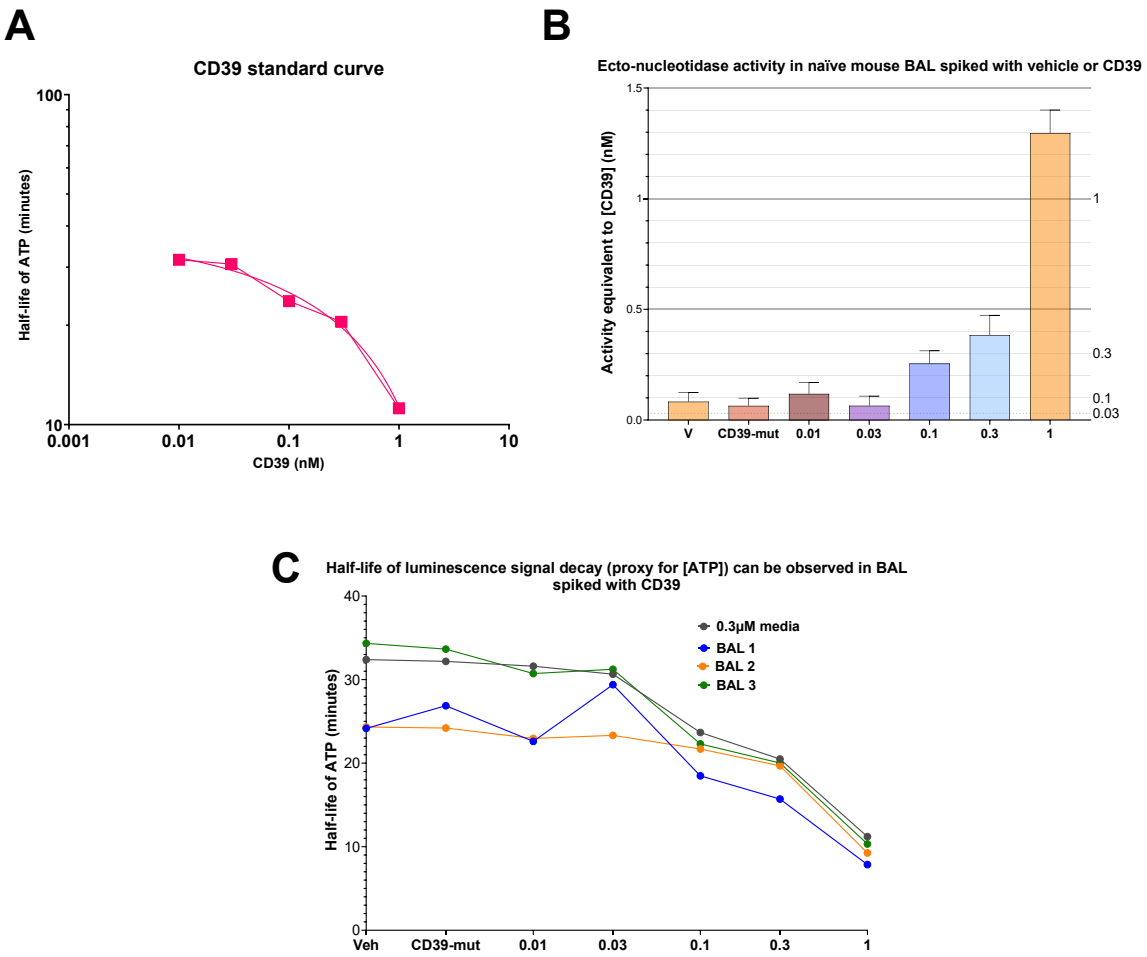


Figure 8. 3 Assessing ecto-nucleotidase activity in naïve mouse BALF.

(A) CD39 standard curve (0.01nM – 1nM CD39) used to extrapolate CD39 activity. (B) Ecto-nucleotidase activity equivalent to CD39 (nM) in naïve mouse BALF spiked with vehicle, CD39-mut of CD39 (0.01nM – 1nM). (C) Half-life of naïve mouse BALF samples spiked with vehicle, CD39-mut or CD39 (0.01nM – 1nM).

This approach using the determination of ecto-nucleotidase activity could be used to investigate whether cigarette smoke, ozone or Poly I:C challenge triggers an upregulation in ATP breakdown which may explain why an increase in BALF eATP is not observed in these disease models. This approach could also be used to investigate whether there is increased ecto-nucleotidase activity in refractory and unexplained chronic cough BALF samples given that increased eATP was not observed in patients compared to healthy controls.

8.3.5 Investigating levels of eATP in a systemic bleomycin model of IPF

In **Chapter 5**, CD39-His was shown to inhibit airway sensory nerve activation. Given that cough is a major symptom of idiopathic pulmonary fibrosis (IPF) and that increased eATP has been found in BALF from IPF patients compared to healthy controls (Müller et al., 2017, Riteau et al., 2010), future work could investigate CD39-His in IPF disease models.

Bleomycin mouse models are typically used to model IPF and a study by Riteau et al demonstrated that 4 hours after intranasal administration of bleomycin in mice, there were significantly increased levels of eATP in BALF which were followed by increased neutrophil recruitment, increased lung IL-1β and an increase in fibrotic markers. These were reduced in P2X7-/- mice and following dosing with apyrase, an enzyme that breaks down ATP. These data suggest that ATP-induced activation of P2X7 plays an important role in inflammation and fibrosis development in this model (Riteau et al., 2010). This was further supported by a separate study which showed that intratracheal dosing of bleomycin in mice caused significant increases in BALF eATP (Müller et al., 2017). BALF samples from a bleomycin mouse model ran by collaborators in the 'Bioscience In Vivo' team at AstraZeneca, Sweden, were also sent to Imperial College London for analysis using the ATP detection assay. Across pre-determined time-points, from 7 – 28 days, animals were culled and BALF collected. eATP levels were elevated all time points compared to vehicle controls with significant increases at day 14 and at the later time points (Figure 8.4).

Having determined the dose-range, duration of action and route of administration of CD39-His in naïve mice, the putative inhibitory effect of CD39-His could be investigated in the bleomycin mouse model where significant increases in lung eATP was observed. The impact of CD39-His on reducing eATP could determine whether the breakdown of eATP has a positive impact on disease pathogenesis in this model, indicating possible translational applications for CD39-His.

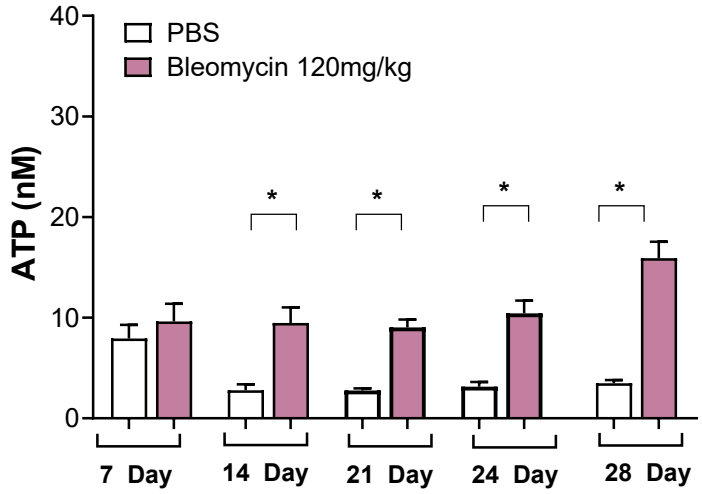


Figure 8. 4 eATP levels in BALF from a systemic bleomycin model.

*Vehicle (PBS) or bleomycin 120mg/kg was dosed i.t to naïve C57BL/6 mice. At 7, 14, 21, 24 and 28 days post dose, animals were culled and BALF sample were collected for ATP analysis using the ATP detection assay. N=8 per group. Data shown are mean ± SEM. * indicates statistical significance ($p < 0.05$), Kruskal Wallis with Dunn's Post Test.*

8.3.6 BALF collection using bronchosorption

Although BALF samples are used to indicate lung levels of eATP, it is also important to note that during the lavaging process, eATP and other analytes are heavily diluted in the lavage solution. Furthermore, the volume of BALF recovered from both animals and humans are variable. An alternative method that can be explored is bronchosorption. This involves the use of synthetic absorptive matrices (SAM).

These are placed in the lungs through a bronchoscope with a SAM probe and has the benefit of reducing analyte dilution and measuring eATP at the site of nerve terminals. This technique has been used in several studies which report higher levels of cytokines in lavage samples and had no safety concerns (Hansel et al., 2017, Sadiq et al., 2021, Jackson et al., 2014, Farne et al., 2018). This technique may therefore reduce variability between samples as there are less variations in the volume and dilution of samples recovered. The technique could be trialled by clinical collaborators to determine whether eATP levels in samples collected by the SAM are significantly higher in refractory and unexplained chronic cough patients compared to healthy controls.

8.4 Concluding Remarks

The work carried out for this thesis has shown that the endogenous ATP ligand causes activation of airway sensory nerves which can be reduced using ecto-nucleotidases such as CD39. This supports the overall hypothesis that eATP is involved in the activation of airway sensory nerves. A more reliable and reproducible methodology for the retrieval and measurement of eATP in biological samples was also developed. Unexpectedly, levels of eATP measured in BALF samples from three different airway disease models showed a significant decrease in eATP compared to healthy controls. Surprisingly, the same observation was observed in clinical BALF samples from RUCC patients. The future work that has been outlined above should help further investigate why a decrease in eATP is observed through investigation of ecto-nucleotidase activity (which may control elevated eATP in early disease) in these samples.

Given that P2X3 antagonists have shown antitussive efficacy in chronic cough patients, perhaps the eATP measured in BALF is not truly reflective of local increases in eATP release given that eATP is heavily diluted in the lavaging process. Although BALF samples are reflective of eATP lavaged in the airways, perhaps interstitial eATP within the lung tissues should also be considered. The role of eATP in driving chronic cough is also supported by a significant increase in eATP in RUCC patient plasma samples compared to healthy controls. Although more data is required to confirm this finding, across a larger cohort of RUCC patients, perhaps plasma eATP levels may be more reflective of increases in tissue/interstitial pulmonary eATP.

The use of ecto-nucleotidases in reducing ATP driven activation of airway sensory nerves in both *in vitro* experiments, *ex vivo* experiments, and an *in vivo* conscious guinea pig cough model suggests it could be an alternative strategy to P2X3 antagonists by reducing eATP in chronic respiratory diseases. Future work will address the efficacy of ecto-nucleotidases in airway disease models where a clear increase in eATP is observed. Taken together, high pulmonary eATP could potentially be a useful biomarker in the identification of patient populations with airway diseases and cough who may be more likely to respond to ATP targeted therapies; this would allow for a precision medicine approach to be taken for the treatment of chronic respiratory diseases such as chronic cough.

Chapter 9: Bibliography

ABBAFATI, C., ABBAS, K., ABBASI-KANGEVARI, M., ABD-ALLAH, F., ABDELALIM, A. & ABDOLLAHI, M. E. A. 2020. Global burden of 369 diseases and injuries in 204 countries and territories, 1990-2019: a systematic analysis for the Global Burden of Disease Study 2019. *Lancet,* 396**,** 1204-1222.

ABDULQAWI, R., DOCKRY, R., HOLT, K., LAYTON, G., MCCARTHY, B. G., FORD, A. P. & SMITH, J. A. 2015. P2X3 receptor antagonist (AF-219) in refractory chronic cough: a randomised, double-blind, placebo-controlled phase 2 study. *Lancet,* 385**,** 1198-205.

ABUDARA, V., RETAMAL, M. A., DEL RIO, R. & ORELLANA, J. A. 2018. Synaptic Functions of Hemichannels and Pannexons: A Double-Edged Sword. *Front Mol Neurosci,* 11**,** 435.

ADCOCK, J. J., BIRRELL, M. A., MAHER, S. A., BONVINI, S. J., DUBUIS, E., WORTLEY, M. A., BAKER, K. E. & BELVISI, M. G. 2014. Making Sense Of Sensory Nerves: An In Vivo Characterisation Of Aδ- And C-Fibres Innervating Guinea-Pig Airways. *C19. NEW SENSATIONS IN THE LUNG: THE GOOD, THE BAD, AND THE NERVE.* American Thoracic Society.

ADCOCK, J. J., DOUGLAS, G. J., GARABETTE, M., GASCOIGNE, M., BEATCH, G., WALKER, M. & PAGE, C. P. 2003. RSD931, a novel anti-tussive agent acting on airway sensory nerves. *Br J Pharmacol,* 138**,** 407-16.

ADRIAENSEN, D. & TIMMERMANS, J.-P. 2004. Purinergic signalling in the lung: important in asthma and COPD? *Current Opinion in Pharmacology,* 4**,** 207-214.

ALIAGAS, E., MUÑOZ-ESQUERRE, M., CUEVAS, E., CARETA, O., HUERTAS, D., LÓPEZ-SÁNCHEZ, M., ESCOBAR, I., DORCA, J. & SANTOS, S. 2018. Is the purinergic pathway involved in the pathology of COPD? Decreased lung CD39 expression at initial stages of COPD. *Respir Res,* 19**,** 103.

ANDO, A., SMALLWOOD, D., MCMAHON, M., IRVING, L., MAZZONE, S. B. & FARRELL, M. J. 2016. Neural correlates of cough hypersensitivity in humans: evidence for central sensitisation and dysfunctional inhibitory control. *Thorax,* 71**,** 323-9.

ANDRE, E., GATTI, R., TREVISANI, M., PRETI, D., BARALDI, P. G., PATACCHINI, R. & GEPPETTI, P. 2009. Transient receptor potential ankyrin receptor 1 is a novel target for pro-tussive agents. *Br J Pharmacol,* 158**,** 1621-8.

ANDRÈ, E., CAMPI, B., MATERAZZI, S., TREVISANI, M., AMADESI, S., MASSI, D., CREMINON, C., VAKSMAN, N., NASSINI, R., CIVELLI, M., BARALDI, P. G., POOLE, D. P., BUNNETT, N. W., GEPPETTI, P. & PATACCHINI, R. 2008. Cigarette smoke-induced neurogenic inflammation is mediated by alpha,beta-unsaturated aldehydes and the TRPA1 receptor in rodents. *J Clin Invest,* 118**,** 2574-82.

ATSUMI, K., YAJIMA, T., TACHIYA, D., KOKUBUN, S., SHOJI, N., SASANO, T., ICHIKAWA, H. & SATO, T. 2020. Sensory neurons in the human jugular ganglion. *Tissue Cell,* 64**,** 101344.

BALESTRINI, A., JOSEPH, V., DOURADO, M., REESE, R. M., SHIELDS, S. D., ROUGÉ, L., BRAVO, D. D., CHERNOV-ROGAN, T., AUSTIN, C. D., CHEN, H., WANG, L., VILLEMURE, E., SHORE, D. G. M., VERMA, V. A., HU, B., CHEN, Y., LEONG, L., BJORNSON, C., HÖTZEL, K., GOGINENI, A., LEE, W. P., SUTO, E., WU, X., LIU, J., ZHANG, J., GANDHAM, V., WANG, J., PAYANDEH, J., CIFERRI, C., ESTEVEZ, A., ARTHUR, C. P., KORTMANN, J., WONG, R. L., HEREDIA, J. E., DOERR, J., JUNG, M., VANDER HEIDEN, J. A., ROOSE-GIRMA, M., TAM, L., BARCK, K. H., CARANO, R. A. D., DING, H. T., BRILLANTES, B., TAM, C., YANG, X., GAO, S. S., LY, J. Q., LIU, L., CHEN, L., LIEDERER, B. M., LIN, J. H., MAGNUSON, S., CHEN, J., HACKOS, D. H., ELSTROTT, J., ROHOU, A., SAFINA, B. S., VOLGRAF, M., BAUER, R. N. & RIOL-BLANCO, L. 2021. A TRPA1 inhibitor suppresses neurogenic inflammation and airway contraction for asthma treatment. *J Exp Med,* 218.

BANFI, G., SALVAGNO, G. L. & LIPPI, G. 2007. The role of ethylenediamine tetraacetic acid (EDTA) as in vitro anticoagulant for diagnostic purposes. *Clin Chem Lab Med,* 45**,** 565-76.

BARNES, P. J. 2013. New anti-inflammatory targets for chronic obstructive pulmonary disease. *Nat Rev Drug Discov,* 12**,** 543-59.
BARNES, P. J. 2014. Cellular and molecular mechanisms of chronic obstructive pulmonary disease. *Clin Chest Med,* 35**,** 71-86.
BARNES, P. J., BURNEY, P. G. J., SILVERMAN, E. K., CELLI, B. R., VESTBO, J., WEDZICHA, J. A. & WOUTERS, E. F. M. 2015. Chronic obstructive pulmonary disease. *Nature Reviews Disease Primers,* 1**,** 15076.
BARNETT, M. W. & LARKMAN, P. M. 2007. The action potential. *Pract Neurol,* 7**,** 192-7.
BAROJA-MAZO, A., BARBERÀ-CREMADES, M. & PELEGRÍN, P. 2013. The participation of plasma membrane hemichannels to purinergic signaling. *Biochim Biophys Acta,* 1828**,** 79-93.
BARTLETT, D., JR., JEFFERY, P., SANT'AMBROGIO, G. & WISE, J. C. 1976. Location of stretch receptors in the trachea and bronchi of the dog. *J Physiol,* 258**,** 409-20.
BASOGLU, O. K., BARNES, P. J., KHARITONOV, S. A. & PELLEG, A. 2015. Effects of Aerosolized Adenosine 5'-Triphosphate in Smokers and Patients With COPD. *Chest,* 148**,** 430-435.
BASOGLU, O. K., PELLEG, A., ESSILFIE-QUAYE, S., BRINDICCI, C., BARNES, P. J. & KHARITONOV, S. A. 2005. Effects of Aerosolized Adenosine 5′-Triphosphate vs Adenosine 5′-Monophosphate on Dyspnea and Airway Caliber in Healthy Nonsmokers and Patients With Asthma. *Chest,* 128**,** 1905-1909.
BATEMAN, E. D., HURD, S. S., BARNES, P. J., BOUSQUET, J., DRAZEN, J. M., FITZGERALD, J. M., GIBSON, P., OHTA, K., O'BYRNE, P., PEDERSEN, S. E., PIZZICHINI, E., SULLIVAN, S. D., WENZEL, S. E. & ZAR, H. J. 2008. Global strategy for asthma management and prevention: GINA executive summary. *Eur Respir J,* 31**,** 143-78.
BAUTISTA, D. M., JORDT, S. E., NIKAI, T., TSURUDA, P. R., READ, A. J., POBLETE, J., YAMOAH, E. N., BASBAUM, A. I. & JULIUS, D. 2006. TRPA1 mediates the inflammatory actions of environmental irritants and proalgesic agents. *Cell,* 124**,** 1269-82.
BAXTER, M., ELTOM, S., DEKKAK, B., YEW-BOOTH, L., DUBUIS, E. D., MAHER, S. A., BELVISI, M. G. & BIRRELL, M. A. 2014. Role of transient receptor potential and pannexin channels in cigarette smoke-triggered ATP release in the lung. *Thorax,* 69**,** 1080-9.
BELVISI, M. G. 2003. Sensory nerves and airway inflammation: role of A delta and C-fibres. *Pulm Pharmacol Ther,* 16**,** 1-7.
BELVISI, M. G., BIRRELL, M. A., KHALID, S., WORTLEY, M. A., DOCKRY, R., COOTE, J., HOLT, K., DUBUIS, E., KELSALL, A., MAHER, S. A., BONVINI, S., WOODCOCK, A. & SMITH, J. A. 2016. Neurophenotypes in Airway Diseases. Insights from Translational Cough Studies. *American journal of respiratory and critical care medicine,* 193**,** 1364-1372.
BELVISI, M. G., BIRRELL, M. A., WORTLEY, M. A., MAHER, S. A., SATIA, I., BADRI, H., HOLT, K., ROUND, P., MCGARVEY, L., FORD, J. & SMITH, J. A. 2017. XEN-D0501, a Novel Transient Receptor Potential Vanilloid 1 Antagonist, Does Not Reduce Cough in Patients with Refractory Cough. *Am J Respir Crit Care Med,* 196**,** 1255-1263.
BELVISI, M. G., DUBUIS, E. & BIRRELL, M. A. 2011. Transient receptor potential A1 channels: insights into cough and airway inflammatory disease. *Chest,* 140**,** 1040-1047.
BELVISI, M. G. & SMITH, J. A. 2017. ATP and cough reflex hypersensitivity: a confusion of goals? *Eur Respir J,* 50.
BESNARD, A. G., GUILLOU, N., TSCHOPP, J., ERARD, F., COUILLIN, I., IWAKURA, Y., QUESNIAUX, V., RYFFEL, B. & TOGBE, D. 2011. NLRP3 inflammasome is required in murine asthma in the absence of aluminum adjuvant. *Allergy,* 66**,** 1047-57.
BIANCO, S., ROBUSCHI, M., VAGHI, A. & PASARGIKLIAN, M. 1988. PREVENTION OF EXERCISE-INDUCED BRONCHOCONSTRICTION BY INHALED FRUSEMIDE. *The Lancet,* 332**,** 252-255.
BIRRELL, M. A., BELVISI, M. G., GRACE, M., SADOFSKY, L., FARUQI, S., HELE, D. J., MAHER, S. A., FREUND-MICHEL, V. & MORICE, A. H. 2009. TRPA1 agonists evoke coughing in guinea pig and human volunteers. *Am J Respir Crit Care Med,* 180**,** 1042-7.

BIRRELL, M. A., CRISPINO, N., HELE, D. J., PATEL, H. J., YACOUB, M. H., BARNES, P. J. & BELVISI, M. G. 2002. Effect of dopamine receptor agonists on sensory nerve activity: possible therapeutic targets for the treatment of asthma and COPD. *Br J Pharmacol,* 136**,** 620-8.

BIRRELL, M. A. & ELTOM, S. 2011. The role of the NLRP3 inflammasome in the pathogenesis of airway disease. *Pharmacol Ther,* 130**,** 364-70.

BIRRING, S. S., FLEMING, T., MATOS, S., RAJ, A. A., EVANS, D. H. & PAVORD, I. D. 2008. The Leicester Cough Monitor: preliminary validation of an automated cough detection system in chronic cough. *Eur Respir J,* 31**,** 1013-8.

BIRRING, S. S., MATOS, S., PATEL, R. B., PRUDON, B., EVANS, D. H. & PAVORD, I. D. 2006. Cough frequency, cough sensitivity and health status in patients with chronic cough. *Respir Med,* 100**,** 1105-9.

BIRRING, S. S., PRUDON, B., CARR, A. J., SINGH, S. J., MORGAN, M. D. & PAVORD, I. D. 2003. Development of a symptom specific health status measure for patients with chronic cough: Leicester Cough Questionnaire (LCQ). *Thorax,* 58**,** 339-43.

BIRRING, S. S., SMITH, J. A., MCGARVEY, L., MORICE, A. H., GOLDSOBEL, A., LANOUETTE, S., YANG, R., LEVENGOOD, A., GARIN, M. & BONUCCELLI, C. M. 2022. Efficacy in SOOTHE, A Phase 2b Trial of BLU-5937 In Refractory Chronic Cough, Was Not Dependant of Taste Disturbance Adverse Events. *European Respiratory Journal,* 60**,** 807.

BIRRING, S. S., WIJSENBEEK, M. S., AGRAWAL, S., VAN DEN BERG, J. W. K., STONE, H., MAHER, T. M., TUTUNCU, A. & MORICE, A. H. 2017. A novel formulation of inhaled sodium cromoglicate (PA101) in idiopathic pulmonary fibrosis and chronic cough: a randomised, double-blind, proof-of-concept, phase 2 trial. *Lancet Respir Med,* 5**,** 806-815.

BODIN, P. & BURNSTOCK, G. 2001. Purinergic signalling: ATP release. *Neurochem Res,* 26**,** 959-69.

BONVINI, S. J., BIRRELL, M. A., DUBUIS, E., ADCOCK, J. J., WORTLEY, M. A., FLAJOLET, P., BRADDING, P. & BELVISI, M. G. 2020. Novel airway smooth muscle-mast cell interactions and a role for the TRPV4-ATP axis in non-atopic asthma. *Eur Respir J,* 56.

BONVINI, S. J., BIRRELL, M. A., GRACE, M. S., MAHER, S. A., ADCOCK, J. J., WORTLEY, M. A., DUBUIS, E., CHING, Y. M., FORD, A. P., SHALA, F., MIRALPEIX, M., TARRASON, G., SMITH, J. A. & BELVISI, M. G. 2016. Transient receptor potential cation channel, subfamily V, member 4 and airway sensory afferent activation: Role of adenosine triphosphate. *J Allergy Clin Immunol,* 138**,** 249-261.e12.

BONVINI, S. J., BIRRELL, M. A., SMITH, J. A. & BELVISI, M. G. 2015. Targeting TRP channels for chronic cough: from bench to bedside. *Naunyn Schmiedebergs Arch Pharmacol,* 388**,** 401-20.

BROUNS, I., PINTELON, I., TIMMERMANS, J.-P. & ADRIAENSEN, D. 2012. Novel insights in the neurochemistry and function of pulmonary sensory receptors. *Advances in anatomy, embryology, and cell biology,* 211**,** 1-115, vii.

BROZMANOVA, M., RU, F., SURDENIKOVA, L., MAZUROVA, L., TAYLOR-CLARK, T. & KOLLARIK, M. 2011. Preferential activation of the vagal nodose nociceptive subtype by TRPA1 agonists in the guinea pig esophagus. *Neurogastroenterol Motil,* 23**,** e437-45.

BURCH, L. H. & PICHER, M. 2006. E-NTPDases in human airways: Regulation and relevance for chronic lung diseases. *Purinergic Signal,* 2**,** 399-408.

BURGERS, J. A., SCHWEIZER, R. C., KOENDERMAN, L., BRUIJNZEEL, P. L. & AKKERMAN, J. W. 1993. Human platelets secrete chemotactic activity for eosinophils.

BURNSTOCK, G. 2018. Purine and purinergic receptors. *Brain and Neuroscience Advances,* 2**,** 2398212818817494.

BURNSTOCK, G., BROUNS, I., ADRIAENSEN, D. & TIMMERMANS, J. P. 2012. Purinergic signaling in the airways. *Pharmacol Rev,* 64**,** 834-68.

BÉRUBÉ, J., BOURDON, C., YAO, Y. & ROUSSEAU, S. 2009. Distinct intracellular signaling pathways control the synthesis of IL-8 and RANTES in TLR1/TLR2, TLR3 or NOD1 activated human airway epithelial cells. *Cell Signal,* 21**,** 448-56.

CACERES, A. I., BRACKMANN, M., ELIA, M. D., BESSAC, B. F., DEL CAMINO, D., D'AMOURS, M., WITEK, J. S., FANGER, C. M., CHONG, J. A., HAYWARD, N. J., HOMER, R. J., COHN, L., HUANG, X., MORAN, M. M. & JORDT, S. E. 2009. A sensory neuronal ion channel essential for airway inflammation and hyperreactivity in asthma. *Proc Natl Acad Sci U S A,* 106**,** 9099-104.

CANNING, B. J. 2006. Anatomy and neurophysiology of the cough reflex: ACCP evidence-based clinical practice guidelines. *Chest,* 129**,** 33s-47s.

CANNING, B. J., LIU, Q., TAO, M., DEVITA, R., PERELMAN, M., HAY, D. W., DICPINIGAITIS, P. V. & LIANG, J. 2022. Evidence for Alpha(7) Nicotinic Receptor Activation During the Cough Suppressing Effects Induced by Nicotine and Identification of ATA-101 as a Potential Novel Therapy for the Treatment of Chronic Cough. *J Pharmacol Exp Ther,* 380**,** 94-103.

CANNING, B. J., MAZZONE, S. B., MEEKER, S. N., MORI, N., REYNOLDS, S. M. & UNDEM, B. J. 2004. Identification of the tracheal and laryngeal afferent neurones mediating cough in anaesthetized guinea-pigs. *The Journal of physiology,* 557**,** 543-558.

CANNING, B. J. & MORI, N. 2011. Encoding of the cough reflex in anesthetized guinea pigs. *Am J Physiol Regul Integr Comp Physiol,* 300**,** R369-77.

CARETA, O., CUEVAS, E., MUÑOZ-ESQUERRE, M., LÓPEZ-SÁNCHEZ, M., PASCUAL-GONZÁLEZ, Y., DORCA, J., ALIAGAS, E. & SANTOS, S. 2019. Imbalance in the Expression of Genes Associated with Purinergic Signalling in the Lung and Systemic Arteries of COPD Patients. *Scientific Reports,* 9**,** 2796.

CARR, M. J., KOLLARIK, M., MEEKER, S. N. & UNDEM, B. J. 2003. A role for TRPV1 in bradykinin-induced excitation of vagal airway afferent nerve terminals. *J Pharmacol Exp Ther,* 304**,** 1275-9.

CARTER, D. S., ALAM, M., CAI, H., DILLON, M. P., FORD, A. P. D. W., GEVER, J. R., JAHANGIR, A., LIN, C., MOORE, A. G., WAGNER, P. J. & ZHAI, Y. 2009. Identification and SAR of novel diaminopyrimidines. Part 1: The discovery of RO-4, a dual P2X3/P2X2/3 antagonist for the treatment of pain. *Bioorganic & Medicinal Chemistry Letters,* 19**,** 1628-1631.

CATERINA, M. J., SCHUMACHER, M. A., TOMINAGA, M., ROSEN, T. A., LEVINE, J. D. & JULIUS, D. 1997. The capsaicin receptor: a heat-activated ion channel in the pain pathway. *Nature,* 389**,** 816-24.

CHADWICK, B. P. & FRISCHAUF, A. M. 1998. The CD39-like gene family: identification of three new human members (CD39L2, CD39L3, and CD39L4), their murine homologues, and a member of the gene family from Drosophila melanogaster. *Genomics,* 50**,** 357-67.

CHAMBERLAIN MITCHELL, S. A., GARROD, R., CLARK, L., DOUIRI, A., PARKER, S. M., ELLIS, J., FOWLER, S. J., LUDLOW, S., HULL, J. H., CHUNG, K. F., LEE, K. K., BELLAS, H., PANDYAN, A. & BIRRING, S. S. 2017. Physiotherapy, and speech and language therapy intervention for patients with refractory chronic cough: a multicentre randomised control trial. *Thorax,* 72**,** 129-136.

CHAMBERLAIN, S. A., GARROD, R., DOUIRI, A., MASEFIELD, S., POWELL, P., BÜCHER, C., PANDYAN, A., MORICE, A. H. & BIRRING, S. S. 2015. The impact of chronic cough: a cross-sectional European survey. *Lung,* 193**,** 401-8.

CHOU, Y. L., SCARUPA, M. D., MORI, N. & CANNING, B. J. 2008. Differential effects of airway afferent nerve subtypes on cough and respiration in anesthetized guinea pigs. *Am J Physiol Regul Integr Comp Physiol,* 295**,** R1572-84.

CHOUDRY, N. B. & FULLER, R. W. 1992. Sensitivity of the cough reflex in patients with chronic cough. *Eur Respir J,* 5**,** 296-300.

CHOUDRY, N. B., FULLER, R. W. & PRIDE, N. B. 1989. Sensitivity of the human cough reflex: effect of inflammatory mediators prostaglandin E2, bradykinin, and histamine. *Am Rev Respir Dis,* 140**,** 137-41.

CHUNG, K. F. 2011. Chronic 'cough hypersensitivity syndrome': a more precise label for chronic cough. *Pulm Pharmacol Ther,* 24**,** 267-71.

CHUNG, K. F., MCGARVEY, L. & MAZZONE, S. B. 2013. Chronic cough as a neuropathic disorder. *Lancet Respir Med,* 1**,** 414-22.

CHUNG, K. F., MCGARVEY, L., SONG, W.-J., CHANG, A. B., LAI, K., CANNING, B. J., BIRRING, S. S., SMITH, J. A. & MAZZONE, S. B. 2022. Cough hypersensitivity and chronic cough. *Nature Reviews Disease Primers,* 8**,** 45.

CHUNG, K. F. & PAVORD, I. D. 2008. Prevalence, pathogenesis, and causes of chronic cough. *Lancet,* 371**,** 1364-74.

CHURG, A., ZHOU, S., WANG, X., WANG, R. & WRIGHT, J. L. 2009. The role of interleukin-1beta in murine cigarette smoke-induced emphysema and small airway remodeling. *Am J Respir Cell Mol Biol,* 40**,** 482-90.

CICKO, S., KÖHLER, T. C., AYATA, C. K., MÜLLER, T., EHRAT, N., MEYER, A., HOSSFELD, M., ZECH, A., DI VIRGILIO, F. & IDZKO, M. 2018. Extracellular ATP is a danger signal activating P2X7 receptor in a LPS mediated inflammation (ARDS/ALI). *Oncotarget,* 9**,** 30635-30648.

CICKO, S., LUCATTELLI, M., MÜLLER, T., LOMMATZSCH, M., DE CUNTO, G., CARDINI, S., SUNDAS, W., GRIMM, M., ZEISER, R., DÜRK, T., ZISSEL, G., BOEYNAEMS, J. M., SORICHTER, S., FERRARI, D., DI VIRGILIO, F., VIRCHOW, J. C., LUNGARELLA, G. & IDZKO, M. 2010. Purinergic receptor inhibition prevents the development of smoke-induced lung injury and emphysema. *J Immunol,* 185**,** 688-97.

COLERIDGE, J. C. & COLERIDGE, H. M. 1984. Afferent vagal C fibre innervation of the lungs and airways and its functional significance. *Rev Physiol Biochem Pharmacol,* 99**,** 1-110.

COSTELLO, J. F., DUNLOP, L. S. & GARDINER, P. J. 1985. Characteristics of prostaglandin induced cough in man. *Br J Clin Pharmacol,* 20**,** 355-9.

DACCORD, C. & MAHER, T. M. 2016. Recent advances in understanding idiopathic pulmonary fibrosis. *F1000Res,* 5.

DECALMER, S. C., WEBSTER, D., KELSALL, A. A., MCGUINNESS, K., WOODCOCK, A. A. & SMITH, J. A. 2007. Chronic cough: how do cough reflex sensitivity and subjective assessments correlate with objective cough counts during ambulatory monitoring? *Thorax,* 62**,** 329-34.

DI POTO, C., TIAN, X., MELLORS, S., ROSENGREN, S., ISSOP, S., BONVINI, S. J., HESS, S. & ALLMAN, E. L. 2024. A microfluidic chip-based capillary zone electrophoresis-mass spectrometry method for measuring adenosine 5'-Triphosphate and its similar nucleotide analogues. *Analytica Chimica Acta,* 1298**,** 342400.

DI VIRGILIO, F., DAL BEN, D., SARTI, A. C., GIULIANI, A. L. & FALZONI, S. 2017. The P2X7 Receptor in Infection and Inflammation. *Immunity,* 47**,** 15-31.

DI VIRGILIO, F. & VUERICH, M. 2015. Purinergic signaling in the immune system. *Auton Neurosci,* 191**,** 117-23.

DICPINIGAITIS, P. V. 2006. Potential future therapies for the management of cough: ACCP evidence-based clinical practice guidelines. *Chest,* 129**,** 284s-286s.

DICPINIGAITIS, P. V. & ALVA, R. V. 2005. Safety of capsaicin cough challenge testing. *Chest,* 128**,** 196-202.

DICPINIGAITIS, P. V., MCGARVEY, L. P. & CANNING, B. J. 2020. P2X3-Receptor Antagonists as Potential Antitussives: Summary of Current Clinical Trials in Chronic Cough. *Lung,* 198**,** 609-616.

DICPINIGAITIS, P. V., MORICE, A. H., BIRRING, S. S., MCGARVEY, L., SMITH, J. A., CANNING, B. J. & PAGE, C. P. 2014. Antitussive drugs--past, present, and future. *Pharmacol Rev,* 66**,** 468-512.

DOSCH, M., GERBER, J., JEBBAWI, F. & BELDI, G. 2018. Mechanisms of ATP Release by Inflammatory Cells. *Int J Mol Sci,* 19.

DRAKE, M. G., MCGARVEY, L. P. & MORICE, A. H. 2023. From bench to bedside: The role of cough hypersensitivity in chronic cough. *Clin Transl Med,* 13**,** e1343.

DUBUIS, E., GRACE, M., WORTLEY, M. A., BIRRELL, M. A. & BELVISI, M. G. 2013. Harvesting, isolation, and functional assessment of primary vagal ganglia cells. *Curr Protoc Pharmacol,* 62**,** 12.15.1-12.15.27.

EKBERG-JANSSON, A., ANDERSSON, B., BAKE, B., BOIJSEN, M., ENANDEN, I., ROSENGREN, A., SKOOGH, B. E., TYLÉN, U., VENGE, P. & LÖFDAHL, C. G. 2001. Neutrophil-associated

activation markers in healthy smokers relates to a fall in DL(CO) and to emphysematous changes on high resolution CT. *Respir Med,* 95**,** 363-73.
ELTOM, S., BELVISI, M. G., STEVENSON, C. S., MAHER, S. A., DUBUIS, E., FITZGERALD, K. A. & BIRRELL, M. A. 2014. Role of the inflammasome-caspase1/11-IL-1/18 axis in cigarette smoke driven airway inflammation: an insight into the pathogenesis of COPD. *PLoS One,* 9**,** e112829.
ELTOM, S., STEVENSON, C. S., RASTRICK, J., DALE, N., RAEMDONCK, K., WONG, S., CATLEY, M. C., BELVISI, M. G. & BIRRELL, M. A. 2011. P2X7 receptor and caspase 1 activation are central to airway inflammation observed after exposure to tobacco smoke. *PLoS One,* 6**,** e24097.
EVERETT, C. F., KASTELIK, J. A., THOMPSON, R. H. & MORICE, A. H. 2007. Chronic persistent cough in the community: a questionnaire survey. *Cough,* 3**,** 5.
FARNE, H., GROVES, H. T., GILL, S. K., STOKES, I., MCCULLOCH, S., KAROLY, E., TRUJILLO-TORRALBO, M. B., JOHNSTON, S. L., MALLIA, P. & TREGONING, J. S. 2018. Comparative Metabolomic Sampling of Upper and Lower Airways by Four Different Methods to Identify Biochemicals That May Support Bacterial Growth. *Front Cell Infect Microbiol,* 8**,** 432.
FERRARI, D., PIZZIRANI, C., ADINOLFI, E., LEMOLI, R. M., CURTI, A., IDZKO, M., PANTHER, E. & DI VIRGILIO, F. 2006. The P2X7 receptor: a key player in IL-1 processing and release. *J Immunol,* 176**,** 3877-83.
FERRARI, D., VUERICH, M., CASCIANO, F., LONGHI, M. S., MELLONI, E., SECCHIERO, P., ZECH, A., ROBSON, S. C., MÜLLER, T. & IDZKO, M. 2020. Eosinophils and Purinergic Signaling in Health and Disease. *Front Immunol,* 11**,** 1339.
FINLEY, C. R., CHAN, D. S., GARRISON, S., KOROWNYK, C., KOLBER, M. R., CAMPBELL, S., EURICH, D. T., LINDBLAD, A. J., VANDERMEER, B. & ALLAN, G. M. 2018. What are the most common conditions in primary care? Systematic review. *Can Fam Physician,* 64**,** 832-840.
FORD, A. P. 2012. In pursuit of P2X3 antagonists: novel therapeutics for chronic pain and afferent sensitization. *Purinergic Signal,* 8**,** 3-26.
FORD, A. P. & UNDEM, B. J. 2013. The therapeutic promise of ATP antagonism at P2X3 receptors in respiratory and urological disorders. *Front Cell Neurosci,* 7**,** 267.
FOWLES, H. E., ROWLAND, T., WRIGHT, C. & MORICE, A. 2017. Tussive challenge with ATP and AMP: does it reveal cough hypersensitivity? *Eur Respir J,* 49.
FOX, A. J., BARNES, P. J. & DRAY, A. 1995. Stimulation of guinea-pig tracheal afferent fibres by non-isosmotic and low-chloride stimuli and the effect of frusemide. *J Physiol,* 482 (Pt 1)**,** 179-87.
FRIEDRICH, C., FRANCKE, K., BIRRING, S. S., VAN DEN BERG, J. W. K., MARSDEN, P. A., MCGARVEY, L., TURNER, A. M., WIELDERS, P., GASHAW, I., KLEIN, S. & MORICE, A. H. 2023. The P2X3 receptor antagonist filapixant in patients with refractory chronic cough: a randomized controlled trial. *Respiratory Research,* 24**,** 109.
FULKERSON, P. C. & ROTHENBERG, M. E. 2013. Targeting eosinophils in allergy, inflammation and beyond. *Nature reviews Drug discovery,* 12**,** 117-129.
FULLER, R. W. & COLLIER, J. G. 1984. Sodium cromoglycate and atropine block the fall in FEV1 but not the cough induced by hypotonic mist. *Thorax,* 39**,** 766-70.
FULLER, R. W., KARLSSON, J. A., CHOUDRY, N. B. & PRIDE, N. B. 1988. Effect of inhaled and systemic opiates on responses to inhaled capsaicin in humans. *J Appl Physiol (1985),* 65**,** 1125-30.
GAO, R., MENG, M., ZHOU, X., YU, M., LI, Z., LI, J., WANG, X., SONG, Y., WANG, H. & HE, J. 2022. TRPV1, a novel biomarker associated with lung cancer via excluding immune infiltration. *MedComm (2020),* 3**,** e139.
GAO, Z.-G. & JACOBSON, K. A. 2017. Purinergic signaling in mast cell degranulation and asthma. *Frontiers in Pharmacology,* 8**,** 947.
GARCEAU, D. & CHAURET, N. 2019. BLU-5937: A selective P2X3 antagonist with potent anti-tussive effect and no taste alteration. *Pulm Pharmacol Ther,* 56**,** 56-62.
GRACE, M., BIRRELL, M. A., DUBUIS, E., MAHER, S. A. & BELVISI, M. G. 2012. Transient receptor potential channels mediate the tussive response to prostaglandin E2 and bradykinin. *Thorax,* 67**,** 891-900.

GRACE, M. S. & BELVISI, M. G. 2011. TRPA1 receptors in cough. *Pulm Pharmacol Ther,* 24**,** 286-8.
GRACE, M. S., BONVINI, S. J., BELVISI, M. G. & MCINTYRE, P. 2017. Modulation of the TRPV4 ion channel as a therapeutic target for disease. *Pharmacology & Therapeutics,* 177**,** 9-22.
GRACE, M. S., DUBUIS, E., BIRRELL, M. A. & BELVISI, M. G. 2013. Pre-clinical studies in cough research: role of Transient Receptor Potential (TRP) channels. *Pulm Pharmacol Ther,* 26**,** 498-507.
GRANT, A. D., COTTRELL, G. S., AMADESI, S., TREVISANI, M., NICOLETTI, P., MATERAZZI, S., ALTIER, C., CENAC, N., ZAMPONI, G. W., BAUTISTA-CRUZ, F., LOPEZ, C. B., JOSEPH, E. K., LEVINE, J. D., LIEDTKE, W., VANNER, S., VERGNOLLE, N., GEPPETTI, P. & BUNNETT, N. W. 2007. Protease-activated receptor 2 sensitizes the transient receptor potential vanilloid 4 ion channel to cause mechanical hyperalgesia in mice. *J Physiol,* 578**,** 715-33.
GRAY, E., HOGWOOD, J. & MULLOY, B. 2012. The anticoagulant and antithrombotic mechanisms of heparin. *Handb Exp Pharmacol***,** 43-61.
GUAN, M., MA, H., FAN, X., CHEN, X., MIAO, M. & WU, H. 2020. Dexamethasone alleviate allergic airway inflammation in mice by inhibiting the activation of NLRP3 inflammasome. *Int Immunopharmacol,* 78**,** 106017.
GUAN, M., YING, S. & WANG, Y. 2021. Increased expression of transient receptor potential channels and neurogenic factors associates with cough severity in a guinea pig model. *BMC Pulm Med,* 21**,** 187.
GUDER, W. G., EHRET, W., DA FONSECA-WOLLHEIM, F., HEIL, W., MULLER-PLATHE, O., SCHMITT, Y., TOPFER, G., WISSER, H. & ZWATA, B. 2002. The quality of diagnostic samples. *Laboratoriums Medizin,* 26**,** 267-283.
HALL, J. I., LOZANO, M., ESTRADA-PETROCELLI, L., BIRRING, S. & TURNER, R. 2020. The present and future of cough counting tools. *J Thorac Dis,* 12**,** 5207-5223.
HANSEL, T. T., TUNSTALL, T., TRUJILLO-TORRALBO, M.-B., SHAMJI, B., DEL-ROSARIO, A., DHARIWAL, J., KIRK, P. D. W., STUMPF, M. P. H., KOOPMANN, J., TELCIAN, A., ANISCENKO, J., GOGSADZE, L., BAKHSOLIANI, E., STANCIU, L., BARTLETT, N., EDWARDS, M., WALTON, R., MALLIA, P., HUNT, T. M., HUNT, T. L., HUNT, D. G., WESTWICK, J., EDWARDS, M., KON, O. M., JACKSON, D. J. & JOHNSTON, S. L. 2017. A Comprehensive Evaluation of Nasal and Bronchial Cytokines and Chemokines Following Experimental Rhinovirus Infection in Allergic Asthma: Increased Interferons (IFN-γ and IFN-λ) and Type 2 Inflammation (IL-5 and IL-13). *EBioMedicine,* 19**,** 128-138.
HERNANDEZ, M. L., MILLS, K., ALMOND, M., TODORIC, K., ALEMAN, M. M., ZHANG, H., ZHOU, H. & PEDEN, D. B. 2015. IL-1 receptor antagonist reduces endotoxin-induced airway inflammation in healthy volunteers. *J Allergy Clin Immunol,* 135**,** 379-85.
HEWITT, M. M., ADAMS, G., JR., MAZZONE, S. B., MORI, N., YU, L. & CANNING, B. J. 2016. Pharmacology of Bradykinin-Evoked Coughing in Guinea Pigs. *J Pharmacol Exp Ther,* 357**,** 620-8.
HIGH, B., JETTÉ, M. E., LI, M., RAMAKRISHNAN, V. R., CLARY, M., PRAGER, J., DRAF, J., HUMMEL, T. & FINGER, T. E. 2023. Variability in P2X receptor composition in human taste nerves: implications for treatment of chronic cough. *ERJ Open Res,* 9.
HILTON, E. C., BAVEREL, P. G., WOODCOCK, A., VAN DER GRAAF, P. H. & SMITH, J. A. 2013. Pharmacodynamic modeling of cough responses to capsaicin inhalation calls into question the utility of the C5 end point. *J Allergy Clin Immunol,* 132**,** 847-55.e1-5.
HLAPČIĆ, I., HULINA-TOMAŠKOVIĆ, A., SOMBORAC-BAČURA, A., RAJKOVIĆ, M. G., DUGAC, A. V., POPOVIĆ-GRLE, S. & RUMORA, L. 2019. Extracellular adenosine triphosphate is associated with airflow limitation severity and symptoms burden in patients with chronic obstructive pulmonary disease. *Scientific Reports,* 9**,** 15349.
HOFMANN, M. H. & BLECKMANN, H. 1999. Effect of temperature and calcium on transneuronal diffusion of DiI in fixed brain preparations. *J Neurosci Methods,* 88**,** 27-31.

HOGG, J. 2004. Peripheral lung remodelling in asthma and chronic obstructive pulmonary disease. *Eur Respir J.* England.
HOPE-GILL, B. D., HILLDRUP, S., DAVIES, C., NEWTON, R. P. & HARRISON, N. K. 2003. A study of the cough reflex in idiopathic pulmonary fibrosis. *Am J Respir Crit Care Med,* 168**,** 995-1002.
HORNICK, I. 2023. *FDA panel votes against gefapixant for unexplained chronic cough* [Online]. Available: https://www.healio.com/news/pulmonology/20231117/fda-panel-votes-against-gefapixant-for-unexplained-chronic-cough [Accessed].
HU, Y., LIU, Z., YU, X., PASRICHA, P. J., UNDEM, B. J. & YU, S. 2014. Increased acid responsiveness in vagal sensory neurons in a guinea pig model of eosinophilic esophagitis. *Am J Physiol Gastrointest Liver Physiol,* 307**,** G149-57.
HUNTER, D. D., MYERS, A. C. & UNDEM, B. J. 2000. Nerve growth factor-induced phenotypic switch in guinea pig airway sensory neurons. *Am J Respir Crit Care Med,* 161**,** 1985-90.
IDZKO, M., FERRARI, D. & ELTZSCHIG, H. K. 2014. Nucleotide signalling during inflammation. *Nature,* 509**,** 310-7.
IDZKO, M., HAMMAD, H., VAN NIMWEGEN, M., KOOL, M., WILLART, M. A., MUSKENS, F., HOOGSTEDEN, H. C., LUTTMANN, W., FERRARI, D., DI VIRGILIO, F., VIRCHOW, J. C., JR. & LAMBRECHT, B. N. 2007. Extracellular ATP triggers and maintains asthmatic airway inflammation by activating dendritic cells. *Nat Med,* 13**,** 913-9.
IMURA, Y., MORIZAWA, Y., KOMATSU, R., SHIBATA, K., SHINOZAKI, Y., KASAI, H., MORIISHI, K., MORIYAMA, Y. & KOIZUMI, S. 2013. Microglia release ATP by exocytosis. *Glia,* 61**,** 1320-30.
IRWIN, R. S., FRENCH, C. T., LEWIS, S. Z., DIEKEMPER, R. L. & GOLD, P. M. 2014. Overview of the management of cough: CHEST Guideline and Expert Panel Report. *Chest,* 146**,** 885-889.
IYER, S. S., PULSKENS, W. P., SADLER, J. J., BUTTER, L. M., TESKE, G. J., ULLAND, T. K., EISENBARTH, S. C., FLORQUIN, S., FLAVELL, R. A., LEEMANS, J. C. & SUTTERWALA, F. S. 2009. Necrotic cells trigger a sterile inflammatory response through the Nlrp3 inflammasome. *Proc Natl Acad Sci U S A,* 106**,** 20388-93.
JACKSON, D. J., MAKRINIOTI, H., RANA, B. M. J., SHAMJI, B. W. H., TRUJILLO-TORRALBO, M.-B., FOOTITT, J., JERICO, D.-R., TELCIAN, A. G., NIKONOVA, A., ZHU, J., ANISCENKO, J., GOGSADZE, L., BAKHSOLIANI, E., TRAUB, S., DHARIWAL, J., PORTER, J., HUNT, D., HUNT, T., HUNT, T., STANCIU, L. A., KHAITOV, M., BARTLETT, N. W., EDWARDS, M. R., KON, O. M., MALLIA, P., PAPADOPOULOS, N. G., AKDIS, C. A., WESTWICK, J., EDWARDS, M. J., COUSINS, D. J., WALTON, R. P. & JOHNSTON, S. L. 2014. IL-33–Dependent Type 2 Inflammation during Rhinovirus-induced Asthma Exacerbations In Vivo. *American Journal of Respiratory and Critical Care Medicine,* 190**,** 1373-1382.
JACOBSON, K. A., PRADHAN, B., WEN, Z. & PRAMANIK, A. 2023. New paradigms in purinergic receptor ligand discovery. *Neuropharmacology,* 230**,** 109503.
JAQUEMAR, D., SCHENKER, T. & TRUEB, B. 1999. An ankyrin-like protein with transmembrane domains is specifically lost after oncogenic transformation of human fibroblasts. *J Biol Chem,* 274**,** 7325-33.
JARVIS, M. F. 2003. Contributions of P2X3 homomeric and heteromeric channels to acute and chronic pain. *Expert Opin Ther Targets,* 7**,** 513-22.
JIA, Y., WANG, X., VARTY, L., RIZZO, C. A., YANG, R., CORRELL, C. C., PHELPS, P. T., EGAN, R. W. & HEY, J. A. 2004. Functional TRPV4 channels are expressed in human airway smooth muscle cells. *Am J Physiol Lung Cell Mol Physiol,* 287**,** L272-8.
JIANG, L. H., KIM, M., SPELTA, V., BO, X., SURPRENANT, A. & NORTH, R. A. 2003. Subunit arrangement in P2X receptors. *J Neurosci,* 23**,** 8903-10.
JOHNSTON-COX, H. A. & RAVID, K. 2011. Adenosine and blood platelets. *Purinergic Signal,* 7**,** 357-65.
JOHNSTON-COX, H. A., YANG, D. & RAVID, K. 2011. Physiological implications of adenosine receptor-mediated platelet aggregation. *Journal of Cellular Physiology,* 226**,** 46-51.

JONES, B., DONOVAN, C., LIU, G., GOMEZ, H. M., CHIMANKAR, V., HARRISON, C. L., WIEGMAN, C. H., ADCOCK, I. M., KNIGHT, D. A., HIROTA, J. A. & HANSBRO, P. M. 2017. Animal models of COPD: What do they tell us? *Respirology,* 22**,** 21-32.

JORDT, S. E., BAUTISTA, D. M., CHUANG, H. H., MCKEMY, D. D., ZYGMUNT, P. M., HÖGESTÄTT, E. D., MENG, I. D. & JULIUS, D. 2004. Mustard oils and cannabinoids excite sensory nerve fibres through the TRP channel ANKTM1. *Nature,* 427**,** 260-5.

JUNGER, W. G. 2011. Immune cell regulation by autocrine purinergic signalling. *Nat Rev Immunol,* 11**,** 201-12.

JÄGER, B., SEELIGER, B., TERWOLBECK, O., WARNECKE, G., WELTE, T., MÜLLER, M., BODE, C. & PRASSE, A. 2021. The NLRP3-Inflammasome-Caspase-1 Pathway Is Upregulated in Idiopathic Pulmonary Fibrosis and Acute Exacerbations and Is Inducible by Apoptotic A549 Cells. *Front Immunol,* 12**,** 642855.

KACZMAREK, E., KOZIAK, K., SÉVIGNY, J., SIEGEL, J. B., ANRATHER, J., BEAUDOIN, A. R., BACH, F. H. & ROBSON, S. C. 1996. Identification and characterization of CD39/vascular ATP diphosphohydrolase. *J Biol Chem,* 271**,** 33116-22.

KAMEI, J. & TAKAHASHI, Y. 2006. Involvement of ionotropic purinergic receptors in the histamine-induced enhancement of the cough reflex sensitivity in guinea pigs. *European journal of pharmacology,* 547**,** 160-164.

KAMEI, J., TAKAHASHI, Y., YOSHIKAWA, Y. & SAITOH, A. 2005. Involvement of P2X receptor subtypes in ATP-induced enhancement of the cough reflex sensitivity. *European journal of pharmacology,* 528**,** 158-161.

KANEMITSU, Y., SMITH, J., BUTERA, P., CANNING, B., DICPINIGAITIS, P., IYER, V. & KITT, M. 2020. The Efficacy of Bradanicline in Refractory Chronic Cough. *European Respiratory Journal,* 56**,** 4564.

KANG, M. J., HOMER, R. J., GALLO, A., LEE, C. G., CROTHERS, K. A., CHO, S. J., ROCHESTER, C., CAIN, H., CHUPP, G., YOON, H. J. & ELIAS, J. A. 2007. IL-18 is induced and IL-18 receptor alpha plays a critical role in the pathogenesis of cigarette smoke-induced pulmonary emphysema and inflammation. *J Immunol,* 178**,** 1948-59.

KARLSSON, J. A. & FULLER, R. W. 1999. Pharmacological regulation of the cough reflex--from experimental models to antitussive effects in Man. *Pulm Pharmacol Ther,* 12**,** 215-28.

KELSALL, A., DECALMER, S., MCGUINNESS, K., WOODCOCK, A. & SMITH, J. A. 2009. Sex differences and predictors of objective cough frequency in chronic cough. *Thorax,* 64**,** 393-8.

KELSALL, A., HOUGHTON, L. A., JONES, H., DECALMER, S., MCGUINNESS, K. & SMITH, J. A. 2011. A novel approach to studying the relationship between subjective and objective measures of cough. *Chest,* 139**,** 569-575.

KHALID, S., MURDOCH, R., NEWLANDS, A., SMART, K., KELSALL, A., HOLT, K., DOCKRY, R., WOODCOCK, A. & SMITH, J. A. 2014. Transient receptor potential vanilloid 1 (TRPV1) antagonism in patients with refractory chronic cough: a double-blind randomized controlled trial. *J Allergy Clin Immunol,* 134**,** 56-62.

KIM, K., KIM, H. J., BINAS, B., KANG, J. H. & CHUNG, I. Y. 2018. Inflammatory mediators ATP and S100A12 activate the NLRP3 inflammasome to induce MUC5AC production in airway epithelial cells. *Biochemical and Biophysical Research Communications,* 503**,** 657-664.

KOHROGI, H., GRAF, P. D., SEKIZAWA, K., BORSON, D. B. & NADEL, J. A. 1988. Neutral endopeptidase inhibitors potentiate substance P- and capsaicin-induced cough in awake guinea pigs. *J Clin Invest,* 82**,** 2063-8.

KOIVISTO, A. P., BELVISI, M. G., GAUDET, R. & SZALLASI, A. 2022. Advances in TRP channel drug discovery: from target validation to clinical studies. *Nat Rev Drug Discov,* 21**,** 41-59.

KOLLARIK, M. & UNDEM, B. J. 2004. Activation of bronchopulmonary vagal afferent nerves with bradykinin, acid and vanilloid receptor agonists in wild-type and TRPV1-/- mice. *J Physiol,* 555**,** 115-23.

KONG, X., BENNETT, W. C., JANIA, C. M., CHASON, K. D., GERMAN, Z., ADOULI, J., BUDNEY, S. D., OBY, B. T., VAN HEUSDEN, C., LAZAROWSKI, E. R., JASPERS, I., RANDELL, S. H., HEDGESPETH,

B. A., CRUSE, G., HUA, X., SCHWORER, S. A., SMITH, G. J., KELADA, S. N. & TILLEY, S. L. 2021. Identification of an ATP/P2X7/mast cell pathway mediating ozone-induced bronchial hyperresponsiveness. *JCI Insight,* 6.

KOSKELA, H. O., KONTRA, K. M., PUROKIVI, M. K. & RANDELL, J. T. 2005. Interpretation of cough provoked by airway challenges. *Chest,* 128**,** 3329-35.

KOSKELA, H. O., PUROKIVI, M. K., KONTRA, K. M., TAIVAINEN, A. H. & TUKIAINEN, H. O. 2008. Hypertonic saline cough provocation test with salbutamol pre-treatment: evidence for sensorineural dysfunction in asthma. *Clin Exp Allergy,* 38**,** 1100-7.

KROPSKI, J. A., LAWSON, W. E., YOUNG, L. R. & BLACKWELL, T. S. 2013. Genetic studies provide clues on the pathogenesis of idiopathic pulmonary fibrosis. *Dis Model Mech,* 6**,** 9-17.

KUZNIAR, T. J., MORGENTHALER, T. I., AFESSA, B. & LIM, K. G. 2007. Chronic cough from the patient's perspective. *Mayo Clin Proc,* 82**,** 56-60.

KWONG, K., KOLLARIK, M., NASSENSTEIN, C., RU, F. & UNDEM, B. J. 2008. P2X2 receptors differentiate placodal vs. neural crest C-fiber phenotypes innervating guinea pig lungs and esophagus. *Am J Physiol Lung Cell Mol Physiol,* 295**,** L858-65.

LALLOO, U. G., FOX, A. J., BELVISI, M. G., CHUNG, K. F. & BARNES, P. J. 1995. Capsazepine inhibits cough induced by capsaicin and citric acid but not by hypertonic saline in guinea pigs. *J Appl Physiol (1985),* 79**,** 1082-7.

LATORRE, R. & DÍAZ-FRANULIC, I. 2022. Profile of David Julius and Ardem Patapoutian: 2021 Nobel Laureates in Physiology or Medicine. *Proc Natl Acad Sci U S A,* 119.

LECHTZIN, N., HILLIARD, M. E. & HORTON, M. R. 2013. Validation of the Cough Quality-of-Life Questionnaire in patients with idiopathic pulmonary fibrosis. *Chest,* 143**,** 1745-1749.

LEE, L.-Y. & PISARRI, T. E. 2001. Afferent properties and reflex functions of bronchopulmonary C-fibers. *Respiration Physiology,* 125**,** 47-65.

LEMANSKE, R. F., JR. & BUSSE, W. W. 2003. 6. Asthma. *J Allergy Clin Immunol,* 111**,** S502-19.

LESZCZYŃSKA, K., JAKUBCZYK, D. & GÓRSKA, S. 2022. The NLRP3 inflammasome as a new target in respiratory disorders treatment. *Front Immunol,* 13**,** 1006654.

LEVER, A. R., PARK, H., MULHERN, T. J., JACKSON, G. R., COMOLLI, J. C., BORENSTEIN, J. T., HAYDEN, P. J. & PRANTIL-BAUN, R. 2015. Comprehensive evaluation of poly(I:C) induced inflammatory response in an airway epithelial model. *Physiol Rep,* 3.

LEY, B. & COLLARD, H. R. 2013. Epidemiology of idiopathic pulmonary fibrosis. *Clin Epidemiol,* 5**,** 483-92.

LI, R., SHANG, Y., HU, X., YU, Y., ZHOU, T., XIONG, W. & ZOU, X. 2020. ATP/P2X7r axis mediates the pathological process of allergic asthma by inducing M2 polarization of alveolar macrophages. *Exp Cell Res,* 386**,** 111708.

LIEDTKE, W., CHOE, Y., MARTÍ-RENOM, M. A., BELL, A. M., DENIS, C. S., SALI, A., HUDSPETH, A. J., FRIEDMAN, J. M. & HELLER, S. 2000. Vanilloid receptor-related osmotically activated channel (VR-OAC), a candidate vertebrate osmoreceptor. *Cell,* 103**,** 525-35.

LIEU, T. M., MYERS, A. C., MEEKER, S. & UNDEM, B. J. 2012. TRPV1 induction in airway vagal low-threshold mechanosensory neurons by allergen challenge and neurotrophic factors. *Am J Physiol Lung Cell Mol Physiol,* 302**,** L941-8.

LOMMATZSCH, M., CICKO, S., MULLER, T., LUCATTELLI, M., BRATKE, K., STOLL, P., GRIMM, M., DURK, T., ZISSEL, G., FERRARI, D., DI VIRGILIO, F., SORICHTER, S., LUNGARELLA, G., VIRCHOW, J. C. & IDZKO, M. 2010. Extracellular adenosine triphosphate and chronic obstructive pulmonary disease. *Am J Respir Crit Care Med,* 181**,** 928-34.

LOPEZ, W., RAMACHANDRAN, J., ALSAMARAH, A., LUO, Y., HARRIS, A. L. & CONTRERAS, J. E. 2016. Mechanism of gating by calcium in connexin hemichannels. *Proc Natl Acad Sci U S A,* 113**,** E7986-e7995.

LUCEY, E. C., KEANE, J., KUANG, P. P., SNIDER, G. L. & GOLDSTEIN, R. H. 2002. Severity of elastase-induced emphysema is decreased in tumor necrosis factor-alpha and interleukin-1beta receptor-deficient mice. *Lab Invest,* 82**,** 79-85.

LUDBROOK, V. J., HANROTT, K. E., KREINDLER, J. L., MARKS-KONCZALIK, J. E., BIRD, N. P., HEWENS, D. A., BEERAHEE, M., BEHM, D. J., MORICE, A., MCGARVEY, L., PARKER, S. M., BIRRING, S. S. & SMITH, J. 2021. Adaptive study design to assess effect of TRPV4 inhibition in patients with chronic cough. *ERJ Open Res,* 7.

LV, H., YUE, J., CHEN, Z., CHAI, S., CAO, X., ZHAN, J., JI, Z., ZHANG, H., DONG, R. & LAI, K. 2016. Effect of transient receptor potential vanilloid-1 on cough hypersensitivity induced by particulate matter 2.5. *Life Sci,* 151**,** 157-166.

LÁZÁR, Z., HUSZÁR, E., KULLMANN, T., BARTA, I., ANTUS, B., BIKOV, A., KOLLAI, M. & HORVÁTH, I. 2008. Adenosine triphosphate in exhaled breath condensate of healthy subjects and patients with chronic obstructive pulmonary disease. *Inflamm Res,* 57**,** 367-73.

MAES, T., BRACKE, K. R., VERMAELEN, K. Y., DEMEDTS, I. K., JOOS, G. F., PAUWELS, R. A. & BRUSSELLE, G. G. 2006. Murine TLR4 is implicated in cigarette smoke-induced pulmonary inflammation. *Int Arch Allergy Immunol,* 141**,** 354-68.

MAHER, S. A., BIRRELL, M. A. & BELVISI, M. G. 2009. Prostaglandin E2 mediates cough via the EP3 receptor: implications for future disease therapy. *Am J Respir Crit Care Med,* 180**,** 923-8.

MARKHAM, A. 2022. Gefapixant: First Approval. *Drugs,* 82**,** 691-695.

MARTENS, S. & MCMAHON, H. T. 2008. Mechanisms of membrane fusion: disparate players and common principles. *Nat Rev Mol Cell Biol,* 9**,** 543-56.

MARTINON, F., BURNS, K. & TSCHOPP, J. 2002. The inflammasome: a molecular platform triggering activation of inflammatory caspases and processing of proIL-β. *Molecular cell,* 10**,** 417-426.

MAZZONE, S. B. 2004. Sensory regulation of the cough reflex. *Pulm Pharmacol Ther,* 17**,** 361-8.

MAZZONE, S. B., CANNING, B. J. & WIDDICOMBE, J. G. 2003. Sensory Pathways for the Cough Reflex. *Cough: Causes, Mechanisms and Therapy.*

MAZZONE, S. B. & MCGARVEY, L. 2021. Mechanisms and Rationale for Targeted Therapies in Refractory and Unexplained Chronic Cough. *Clin Pharmacol Ther,* 109**,** 619-636.

MAZZONE, S. B., MCGOVERN, A. E., COLE, L. J. & FARRELL, M. J. 2011. Central nervous system control of cough: pharmacological implications. *Curr Opin Pharmacol,* 11**,** 265-71.

MAZZONE, S. B. & UNDEM, B. J. 2016. Vagal Afferent Innervation of the Airways in Health and Disease. *Physiol Rev,* 96**,** 975-1024.

MCELROY, W. D. 1947. The Energy Source for Bioluminescence in an Isolated System. *Proc Natl Acad Sci U S A,* 33**,** 342-5.

MCGARVEY, L., MORICE, A., WAY, N., LI, V., WEAVER, J., DOSHI, I., URDANETA, E. & BOGGS, R. 2019. Prevalence of chronic cough, patient characteristics and health outcomes among UK adults. *European Respiratory Journal,* 54**,** PA3327.

MCGARVEY, L., SHER, M., SHVARTS, Y. G., LU, S., WU, W. C., XU, P., SCHELFHOUT, J., LA ROSA, C., NGUYEN, A. M., REYFMAN, P. A. & AFZAL, A. S. 2023a. The Efficacy and Safety of Gefapixant in a Phase 3b Trial of Patients with Recent-Onset Chronic Cough. *Lung,* 201**,** 111-118.

MCGARVEY, L., SMITH, J. A., MORICE, A., BIRRING, S. S., CHUNG, K. F., DICPINIGAITIS, P. V., NIIMI, A., BENNINGER, M. S., SHER, M., MATSUNAGA, Y., MIYAZAKI, S., MACHIDA, M., ISHIHARA, H., MAHMOOD, A. & GOMEZ, J. C. 2023b. A Randomized, Double-Blind, Placebo-Controlled, Parallel-Group Phase 2b Trial of P2X3 Receptor Antagonist Sivopixant for Refractory or Unexplained Chronic Cough. *Lung,* 201**,** 25-35.

MCGARVEY, L. P., BIRRING, S. S., MORICE, A. H., DICPINIGAITIS, P. V., PAVORD, I. D., SCHELFHOUT, J., NGUYEN, A. M., LI, Q., TZONTCHEVA, A., ISKOLD, B., GREEN, S. A., ROSA, C. L., MUCCINO, D. R. & SMITH, J. A. 2022. Efficacy and safety of gefapixant, a P2X3 receptor antagonist, in refractory chronic cough and unexplained chronic cough (COUGH-1 and COUGH-2): results from two double-blind, randomised, parallel-group, placebo-controlled, phase 3 trials. *The Lancet,* 399**,** 909-923.

MCGARVEY, L. P., BUTLER, C. A., STOKESBERRY, S., POLLEY, L., MCQUAID, S., ABDULLAH, H., ASHRAF, S., MCGAHON, M. K., CURTIS, T. M., ARRON, J., CHOY, D., WARKE, T. J., BRADDING, P., ENNIS, M., ZHOLOS, A., COSTELLO, R. W. & HEANEY, L. G. 2014. Increased expression of bronchial

epithelial transient receptor potential vanilloid 1 channels in patients with severe asthma. *J Allergy Clin Immunol,* 133**,** 704-12.e4.
MCGARVEY, L. P., HEANEY, L. G., LAWSON, J. T., JOHNSTON, B. T., SCALLY, C. M., ENNIS, M., SHEPHERD, D. R. & MACMAHON, J. 1998. Evaluation and outcome of patients with chronic non-productive cough using a comprehensive diagnostic protocol. *Thorax,* 53**,** 738-43.
MCNAMARA, N., GALLUP, M., KHONG, A., SUCHER, A., MALTSEVA, I., FAHY, J. & BASBAUM, C. 2004. Adenosine up-regulation of the mucin gene, MUC2, in asthma. *Faseb j,* 18**,** 1770-2.
MEI, X., LU, R., CUI, L., TIAN, Y., ZHAO, P. & LI, J. 2022. Poly I:C Exacerbates Airway Inflammation and Remodeling in Cigarette Smoke-Exposed Mice. *Lung,* 200**,** 677-686.
MELTZER, E. O., ZEIGER, R. S., DICPINIGAITIS, P., BERNSTEIN, J. A., OPPENHEIMER, J. J., WAY, N. A., LI, V. W., BOGGS, R., DOANE, M. J., URDANETA, E., WEAVER, J. P., SCHELFHOUT, J. & FONSECA, E. 2021. Prevalence and Burden of Chronic Cough in the United States. *J Allergy Clin Immunol Pract,* 9**,** 4037-4044.e2.
MEYER, K. C., RAGHU, G., BAUGHMAN, R. P., BROWN, K. K., COSTABEL, U., DU BOIS, R. M., DRENT, M., HASLAM, P. L., KIM, D. S., NAGAI, S., ROTTOLI, P., SALTINI, C., SELMAN, M., STRANGE, C. & WOOD, B. 2012. An official American Thoracic Society clinical practice guideline: the clinical utility of bronchoalveolar lavage cellular analysis in interstitial lung disease. *Am J Respir Crit Care Med,* 185**,** 1004-14.
MILLQVIST, E. 2011. The airway sensory hyperreactivity syndrome. *Pulm Pharmacol Ther,* 24**,** 263-6.
MIYAJI, T., SAWADA, K., OMOTE, H. & MORIYAMA, Y. 2011. Divalent cation transport by vesicular nucleotide transporter. *J Biol Chem,* 286**,** 42881-7.
MOHANTY, J. G., RAIBLE, D. G., MCDERMOTT, L. J., PELLEG, A. & SCHULMAN, E. S. 2001. Effects of purine and pyrimidine nucleotides on intracellular Ca2+ in human eosinophils: activation of purinergic P2Y receptors. *Journal of allergy and clinical immunology,* 107**,** 849-855.
MORCIANO, G., SARTI, A. C., MARCHI, S., MISSIROLI, S., FALZONI, S., RAFFAGHELLO, L., PISTOIA, V., GIORGI, C., DI VIRGILIO, F. & PINTON, P. 2017. Use of luciferase probes to measure ATP in living cells and animals. *Nature Protocols,* 12**,** 1542-1562.
MOREAUX, B., NEMMAR, A., VINCKE, G., HALLOY, D., BEERENS, D., ADVENIER, C. & GUSTIN, P. 2000. Role of substance P and tachykinin receptor antagonists in citric acid-induced cough in pigs. *Eur J Pharmacol,* 408**,** 305-12.
MORELLO, S., CAIAZZO, E., TURIELLO, R. & CICALA, C. 2021. Thrombo-Inflammation: A Focus on NTPDase1/CD39. *Cells,* 10.
MORICE, A., SMITH, J. A., MCGARVEY, L., BIRRING, S. S., PARKER, S. M., TURNER, A., HUMMEL, T., GASHAW, I., FELS, L., KLEIN, S., FRANCKE, K. & FRIEDRICH, C. 2021. Eliapixant (BAY 1817080), a P2X3 receptor antagonist, in refractory chronic cough: a randomised, placebo-controlled, crossover phase 2a study. *Eur Respir J,* 58.
MORICE, A. H. 2010. The cough hypersensitivity syndrome: a novel paradigm for understanding cough. *Lung,* 188 Suppl 1**,** S87-90.
MORICE, A. H., FONTANA, G. A., BELVISI, M. G., BIRRING, S. S., CHUNG, K. F., DICPINIGAITIS, P. V., KASTELIK, J. A., MCGARVEY, L. P., SMITH, J. A., TATAR, M. & WIDDICOMBE, J. 2007a. ERS guidelines on the assessment of cough. *European Respiratory Journal,* 29**,** 1256.
MORICE, A. H., JAKES, A. D., FARUQI, S., BIRRING, S. S., MCGARVEY, L., CANNING, B., SMITH, J. A., PARKER, S. M., CHUNG, K. F., LAI, K., PAVORD, I. D., VAN DEN BERG, J., SONG, W. J., MILLQVIST, E., FARRELL, M. J., MAZZONE, S. B. & DICPINIGAITIS, P. 2014a. A worldwide survey of chronic cough: a manifestation of enhanced somatosensory response. *Eur Respir J,* 44**,** 1149-55.
MORICE, A. H., KITT, M. M., FORD, A. P., TERSHAKOVEC, A. M., WU, W. C., BRINDLE, K., THOMPSON, R., THACKRAY-NOCERA, S. & WRIGHT, C. 2019. The effect of gefapixant, a P2X3 antagonist, on cough reflex sensitivity: a randomised placebo-controlled study. *Eur Respir J,* 54.
MORICE, A. H., LOWRY, R., BROWN, M. J. & HIGENBOTTAM, T. 1987. Angiotensin-converting enzyme and the cough reflex. *Lancet,* 2**,** 1116-8.

MORICE, A. H., MENON, M. S., MULRENNAN, S. A., EVERETT, C. F., WRIGHT, C., JACKSON, J. & THOMPSON, R. 2007b. Opiate therapy in chronic cough. *Am J Respir Crit Care Med,* 175**,** 312-5.

MORICE, A. H., MILLQVIST, E., BELVISI, M. G., BIEKSIENE, K., BIRRING, S. S., CHUNG, K. F., DAL NEGRO, R. W., DICPINIGAITIS, P., KANTAR, A., MCGARVEY, L. P., PACHECO, A., SAKALAUSKAS, R. & SMITH, J. A. 2014b. Expert opinion on the cough hypersensitivity syndrome in respiratory medicine. *Eur Respir J,* 44**,** 1132-48.

MORICE, A. H., MILLQVIST, E., BIEKSIENE, K., BIRRING, S. S., DICPINIGAITIS, P., DOMINGO RIBAS, C., HILTON BOON, M., KANTAR, A., LAI, K., MCGARVEY, L., RIGAU, D., SATIA, I., SMITH, J., SONG, W. J., TONIA, T., VAN DEN BERG, J. W. K., VAN MANEN, M. J. G. & ZACHARASIEWICZ, A. 2020. ERS guidelines on the diagnosis and treatment of chronic cough in adults and children. *Eur Respir J,* 55.

MORIYAMA, Y., HIASA, M., SAKAMOTO, S., OMOTE, H. & NOMURA, M. 2017. Vesicular nucleotide transporter (VNUT): appearance of an actress on the stage of purinergic signaling. *Purinergic Signal,* 13**,** 387-404.

MORTAZ, E., BRABER, S., NAZARY, M., GIVI, M. E., NIJKAMP, F. P. & FOLKERTS, G. 2009. ATP in the pathogenesis of lung emphysema. *Eur J Pharmacol,* 619**,** 92-6.

MORTAZ, E., FOLKERTS, G., NIJKAMP, F. P. & HENRICKS, P. A. J. 2010. ATP and the pathogenesis of COPD. *European Journal of Pharmacology,* 638**,** 1-4.

MUNCHEL, J. K. & SHEA, B. S. 2021. Diagnosis and Management of Idiopathic Pulmonary Fibrosis. *R I Med J (2013),* 104**,** 26-29.

MÜLLER, T., FAY, S., VIEIRA, R. P., KARMOUTY-QUINTANA, H., CICKO, S., AYATA, K., ZISSEL, G., GOLDMANN, T., LUNGARELLA, G., FERRARI, D., DI VIRGILIO, F., ROBAYE, B., BOEYNAEMS, J. M., BLACKBURN, M. R. & IDZKO, M. 2017. The purinergic receptor subtype P2Y2 mediates chemotaxis of neutrophils and fibroblasts in fibrotic lung disease. *Oncotarget,* 8**,** 35962-35972.

NACHMIAS, N., LANGIER, S., BRZEZINSKI, R. Y., SITERMAN, M., STARK, M., ETKIN, S., AVRIEL, A., SCHWARZ, Y., SHENHAR-TSARFATY, S. & BAR-SHAI, A. 2019. NLRP3 inflammasome activity is upregulated in an in-vitro model of COPD exacerbation. *PLoS One,* 14**,** e0214622.

NASRA, J. & BELVISI, M. G. 2009. Modulation of sensory nerve function and the cough reflex: understanding disease pathogenesis. *Pharmacol Ther,* 124**,** 354-75.

NASSENSTEIN, C., KWONG, K., TAYLOR-CLARK, T., KOLLARIK, M., MACGLASHAN, D. M., BRAUN, A. & UNDEM, B. J. 2008. Expression and function of the ion channel TRPA1 in vagal afferent nerves innervating mouse lungs. *J Physiol,* 586**,** 1595-604.

NASSINI, R., PEDRETTI, P., MORETTO, N., FUSI, C., CARNINI, C., FACCHINETTI, F., VISCOMI, A. R., PISANO, A. R., STOKESBERRY, S., BRUNMARK, C., SVITACHEVA, N., MCGARVEY, L., PATACCHINI, R., DAMHOLT, A. B., GEPPETTI, P. & MATERAZZI, S. 2012. Transient receptor potential ankyrin 1 channel localized to non-neuronal airway cells promotes non-neurogenic inflammation. *PLoS One,* 7**,** e42454.

NAUMOV, D. E., KOLOSOV, V. P., PERELMAN, J. M. & PRIKHODKO, A. G. 2016. Influence of TRPV4 gene polymorphisms on the development of osmotic airway hyperresponsiveness in patients with bronchial asthma. *Dokl Biochem Biophys,* 469**,** 260-3.

NEWTON, K. & DIXIT, V. M. 2012. Signaling in innate immunity and inflammation. *Cold Spring Harb Perspect Biol,* 4.

NIGAM, P. K. 2016. Correct Blood Sampling for Blood Gas Analysis. *J Clin Diagn Res,* 10**,** Bl01-bl02.

NIIMI, A. & CHUNG, K. F. 2015. Evidence for neuropathic processes in chronic cough. *Pulm Pharmacol Ther,* 35**,** 100-4.

NIIMI, A., SAITO, J., KAMEI, T., SHINKAI, M., ISHIHARA, H., MACHIDA, M. & MIYAZAKI, S. 2022. Randomised trial of the P2X(3) receptor antagonist sivopixant for refractory chronic cough. *Eur Respir J,* 59.

NILIUS, B. & SZALLASI, A. 2014. Transient receptor potential channels as drug targets: from the science of basic research to the art of medicine. *Pharmacol Rev,* 66**,** 676-814.
NIRODY, J. A., BUDIN, I. & RANGAMANI, P. 2020. ATP synthase: Evolution, energetics, and membrane interactions. *J Gen Physiol,* 152.
NORTH, R. A. & JARVIS, M. F. 2013. P2X receptors as drug targets. *Mol Pharmacol,* 83**,** 759-69.
NURMI, H. M., LÄTTI, A. M., BRANNAN, J. D. & KOSKELA, H. O. 2019. Comparison of mannitol and citric acid cough provocation tests. *Respir Med,* 158**,** 14-20.
OTSUKA, K., NIIMI, A., MATSUMOTO, H., ITO, I., YAMAGUCHI, M., MATSUOKA, H., JINNAI, M., OGUMA, T., TAKEDA, T., NAKAJI, H., CHIN, K., SASAKI, K., AOYAMA, N. & MISHIMA, M. 2011. Plasma substance P levels in patients with persistent cough. *Respiration,* 82**,** 431-8.
PACHECO, A. 2014. Chronic cough: from a complex dysfunction of the neurological circuit to the production of persistent cough. *Thorax,* 69**,** 881-3.
PATEL, H. J., BIRRELL, M. A., CRISPINO, N., HELE, D. J., VENKATESAN, P., BARNES, P. J., YACOUB, M. H. & BELVISI, M. G. 2003. Inhibition of guinea-pig and human sensory nerve activity and the cough reflex in guinea-pigs by cannabinoid (CB2) receptor activation. *Br J Pharmacol,* 140**,** 261-8.
PELLEG, A., SCHULMAN, E. S. & BARNES, P. J. 2016. Extracellular Adenosine 5'-Triphosphate in Obstructive Airway Diseases. *Chest,* 150**,** 908-915.
PELLEG, A., XU, F., ZHUANG, J., UNDEM, B. & BURNSTOCK, G. 2019. DT-0111: a novel drug-candidate for the treatment of COPD and chronic cough. *Therapeutic advances in respiratory disease,* 13**,** 1753466619877960.
PENUELA, S., GEHI, R. & LAIRD, D. W. 2013. The biochemistry and function of pannexin channels. *Biochim Biophys Acta,* 1828**,** 15-22.
PERO, J. E., MCATEE, J. J., BEHM, D. J., BRIAND, J., GRACZYK-MILLBRANDT, G., ERHARD, K., ROBERTS, A. D., RIVERO, R. A., HOLT, D. A. & LAWHORN, B. G. 2021. Identification, Synthesis, and Characterization of a Major Circulating Human Metabolite of TRPV4 Antagonist GSK2798745. *ACS Med Chem Lett,* 12**,** 1498-1502.
PETERSEN, A. M., PENKOWA, M., IVERSEN, M., FRYDELUND-LARSEN, L., ANDERSEN, J. L., MORTENSEN, J., LANGE, P. & PEDERSEN, B. K. 2007. Elevated levels of IL-18 in plasma and skeletal muscle in chronic obstructive pulmonary disease. *Lung,* 185**,** 161-71.
PICHER, M., BURCH, L. H., HIRSH, A. J., SPYCHALA, J. & BOUCHER, R. C. 2003. Ecto 5'-nucleotidase and nonspecific alkaline phosphatase. Two AMP-hydrolyzing ectoenzymes with distinct roles in human airways. *J Biol Chem,* 278**,** 13468-79.
POLIACEK, I. 2020. Sensory Pathways and Neural Modulation of Cough.
POLIACEK, I., ROSE, M. J., PITTS, T. E., MORTENSEN, A., CORRIE, L. W., DAVENPORT, P. W. & BOLSER, D. C. 2015. Central administration of nicotine suppresses tracheobronchial cough in anesthetized cats. *J Appl Physiol (1985),* 118**,** 265-72.
POLVERINO, M., POLVERINO, F., FASOLINO, M., ANDÒ, F., ALFIERI, A. & DE BLASIO, F. 2012. Anatomy and neuro-pathophysiology of the cough reflex arc. *Multidiscip Respir Med,* 7**,** 5.
RAEMDONCK, K., DE ALBA, J., BIRRELL, M. A., GRACE, M., MAHER, S. A., IRVIN, C. G., FOZARD, J. R., O'BYRNE, P. M. & BELVISI, M. G. 2012. A role for sensory nerves in the late asthmatic response. *Thorax,* 67**,** 19-25.
RAGHU, G., REMY-JARDIN, M., RICHELDI, L., THOMSON, C. C., INOUE, Y., JOHKOH, T., KREUTER, M., LYNCH, D. A., MAHER, T. M., MARTINEZ, F. J., MOLINA-MOLINA, M., MYERS, J. L., NICHOLSON, A. G., RYERSON, C. J., STREK, M. E., TROY, L. K., WIJSENBEEK, M., MAMMEN, M. J., HOSSAIN, T., BISSELL, B. D., HERMAN, D. D., HON, S. M., KHEIR, F., KHOR, Y. H., MACREA, M., ANTONIOU, K. M., BOUROS, D., BUENDIA-ROLDAN, I., CARO, F., CRESTANI, B., HO, L., MORISSET, J., OLSON, A. L., PODOLANCZUK, A., POLETTI, V., SELMAN, M., EWING, T., JONES, S., KNIGHT, S. L., GHAZIPURA, M. & WILSON, K. C. 2022. Idiopathic Pulmonary Fibrosis (an Update) and Progressive Pulmonary Fibrosis in Adults: An Official ATS/ERS/JRS/ALAT Clinical Practice Guideline. *Am J Respir Crit Care Med,* 205**,** e18-e47.

RAHMAN, M., SUN, R., MUKHERJEE, S., NILIUS, B. & JANSSEN, L. J. 2018. TRPV4 Stimulation Releases ATP via Pannexin Channels in Human Pulmonary Fibroblasts. *Am J Respir Cell Mol Biol,* 59**,** 87-95.

RAMSDELL, J. W. 2003. Adenosine airways responsiveness: what does it mean? *Chest.* United States.

RAYEES, S., JOSHI, J. C., TAUSEEF, M., ANWAR, M., BAWEJA, S., ROCHFORD, I., JOSHI, B., HOLLENBERG, M. D., REDDY, S. P. & MEHTA, D. 2019. PAR2-Mediated cAMP Generation Suppresses TRPV4-Dependent Ca(2+) Signaling in Alveolar Macrophages to Resolve TLR4-Induced Inflammation. *Cell Rep,* 27**,** 793-805.e4.

RETAMAL, M. A., SCHALPER, K. A., SHOJI, K. F., ORELLANA, J. A., BENNETT, M. V. & SÁEZ, J. C. 2007. Possible involvement of different connexin43 domains in plasma membrane permeabilization induced by ischemia-reperfusion. *J Membr Biol,* 218**,** 49-63.

RICCIO, M. M., MYERS, A. C. & UNDEM, B. J. 1996. Immunomodulation of afferent neurons in guinea-pig isolated airway. *J Physiol,* 491 (Pt 2)**,** 499-509.

RICCO, M. M., KUMMER, W., BIGLARI, B., MYERS, A. C. & UNDEM, B. J. 1996. Interganglionic segregation of distinct vagal afferent fibre phenotypes in guinea-pig airways. *J Physiol,* 496 (Pt 2)**,** 521-30.

RICHARDS, D., GEVER, J. R., FORD, A. P. & FOUNTAIN, S. J. 2019. Action of MK-7264 (gefapixant) at human P2X3 and P2X2/3 receptors and in vivo efficacy in models of sensitisation. *British Journal of Pharmacology,* 176**,** 2279-2291.

RITEAU, N., GASSE, P., FAUCONNIER, L., GOMBAULT, A., COUEGNAT, M., FICK, L., KANELLOPOULOS, J., QUESNIAUX, V. F., MARCHAND-ADAM, S., CRESTANI, B., RYFFEL, B. & COUILLIN, I. 2010. Extracellular ATP is a danger signal activating P2X7 receptor in lung inflammation and fibrosis. *Am J Respir Crit Care Med,* 182**,** 774-83.

ROBINSON, R., BIRRELL, M., WORTLEY, M., DUBUIS, E., CHEN, S., MCGILVERY, C., HU, S., BONVINI, S., MAHER, S., ADCOCK, J., MUDWAY, I., PORTER, A., TETLEY, T. & BELVISI, M. 2016. Direct activation of sensory afferents by diesel exhaust particles can trigger respiratory symptoms. *European Respiratory Journal,* 48**,** PA5071.

ROBINSON, R. K., BIRRELL, M. A., ADCOCK, J. J., WORTLEY, M. A., DUBUIS, E. D., CHEN, S., MCGILVERY, C. M., HU, S., SHAFFER, M. S. P., BONVINI, S. J., MAHER, S. A., MUDWAY, I. S., PORTER, A. E., CARLSTEN, C., TETLEY, T. D. & BELVISI, M. G. 2018. Mechanistic link between diesel exhaust particles and respiratory reflexes. *J Allergy Clin Immunol,* 141**,** 1074-1084.e9.

ROMAN, J., RIVERA, H. N., ROSER-PAGE, S., SITARAMAN, S. V. & RITZENTHALER, J. D. 2006. Adenosine induces fibronectin expression in lung epithelial cells: implications for airway remodeling. *Am J Physiol Lung Cell Mol Physiol,* 290**,** L317-25.

RUVUNA, L. & SOOD, A. 2020. Epidemiology of Chronic Obstructive Pulmonary Disease. *Clin Chest Med,* 41**,** 315-327.

RYAN, N. M., BIRRING, S. S. & GIBSON, P. G. 2012. Gabapentin for refractory chronic cough: a randomised, double-blind, placebo-controlled trial. *Lancet,* 380**,** 1583-9.

RYAN, R., MARK, B., MICHAEL, W., ERIC, D., SHU, C., CATRIONA, M., SHENG, H., SARA, B., SARAH, M., JOHN, A., IAN, M., ALEXANDRA, P., TERRY, T. & MARIA, B. 2016. Direct activation of sensory afferents by diesel exhaust particles can trigger respiratory symptoms. *European Respiratory Journal,* 48**,** PA5071.

SADIQ, M. W., HOLZ, O., ELLINGHUSEN, B. D., FAULENBACH, C., MÜLLER, M., BADORREK, P., ERIKSSON, U. G., FRIDÉN, M., STOMILOVIC, S., LUNDQVIST, A. J. & HOHLFELD, J. M. 2021. Lung pharmacokinetics of inhaled and systemic drugs: A clinical evaluation. *British Journal of Pharmacology,* 178**,** 4440-4451.

SAMITAS, K., ZERVAS, E. & GAGA, M. 2017. T2-low asthma: current approach to diagnosis and therapy. *Curr Opin Pulm Med,* 23**,** 48-55.

SANT'AMBROGIO, G. & WIDDICOMBE, J. 2001. Reflexes from airway rapidly adapting receptors. *Respir Physiol,* 125**,** 33-45.

SATIA, I., TSAMANDOURAS, N., HOLT, K., BADRI, H., WOODHEAD, M., OGUNGBENRO, K., FELTON, T. W., O'BYRNE, P. M., FOWLER, S. J. & SMITH, J. A. 2017. Capsaicin-evoked cough responses in asthmatic patients: Evidence for airway neuronal dysfunction. *J Allergy Clin Immunol,* 139**,** 771-779.e10.

SATO, D., SATO, T., URATA, Y., OKAJIMA, T., KAWAMURA, S., KURITA, M., TAKAHASHI, K., NANNO, M., WATAHIKI, A., KOKUBUN, S., SHIMIZU, Y., KASAHARA, E., SHOJI, N., SASANO, T. & ICHIKAWA, H. 2014. Distribution of TRPVs, P2X3, and parvalbumin in the human nodose ganglion. *Cell Mol Neurobiol,* 34**,** 851-8.

SAUL, A., HAUSMANN, R., KLESS, A. & NICKE, A. 2013. Heteromeric assembly of P2X subunits. *Front Cell Neurosci,* 7**,** 250.

SAWADA, K., ECHIGO, N., JUGE, N., MIYAJI, T., OTSUKA, M., OMOTE, H., YAMAMOTO, A. & MORIYAMA, Y. 2008. Identification of a vesicular nucleotide transporter. *Proc Natl Acad Sci U S A,* 105**,** 5683-6.

SCHELEGLE, E. S. 2003. Functional morphology and physiology of slowly adapting pulmonary stretch receptors. *Anat Rec A Discov Mol Cell Evol Biol,* 270**,** 11-6.

SCHELEGLE, E. S. & GREEN, J. F. 2001. An overview of the anatomy and physiology of slowly adapting pulmonary stretch receptors. *Respir Physiol,* 125**,** 17-31.

SCHOEFFEL, R. E., ANDERSON, S. D. & ALTOUNYAN, R. E. 1981. Bronchial hyperreactivity in response to inhalation of ultrasonically nebulised solutions of distilled water and saline. *Br Med J (Clin Res Ed),* 283**,** 1285-7.

SCHWIEBERT, E. M. & ZSEMBERY, A. 2003. Extracellular ATP as a signaling molecule for epithelial cells. *Biochimica et Biophysica Acta (BBA) - Biomembranes,* 1615**,** 7-32.

SHAPIRO, C. O., PROSKOCIL, B. J., OPPEGARD, L. J., BLUM, E. D., KAPPEL, N. L., CHANG, C. H., FRYER, A. D., JACOBY, D. B., COSTELLO, R. W. & DRAKE, M. G. 2021. Airway Sensory Nerve Density Is Increased in Chronic Cough. *Am J Respir Crit Care Med,* 203**,** 348-355.

SHISHIKURA, Y., KOARAI, A., AIZAWA, H., YAMAYA, M., SUGIURA, H., WATANABE, M., HASHIMOTO, Y., NUMAKURA, T., MAKIGUTI, T., ABE, K., YAMADA, M., KIKUCHI, T., HOSHIKAWA, Y., OKADA, Y. & ICHINOSE, M. 2016. Extracellular ATP is involved in dsRNA-induced MUC5AC production via P2Y2R in human airway epithelium. *Respiratory Research,* 17**,** 121.

SMITH, J. 2010. Monitoring chronic cough: current and future techniques. *Expert Rev Respir Med,* 4**,** 673-83.

SMITH, J., ALLMAN, D., BADRI, H., MILLER, R., MORRIS, J., SATIA, I., WOOD, A. & M, K. T. 2020a. The Neurokinin-1 Receptor Antagonist Orvepitant Is a Novel Antitussive Therapy for Chronic Refractory Cough: Results From a Phase 2 Pilot Study (VOLCANO-1). *Chest,* 157**,** 111-118.

SMITH, J., MORICE, A. H., BIRRING, S. S., PARKER, S., MARSDEN, P. A., HOLCOMB, J., PRENNER, B. M., SHER, M. R., STEVEN, G. C., MCGARVEY, L., GARCEAU, D., BONUCCELLI, C. M. & HARVEY, L. 2021a. Improvements in Cough Frequency Over 24 Hours with BLU-5937, a Selective P2X3 Antagonist, in Patient Subgroups Defined by Baseline Awake Cough Frequencies. *A6. A006 HOT TAKES FROM CLINICAL TRIALS IN LUNG DISEASE.* American Thoracic Society.

SMITH, J. & WOODCOCK, A. 2008. New developments in the objective assessment of cough. *Lung,* 186 Suppl 1**,** S48-54.

SMITH, J. A. & BADRI, H. 2019. Cough: New Pharmacology. *J Allergy Clin Immunol Pract,* 7**,** 1731-1738.

SMITH, J. A., HILTON, E. C. Y., SAULSBERRY, L. & CANNING, B. J. 2012. Antitussive effects of memantine in guinea pigs. *Chest,* 141**,** 996-1002.

SMITH, J. A., HOLT, K., DOCKRY, R., SEN, S., SHEPPARD, K., TURNER, P., CZYZYK, P. & MCGUINNESS, K. 2021b. Performance of a digital signal processing algorithm for the accurate quantification of cough frequency. *Eur Respir J,* 58.

SMITH, J. A., KITT, M. M., MORICE, A. H., BIRRING, S. S., MCGARVEY, L. P., SHER, M. R., LI, Y.-P., WU, W.-C., XU, Z. J., MUCCINO, D. R., FORD, A. P., SMITH, J., MCGARVEY, L., BIRRING, S., HULL, J., CARR, W. W., GOLDSOBEL, A. B., GROSS, G. N., HOLCOMB, J. R., HUSSAIN, I., SHER, M.,

SPANGENTHAL, S., STORMS, W., MORICE, A., ELKAYAM, D., STEVEN, G. C., KRAINSON, J., FAKIH, F. A., MATZ, J., BROOKS, G. D., CASALE, T., BERMAN, G. D., CONDEMI, J. J., GREOS, L. S., GOGATE, S. U., SHER, E. R., FRIESEN, J. H., SCHENKEL, E. J., BERNSTEIN, D. I., CORREN, J., SUNDAR, K., GOTFRIED, M. H., MONTANARO, A., LUMRY, W. R., AMAR, N. J., KAPLAN, M. S., PRENNER, B. M., MURPHY, T. R., GOOD, J. S., PARKER, S., HARRISON, T., PAVORD, I., BRIGHTLING, C., DJUKANOVIC, R., MCQUAID, D., DENENBERG, M., ETTINGER, N. A. & IYER, V. 2020b. Gefapixant, a P2X3 receptor antagonist, for the treatment of refractory or unexplained chronic cough: a randomised, double-blind, controlled, parallel-group, phase 2b trial. *The Lancet Respiratory Medicine,* 8**,** 775-785.

SMITH, J. A., MCGARVEY, L., MORICE, A. H., BIRRING, S. S., HULL, J., LANOUETTE, S., YANG, R., BARTHOLOMEW, K., HARVEY, L., GARIN, M. & BONUCCELLI, C. M. 2022. Improvements in Awake Cough Frequency in SOOTHE, A Phase 2b Trial of BLU-5937 in Refractory Chronic Cough. *European Respiratory Journal,* 60**,** 810.

SMITH, J. A., MCGARVEY, L. P. A., BADRI, H., SATIA, I., WARREN, F., SIEDERER, S., LIEFAARD, L., MURDOCH, R. D., POVEY, K. & MARKS-KONCZALIK, J. 2017. Effects of a novel sodium channel blocker, GSK2339345, in patients with refractory chronic cough. *Int J Clin Pharmacol Ther,* 55**,** 712-719.

SMITH, J. A. & WEST, P. W. 2021. Branching Out in Chronic Cough: Evidence for Increased Airway Nerve Density. American Thoracic Society.

SOKOLOWSKA, M., QUESNIAUX, V. F. J., AKDIS, C. A., CHUNG, K. F., RYFFEL, B. & TOGBE, D. 2019. Acute Respiratory Barrier Disruption by Ozone Exposure in Mice. *Front Immunol,* 10**,** 2169.

SOSINSKY, G. E., BOASSA, D., DERMIETZEL, R., DUFFY, H. S., LAIRD, D. W., MACVICAR, B., NAUS, C. C., PENUELA, S., SCEMES, E., SPRAY, D. C., THOMPSON, R. J., ZHAO, H. B. & DAHL, G. 2011. Pannexin channels are not gap junction hemichannels. *Channels (Austin),* 5**,** 193-7.

SPICUZZA, L., DI MARIA, G. & POLOSA, R. 2006. Adenosine in the airways: implications and applications. *Eur J Pharmacol,* 533**,** 77-88.

STERN, J., PIER, J. & LITONJUA, A. A. 2020. Asthma epidemiology and risk factors. *Semin Immunopathol,* 42**,** 5-15.

STORY, G. M., PEIER, A. M., REEVE, A. J., EID, S. R., MOSBACHER, J., HRICIK, T. R., EARLEY, T. J., HERGARDEN, A. C., ANDERSSON, D. A., HWANG, S. W., MCINTYRE, P., JEGLA, T., BEVAN, S. & PATAPOUTIAN, A. 2003. ANKTM1, a TRP-like channel expressed in nociceptive neurons, is activated by cold temperatures. *Cell,* 112**,** 819-29.

STOWELL, N. C., SEIDEMAN, J., RAYMOND, H. A., SMALLEY, K. A., LAMB, R. J., EGENOLF, D. D., BUGELSKI, P. J., MURRAY, L. A., MARSTERS, P. A., BUNTING, R. A., FLAVELL, R. A., ALEXOPOULOU, L., SAN MATEO, L. R., GRISWOLD, D. E., SARISKY, R. T., MBOW, M. L. & DAS, A. M. 2009. Long-term activation of TLR3 by poly(I:C) induces inflammation and impairs lung function in mice. *Respir Res,* 10**,** 43.

STROTMANN, R., HARTENECK, C., NUNNENMACHER, K., SCHULTZ, G. & PLANT, T. D. 2000. OTRPC4, a nonselective cation channel that confers sensitivity to extracellular osmolarity. *Nat Cell Biol,* 2**,** 695-702.

SUZUKI, M., MIZUNO, A., KODAIRA, K. & IMAI, M. 2003. Impaired pressure sensation in mice lacking TRPV4. *J Biol Chem,* 278**,** 22664-8.

SÜDHOF, T. C. & ROTHMAN, J. E. 2009. Membrane fusion: grappling with SNARE and SM proteins. *Science,* 323**,** 474-7.

TAKAHARA, N., ITO, S., FURUYA, K., NARUSE, K., ASO, H., KONDO, M., SOKABE, M. & HASEGAWA, Y. 2014. Real-time imaging of ATP release induced by mechanical stretch in human airway smooth muscle cells. *Am J Respir Cell Mol Biol,* 51**,** 772-82.

TAKAHASHI, A., CAMACHO, P., LECHLEITER, J. D. & HERMAN, B. 1999. Measurement of intracellular calcium. *Physiol Rev,* 79**,** 1089-125.

TAKAHASHI, K., ITO, S., FURUYA, K., ASANO, S., SOKABE, M. & HASEGAWA, Y. 2017. Real-time imaging of mechanically and chemically induced ATP release in human lung fibroblasts. *Respir Physiol Neurobiol,* 242**,** 96-101.

TAKEYAMA, M., NAGAI, S., MORI, K., IKAWA, K., SATAKE, N. & IZUMI, T. 1996. Substance P-like immunoreactive substance in bronchoalveolar lavage fluids from patients with idiopathic pulmonary fibrosis and pulmonary sarcoidosis. *Sarcoidosis Vasc Diffuse Lung Dis,* 13**,** 33-7.

TANG, D., KANG, R., COYNE, C. B., ZEH, H. J. & LOTZE, M. T. 2012. PAMPs and DAMPs: signal 0s that spur autophagy and immunity. *Immunol Rev,* 249**,** 158-75.

TARUNO, A. 2018. ATP Release Channels. *Int J Mol Sci,* 19.

TATAR, M., SANT'AMBROGIO, G. & SANT'AMBROGIO, F. B. 1994. Laryngeal and tracheobronchial cough in anesthetized dogs. *J Appl Physiol (1985),* 76**,** 2672-9.

TAYLOR-CLARK, T. E. & UNDEM, B. J. 2011. Sensing pulmonary oxidative stress by lung vagal afferents. *Respir Physiol Neurobiol,* 178**,** 406-13.

THOMPSON, R. J., SAYERS, I., KUOKKANEN, K. & HALL, I. P. 2021. Purinergic Receptors in the Airways: Potential Therapeutic Targets for Asthma? *Front Allergy,* 2**,** 677677.

THORNELOE, K. S., SULPIZIO, A. C., LIN, Z., FIGUEROA, D. J., CLOUSE, A. K., MCCAFFERTY, G. P., CHENDRIMADA, T. P., LASHINGER, E. S., GORDON, E., EVANS, L., MISAJET, B. A., DEMARINI, D. J., NATION, J. H., CASILLAS, L. N., MARQUIS, R. W., VOTTA, B. J., SHEARDOWN, S. A., XU, X., BROOKS, D. P., LAPING, N. J. & WESTFALL, T. D. 2008. N-((1S)-1-{[4-((2S)-2-{[(2,4-dichlorophenyl)sulfonyl]amino}-3-hydroxypropanoyl)-1-piperazinyl]carbonyl}-3-methylbutyl)-1-benzothiophene-2-carboxamide (GSK1016790A), a novel and potent transient receptor potential vanilloid 4 channel agonist induces urinary bladder contraction and hyperactivity: Part I. *J Pharmacol Exp Ther,* 326**,** 432-42.

TRAUTMANN, A. 2009. Extracellular ATP in the immune system: more than just a "danger signal". *Sci Signal,* 2**,** pe6.

TREVISANI, M., MILAN, A., GATTI, R., ZANASI, A., HARRISON, S., FONTANA, G., MORICE, A. H. & GEPPETTI, P. 2004. Antitussive activity of iodo-resiniferatoxin in guinea pigs. *Thorax,* 59**,** 769-72.

TURNER, R. D. & BIRRING, S. S. 2023. Measuring cough: what really matters? *J Thorac Dis,* 15**,** 2288-2299.

UNDEM, B. J., CHUAYCHOO, B., LEE, M. G., WEINREICH, D., MYERS, A. C. & KOLLARIK, M. 2004. Subtypes of vagal afferent C-fibres in guinea-pig lungs. *J Physiol,* 556**,** 905-17.

UNDEM, B. J. & KOLLARIK, M. 2002. Characterization of the vanilloid receptor 1 antagonist iodo-resiniferatoxin on the afferent and efferent function of vagal sensory C-fibers. *J Pharmacol Exp Ther,* 303**,** 716-22.

UNDEM, B. J. & NASSENSTEIN, C. 2009. Airway nerves and dyspnea associated with inflammatory airway disease. *Respir Physiol Neurobiol.* Netherlands.

UNDEM, B. J., OH, E. J., LANCASTER, E. & WEINREICH, D. 2003. Effect of extracellular calcium on excitability of guinea pig airway vagal afferent nerves. *J Neurophysiol,* 89**,** 1196-204.

VANDIVIER, R. W. & GHOSH, M. 2017. Understanding the Relevance of the Mouse Cigarette Smoke Model of COPD: Peering through the Smoke. *Am J Respir Cell Mol Biol,* 57**,** 3-4.

VARECHOVA, S., PLEVKOVA, J., HANACEK, J. & TATAR, M. 2008. Role of gender and pubertal stage on cough sensitivity in childhood and adolescence. *J Physiol Pharmacol,* 59 Suppl 6**,** 719-26.

VERTIGAN, A. E., KAPELA, S. L., RYAN, N. M., BIRRING, S. S., MCELDUFF, P. & GIBSON, P. G. 2016. Pregabalin and Speech Pathology Combination Therapy for Refractory Chronic Cough: A Randomized Controlled Trial. *Chest,* 149**,** 639-48.

VLAHOS, R. & BOZINOVSKI, S. 2014. Recent advances in pre-clinical mouse models of COPD. *Clin Sci (Lond),* 126**,** 253-65.

VULTAGGIO-POMA, V., SARTI, A. C. & DI VIRGILIO, F. 2020. Extracellular ATP: A Feasible Target for Cancer Therapy. *Cells,* 9.

WANG, H., LV, C., WANG, S., YING, H., WENG, Y. & YU, W. 2018. NLRP3 Inflammasome Involves in the Acute Exacerbation of Patients with Chronic Obstructive Pulmonary Disease. *Inflammation,* 41**,** 1321-1333.

WANG, J., TAKEMURA, N. & SAITOH, T. 2021. Macrophage Response Driven by Extracellular ATP. *Biol Pharm Bull,* 44**,** 599-604.

WANG, L. L., TANG, P. H., SHI, C. G., WAN, Y. H., TANG, W., HOU, X. X., PAN, N. L., SHI, Y. B. & TAO, Q. L. 2014. Expression of CD39 mRNA is altered in the peripheral blood of patients with allergic asthma. *Biomed Rep,* 2**,** 75-78.

WANG, N., DE BOCK, M., DECROCK, E., BOL, M., GADICHERLA, A., VINKEN, M., ROGIERS, V., BUKAUSKAS, F. F., BULTYNCK, G. & LEYBAERT, L. 2013. Paracrine signaling through plasma membrane hemichannels. *Biochim Biophys Acta,* 1828**,** 35-50.

WATANABE, H., DAVIS, J. B., SMART, D., JERMAN, J. C., SMITH, G. D., HAYES, P., VRIENS, J., CAIRNS, W., WISSENBACH, U., PRENEN, J., FLOCKERZI, V., DROOGMANS, G., BENHAM, C. D. & NILIUS, B. 2002. Activation of TRPV4 channels (hVRL-2/mTRP12) by phorbol derivatives. *J Biol Chem,* 277**,** 13569-77.

WEBER, J., RAJAN, S., SCHREMMER, C., CHAO, Y. K., KRASTEVA-CHRIST, G., KANNLER, M., YILDIRIM, A., BROSIEN, M., SCHREDELSEKER, J., WEISSMANN, N., GRIMM, C., GUDERMANN, T. & DIETRICH, A. 2020. TRPV4 channels are essential for alveolar epithelial barrier function as protection from lung edema. *JCI Insight,* 5.

WEST, P. W., KELSALL, A., DECALMER, S., DOVE, W., BISHOP, P. W., STEWART, J. P., WOODCOCK, A. A. & SMITH, J. A. 2012. PCR based bronchoscopic detection of common respiratory pathogens in chronic cough: a case control study. *Cough,* 8**,** 5.

WIDDICOMBE, J. 2002. Neuroregulation of cough: implications for drug therapy. *Current Opinion in Pharmacology,* 2**,** 256-263.

WIDDICOMBE, J. 2003. Functional morphology and physiology of pulmonary rapidly adapting receptors (RARs). *Anat Rec A Discov Mol Cell Evol Biol,* 270**,** 2-10.

WIDDICOMBE, J. G. & UNDEM, B. J. 2002. Summary: central nervous pharmacology of cough. *Pulm Pharmacol Ther,* 15**,** 251-2.

WONG, C. H., MATAI, R. & MORICE, A. H. 1999. Cough induced by low pH. *Respir Med,* 93**,** 58-61.

WONG, Q. Y. A., LIM, J. J., NG, J. Y., MALIPEDDI, P., LIM, Y. Y. E., SIO, Y. Y. & CHEW, F. T. 2023. An updated prevalence of asthma, its phenotypes, and the identification of the potential asthma risk factors among young Chinese adults recruited in Singapore. *World Allergy Organ J,* 16**,** 100757.

WOOD, R. E., WISHART, C., WALKER, P. J., ASKEW, C. D. & STEWART, I. B. 2009. Plasma ATP concentration and venous oxygen content in the forearm during dynamic handgrip exercise. *BMC Physiol,* 9**,** 24.

WORTLEY, M. A., DUBUIS, E., BONVINI, S. J., WONG, S., SHALA, F., MAHER, S. A., ADCOCK, J. J., SMITH, J. A., BIRRELL, M. A. & BELVISI, M. G. 2016. Making Sense of Sensory Nerves: An In Vitro Characterisation of Gene Expression Profiles of Airway-Innervating Guinea-Pig Airway Neurons Using Single-Cell Analysis. *C78. NOT STRANGERS IN THE NIGHT: SLEEP AND THORACIC DISEASES.* American Thoracic Society.

WRIGHT, J. L., COSIO, M. & CHURG, A. 2008. Animal models of chronic obstructive pulmonary disease. *Am J Physiol Lung Cell Mol Physiol,* 295**,** L1-15.

YAN, Z., JIN, Y., AN, Z., LIU, Y., SAMET, J. M. & WU, W. 2016. Inflammatory cell signaling following exposures to particulate matter and ozone. *Biochimica et Biophysica Acta (BBA) - General Subjects,* 1860**,** 2826-2834.

YI, G., LIANG, M., LI, M., FANG, X., LIU, J., LAI, Y., CHEN, J., YAO, W., FENG, X., HU, L., LIN, C., ZHOU, X. & LIU, Z. 2018. A large lung gene expression study identifying IL1B as a novel player in airway inflammation in COPD airway epithelial cells. *Inflamm Res,* 67**,** 539-551.

YILMAZ, İ. 2019. Angiotensin-Converting Enzyme Inhibitors Induce Cough. *Turk Thorac J,* 20**,** 36-42.

YOUNG, E. C. & SMITH, J. A. 2011. Pharmacologic therapy for cough. *Curr Opin Pharmacol,* 11**,** 224-30.

ZHANG, F., SU, X., HUANG, G., XIN, X. F., CAO, E. H., SHI, Y. & SONG, Y. 2017. Adenosine Triphosphate Promotes Allergen-Induced Airway Inflammation and Th17 Cell Polarization in Neutrophilic Asthma. *J Immunol Res,* 2017**,** 5358647.

ZHOU, R., YAZDI, A. S., MENU, P. & TSCHOPP, J. 2011. A role for mitochondria in NLRP3 inflammasome activation. *Nature,* 469**,** 221-5.

ZIMMERMANN, H., ZEBISCH, M. & STRÄTER, N. 2012. Cellular function and molecular structure of ecto-nucleotidases. *Purinergic Signal,* 8**,** 437-502.

ÇOLAK, Y., NORDESTGAARD, B. G., LAURSEN, L. C., AFZAL, S., LANGE, P. & DAHL, M. 2017. Risk Factors for Chronic Cough Among 14,669 Individuals From the General Population. *Chest,* 152**,** 563-573.

Appendix

The table below outlines reagents used in this thesis.

Reagent	Source	Vehicle (where applicable)
αβ-MeATP	Sigma-Aldrich, USA	0.1% dH_2O in KH *in vitro*
AF-353	Sigma-Aldrich, USA	0.1% DMSO in KH *in vitro*
ATP	Sigma-Aldrich, USA	1% dH_2O in ECS *in vitro*
$CaCl_2$	VWR, USA	
Capsaicin	Sigma-Aldrich, USA	0.1% DMSO in KH *in vitro*
CD39-analogue	AstraZeneca, Sweden	0.1% DMSO in KH *in vitro*
CD39-His	AstraZeneca, Sweden	0.1% DMSO in KH *in vitro* 0.1% DMSO in 0.9% saline in vivo
CD39-Mut	AstraZeneca, Sweden	0.1% DMSO in KH *in vitro* 0.1% DMSO in 0.9% saline in vivo
DMSO	Sigma-Aldrich, USA	
EDTA	Sigma-Aldrich, USA	
Ethanol	VWR, USA	
FBS	ThermoFisher Scientific, USA	
Gefapixant	Selleckchem, UK	0.1% DMSO in KH *in vitro*
GSK1016790A	Sigma-Aldrich, USA	0.1% DMSO in KH *in vitro* 0.1% DMSO in 0.9% saline *in vivo*
HBSS	Sigma-Aldrich, USA	
Heparin Sodium Salt	Sigma-Aldrich, USA	
HEPES	Sigma-Aldrich, USA	
Isoflurane	Abbott laboratories, USA	
KCl	VWR, USA	
$MgSO_4$	VWR, USA	
NaCl	VWR, USA	
NaH_2PO_4	VWR, USA	
$NaHCO_3$	Sigma-Aldrich, USA	
Nuclease free water	Promega, USA	
Papain	Sigma-Aldrich, USA	
Petroleum Jelly	Vaseline	
Poly I:C potassium salt	InvivoGen, USA	0.1% DMSO in 0.9% saline *in vivo*
Saline (0.9% NaCl)	Fresenius Kabi, Germany	